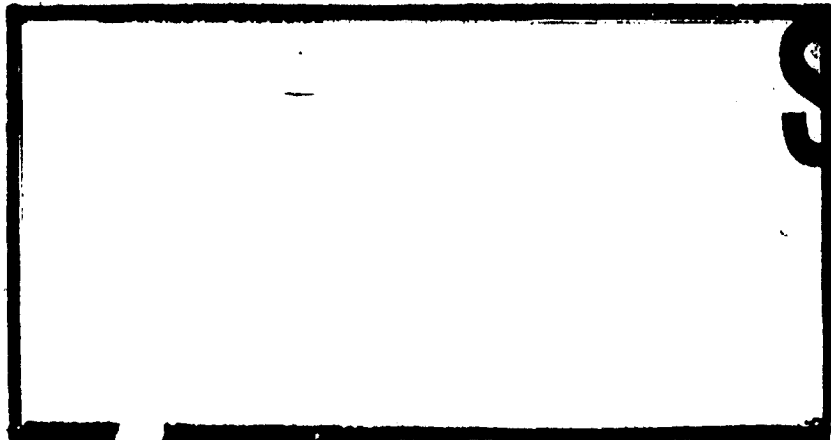


AD-A280 593



0



DTIC
ELECTE
JUN 24 1994

S

D

G



DTIC QUALITY INSPECTED 2

DEPARTMENT OF THE AIR FORCE
AIR UNIVERSITY

AIR FORCE INSTITUTE OF TECHNOLOGY

Wright-Patterson Air Force Base, Ohio

AFIT/DS/AA/94-2

H_2 OPTIMAL CONTROL WITH H_∞ ,
 μ , AND L_1 CONSTRAINTS

DISSERTATION
David Earl Walker
Lieutenant Colonel, USAF

AFIT/DS/AA/94-2

94-19401



Approved for public release; distribution unlimited

94 6 24 016

AFIT/DS/AA/94-2

H_2 OPTIMAL CONTROL WITH H_∞ , μ , AND L_1 CONSTRAINTS

DISSERTATION

Presented to the Faculty of the Graduate School of Engineering
of the Air Force Institute of Technology

Air University

In Partial Fulfillment of the
Requirements for the Degree of
Doctor of Philosophy

David Earl Walker, B.S., M.S.

Lieutenant Colonel, USAF

June, 1994

Approved for public release; distribution unlimited

REPORT DOCUMENTATION PAGE

Form Approved
OMB No. 0704-0188

Public reporting burden for this collection of information is estimated to average 1 hour per response, including the time for reviewing instructions, searching existing data sources, gathering and maintaining the data needed, and completing and reviewing the collection of information. Send comments regarding this burden estimate or any other aspect of this collection of information, including suggestions for reducing this burden, to Washington Headquarters Services, Directorate for Information Operations and Reports, 1215 Jefferson Davis Highway, Suite 1204, Arlington, VA 22202-4302, and to the Office of Management and Budget, Paperwork Reduction Project (0704-0188), Washington, DC 20503.

1. AGENCY USE ONLY (Leave blank)		2. REPORT DATE June 1994	3. REPORT TYPE AND DATES COVERED Doctoral Dissertation	
4. TITLE AND SUBTITLE H2 OPTIMAL CONTROL WITH H-INF, MU, AND L1 CONSTRAINTS			5. FUNDING NUMBERS	
6. AUTHOR(S) David E. Walker, Lt Col, USAF				
7. PERFORMING ORGANIZATION NAME(S) AND ADDRESS(ES) Air Force Institute of Technology, WPAFB OH 45433-6583			8. PERFORMING ORGANIZATION REPORT NUMBER AFIT/DS/AA/94-2	
9. SPONSORING / MONITORING AGENCY NAME(S) AND ADDRESS(ES) Dr Marc Jacobs AFOSR/NM 110 Duncan Ave, Suite B115 Bolling AFB DC 20332-0001			10. SPONSORING / MONITORING AGENCY REPORT NUMBER	
11. SUPPLEMENTARY NOTES				
12a. DISTRIBUTION / AVAILABILITY STATEMENT Approved For Public Release; Distribution Unlimited			12b. DISTRIBUTION CODE	
13. ABSTRACT (Maximum 200 words) H2 optimization with convex constraints is considered. The optimal (order-free) solution is shown to be unique through convex analysis. H-inf constraints with feedforward terms and singular constraints are also allowed. The optimal fixed-order solution is shown to have the same characteristics as a mixed problem with regular H-inf constraints. Furthermore, these results are shown to hold for controller orders as low as the optimal H2 order. A numerical method is developed based on analytical gradients which results in sub- and super-optimal fixed-order controllers. The problem is extended to include an upper bound on a mu constraint through a modification of the D-K iteration method. Next, multiple H-inf constraints are developed. Fixed-order solutions to the multiple constraint problem are characterized and the numerical method is extended to include multiple constraints. Next, a continuous L1 constraint is added. A numerical approach is proposed based on bounding the L1-norm by the l1-norm of an Euler approximating system. Finally, H2 optimization with a finite set of H-inf, mu, and L1 constraints is characterized. SISO and MIMO numerical examples demonstrate the application of these methods.				
14. SUBJECT TERMS Control Theory, Mathematical Programming, Riccati Equation, H2 Optimization, H-inf Optimization, Mu-Synthesis, L1 Optimization, Multiobjective Optimal Control			15. NUMBER OF PAGES 237	
			16. PRICE CODE	
17. SECURITY CLASSIFICATION OF REPORT UNCLASSIFIED	18. SECURITY CLASSIFICATION OF THIS PAGE UNCLASSIFIED	19. SECURITY CLASSIFICATION OF ABSTRACT UNCLASSIFIED	20. LIMITATION OF ABSTRACT UL	

The views expressed in this dissertation are those of the author and do not reflect the official policy or position of the Department of Defense or the U. S. Government.

Accession For	
NTIS	CRA&I <input checked="" type="checkbox"/>
DTIC	TAB <input type="checkbox"/>
Unannounced	<input type="checkbox"/>
Justification _____	
By _____	
Distribution / _____	
Availability Codes	
Dist	Avail and/or Special
A-1	

AFIT/DS/AA/94-2

H_2 OPTIMAL CONTROL WITH H_∞ , μ , AND L_1 CONSTRAINTS

David Earl Walker, B.S., M.S.

Lieutenant Colonel, USAF

Approved:

D. Brett Ridgely 19 May 1994

Dr. D. Brett Ridgely, Research Advisor

Brad S. Liebst 16 May 1994

Dr. Brad S. Liebst

Mark E. Oxley 16 May 1994

Dr. Mark E. Oxley

Peter S. Maybeck 16 May 1994

Dr. Peter S. Maybeck

J. S. Przemieniecki 19 May 1994

Dr. J. S. Przemieniecki

Institute Senior Dean

Acknowledgements

There have been many people in my life who have influenced the completion of this work. While I cannot possibly thank everyone who has guided, influenced or inspired me, I would like to acknowledge some people who have had a direct impact.

First and foremost, I want to thank Dr. Brett Ridgely who challenged me with the mixed optimization problem. It was only with his insight and guidance throughout this endeavor that I was able to complete my research. In addition, his editorial abilities were indispensable. Furthermore, the research group Dr Ridgely established allowed this work to be approached with the synergy available only through a collection of enthusiastic and capable people.

I am indebted to all the members of this research group. In particular, I want to thank Jim Luke, Julio Ullauri, and Bill Reigelsperger for demonstrating to the world that the theory we have developed has real world applications. Furthermore, I want to thank Dave Jacques for all the hours of discussion and help he provided.

I would like to thank my research committee members, Dr. Brad Liebst and Dr Mark Oxley. Their assistance in answering questions and providing leads to research in areas associated with my work was invaluable. I also want to thank Dr. Peter Maybeck for acting as the Dean's representative on my committee. His thorough review and excellent comments on this work have led to much more polished and usable document.

I want to thank Dr. Bob Canfield for his suggestions on how to improve the numerical approaches to my problem. Dr Alan Lair provided the mathematical insight necessary for the duality work in the dissertation, and I am deeply grateful for his assistance. For the last two years Dr. Brian Jones has always provided me a place to escape and philosophize on the problems of the world. I want to thank him for keeping my work in perspective and for his assistance in reviewing this document.

Most importantly, I could not have completed this work without the support and understanding of my loving wife Takako and my children Christine, Cathy, Frances, and Anne. They are the ones who have sacrificed the most during the past three years and I know that I will never be able to make up for it.

Finally, I want to thank the man who always challenged me to go one step beyond and never be satisfied until I reached my ultimate goal. For this reason, I dedicate this work to the memory of my Father.

David Earl Walker

Table of Contents

	Page
Acknowledgements	iii
List of Figures	ix
List of Tables	xiv
Abstract	xv
I. Introduction	1-1
1.1 Overview	1-1
1.2 Review of Related Work	1-7
1.2.1 Mixed H_2/H_∞ with a single input or single out- put	1-7
1.2.2 General Mixed H_2/H_∞ optimization	1-7
1.2.3 Mixed H_2/μ optimization	1-8
1.3 Research Objectives and Contributions	1-9
1.4 Outline	1-11
II. Mathematical Preliminaries	2-1
2.1 State Space and Transfer Functions	2-1
2.2 Stability Theory	2-5
2.3 Operator Spaces	2-6
2.3.1 H_2 Space	2-7
2.3.2 H_∞ Space	2-9
2.3.3 L_1 and ℓ_1 Spaces	2-10
2.4 Lyapunov Equations	2-15
2.5 Riccati Equations	2-16

	Page
2.5.1 H_2 Type	2-16
2.5.2 H_∞ Type	2-17
2.6 Convex Optimization	2-25
2.7 Duality in Minimum Norm Problems	2-27
2.8 Summary	2-29
III. Review of H_2 , H_∞ , and μ	3-1
3.1 Parametrization of All Stabilizing Controllers	3-1
3.1.1 Coprime Factorizations	3-1
3.1.2 Parametrization	3-2
3.2 H_2 Optimization	3-4
3.3 H_∞ Optimization	3-7
3.4 The Complex Structured Singular Value	3-12
3.4.1 Structured Singular Value	3-12
3.4.2 Frequency Domain μ -synthesis	3-15
3.5 Summary	3-17
IV. The Optimal H_2/H_∞ Controller	4-1
4.1 Parametrization of the H_2/H_∞ Controller	4-1
4.2 Uniqueness of the Optimal (Order-Free) H_2/H_∞ Controller	4-7
4.3 Dual Approach to H_2/H_∞	4-10
4.4 Summary	4-16
V. Fixed-Order H_2/H_∞ Optimal Control	5-1
5.1 State Space Formulation	5-3
5.2 The Lagrangian and Necessary Conditions	5-7
5.3 H_2 Order or Greater Order Solution	5-12
5.4 Summary	5-15

	Page
VI. Numerical Approach	6-1
6.1 Numerical Method	6-2
6.1.1 Equality Constraint Approach	6-3
6.1.2 Inequality Constraint Approach	6-4
6.1.3 Computing Gradients of the Two-Norm	6-6
6.1.4 Computing Gradients of the Infinity-Norm	6-8
6.1.5 Initial Conditions and Controller Realizations	6-12
6.2 Numerical Example: SISO F-16 Longitudinal Controller	6-13
6.2.1 H_2 Problem	6-14
6.2.2 H_∞ Problem	6-17
6.2.3 Results	6-21
6.2.4 Modified H_2 Problem	6-30
6.2.5 Convergence	6-33
6.3 Summary	6-34
VII. Mixed H_2/μ Optimal Control	7-1
7.1 Mixed H_2/μ	7-2
7.2 Robust Controllers Using H_2/μ	7-5
7.2.1 Robust Stability	7-5
7.2.2 Robust Performance	7-5
7.3 Examples	7-7
7.3.1 SISO F-16 Design	7-7
7.3.2 MIMO HIMAT Design	7-21
7.4 Summary	7-37
VIII. Multiple H_∞ Constraints	8-1
8.1 Uniqueness of the Optimal Controller	8-4
8.2 Fixed-order Solutions	8-12

	Page
8.2.1 State Space Formulation	8-12
8.2.2 The Lagrangian and Necessary Conditions . .	8-15
8.2.3 H_2 Order or Greater Solution	8-20
8.3 Numerical Solution	8-22
8.3.1 Grid Method	8-22
8.3.2 Direct Method	8-23
8.4 SISO F-16 Example	8-24
8.4.1 Problem Setup	8-25
8.4.2 Results	8-26
8.5 Summary	8-31
 IX. Mixed H_2/L_1 and $H_2/H_\infty/\mu/L_1$ Optimal Control	 9-1
9.1 Mixed H_2/L_1 Optimization	9-1
9.1.1 Uniqueness of the Optimal H_2/L_1 Controller .	9-2
9.1.2 Fixed-Order Controllers—Numerical Approach	9-4
9.2 H_2 Optimization with H_∞ , μ , and L_1 Constraints . . .	9-5
9.3 Application of Mixed Optimization	9-8
 X. Conclusions and Recommendations	 10-1
10.1 Summary	10-1
10.2 Recommendations for Future Research	10-4
 Appendix A. SISO F-16 Short Period Model	 A-1
 Appendix B. MIMO HIMAT Model	 B-1
 Bibliography	 BIB-1
 Vita	 VITA-1

List of Figures

Figure	Page
1.1. General nominal block diagram	1-2
1.2. General perturbed block diagram	1-3
1.3. Mixed block diagram	1-4
1.4. Perturbed stability diagram	1-5
2.1. Nominal feedback system	2-3
2.2. Perturbed system	2-4
2.3. Internal stability system	2-7
3.1. Feedback system	3-1
3.2. H_2 system with parametrized controller	3-6
3.3. H_∞ feedback system	3-8
3.4. H_∞ system with parametrized controller	3-10
3.5. M- Δ system	3-14
4.1. General mixed H_2/H_∞ optimization problem	4-2
4.2. Q-parametrization	4-6
4.3. Admissible region, $\gamma \geq \bar{\gamma}$	4-9
4.4. Admissible region, $\gamma \leq \bar{\gamma}$	4-10
5.1. General mixed H_2/H_∞ optimization problem	5-4
5.2. Typical mixed H_2/H_∞ α versus γ curve	5-14
6.1. $j\omega$ -axis intercept	6-10
6.2. F-16 H_2 block diagram	6-15
6.3. F-16, H_2 controller, response to initial 5° angle of attack perturbation	6-17
6.4. F-16, H_2 controller, response to unit normal acceleration step . .	6-18

Figure	Page
6.5. F-16, H_2 controller, control usage for initial 5° angle of attack perturbation	6-18
6.6. F-16, H_2 controller, control usage for unit normal acceleration step	6-19
6.7. F-16, H_2 controller, open-loop GK	6-19
6.8. F-16 H_∞ block diagram	6-20
6.9. F-16, α versus γ	6-23
6.10. F-16, α versus γ , expanded	6-23
6.11. F-16, H_2/H_∞ , $n_c = 4$, closed-loop sensitivity	6-24
6.12. F-16, H_2/H_∞ , $n_c = 4$, closed-loop complementary sensitivity . . .	6-25
6.13. F-16, H_2/H_∞ , $n_c = 4$, open-loop GK	6-25
6.14. F-16, H_2/H_∞ , $n_c = 4$, response to a unit step in normal acceleration	6-26
6.15. F-16, H_2/H_∞ , $n_c = 4$, control usage for a unit step in normal acceleration	6-26
6.16. F-16, H_2/H_∞ , $n_c = 4$, response to a 5° initial angle of attack perturbation	6-27
6.17. F-16, H_2/H_∞ , $n_c = 4$, control usage for a 5° initial angle of attack perturbation	6-28
6.18. F-16, H_2/H_∞ , $n_c = 8$ and $n_c = 4$, response to a unit step in normal acceleration	6-29
6.19. F-16, H_2/H_∞ , $n_c = 8$, control usage for a unit step in normal acceleration	6-29
6.20. F-16, H_2/H_∞ , $n_c = 8$, closed-loop sensitivity	6-30
6.21. F-16, H_2/H_∞ , $n_c = 4$, open-loop GK, improved process noise . .	6-32
6.22. F-16, H_2/H_∞ , $n_c = 4$, closed-loop sensitivity, improved process noise	6-32
6.23. F-16, H_2/H_∞ , $n_c = 4$, response to a unit step in normal acceleration, improved process noise	6-33
7.1. Perturbed closed-loop system	7-2
7.2. Mixed H_2/μ problem	7-3

Figure	Page
7.3. Mixed H_2/μ boundary plot	7-4
7.4. Robust performance closed-loop system	7-6
7.5. μ block diagram	7-7
7.6. F-16, step response, 10th order μ controller	7-13
7.7. F-16, step response, 10th order H_2/μ controller	7-13
7.8. F-16, control usage for step response, 10th order μ controller	7-14
7.9. F-16, control usage for step response, 10th order H_2/μ controller	7-14
7.10. F-16, step response, 8th order μ controller	7-15
7.11. F-16, step response, 8th order H_2/μ controller	7-15
7.12. F-16, control usage for step response, 8th order μ controller	7-16
7.13. F-16, control usage for step response, 8th order H_2/μ controller	7-16
7.14. F-16, step response, 6th order μ controller	7-17
7.15. F-16, step response, 6th order H_2/μ controller	7-17
7.16. F-16, control usage for step response, 6th order μ controller	7-18
7.17. F-16, control usage for step response, 6th order H_2/μ controller	7-18
7.18. F-16, step response, 4th order H_2/μ controller	7-19
7.19. F-16, control usage for step response, 4th order H_2/μ controller	7-19
7.20. F-16, initial 5° angle of attack perturbation response	7-21
7.21. HIMAT system block diagram	7-22
7.22. HIMAT, H_2 controller-velocity response to initial 5° angle of attack perturbation	7-23
7.23. HIMAT, H_2 controller-angle of attack response to initial 5° angle of attack perturbation	7-24
7.24. HIMAT, H_2 controller-pitch rate response to initial 5° angle of at- tack perturbation	7-24
7.25. HIMAT, H_2 controller-pitch angle response to initial 5° angle of attack perturbation	7-25
7.26. HIMAT, H_2 controller-control usage for an initial 5° angle of attack perturbation	7-25

Figure	Page
7.27. HIMAT, H_2 controller—angle of attack response to angle of attack unit step input	7-26
7.28. HIMAT, H_2 controller—pitch angle response to angle of attack unit step input	7-26
7.29. HIMAT, H_2 controller—control usage for angle of attack unit step input	7-27
7.30. HIMAT, H_2 controller—angle of attack response to pitch angle unit step input	7-27
7.31. HIMAT, H_2 controller—pitch angle response to pitch angle unit step input	7-28
7.32. HIMAT, H_2 controller—control usage for pitch angle unit step input	7-28
7.33. HIMAT, μ controller—angle of attack response to angle of attack unit step input	7-30
7.34. HIMAT, μ controller—pitch angle response to angle of attack unit step input	7-31
7.35. HIMAT, μ controller—control usage for angle of attack unit step input	7-31
7.36. HIMAT, μ controller—angle of attack response to pitch angle unit step input	7-32
7.37. HIMAT, μ controller—pitch angle response to pitch angle unit step input	7-32
7.38. HIMAT, μ controller—control usage for pitch angle unit step input	7-33
7.39. HIMAT, H_2/μ , $n_c = 4$, angle of attack response to angle of attack unit step input	7-34
7.40. HIMAT, H_2/μ , $n_c = 4$, pitch angle response to angle of attack unit step input	7-35
7.41. HIMAT, H_2/μ , $n_c = 4$, control usage for angle of attack unit step input	7-35
7.42. HIMAT, H_2/μ , $n_c = 4$, angle of attack response to pitch angle unit step input	7-36
7.43. HIMAT, H_2/μ , $n_c = 4$, pitch angle response to pitch angle unit step input	7-36

Figure	Page
7.44. HIMAT, H_2/μ , $n_c = 4$, control usage for pitch angle unit step input	7-37
8.1. System with uncertainties	8-2
8.2. System with uncertainties "pulled out"	8-2
8.3. General mixed H_2/H_∞ optimization problem	8-5
8.4. J-Q parametrization of the mixed H_2/H_∞ problem	8-6
8.5. Admissible solution regions	8-7
8.6. $\ T_{zw}\ _2/\ T_{ed_1}\ _\infty/\ T_{ed_2}\ _\infty$ surface	8-8
8.7. Admissible solutions-Region IV	8-8
8.8. Admissible solutions-Region II	8-9
8.9. Admissible solutions-Region I	8-10
8.10. Typical surface generated by the grid method	8-23
8.11. F-16, $H_2/\ T_{ed_1}\ _\infty$ α versus γ_1 curve	8-27
8.12. F-16, $H_2/\ T_{ed_2}\ _\infty$ α versus γ_2 curve	8-28
8.13. F-16, $H_2/\ T_{ed_2}\ _\infty$ α versus γ_2 curve, expanded	8-28
8.14. F-16, constraint plane solution regions	8-29
8.15. F-16, $H_2/\ T_{ed_1}\ _\infty/\ T_{ed_2}\ _\infty$ surface	8-30
8.16. F-16, projection of the $H_2/\ T_{ed_1}\ _\infty/\ T_{ed_2}\ _\infty$ surface in the constraint plane	8-30
8.17. F-16, H_2/H_∞ and H_2/μ /multiple H_∞ controllers, response to unit normal acceleration step	8-31
9.1. General mixed H_2/L_1 optimization problem	9-2
9.2. General mixed $H_2/H_\infty/\mu/L_1$ optimization problem	9-6
A.1. F-16 model block diagram	A-2
B.1. HIMAT model block diagram	B-2

List of Tables

Table	Page
6.1. F-16 H_2/H_∞ Vector Margins	6-22
7.1. F-16 H_2/μ Optimization Results	7-11
7.2. F-16 H_2/μ Vector Margins	7-20
7.3. HIMAT H_2/μ Optimization Results	7-33

Abstract

H_2 optimization with convex constraints is considered. The optimal (order-free) solution is shown to be unique through convex analysis. H_∞ constraints with feedforward terms and singular constraints (those with no direct control usage penalty or perfect measurements and those with associated Hamiltonians that have $j\omega$ -axis zeros) are also allowed. The optimal fixed-order solution is shown to have the same characteristics as a mixed problem with regular H_∞ constraints. Furthermore, these results are shown to hold for controller orders as low as the optimal H_2 order. A numerical method is developed based on analytical gradients which results in sub- and super-optimal fixed-order controllers. The problem is extended to include an upper bound on a μ constraint through a modification of the D-K iteration method. Next, multiple H_∞ constraints are developed. Fixed-order solutions to the multiple constraint problem are characterized and the numerical method is extended to include multiple constraints. Next, a continuous L_1 constraint is added. A numerical approach is proposed based on bounding the L_1 -norm by the ℓ_1 -norm of an Euler approximating system. Finally, H_2 optimization with a finite set of H_∞ , μ , and L_1 constraints is characterized. SISO and MIMO numerical examples demonstrate the application of these methods.

H_2 OPTIMAL CONTROL WITH H_∞ , μ , AND L_1 CONSTRAINTS

I. Introduction

1.1 Overview

Controller design for a nonlinear system is often based on a linear, time-invariant model of the system as it operates near an operating point or nominal. While this approach simplifies the design process and allows powerful tools and techniques to be applied, there are distinct drawbacks to the method due to the imprecise modeling of a nonlinear system by a linear model. Moreover, the model is assumed to be time-invariant, and thus cannot account for changes in the system that are time-dependent. One can argue that the primary purpose of feedback control is to provide stability in light of any unmodeled dynamics and system perturbations. A second, but just as important, use of feedback control is to provide some desired level of system performance.

Due to the nature of the control problem, the design process is broken down into two categories, each of which has two parts. This first category is to provide nominal control—that is, to provide stability and performance for the nominal linear model. Consider the linear system in Figure 1.1 where $w(s)$ is an exogenous input and $z(s)$ is the output which we are trying to control (not necessarily realizable). The plant $P(s)$ is based on some underlying linear model $G(s)$ which transfers the control $u(s)$ to the measured output $y(s)$. $K(s)$ is a linear, time-invariant controller which has the measured output $y(s)$ as its input and the control $u(s)$ is its output. *Nominal stability* is achieved if the closed-loop system in Figure 1.1, where the feedback loop is closed with the controller $K(s)$, is asymptotically stable. If we only consider the underlying linear model with no input to the system ($P(s)=G(s)$, $z(s)=y(s)$), and

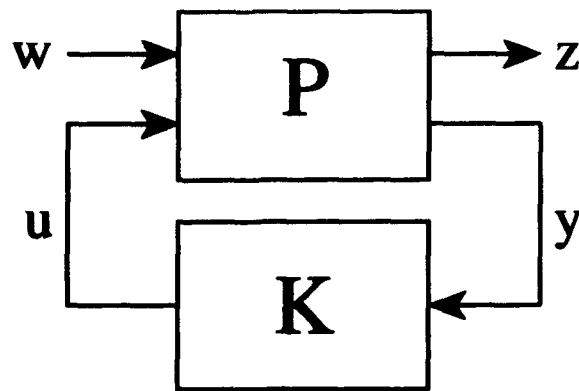


Figure 1.1. General nominal block diagram

$w(s)=0$), this requirement is met if the poles of $P(s)[I - P(s)K(s)]^{-1}$ lie in the open left-half complex-plane. A broader concept of internal stability will be explored later, but is equivalent for this closed-loop system.

For the *nominal performance* problem, $z(s)$ generally differs from $y(s)$ and $w(s)$ is not zero; thus, $P(s)$ is, in general, not equal to $G(s)$. It is assumed that $P(s)$ is known and $w(s)$ is some exogenous input with known properties such as white noise of fixed intensity or a deterministic signal with bounded energy. Some performance measure is defined and the nominal performance problem is to find a $K(s)$ which provides nominal stability and an acceptable level of the performance measure. If the performance problem can be expressed as a mathematical program over the set of possible controllers, the minimization or maximization problem is called an optimal control problem.

Robust control is the second category the designer must consider. In this problem, the systems under consideration are every element \mathcal{P}_i in the set $\mathcal{P} := P(s) + \Delta P$ where ΔP is a set of unknown perturbation to the nominal plant. The *robust stability* problem is to design a controller $K(s)$ which provides asymptotic stability for every \mathcal{P}_i . One way to consider this problem is to combine all the perturbations to the system into a single unstructured perturbation $\Delta(s)$, which has input $e(s)$ and output $d(s)$ which are outputs and inputs of $P(s)$, respectively. The resulting system

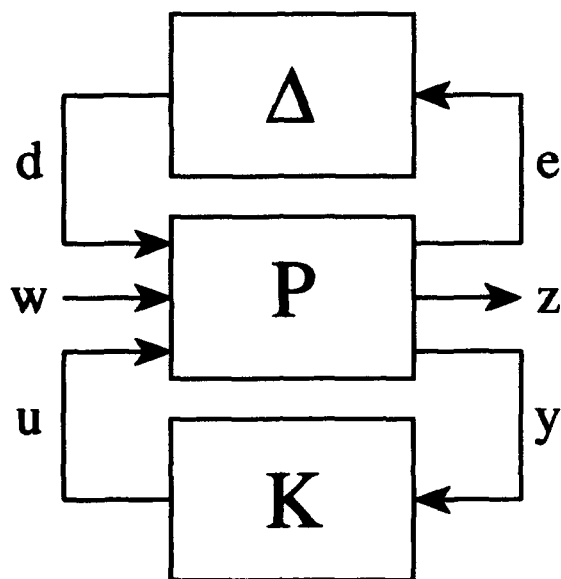


Figure 1.2. General perturbed block diagram

is shown in Figure 1.2. Then, robust stability requires $K(s)$ to internally stabilize the system for all possible $\Delta(s)$.

Finally, the feedback controller should provide some measure of *robust performance*—that is, produce a controller $K(s)$ which internally stabilizes the closed-loop system and provides an acceptable measure of performance under all expected plant perturbations. This problem is not as easy to handle as the previous problems, but μ -synthesis is generally acknowledged as the best approach to solving the robust performance problem [1, 2]. μ -synthesis is based on exploiting the known structure of the perturbation Δ and will be developed later in this work.

The performance of a system is often measured by the maximum energy of some controlled output due to some specified input. One example is the familiar linear quadratic Gaussian (LQG) control problem, where the exogenous input is zero-mean, white Gaussian noise of unit intensity. This problem is equivalent to minimizing the two-norm of the transfer function from the input to the output and is referred to as H_2 optimization. Another measure of performance is the model matching problem, where it is desired to minimize the energy of the controlled output resulting from

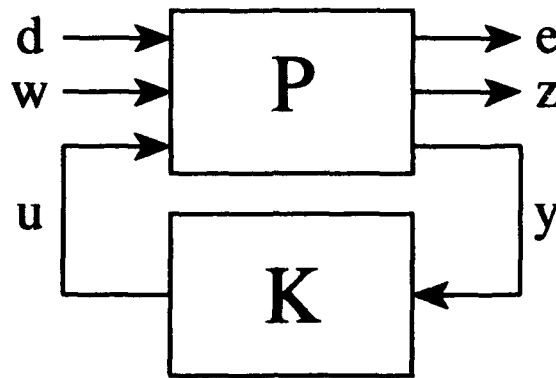


Figure 1.3. Mixed block diagram

some exogenous but bounded energy input. This is equivalent to minimizing the infinity-norm of the transfer function from the input to the output and is referred to as H_∞ optimization. An example of this problem is the weighted sensitivity problem, which will be discussed in detail later.

In general, it will be desirable to solve both the LQG and model matching problems concurrently for a given system, thus leading to a multi-objective or mixed optimal control problem. Consider the system in Figure 1.3, where the transfer function from w to z , T_{zw} , is associated with the LQG problem and the transfer function from d to e , T_{ed} , represents the model matching problem. The problem now is to find an internally stabilizing $K(s)$ which minimizes $\|T_{zw}\|_2$ for some level of model matching, $\|T_{ed}\|_\infty \leq \gamma$. This implies a potential trade-off exists between the two measures of performance. Furthermore, robustness has not yet been considered.

To add robust stability to the above problem, the Small Gain Theorem can be used. Define H_∞ as the space of all transfer functions which are analytic and bounded in the closed right-half complex-plane. Internal stability implies that all the states of the system are asymptotically stable (the concept of internal stability will be developed more in Chapter II). Then the following theorem gives us a condition for stability robustness.

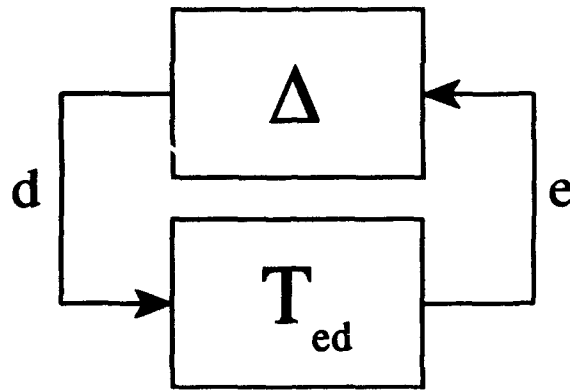


Figure 1.4. Perturbed stability diagram

Theorem 1.1.1 (Small Gain Theorem) *Let $T_{ed} \in H_\infty$. Assume $\Delta \in H_\infty$ is connected from e to d as shown in Figure 1.4. Then the closed-loop system is internally stable if*

$$\|T_{ed}(s)\Delta(s)\|_\infty \leq \|T_{ed}(s)\|_\infty \|\Delta(s)\|_\infty < 1 \quad (1.1)$$

Proof: See [3]. ■

Therefore, as $\|T_{ed}\|_\infty$ is decreased, a larger level of unstructured uncertainty can be allowed and internal stability still be guaranteed. Thus, robust stability can be incorporated into the mixed problem using an H_∞ constraint. However, this measure of robustness is conservative since it does not account for the structure of the perturbations and only provides information for the worst case frequency. Through μ -synthesis, a less conservative measure of robust stability can be added to the mixed problem by exploiting the structure and frequency content of the perturbation. Moreover, μ -synthesis can be used to add robust performance into the mixed problem. While H_∞ optimization and μ -synthesis provide powerful techniques for designing optimal controllers, both methods have limitations. In general, the methods tend to result in high bandwidth controllers and thus have increased high frequency noise response. A slight increase in the infinity-norm often results in a substantial

reduction in the high frequency response, which demonstrates an available trade-off which will be exploited in the mixed problem.

Finally, H_∞ and μ -synthesis are based on bounded energy inputs and outputs. It is often the case that the designer is interested in bounding the magnitude of a controlled output due to a worst case bounded magnitude input. This is particularly important when considering surface deflections and aircraft rotation rates where physical limitations are not modeled by the linear system. L_1 optimal control can handle this control problem. This technique minimizes the magnitude of the controlled output due to an exogenous but bounded magnitude input by minimizing the L_1 -norm of the resulting transfer function. Moreover, we can replace the infinity-norm in the above discussion with the one-norm, and the robustness properties hold. Thus, we desire a method of including L_1 constraints into the mixed optimization problem.

To solve the mixed control problem, the H_2 problem will be selected as the objective function. Throughout this dissertation, we will assume the H_2 problem has tractable solutions. To incorporate a desired level of robustness and/or nominal performance, an inequality constraint will be appended to the H_2 problem. Thus, the problem to be addressed in this dissertation is: Find an internally stabilizing $K(s)$ that achieves

$$\inf_{K(s) \text{ stabilizing}} \{ \|T_{zw}\|_2 \mid \|T_{ed}\|_\alpha \leq \gamma \} \quad (1.2)$$

where $\alpha = \{\infty, \mu, 1\}$ and γ is fixed *a priori* and is based on the desired level of robustness and/or nominal performance. This problem is a mathematical programming problem which can be approached using the rich theory which exists for optimization problems.

There has been a great deal of interest in the mixed H_2/H_∞ problem and variations on it with simplifying assumptions. This work will take the most general approach to date and remove some of the remaining simplifying assumptions. In

addition, the mixed framework will be extended to a more general multi-objective problem. First, a review of previous work is necessary to set the stage.

1.2 Review of Related Work

1.2.1 Mixed H_2/H_∞ with a single input or single output. The initial approaches to the mixed objective control problem were taken on a subset of the problem given in Figure 1.3, where it is assumed that either $d = w$ or $z = e$. Bernstein and Haddad [4] presented one of the earliest formulations of the problem with $d = w$. Their formulation used a Lagrange multiplier approach and resulted in necessary conditions for a fixed-order controller which provides an overbound to the H_2 problem and satisfies the H_∞ constraint. The controller order must be determined *a priori*. While this technique allows reduced order controllers which are desirable, it does not provide conditions for determining the order of the controller which is globally optimal. Zhou, *et al*, [5, 6] formed the mixed problem for two independent inputs with $e = z$. Their approach defined a new performance index which reduced to the H_2 performance index when $d \equiv 0$ and the H_∞ performance index when $w \equiv 0$. If both inputs are non-zero, a mixed performance index is obtained. Necessary and sufficient conditions for the existence of a mixed controller were derived and controllers were parametrized through a set of coupled matrix equations. Yeh, *et al* [7], showed that, when the order of the controller is fixed to that of the plant, the results of the above two works are the duals of each other.

1.2.2 General Mixed H_2/H_∞ optimization. Rotea and Khargonekar [8] presented the first attempt at solving the general problem shown in Figure 1.3, where no relationship is assumed between d and w or e and z . Their formulation was based on full state availability only. In addition, their approach was nonconservative in regards to optimizing the actual H_2 norm, rather than just providing an overbound to the norm. Ridgely, *et al* [9, 10], added output feedback into the formulation of the general mixed optimal control problem. They derived the necessary conditions

for an optimal fixed-order controller. The formulation assumed a strictly proper, regular H_∞ constraint. In addition, Ridgely, *et al*, developed a numerical solution which requires unique solutions to Lyapunov equations and stabilizing solutions to Riccati equations. A homotopy method was used between the central H_∞ problem [11] and the optimal mixed problem. The method was shown to converge to the optimal mixed problem.

The above approaches are based on a single H_2 and a single H_∞ transfer function. Schömig, *et al*, [12] developed a time domain approach for solving the mixed problem with multiple transfer functions. The approach combined the optimal H_2 problem with a penalty function, which incorporates the H_∞ constraint. A fixed-order controller and a finite final time were used. The resulting controller approaches a controller which infimizes a linear combination of H_2 performance bounds while satisfying a set of H_∞ constraints as the final time approaches infinity. However, there was no attempt to characterize the optimal controller or provide conditions for its existence.

All of the above works based their results on a fixed-order controller with order equal to the plant order.

1.2.3 Mixed H_2/μ optimization. Madiwale [13] first proposed adding robustness to the mixed control problem. His approach was based on the work of Bernstein and Haddad [4], and thus only provides an overbound to the H_2 portion. However, his development does attempt to provide robustness to both the H_2 and H_∞ performance. Bambang, *et al*, [14] presented a static state feedback solution to the mixed H_2/μ problem based on the work of Rotea and Khargonekar [15]. Both of these approaches only address a subproblem due the restrictive assumptions on the inputs, outputs, and controller.

Hall and How [16] used a dissipative system approach to develop a worst case bound on H_2 robust performance for a system with uncertainty. Their work gener-

alizes a measure of robust performance to the H_2 framework. However, it does not address a mixed norm approach to the optimization.

1.3 Research Objectives and Contributions

The purpose of this research is to first explore the nature of the optimal solution to the mixed H_2/H_∞ optimal control problem. Next, the set of problems which can be handled by the mixed H_2/H_∞ optimal control problem will be extended beyond the set discussed in the previous section. Furthermore, formal incorporation of multiple H_∞ constraints and μ into the general framework will be accomplished. A general numerical approach for fixed-order controllers will be developed. Finally, the H_2 problem with a finite set of convex constraints, including H_∞ , μ , and L_1 , will be examined.

The first contribution of this dissertation will be to characterize the optimal controller for a mixed H_2/H_∞ optimization problem where the controller order is not assumed *a priori* but allowed to be free. It will be shown that the optimal solution is unique by approaching the problem through convex programming. Moreover, necessary conditions for optimality will be derived. Next, a dual approach to computing the optimal controller will show that the optimal controller for a class of mixed H_2/H_∞ problems is a non-rational H_2 function. Furthermore, this method will be used to develop an analytical method for determining the minimum two-norm for a fixed γ for a class of mixed H_2/H_∞ problem.

The second contribution of this work is to extend the set of H_∞ constraints which can be handled by the fixed-order mixed problem. As discussed in Section 1.2, previous methods for solving the fixed order H_2/H_∞ problem have been based on the assumptions that the H_∞ constraint is non-singular and strictly proper. However, it is often desirable to allow both singular and non-strictly proper constraints. A common example of this is the weighted sensitivity problem, which is singular and can also be non-strictly proper. Thus, the set of allowable H_∞ constraints will be

expanded to include singular constraints as well as non-strictly proper ones. Furthermore, for practical applications, the order of the controller must be as low as possible. Previous approaches to the general mixed problem have assumed the controller order is equal to or greater than the order of the plant augmented with both the H_2 and H_∞ weighting transfer functions. It will be shown that the conditions developed for a fixed-order solution in this work hold for a controller order as low as the order of the H_2 problem alone.

Next, a numerical approach for finding fixed-order controllers in the neighborhood of the optimal fixed-order controller will be developed. This approach has the advantage (over previous methods) of handling singular H_∞ constraints and those with a feedforward term. Furthermore, the order of the solutions can be reduced to greater than or equal to that of the H_2 problem. Finally, the computation time for the new method is significantly reduced from that of the existing method.

The fourth contribution of this work is to extend the method to include incorporate μ -synthesis into the framework. This will allow a less conservative measure of robust stability and also allow robust performance to be included in the mixed framework.

The next contribution is to extend the above results to mixed problems with multiple H_∞ constraints. The uniqueness of the optimal controller is shown and necessary conditions for order-free and fixed-order solutions will be developed. Furthermore, numerical approaches for finding solutions to the multiple constraint problem are given.

The last contribution will show that any finite set of convex constraints can be augmented to the H_2 optimization problem in the framework developed in this dissertation. First, the H_2/L_1 problem will be set up and a numerical approach for designing fixed-order controllers will be given. This allows the mixed approach to be applied to bounded magnitude outputs. Finally, the framework will be expanded to allow H_2 problems with a finite set of H_∞ , μ , and l_1 constraints. It will be

shown that all these constraints can be augmented and the problem solved in an analogous manner to the multiple H_∞ constraint problem. Thus, all the design methodologies discussed in this work can be combined into a single problem allowing the design engineer a wide latitude in setting up competing objectives for synthesizing a controller which provides nominal and robust stability and performance.

1.4 Outline

This dissertation consists of 10 chapters including this introduction. Chapter 2 will present some necessary mathematical review, including a discussion of linear vector spaces, Lyapunov and Riccati equations, convex programming, and minimum norm duality theory. Next, Chapter 3 will review H_2 and H_∞ optimization techniques and present an introduction to μ -synthesis.

Chapter 4 will develop the key theoretical results for mixed H_2/H_∞ optimization. To begin, the set of all stabilizing controllers will be parametrized over a convex set. Then, the uniqueness of the optimal controller will be shown through convex analysis. Furthermore, a duality approach to the minimum norm problem will be developed to characterize the optimal controller. This development will solve a special case of the optimal problem with a particular form of the H_∞ constraint.

Fixed-order solutions to the mixed problem will be addressed in Chapter 5. A Lagrange multiplier approach will be taken by appending a Lyapunov equation associated with the H_2 problem and a Riccati equation associated with the H_∞ constraint. This development will allow singular and non-strictly proper H_∞ constraints, and can handle controllers with order fixed to greater than or equal to the H_2 problem. Chapter 6 will develop a numerical method based in the frequency domain which computes fixed-order controllers in the neighborhood of the optimal. The resulting algorithm will be demonstrated through the design of a single input/single output (SISO) F-16 longitudinal controller.

Robust performance will be added into the framework in Chapter 7 by incorporating μ -synthesis into the mixed H_2/H_∞ optimal control problem. The fixed-order controller will be characterized and the trade-off between robustness and disturbance rejection will be demonstrated through an F-16 normal acceleration control problem and a multiple input/multiple output (MIMO) HIMAT pitch control design example.

The utility of the mixed problem will be further increased in Chapter 8 by including multiple H_∞ constraints. First, the uniqueness of the optimal controller will be addressed and the question of existence will be discussed. Next, the fixed-order solution will be developed and the nature of fixed-order controllers with order greater than or equal to the H_2 problem will be characterized. The numerical approach from Chapter 6 will be modified to handle multiple constraints, and methods for finding controllers will be developed. Finally, an F-16 normal acceleration example will be used to demonstrate the power of the multiple constraint optimization.

In Chapter 9, an approach to H_2/L_1 problems will be developed. Suggestions on how to extend this work to include H_2 optimization with any combination of H_∞ , μ , and L_1 constraints will be discussed. Finally, Chapter 10 presents some conclusions and recommendations.

II. Mathematical Preliminaries

2.1 State Space and Transfer Functions

This section will consider linear, time-invariant systems in continuous state space form

$$\begin{aligned}\dot{x}(t) &= Ax(t) + Bw(t) \\ z(t) &= Cx(t) + Dw(t)\end{aligned}\tag{2.1}$$

or in discrete state space form

$$\begin{aligned}x(k+1) &= A_d x(k) + B_d w(k) \\ z(k) &= C_d x(k) + D_d w(k)\end{aligned}\tag{2.2}$$

where $A, A_d \in \mathfrak{R}^{n \times n}$, $B, B_d \in \mathfrak{R}^{n \times m}$, $C, C_d \in \mathfrak{R}^{p \times n}$, and $D, D_d \in \mathfrak{R}^{p \times m}$ are constant matrices. The vectors $x \in \mathfrak{R}^n$, $w \in \mathfrak{R}^m$, and $z \in \mathfrak{R}^p$ are the state, control, and output vectors, respectively. $[\cdot](t)$ represents functions of time for $t \in [0, +\infty)$, $[\cdot](k)$ represents sequences with index $k \in \{0, 1, 2, \dots\}$, and $\dot{[\cdot]}$ represents the time derivative of $[\cdot]$.

The stability of systems (2.1) and (2.2) is determined by the eigenvalues of A or A_d . For the continuous case, the system is *stable* if all the eigenvalues of A are in the open left-half complex plane; the system is *neutrally stable* if the eigenvalues are in the closed left-half complex plane and at least one eigenvalue is on the imaginary axis; and the system is *unstable* otherwise. For the discrete case, the system is *stable* if all the eigenvalues of A_d are in the open unit disk centered at the origin; the system is *neutrally stable* if the eigenvalues are in the closed unit disk and at least one eigenvalue is on the unit circle; and the system is *unstable* otherwise.

The state space forms can be realized as input-output *transfer functions* in the *s-domain* for the continuous case through the Laplace transform

$$T_{zw}(s) := C(sI - A)^{-1}B + D\tag{2.3}$$

and in the z -domain for the discrete case through the z transform

$$T_{zw}(z) := C_d(zI - A_d)^{-1} B_d + D_d \quad (2.4)$$

For the remainder of this section, only the continuous case will be considered; similar results can be derived for the discrete case. The shorthand notation

$$\left[\begin{array}{c|c} A & B \\ \hline C & D \end{array} \right] := C(sI - A)^{-1} B + D \quad (2.5)$$

will be used. Conversely, for any real-rational, *proper* (i. e., analytical at $s = \infty$) transfer function T_{zw} there exists a *realization* (non-unique) (A, B, C, D) such that

$$T_{zw} = \left[\begin{array}{c|c} A & B \\ \hline C & D \end{array} \right] \quad (2.6)$$

The realization is *minimal* if A is of smallest possible dimension. A realization is minimal if and only if (A, B) is *controllable* and (C, A) is *observable*.

The following definitions and properties will be useful:

$$T_{zw}^T(s) := \left[\begin{array}{c|c} A^T & C^T \\ \hline B^T & D^T \end{array} \right] \quad (2.7)$$

$$T_{zw}(-s) := \left[\begin{array}{c|c} -A & B \\ \hline -C & D \end{array} \right] \quad (2.8)$$

Further, the *conjugate* of T_{zw} is defined by

$$T_{zw}^*(s) := T_{zw}^T(-s) = \left[\begin{array}{c|c} -A^T & -C^T \\ \hline B^T & D^T \end{array} \right] \quad (2.9)$$

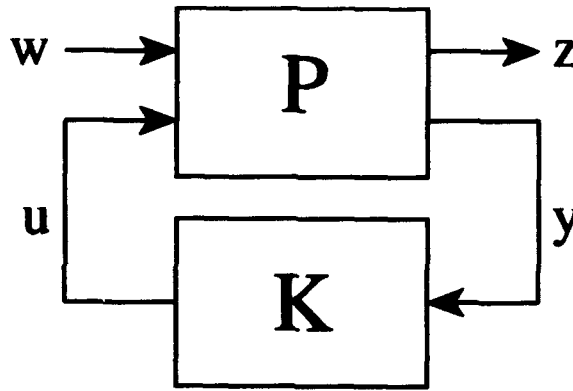


Figure 2.1. Nominal feedback system

and

$$\text{poles } [T_{zw}(s)] = \text{poles } [T_{zw}^T(s)] = -\text{poles } [T_{zw}(-s)] = -\text{poles } [T_{zw}^*(s)] \quad (2.10)$$

For $T_{zw} \in C^{p \times m}$, let $l = \min\{m, p\}$. The *singular values* σ_i , $i = 1, \dots, l$, satisfy

$$\sigma_i [T_{zw}(s)] = \sigma_i [T_{zw}^T(s)] = \sigma_i [T_{zw}(-s)] = \sigma_i [T_{zw}^*(s)] \quad (2.11)$$

To complete this section, consider the nominal feedback system given in Figure 2.1. Let $P(s)$ and $K(s)$ be known proper transfer functions matrices; then Figure 2.1 represents

$$\begin{bmatrix} z \\ y \end{bmatrix} = P \begin{bmatrix} w \\ u \end{bmatrix} \quad u = Ky \quad (2.12)$$

where P can be partitioned as

$$P = \begin{bmatrix} P_{zw} & P_{zu} \\ P_{yw} & P_{yu} \end{bmatrix} \quad (2.13)$$

To simplify notation, it will be assumed that transfer functions and signals are functions-of- s for the remainder of this dissertation unless otherwise stated. If P and

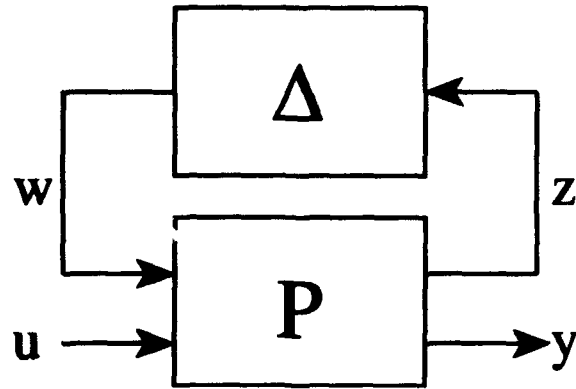


Figure 2.2. Perturbed system

K are minimal order, then the *closed-loop transfer function* T_{zw} can be determined from the *lower fractional transformation* (LFT) as

$$T_{zw} = F_l(P, K) := P_{zw} + P_{zu}K(I - P_{yu}K)^{-1}P_{yw} \quad (2.14)$$

Similarly, an *upper fractional transformation* (UFT) is defined for some block Δ with input z and output w shown in Figure 2.2 as

$$T_{yw} = F_u(P, \Delta) := P_{yu} + P_{yw}\Delta(I - P_{zw}\Delta)^{-1}P_{zu} \quad (2.15)$$

The system in Figure 2.1 is said to be *well posed* if and only if $(I - P_{yu}K)$ is invertible. If P_{yu} or K is *strictly proper* (i. e., $P_{yu}(\infty) = 0$ or $K(\infty) = 0$), as will be assumed in this work, then the system is well posed.

The system in Figure 2.1 can be written in state space form as

$$P = \left[\begin{array}{c|cc} A & B_w & B_u \\ \hline C_z & D_{zw} & D_{zu} \\ C_y & D_{yw} & D_{yu} \end{array} \right] \quad K = \left[\begin{array}{c|c} A_c & B_c \\ \hline C_c & D_c \end{array} \right] \quad (2.16)$$

The well posedness of the system can now be seen as $(I - D_c D_{yu})$ being invertible. Furthermore, the closed-loop transfer function T_{zw} can be written in state space form as

$$T_{zw} = \left[\begin{array}{c|c} A & B \\ \hline C & D \end{array} \right] \quad (2.17)$$

where

$$A = \left[\begin{array}{cc} A + B_u(I - D_c D_{yu})^{-1} D_c C_y & B_u(I - D_c D_{yu})^{-1} C_c \\ B_c(I - D_{yu} D_c)^{-1} C_y & A + B_c(I - D_{yu} D_c)^{-1} D_{yu} C_c \end{array} \right] \quad (2.18)$$

$$B = \left[\begin{array}{c} B_w + B_u(I - D_c D_{yu})^{-1} D_c D_{yw} \\ B_c(I - D_{yu} D_c)^{-1} D_{yw} \end{array} \right] \quad (2.19)$$

$$C = \left[C_z + D_{zu} D_c(I - D_{yu} D_c)^{-1} C_y \quad D_{zu}(I - D_c D_{yu})^{-1} C_c \right] \quad (2.20)$$

$$D = \left[D_{zw} + D_{zu} D_c(I - D_{yu} D_c)^{-1} D_{yw} \right] \quad (2.21)$$

Thus, given a realization of the open-loop system and the feedback controller, we can always determine the resulting closed-loop transfer function.

2.2 Stability Theory

This section will examine the stability of open- and closed-loop systems and give some useful theorems relating to internal stability. The open-loop system (2.1) is said to be *stable* if the A matrix is stable. Similarly, the closed-loop system is said to be *internally stable* if the closed-loop A matrix defined by (2.18) is stable. The following theorems give some conditions for internal stability.

Theorem 2.2.1 *Assume the realization of P in (2.16) is minimal. Then there exists a proper K which achieves internal stability for the system in Figure 2.1 iff (A, B_u) is stabilizable and (C_y, A) is detectable.*

Proof: See [17], Chapter 4. ■

A controller K which achieves internal stability is said to be a *stabilizing controller*. If such a K exists, then P is said to be *stabilizable*.

Theorem 2.2.2 K is a stabilizing controller for P iff K is a stabilizing controller for P_{yu} .

Proof: See [17], Theorem 4.2. ■

Thus, from Theorem 2.2.2, only P_{yu} must be considered for analyzing the internal stability of a system. Internal stability can now be viewed as bounded input-bounded output stability for the system shown in Figure 2.3 where the input is $[v_1^T \ v_2^T]^T$, and the output is $[e_1^T \ e_2^T]^T$. The system in Figure 2.1 is internally stable if and only if the system in Figure 2.3 is internally stable. Finally, the internal stability of the system in Figure 2.3 is given by the following theorem.

Theorem 2.2.3 The system in Figure 2.3 is internally stable iff $(I - P_{yu}K)$ is invertible and all four transfer functions in

$$\begin{bmatrix} I & -K \\ -P_{yu} & I \end{bmatrix} = \begin{bmatrix} I + K(I - P_{yu}K)^{-1}P_{yu} & K(I - P_{yu}K)^{-1} \\ (I - P_{yu}K)^{-1}P_{yu} & (I - P_{yu}K)^{-1} \end{bmatrix} \quad (2.22)$$

which transfers the input $[v_1^T \ v_2^T]^T$ to $[e_1^T \ e_2^T]^T$, are proper and stable.

Proof: See [17], Chapter 4. ■

2.3 Operator Spaces

The transfer functions in this work can be treated as elements of operator (vector) spaces. In particular, we will consider members of the Hardy spaces H_2 and H_∞ , the function space L_1 , and the sequence space ℓ_1 . The functions in these spaces are representations of the actual operators, but we shall abuse the notation and refer to the functions as operators in this work. For further information on operators and their representations, the reader is referred to [18]. This section will define these

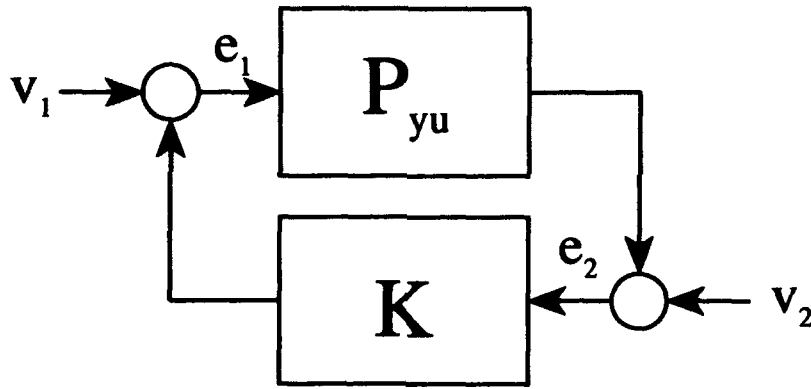


Figure 2.3. Internal stability system

spaces, the associated norms, and methods for computing the norms. First we need to define the following Lebesgue spaces. $L_2(-j\infty, +j\infty)$ is defined as the space of all functions $F(s)$ which are analytic on the imaginary axis and

$$\left[\int_{-\infty}^{+\infty} F^*(j\omega)F(j\omega)d\omega \right]^{\frac{1}{2}} < +\infty \quad (2.23)$$

$L_\infty(-j\infty, +j\infty)$ is defined as the space of all functions $F(s)$ which are analytic on the imaginary axis and

$$\text{ess sup}_{\omega \in \mathbb{R}} \bar{\sigma}[F(j\omega)] < +\infty \quad (2.24)$$

where $\bar{\sigma}(\cdot)$ denotes the maximum singular value.

2.3.1 H_2 Space. H_2 is defined as the space of all transfer function matrices which are analytic in the open right-half complex plane and have a bounded two-norm, where

$$\|T_{zw}\|_2^2 := \frac{1}{2\pi} \int_{-\infty}^{+\infty} \text{tr} [T_{zw}^*(j\omega)T_{zw}(j\omega)] d\omega \quad (2.25)$$

Furthermore, we shall define the subspace \mathfrak{RH}_2 as the space of *real-rational* functions (rational functions with real coefficients) in H_2 . H_2 is a closed subspace of the *Hilbert space* (or complete inner product space) L_2 .

Unfortunately, (2.25) is not easy to compute, but there is a fairly standard method for finding the two-norm of a transfer function (see, for example, [19]). Consider the transfer function

$$G(s) = \left[\begin{array}{c|c} A & B \\ \hline C & 0 \end{array} \right] \in \mathfrak{RH}_2 \quad (2.26)$$

Then the two-norm is given by

$$\|G(s)\|_2^2 = \text{tr} (L_c C^T C) = \text{tr} (L_o B B^T) \quad (2.27)$$

where L_c and L_o are the *controllability* and *observability gramians* of $G(s)$, respectively. The gramians are the positive semidefinite solutions to the *Lyapunov equations*

$$A L_c + L_c A^T + B B^T = 0 \quad (2.28)$$

$$L_o A + A^T L_o + C^T C = 0 \quad (2.29)$$

If $G(s) \in \mathfrak{RL}_2 := \mathfrak{RH}_2 \oplus \mathfrak{RH}_2^\perp$, then the transfer function $G(s)$ can be written as

$$G(s) = G_1(s) + G_2(s) \quad (2.30)$$

where $G_1(s) \in \mathfrak{RH}_2$ and $G_2(s) \in \mathfrak{RH}_2^\perp$. Since the inner product $\langle G_1, G_2 \rangle = 0$,

$$\|G(s)\|_2^2 = \|G_1(s)\|_2^2 + \|G_2(s)\|_2^2 \quad (2.31)$$

The two-norm of $G_2(s)$ is

$$\|G_2\|_2 = \|G_2^*(s)\|_2 \quad (2.32)$$

where $G_2^*(s) \in \mathfrak{RH}_2$ and its two-norm can be computed using (2.27).

2.3.2 H_∞ Space. The next space of operators which will be discussed is H_∞ . H_∞ is defined as the space of transfer function matrices which are analytic and bounded in the open right-half complex plane. Again, the subspace of real-rational H_∞ functions will be denoted as $\Re H_\infty$. H_∞ is a closed subspace of the *Banach space* (or complete normed linear space) L_∞ . Furthermore, H_∞ is the space of bounded operators which map $L_2(0, +\infty)$ into $L_2(0, +\infty)$; thus the norm of interest is the induced operator norm

$$\|T_{zw}\| := \|T_{zw}\|_\infty \quad (2.33)$$

$$= \sup_{w \neq 0} \frac{\|T_{zw}w\|_2}{\|w\|_2} \quad (2.34)$$

$$= \sup_{\|w\|_2 \leq 1} \|z\|_2 \quad (2.35)$$

$$= \sup_{\omega} \bar{\sigma}[T_{zw}(j\omega)] \quad (2.36)$$

This norm will be referred to as the *infinity-norm*. The infinity-norm can be seen to be the maximum possible gain of the system; thus, to minimize the energy of the output due to a unknown but deterministic bounded energy input, one must minimize the infinity-norm of the transfer function. Another important property of the infinity-norm is the submultiplicative property of induced operator norms [18]; given $F, G \in H_\infty$ then

$$\|FG\|_\infty \leq \|F\|_\infty \|G\|_\infty \quad (2.37)$$

This property, which does not hold for two-norms, is very important for robustness problems, as was seen in Theorem 1.1.1.

The infinity-norm can be determined by computing the maximum singular value of the transfer function over a sufficiently large range of frequencies and selecting the maximum value. However, this is not always numerically practical since some *a priori* knowledge of the maximum singular value behavior over frequency is

needed. Another more precise approach is based on the eigenstructure of a Hamiltonian matrix associated with a state space realization of a proper stable transfer function [17]. Consider the transfer function

$$G(s) = \left[\begin{array}{c|c} A & B \\ \hline C & D \end{array} \right] \quad (2.38)$$

Then the associated *Hamiltonian* is

$$H = \left[\begin{array}{cc} A + BR^{-1}D^T C & BR^{-1}B^T \\ -C^T(I + DD^T)^{-1}C & -(A + BR^{-1}D^T C)^T \end{array} \right] \quad (2.39)$$

where $R := \gamma^2 I - D^T D$. The infinity-norm of the transfer function is the smallest γ such that the eigenvalues of H on the imaginary axis (if any) have even partial multiplicities. Effectively, this reduces to finding the smallest γ such that H has no eigenvalues on the imaginary axis. In Chapter VI, a refined method for computing the infinity-norm will be developed.

2.3.3 L_1 and ℓ_1 Spaces. The final spaces discussed in this work are the L_1 function space and the ℓ_1 sequence space. As with the H_2 - and H_∞ -norms, the L_1 -norm will be developed for continuous-time systems; however, the ℓ_1 -norm will be developed in discrete-time. Furthermore, we will only discuss scalar transfer functions (SISO) in this section.

2.3.3.1 L_1 Space. Let $L_1(0, +\infty)$ denote the space of all causal functions $g(t)$ such that

$$\|g\|_1 = \int_0^{+\infty} |g(t)| dt < +\infty \quad (2.40)$$

For convenience, we will denote the space as L_1 . Associated with each $g(t) \in L_1$ there is a Laplace transform $\mathcal{G}(s)$, where

$$\mathcal{G}(s) := \int_0^{+\infty} g(t)e^{-st} dt \quad (2.41)$$

Let $\hat{\mathcal{A}}$ denote the space of all bounded linear operators on L_1 . Given $\mathcal{G} \in \hat{\mathcal{A}}$, the induced norm on $\hat{\mathcal{A}}$ is given by

$$\|\mathcal{G}\|_{\hat{\mathcal{A}}} := \sup_{r \neq 0} \frac{\|\mathcal{G}r\|_{\infty}}{\|r\|_{\infty}} \quad (2.42)$$

$$= \|g\|_1 \quad (2.43)$$

$$= \int_0^{+\infty} |g(t)| dt \quad (2.44)$$

where $r \in L_{\infty}(0, +\infty)$.

Since this is an induced operator norm, the submultiplicative property holds and the norm can be used for robustness analysis. Computation of the L_1 -norm is not as convenient as the previous norms. Since we will only consider stable systems, the impulse response will be bounded below by some epsilon after a fixed time. Therefore, an approximation of the L_1 -norm can be made through a truncated approximation of the integral (2.44).

2.3.3.2 ℓ_1 Space. Let ℓ_1 denote the space of all sequences $h = \{h(k)\}$ such that

$$\|h\|_1 = \sum_{k=0}^{+\infty} |h(k)| < +\infty \quad (2.45)$$

Given a sequence $h \in \ell_1$ we can define the z-transform

$$\mathcal{H}(\zeta) := \sum_{k=0}^{\infty} h(k)\zeta^k \quad (2.46)$$

If \mathcal{H} is the z-transform of the pulse response h of a linear system, then \mathcal{H} is stable if and only if $h \in \ell_1$ [20]. Let ℓ_∞ denote the space of all bounded sequences $f = \{f(k)\}$ with a norm defined by

$$\|f\|_\infty = \max_k |f(k)| \quad (2.47)$$

Define $\tilde{\mathcal{A}}$ as the space of all stable functions and let $\mathcal{H} \in \tilde{\mathcal{A}}$ be a particular function which maps $r \in \ell_\infty$ to $m \in \ell_\infty$. Then $h \in \ell_1$ is the pulse response associated with \mathcal{H} . The induced operator norm of \mathcal{H} on $\tilde{\mathcal{A}}$ is given by

$$\|\mathcal{H}\|_{\tilde{\mathcal{A}}} := \sum_{k=1}^{+\infty} |h(k)| \quad (2.48)$$

Thus,

$$\|\mathcal{H}\|_{\tilde{\mathcal{A}}} = \|h\|_1 \quad (2.49)$$

If r is an unknown but deterministic bounded magnitude input, and it is desired to minimize the worst case maximum magnitude of the output m , then the ℓ_1 -norm of the pulse response function should be minimized. For convenience, the induced norm on $\tilde{\mathcal{A}}$ will be referred to as the ℓ_1 -norm of the transfer function. The ℓ_1 -norm is an induced norm; therefore, the submultiplicative property holds and the norm can be used for robustness analysis.

For the SISO case, the ℓ_1 -norm can be approximated to an *a priori* tolerance ϵ through the sum of a truncated series [21]. Let h be a finite dimensional linear, time-invariant system, and let \mathcal{H} be the z-transform of h with a minimal realization

$$\mathcal{H}(z) = \left[\begin{array}{c|c} A_d & B_d \\ \hline C_d & D_d \end{array} \right] \quad (2.50)$$

The ℓ_1 -norm of h is given by

$$\|h\|_1 = \sum_{k=0}^{+\infty} |h(k)| \quad (2.51)$$

This sum can be rewritten in state space form as

$$\|h\|_1 = \sum_{k=0}^{+\infty} |C_d A_d^k B_d| + |D_d| \quad (2.52)$$

If h is stable, A_d^k approaches zero as k approaches infinity; thus, (2.52) can be approximated by truncating at some integer N . Suppose A_d has distinct roots a_1, a_2, \dots, a_n . These a_i are the poles of the z -transform $\mathcal{H}(z)$ of h , and since h is stable, $|a_i| < 1$ for $i = 1, \dots, n$. Therefore,

$$\mathcal{H}(z) = \sum_{i=1}^n \frac{b_i}{z - a_i} + d = C_d(zI - A_d)^{-1}B_d + D_d \quad (2.53)$$

where

$$b_i = (z - a_i)G(z)|_{z=a_i} \quad (2.54)$$

Let $a_{max} = \max_i |a_i|$ and $b_{max} = \max_i |b_i|$. Given some $\epsilon > 0$, whenever N is such that

$$a_{max}^{N+1} < \frac{\epsilon(1 - a_{max})}{nb_{max}} \quad (2.55)$$

then

$$\sum_{k=0}^N |C_d A_d^k B_d| + |D_d| \leq \|G\|_1 \leq \sum_{k=0}^N |C_d A_d^k B_d| + |D_d| + \epsilon \quad (2.56)$$

Therefore, for the SISO case, the ℓ_1 -norm can be approximated to any desired accuracy.

2.3.3.3 Relationship Between L_1 and ℓ_1 . For a particular transformation from the continuous domain to the discrete domain, an asymptotic relationship between the L_1 -norm and the ℓ_1 -norm can be derived. The transformation is known as a forward rule, which results from substituting

$$s = \frac{z-1}{\tau} \quad (2.57)$$

where τ is the discrete time step. Thus, given a continuous system

$$T_{mr}(s) = \left[\begin{array}{c|c} A & B \\ \hline C & D \end{array} \right] \quad (2.58)$$

then the transformed system is

$$T_{mr}^{EAS}(z) := \left[\begin{array}{c|c} A_E & B_E \\ \hline C_E & D_E \end{array} \right] = \left[\begin{array}{c|c} I + \tau A & \tau B \\ \hline C & D \end{array} \right] \quad (2.59)$$

The system in (2.59) will be referred to as an Euler approximating system (EAS) for the continuous system [22].

Now the relationship between continuous and discrete one-norms is given by the following theorems.

Theorem 2.3.1 *Assume the continuous system*

$$\dot{x} = Ax + Br \quad (2.60)$$

$$m = Cx + Dr \quad (2.61)$$

is stable. Then, given $\tau > 0$, the EAS system

$$x_{k+1} = (I + \tau A)x_k + \tau Br_k \quad (2.62)$$

$$m_k = Cx_k + Dr_k \quad (2.63)$$

is stable, and

$$\|T_{mr}\|_1 \leq \|T_{mr}^{EAS}\|_1 \quad (2.64)$$

Furthermore, $\|T_{mr}^{EAS}\|_1 \rightarrow \|T_{mr}\|_1$ monotonically as $\tau \rightarrow 0$.

Proof: See [22], Theorems 2 and 3. ■

Thus, using the EAS transformation, the ℓ_1 -norm will always provide an upper bound on the L_1 -norm for a given system.

2.4 Lyapunov Equations

As was already seen in the computation of the two-norm, equations of the form

$$A^T X + X A + Z = 0 \quad (2.65)$$

play an integral part in modern control theory. This type of equation is known as a *Lyapunov equation*. This section will present some key theorems on existence and uniqueness of solutions to Lyapunov equations. First, a theorem on uniqueness is presented.

Theorem 2.4.1 *If $Z \geq 0$ and A is stable, the Lyapunov equation (2.65) has a unique solution and $X \geq 0$.*

Proof: See [23], Lemma 12.1 ■

The existence of solutions to (2.65) is related to the stability of A through the following.

Theorem 2.4.2 *Suppose $X \geq 0$, $Z \geq 0$, (\sqrt{Z}, A) is detectable and (2.65) holds. Then A is stable. If (\sqrt{Z}, A) is observable, then $X > 0$.*

Proof: See [23], Lemma 12.2 ■

Theorem 2.4.3 *The Lyapunov equation (2.65) has a unique solution iff A is stable. If A is stable, then $X = 0$ is the unique solution to*

$$A^T X + X A = 0 \quad (2.66)$$

Proof: See [24], Theorem 2.1. ■

2.5 Riccati Equations

Two forms of the algebraic Riccati equation (ARE) which are associated with H_2 and H_∞ optimization will be used in this dissertation. This section will present some existence and uniqueness conditions for solutions to both types of Riccati equations.

2.5.1 H_2 Type. The algebraic Riccati equation associated with the H_2 problem is

$$A^T X + XA - XBR^{-1}B^T X + C^T C = 0 \quad (2.67)$$

where $R = R^T \geq 0$. Given a minimal realization $(A, B, C, 0)$, the following theorem characterizes the solution to (2.67).

Theorem 2.5.1 *Assume (A, B) controllable and (C, A) observable. Then there exists a real symmetric solution X to (2.67) with the property $\Re [\lambda_i(A - BR^{-1}B^T X)] < 0$ (> 0) for all i . Moreover, it is unique and such that $X > 0$ (< 0). Furthermore, it is the only solution in the set of all positive (negative) semidefinite matrices.*

Proof: See [25], Lemma 4. ■

The controllability and observability conditions can be relaxed with the following results.

Theorem 2.5.2 *Assume (A, B) is stabilizable. If (2.67) has a real symmetric solution, then it has a maximal solution X_+ such that $X_+ \geq X$ for all X satisfying (2.67). Moreover, $\Re [\lambda_i(A - BR^{-1}B^T X_+)] \leq 0$ for all i .*

Proof: See [26], Theorem 2.1. ■

Theorem 2.5.3 *Assume (A, B) is stabilizable. Then the real symmetric solution to (2.67) exists and its maximal solution is positive semidefinite. If (C, A) is detectable, then $\Re [\lambda_i(A - BR^{-1}B^T X_+)] < 0$ for all i , and if (C, A) is observable, then $X_+ > 0$.*

Proof: See [26], Theorem 2.2. ■

These results hold for the dual of (2.67)

$$AX + XA^T - XC^T R^{-1} CX + BB^T = 0 \quad (2.68)$$

with the following substitutions: $A = A^T$, $B = C^T$, and $C = B^T$, and making the appropriate substitutions of observability (detectability) and controllability (stabilizability).

The above theorems and their duals can be used to develop a set of assumptions which will ensure the existence of symmetric solutions to an H_2 type Riccati equation. This will be useful in the next chapter when we develop a parametrization of all H_2 controllers.

2.5.2 H_∞ Type. The algebraic Riccati equation of interest for the H_∞ constraint in this work is

$$AX + XA^T + XBR^{-1}B^T X + C^T C = 0 \quad (2.69)$$

Associated with the Riccati equation (2.69) is the Hamiltonian matrix

$$M_\infty = \begin{bmatrix} A & BR^{-1}B^T \\ C^T C & -A^T \end{bmatrix} \quad (2.70)$$

Define

$$\Phi(s) := R - G^*(s)G(s) \quad G(s) = C(sI - A)^{-1}B \quad (2.71)$$

2.5.2.1 Existence and Uniqueness. If (A, B) is controllable, then the existence and uniqueness of the solutions to (2.69) are given by the following theorem.

Theorem 2.5.4 Assume (A, B) is controllable. Then, the following are equivalent:

- i. there exists a solution X of (2.69) such that $X = X^*$
- ii. there exists a solution X_- of (2.69) such that $\Re [\lambda_j(A + BR^{-1}B^T X_-)] \leq 0$ for all j
- iii. there exists a solution X_+ of (2.69) such that $\Re [\lambda_j(A + BR^{-1}B^T X_+)] \geq 0$ for all j
- iv. the partial multiplicities of the imaginary axis eigenvalues of the Hamiltonian (2.70) (if any) are even (the partial multiplicity of an eigenvalue is defined as the order of its associated Jordan block when the matrix is in Jordan form)
- v. $\Phi(j\omega) \geq 0$ for all $\omega \in [0, +\infty]$

Moreover, if i-v hold, then the following are true:

- vi. the solution X_- of (2.69) with the properties of ii is unique
- vii. the solution X_+ of (2.69) with the properties of iii is unique
- viii. $X_- = X_+$ iff all the eigenvalues of (2.70) are on the imaginary axis

Proof: See [27], Theorems 1, 3 and Corollary 5; [28], Theorem 3.11; and [29], Theorem 3. ■

Based on this theorem, the existence of solutions to (2.69) can be determined. Furthermore, the minimal solution, which is the one we are most interested in, is unique. The controllability assumption can be relaxed using the next theorem.

Theorem 2.5.5 Define

$$Q(X) = AX + XA^T + XC^T R^{-1} CX + BB^T \quad (2.72)$$

Assume there exists an $X = X^*$ such that $Q(X) \leq 0$. Then

- i. if (A, B) is stabilizable, there exists a unique minimal solution X_- to (2.69).
Furthermore, $X_- \leq X$ for all X such that $Q(X) \leq 0$ and
 $\Re [\lambda_i(A + BR^{-1}B^T X_-)] \leq 0$ for all i
- ii. if $(-A, B)$ is stabilizable, there exists a unique maximal solution X_+ to (2.69).
Furthermore, $X_+ \geq X$ for all X such that $Q(X) \leq 0$ and
 $\Re [\lambda_i(A + BR^{-1}B^T X_+)] \geq 0$ for all i
- iii. if (A, B) is controllable, both X_+ and X_- exist. Furthermore, $X_+ > X_-$ iff
 $\Re [\lambda_i(A + BR^{-1}B^T X_-)] < 0$ for all i iff $\Re [\lambda_i(A + BR^{-1}B^T X_+)] > 0$ for all
 i
- iv. if $Q(X) < 0$, then i and ii above can be strengthened to
 $X_- < X$, $\Re [\lambda_i(A + BR^{-1}B^T X_-)] < 0$ for all i , and
 $X_+ > X$, $\Re [\lambda_i(A + BR^{-1}B^T X_+)] > 0$ for all i , respectively

Proof: See [28], Corollary 3.4. ■

Thus, if the assumption on (A, B) is relaxed to stabilizable, we can still determine if solutions to (2.69) exist and the uniqueness of the minimal solution.

The next theorems are key results which will be used in this work.

Theorem 2.5.6 Assume (A, B) stabilizable and $\Re [\lambda_i(A)] \leq 0$ for all i . If $X = X^*$ satisfies (2.69), then $X \geq 0$.

Proof: See [30], Lemma. ■

Theorem 2.5.7 If (C, A) is detectable, then there exists an $X \geq 0$ satisfying (2.69) only if A is stable.

Proof: Since (C, A) is detectable, $C^T C \geq 0$, and $BR^{-1}B^T \geq 0$. Then from [23], Theorem 3.6, $(\sqrt{XBR^{-1}B^T X + C^T C}, A)$ is detectable. Furthermore, assume a solution $X \geq 0$ exists, then (2.69) can be treated as a Lyapunov equation and Theorem 2.4.1 implies A is stable. ■

Combining the above two theorems, we can determine what conditions are necessary for a positive semi-definite solution to (2.69) to exist. Further, the nature of real symmetric solutions can be determined from the stability of the matrix A .

2.5.2.2 The Riccati Operator and Stabilizing Solutions. Consider a Hamiltonian matrix M of order $2n$ which has no eigenvalues on the imaginary axis. One can then define two n -dimensional subspaces $\mathcal{X}_-(M)$ and $\mathcal{X}_+(M)$. $\mathcal{X}_-(M)$ is the invariant subspace associated with the eigenvalues of M in the left-half complex plane and $\mathcal{X}_+(M)$ is the invariant subspace associated with the eigenvalues of M in the right-half complex plane. The matrix which is comprised of the basis vectors of $\mathcal{X}_-(M)$ can be partitioned as

$$\mathcal{X}_-(M) = \text{span} \begin{bmatrix} X_1 \\ X_2 \end{bmatrix} \quad (2.73)$$

where $X_1, X_2 \in \mathbb{R}^{n \times n}$. X_1 is nonsingular if and only if the two subspaces

$$\mathcal{X}_-(M) \quad \text{and} \quad \begin{bmatrix} 0 \\ I \end{bmatrix} \quad (2.74)$$

are complementary. In this case, $X := X_2 X_1^{-1}$ and the *Riccati operator* is defined as $\text{Ric} : M \rightarrow X$ or $X = \text{Ric}(M)$. The domain of the Riccati operator, denoted $\text{dom}(\text{Ric})$, is defined by all Hamiltonian matrices such that

- i. M has no eigenvalues on the imaginary axis
- ii. the two subspaces in (2.74) are complementary.

Theorem 2.5.8 *If $M_\infty \in \text{dom}(\text{Ric})$, where M_∞ is defined by (2.70), and $X = \text{Ric}(M_\infty)$, then*

- i. X is symmetric

ii. X satisfies (2.69)

iii. $\Re [\lambda_j(A + BR^{-1}B^T X)] < 0$ for all j

Proof: See [31], Lemma 2.1. ■

The Riccati operator can be extended to include cases where the Hamiltonian M has eigenvalues on the imaginary axis. If M has eigenvalues on the imaginary axis, then there are at least n eigenvalues in the closed left-half plane. Thus, there is an invariant subspace $\mathcal{X}_-(M)$ (not necessarily unique) corresponding to n eigenvalues in the closed left-half plane with a basis defined as in (2.73) which satisfies

$$M \begin{bmatrix} X_1 \\ X_2 \end{bmatrix} = \begin{bmatrix} X_1 \\ X_2 \end{bmatrix} T_* \quad (2.75)$$

where T_* is any $2n \times 2n$ matrix with $\Re [\lambda_i(T_*)] \leq 0$ for all $i = 1, \dots, 2n$. If $\mathcal{X}_-(M)$ satisfies the complementary property (2.74), then $X := X_2 X_1^{-1}$, if X is symmetric. Define the *extended Riccati operator* $\overline{Ric} : M \rightarrow X$ with domain $dom(\overline{Ric})$ consisting of all Hamiltonians which satisfy the following:

- i. an $\mathcal{X}_-(M)$ exists such that the two subspaces in (2.74) are complementary
- ii. the resulting $X = X_2 X_1^{-1}$ is symmetric.

$\overline{Ric}(M)$ may not always be a function since X may not be unique. In this work, whenever $\overline{Ric}(M) = X$ is used, it will be a well-defined and $X = \overline{Ric}(M)$ must be unique.

Theorem 2.5.9 Suppose $M_\infty \in dom(\overline{Ric})$ and $X = \overline{Ric}(M_\infty)$ is unique. Then

- i. X is symmetric
- ii. X satisfies (2.69)
- iii. $\Re [\lambda_j(A + BR^{-1}B^T X)] \leq 0$ for all j

When iii has at least one j such that equality holds, X is referred to as the neutrally stabilizing solution to (2.69).

Proof: Modification of [31], Lemma 2.1 using the above discussion. ■

Finally, to conclude the discussion of Riccati equations, consider

$$G(s) = \left[\begin{array}{c|c} A & B \\ \hline C & D \end{array} \right] \quad (2.76)$$

and the associated Hamiltonian

$$M_\infty = \left[\begin{array}{cc} A + BR^{-1}D^TC & BR^{-1}B^T \\ -C(I - DD^T)^{-1}C & (A + BR^{-1}D^TC)^T \end{array} \right] \quad (2.77)$$

where $R = \gamma^2 I - D^T D$. Then the following theorem defines bounds on the infinity-norm.

Theorem 2.5.10 *Assume A is stable and $R > 0$. Then the following are equivalent:*

- i. $\|G(s)\|_\infty < \gamma$
- ii. M_∞ has no imaginary axis eigenvalues
- iii. $M_\infty \in \text{dom}(\text{Ric})$
- iv. $M_\infty \in \text{dom}(\text{Ric})$ and $X = \text{Ric}(M_\infty) \geq 0$ (> 0 if (C, A) is observable).

Furthermore, the following are equivalent:

- i. $\|G(s)\|_\infty \leq \gamma$
- ii. $M_\infty \in \text{dom}(\overline{\text{Ric}})$
- iii. $M_\infty \in \text{dom}(\overline{\text{Ric}})$ and $X = \overline{\text{Ric}}(M_\infty) \geq 0$ (> 0 if (C, A) is observable) is unique.

Proof: Modification of [31], Lemma 2.4 for general γ . ■

Thus, upper and lower bounds on the infinity-norm of a transfer function can be determined by varying γ so that the Hamiltonian has eigenvalues on and off the imaginary axis. This will be explored further when numerical solutions are discussed.

All of the above theorems hold for the dual of (2.69)

$$AX + XA^T + XC^T R^{-1} CX + BB^T = 0 \quad (2.78)$$

by making the substitutions $A = A^T$, $B = C^T$, $C = B^T$, and $D = D^T$ and making the appropriate substitutions of observability (detectability) and controllability (stabilizability). Furthermore, the matrix $G(s)$ is replaced by $G^T(s)$ and R becomes $\gamma^2 I - DD^T$. With these substitutions, the last theorem of this section is

Theorem 2.5.11 *Suppose A is stable. If there exists an $X = X^T \geq 0$ satisfying*

$$AX + XA^T + (XC^T + BD^T)R^{-1}(XC^T + BD^T)^T + BB^T = 0 \quad (2.79)$$

where

$$R = \gamma^2 I - DD^T > 0 \quad (2.80)$$

then

$$\|C(sI - A)^{-1}B + D\|_\infty \leq \gamma \quad (2.81)$$

Proof: Assume there exists an $X = X^T \geq 0$ satisfying (2.79). Rewrite (2.79) as

$$sX - sX - AX - XA^T = (XC^T + BD^T)R^{-1}(XC^T + BD^T)^T + BB^T \quad (2.82)$$

or

$$(sI - A)X + X(-sI - A^T) = (XC^T + BD^T)R^{-1}(XC^T + BD^T)^T + BB^T \quad (2.83)$$

Premultiply by $C(sI - A)^{-1}$ and postmultiply by $(-sI - A^T)^{-1}C^T$ to get

$$\begin{aligned}
CX(-sI - A^T)^{-1}C^T + C(sI - A)^{-1}XC^T = \\
C(sI - A)^{-1}(XC^T + BD^T)R^{-1}(XC^T + BD^T)^TC(sI - A)^{-1} \\
+ C(sI - A)^{-1}BB^TC(sI - A)^{-1}
\end{aligned} \tag{2.84}$$

Define $L(s) := CX(sI - A)^{-1}C^T$, $L^*(s) := C(-sI - A^T)^{-1}XC^T$, $\tilde{G}(s) := C(sI - A)^{-1}B$, and $P(s) := \tilde{G}(s)D^T$. Then (2.84) becomes

$$\begin{aligned}
L^*(s) + L(s) - L(s)R^{-1}L^*(s) - L(s)R^{-1}P^*(s) \\
-P(s)R^{-1}L^*(s) - P(s)R^{-1}P^*(s) = \tilde{G}(s)\tilde{G}^*(s)
\end{aligned} \tag{2.85}$$

Since $R = R^* > 0$ there exists an $R^{1/2}$ such that $R^{-1/2}(R^{1/2})^* = I$, $R^{1/2}(R^{1/2})^* = R$, and the following is true:

$$\begin{aligned}
(R^{1/2} - L(s)R^{-1/2} - P(s)R^{-1/2})(R^{1/2} - L(s)R^{-1/2} - P(s)R^{-1/2})^* = \\
R - L^*(s) - L(s) - P^*(s) - P(s) + L(s)R^{-1}L^*(s) + L(s)R^{-1}P^*(s) \\
+ P(s)R^{-1}L^*(s) + P(s)R^{-1}P^*(s)
\end{aligned} \tag{2.86}$$

Thus, letting $G(s) = C(sI - A)^{-1}B + D$ and using (2.86) we can rewrite (2.85) as

$$\begin{aligned}
(R^{1/2} - L(s)R^{-1/2} - P(s)R^{-1/2})(R^{1/2} - L(s)R^{-1/2} - P(s)R^{-1/2})^* = \\
\gamma^2 I - DD^T - D\tilde{G}^* - \tilde{G}(s)D^T - \tilde{G}(s)\tilde{G}^*(s) + \gamma^2 I - G(s)G^*(s)
\end{aligned} \tag{2.87}$$

The left term of (2.87) is Hermitian on the $j\omega$ -axis; thus, it is positive semidefinite.

Therefore

$$2\gamma^2 I - G(s)G^*(s) - (\tilde{G}(s)\tilde{G}^*(s) + \tilde{G}(s)D^T + D\tilde{G}^* + DD^T) \leq 0 \quad (2.88)$$

$$\Rightarrow \gamma^2 I - G(s)G^*(s) \leq 0 \quad (2.89)$$

$$\Rightarrow \|G(s)\|_\infty \leq \gamma \quad (2.90)$$

■

The above theorem allows us to determine whether an H_∞ constraint is met based on the stability of the A matrix and the existence of a positive semi-definite symmetric solution to the algebraic Riccati equation (2.79). This theorem will be very useful in setting up the fixed order mixed H_2/H_∞ problem.

2.6 Convex Optimization

This section is an introduction into some key concepts of convex programming which will be necessary for this work. For a complete discussion of this topic, the reader is referred to [32, 33, 34, 35, 36, 37].

Let X be a vector space, $x_1, x_2 \in X$, and $\alpha \in (0, 1)$, then a *convex combination* of x_1 and x_2 is $\alpha x_1 + (1 - \alpha)x_2$. A set $C \subset X$ is said to be a *convex set* if for every $x_1, x_2 \in C$ then all convex combinations of x_1 and x_2 are also contained in C . Defining a functional $f : C \rightarrow \Re$, f is said to be a *convex functional* if

$$f[\alpha x_1 + (1 - \alpha)x_2] \leq \alpha f(x_1) + (1 - \alpha)f(x_2) \quad (2.91)$$

for all $x_1, x_2 \in C$ and all $\alpha \in (0, 1)$. Furthermore, f is said to be a *strictly convex functional* if strict inequality holds in (2.91), whenever $x_1 \neq x_2$.

Suppose $f(x), g_1(x), \dots, g_m(x)$ are functionals defined on some subset C of a vector space X . We are interested in the following *program*:

$$\mathcal{P} \begin{cases} \text{Minimize } f(x) \text{ subject to} \\ g_i(x) \leq 0 \text{ for all } i \\ \text{where } x \in C \subset X \end{cases} \quad (2.92)$$

The functional $f(x)$ is called the *objective*, and the functional inequalities $g_i(x) \leq 0$ are called the *constraints*. A vector $x \in C$ is said to be an *admissible point* for \mathcal{P} if it satisfies all the constraints in \mathcal{P} . The set A of all admissible points is called the *admissible region* for \mathcal{P} . If A is not empty, the \mathcal{P} is said to be *consistent*, and if there exists an $x \in A$ such that $g_i(x) < 0$ for all i , then \mathcal{P} is said to be *superconsistent*. If \mathcal{P} is a consistent program and there exists an $x^* \in A$ such that $f(x^*) \leq f(x)$ for all $x \in A$, then x^* is a *solution* for \mathcal{P} . Furthermore, if \mathcal{P} is superconsistent, then the admissible region has an interior point. This is a necessary assumption for the main theorem of this section.

If the objective $f(x)$, the constraints $g_i(x)$, and the underlying set C are all convex, then \mathcal{P} is called a *convex program*. In this case the admissible set A will always be convex. The *Lagrangian* \mathcal{L} of the convex program \mathcal{P} is defined as

$$\mathcal{L}(x, \Lambda) := f(x) + \sum_{i=1}^m \lambda_i g_i(x) \quad (2.93)$$

where $x \in C$, $\Lambda := [\lambda_1, \dots, \lambda_m]^T \in \Re^m$, and $\lambda_i \geq 0$ for all i .

The following theorem is the central result of convex programming.

Theorem 2.6.1 (Kuhn-Tucker Theorem (Saddle Point Form)) *Suppose \mathcal{P} given in (2.92) is a superconsistent convex program. Then $x^* \in C$ is a solution of \mathcal{P} if and only if there exists a $\Lambda^* \in \Re^m$ such that:*

$$i. \lambda_j^* \geq 0 \text{ for all } j$$

$$\text{ii. } \mathcal{L}(x^*, \Lambda) \leq \mathcal{L}(x^*, \Lambda^*) \leq \mathcal{L}(x, \Lambda^*)$$

for all $x \in C$ and all $\Lambda \in \mathfrak{R}^m$ such that $\lambda_j \geq 0$ for all j

$$\text{iii. } \lambda_j g_j(x^*) = 0 \text{ for all } j$$

Proof: See [37], Theorem 5.2.13. ■

The above theorem is just one form of the famous group of related theorems called Kuhn-Tucker (KT) Theorems. For the convex analysis in this work, the saddle point form will be sufficient. For additional forms of the KT Theorem, see, for instance, [34, 36, 37]. The results of Theorem 2.6.1 are referred to as the *Kuhn-Tucker conditions*, or just the KT conditions.

The next theorem deals with the uniqueness of the solution to a convex program.

Theorem 2.6.2 *Suppose \mathcal{P} is the convex program given in (2.92) and $x^* \in C$ satisfies the Kuhn-Tucker conditions. If $f(x)$ is strictly convex, then x^* is unique.*

Proof: See [35], Corollary to Theorem 9.4.1. ■

2.7 Duality in Minimum Norm Problems

The final section of this chapter will discuss a dual approach for solving minimum norm problems. An excellent source for this subject is [36].

Let X be a vector space. A functional $f : X \rightarrow \mathfrak{R}$ is a *linear functional* if

$$f(\alpha x_1 + \beta x_2) = \alpha f(x_1) + \beta f(x_2) \tag{2.94}$$

for all $x_1, x_2 \in X$ and for all $\alpha, \beta \in \mathfrak{R}$. Further, f is a *bounded linear functional* if there is some $M \in \mathfrak{R}$ such that

$$|f(x)| \leq M \|x\| \tag{2.95}$$

for all $x \in X$. The infimum over all such M is called the norm of f denoted $\|f\|$. The space of all bounded linear functionals on X is called the *dual* of X and is denoted X^* . Given $x^* \in X^*$, then

$$\|x^*\| := \sup_{\|x\| \leq 1} |x^*(x)| \quad (2.96)$$

The spaces under consideration in this work will be H_2 and L_2 , which are Hilbert spaces, and as such have special properties which will simplify the dual problem. Let X be a Hilbert space. Then the following theorem provides a representation of bounded linear functionals on X .

Theorem 2.7.1 Riesz-Fréchet: *Assume X is a Hilbert space. If f is a bounded linear functional on X , then there exists a unique vector $y \in X$ such that*

$$f(x) = \langle x, y \rangle \quad (2.97)$$

for all $x \in X$. Furthermore,

$$\|f\| = \|y\| \quad (2.98)$$

and every $y \in X$ determines a unique bounded linear functional in this way.

Proof: See [36], Theorem 5.3.2. ■

Thus, linear functionals on a Hilbert space can be represented uniquely by a vector in the space. For the remainder of this work it will be assumed that $[\cdot]^*$ is the vector which represents the actual dual; while this is an abuse of notation, it will simplify the discussion.

Another key concept in duality theory is alignment. A vector $x^* \in X^*$ is said to be *aligned* with a vector $x \in X$ if

$$\langle x, x^* \rangle = \|x^*\| \|x\| \quad (2.99)$$

Finally, let X be a normed vector space. Then the *support functional* of a convex set $K \subset X$ is defined on X^* as

$$h(x^*) := \sup_{x \in K} \langle x, x^* \rangle \quad (2.100)$$

The next theorem provides the main results from duality theory for the minimum norm problem.

Theorem 2.7.2 Minimum Norm Duality: *Assume X is a real normed vector space. Let $d > 0$ denote the distance from a point $x_1 \in X$ and some convex set $K \subset X$ having support functional h , then*

$$d = \inf_{x \in K} \|x - x_1\| = \max_{\|x^*\| \leq 1} [\langle x_1, x^* \rangle - h(x^*)] \quad (2.101)$$

where the maximum on the right is achieved by some $x_0^* \in X^*$. If the infimum on the left is achieved by some $x_0 \in K$, then $-x_0^*$ is aligned with $x_0 - x_1$.

Proof: See [36], Theorem 5.13.1. ■

Therefore, the infimal problem in the primal space can be transformed into a maximal problem in the dual space. While this may not always provide a complete solution to the problem, when combined with the alignment condition, optimal solutions can often be found.

2.8 Summary

This chapter introduced state space representations of linear, time-invariant transfer functions. Further, we introduced the concept of internal stability. Next, the operator spaces H_2 , H_∞ , and L_1 and their associated norms were introduced. A brief review of Lyapunov equations and H_2 type algebraic Riccati equations was presented. A more detailed review of the conditions required for the existence and uniqueness of solutions to H_∞ type algebraic Riccati equations was presented. This was followed

by an introduction to the basic concepts of convex programming including the Kuhn-Tucker Theorem. Finally, duality concepts were used to convert an infimal distance problem into a maximal problem in the dual space.

III. Review of H_2 , H_∞ , and μ

As was discussed in Chapter I, this dissertation will deal with H_2 , H_∞ , and μ optimization. This chapter will present an introduction to a state space approach for finding fixed-order controllers which achieve the design goals of the above optimal control problems. First, the important concept of the Youla parametrization of all stabilizing controllers will be introduced.

3.1 Parametrization of All Stabilizing Controllers

Consider the feedback system given in Figure 3.1 where $K \in \mathbf{K}$, the set of all stabilizing controllers. \mathbf{K} is not a convex set; thus, the tools of convex analysis can not be applied directly. However, a parametrization of all stabilizing controllers over a convex set has been developed from the work of Youla, *et al* [38]. A complete discussion of the parametrization can be found in [17, 39]. This will only be an introduction into the key ideas needed for this work. First we need to introduce the idea of a coprime factorization of a transfer function.

3.1.1 Coprime Factorizations. Two function matrices $F(s), G(s) \in H_\infty$ are *right-coprime* if they have an equal number of columns and there exist function

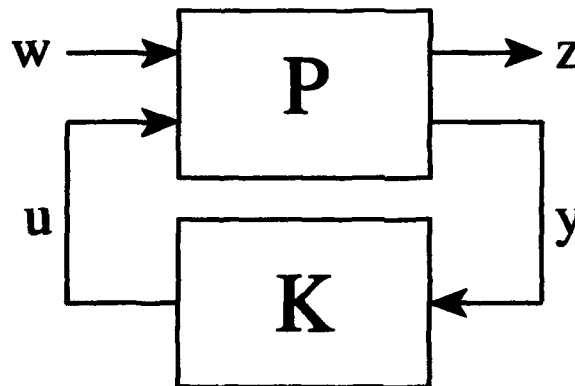


Figure 3.1. Feedback system

matrices $X, Y \in H_\infty$ such that

$$\begin{bmatrix} X & Y \end{bmatrix} \begin{bmatrix} F \\ G \end{bmatrix} = XF + YG = I \quad (3.1)$$

Further, F and G are *left-coprime* if they have an equal number of rows and there exist function matrices $X, Y \in H_\infty$ such that

$$\begin{bmatrix} F & G \end{bmatrix} \begin{bmatrix} X \\ Y \end{bmatrix} = FX + GY = I \quad (3.2)$$

Let G be a proper transfer function matrix. Then writing $G = NM^{-1}$ where N and M are right-coprime is called a *right-coprime factorization* of G . Similarly, the factorization $G = \tilde{M}^{-1}\tilde{N}$ where \tilde{N} and \tilde{M} are left-coprime is called a *left-coprime factorization* of G . Finally, for each proper matrix G , there exist $N, M, \tilde{N}, \tilde{M}, X, Y, \tilde{X}, \tilde{Y} \in H_\infty$ such that

$$G = NM^{-1} = \tilde{M}^{-1}\tilde{N} \quad (3.3)$$

and

$$\begin{bmatrix} \tilde{X} & -\tilde{Y} \\ -\tilde{N} & \tilde{M} \end{bmatrix} \begin{bmatrix} M & Y \\ N & X \end{bmatrix} = I \quad (3.4)$$

(3.3) and (3.4) constitute a *doubly-coprime factorization* of G .

3.1.2 Parametrization. The following presents a method of parametrizing all stabilizing controllers over all $Q \in H_\infty$.

Theorem 3.1.1 Assume G is a proper transfer function matrix with a doubly-coprime factorization given by (3.3) and (3.4). Then the set of all controllers K

which stabilize G is parametrized by

$$K = (Y - MQ)(X - NQ)^{-1} \quad (3.5)$$

$$= (\tilde{X} - Q\tilde{N})^{-1}(\tilde{Y} - Q\tilde{M}) \quad (3.6)$$

where $Q \in H_\infty$.

Proof: See [17], Theorem 4.4.1. ■

Recall that P in Figure 3.1 can be partitioned as

$$P = \begin{bmatrix} P_{zw} & P_{zu} \\ P_{yw} & P_{yu} \end{bmatrix} \quad (3.7)$$

Also, recall from Theorem 2.2.2 that a controller K stabilizes P if and only if it stabilizes P_{yu} . Thus, we get the following theorem which parametrizes all internally stable closed-loop transfer functions T_{zw} .

Theorem 3.1.2 *Let $N, M, \tilde{N}, \tilde{M}, X, Y, \tilde{X}, \tilde{Y} \in H_\infty$ be a doubly-coprime factorization of P_{yu} , K be defined as in Theorem 3.1.1, and define*

$$T_1 = P_{zw} + P_{zu}M\tilde{Y}P_{yw} \quad (3.8)$$

$$T_2 = P_{zu}M \quad (3.9)$$

$$T_3 = \tilde{M}P_{yw} \quad (3.10)$$

Then $T_1, T_2, T_3 \in H_\infty$ and

$$T_{zw} = T_1 - T_2QT_3 \quad (3.11)$$

Proof: See [17], Theorem 4.5.1. ■

3.2 H_2 Optimization

H_2 optimization is a generalization of the standard linear quadratic Gaussian (LQG) problem. Returning to the feedback problem in Figure 3.1, P can be partitioned

$$P = \begin{bmatrix} P_{zw} & P_{zu} \\ P_{yw} & P_{yu} \end{bmatrix} \quad (3.12)$$

such that

$$\begin{aligned} z &= P_{zw}w + P_{zu}u \\ y &= P_{yw}w + P_{yu}u \end{aligned} \quad (3.13)$$

The exogenous input w is zero-mean white Gaussian noise with unit intensity.

The objective of H_2 optimization is to design a controller K which is stabilizing and minimizes the energy, or two-norm, of the output z . This can be written as

$$\alpha = \inf_{K(s) \text{ Stabilizing}} \|z\|_2 \quad (3.14)$$

$$= \inf_{K(s) \text{ Stabilizing}} \|T_{zw}\|_2 \quad (3.15)$$

$$= \inf_{K(s) \text{ Stabilizing}} \|P_{zw} + P_{zu}K(I - P_{yu}K)^{-1}P_{yw}\|_2 \quad (3.16)$$

A state space realization of (3.12) is given by

$$\begin{aligned} \dot{x} &= Ax + B_w w + B_u u \\ z &= C_x x + D_{zw} w + D_{zu} u \\ y &= C_y x + D_{yw} w + D_{yu} u \end{aligned} \quad (3.17)$$

The following assumptions are made:

- i. $D_{zw} = 0$
- ii. $D_{yu} = 0$
- iii. (A, B_u) is stabilizable and (C_y, A) is detectable

$$\text{iv. } D_{zu}^T D_{zu} = I \text{ and } D_{yw} D_{yw}^T = I$$

$$\text{v. } \begin{bmatrix} A - j\omega I & B_u \\ C_z & D_{zu} \end{bmatrix} \text{ has full column rank for all } \omega$$

$$\text{vi. } \begin{bmatrix} A - j\omega I & B_w \\ C_y & D_{yw} \end{bmatrix} \text{ has full row rank for all } \omega$$

Condition i is required to ensure the closed-loop transfer function has a finite two-norm. Condition ii is assumed for ease of development but can be removed completely through loop shifting techniques [40]. Condition iii is necessary for the existence of stabilizing solutions. Condition iv is a regularity condition which insures that there is a direct penalty on all controls and no perfect measurements. This condition can be relaxed to a rank condition through scaling [41]. Finally, conditions v and vi are required to ensure the existence of stabilizing solutions to the two AREs in the following solution. This condition is equivalent to requiring the Hamiltonians associated with AREs be in $\text{dom}(\text{Ric})$.

The controller which minimizes (3.14) is unique and will be denoted $K_{2,opt}$, with a corresponding minimum two-norm $\underline{\alpha}$. It is desired to parametrize sub-optimal controllers for the purpose of trading off H_2 performance for H_∞ performance. All stabilizing controllers can be parametrized by a family of lower fractional transformations (LFT) of a transfer function J and a constrained freedom parameter $Q \in H_2$ as shown in Figure 3.2. One particular form of J is given by

$$J(s) = \begin{bmatrix} J_{uy} & J_{ur} \\ J_{vy} & J_{vr} \end{bmatrix} = \left[\begin{array}{c|cc} A_J & K_f & K_{fl} \\ \hline -K_c & 0 & I \\ K_d & I & 0 \end{array} \right] \quad (3.18)$$

$$\text{where} \quad (3.19)$$

$$A_J = A - K_f C_y - B_u K_c \quad (3.20)$$

$$K_c = B_u^T X_2 + D_{zu}^T C_z \quad (3.21)$$

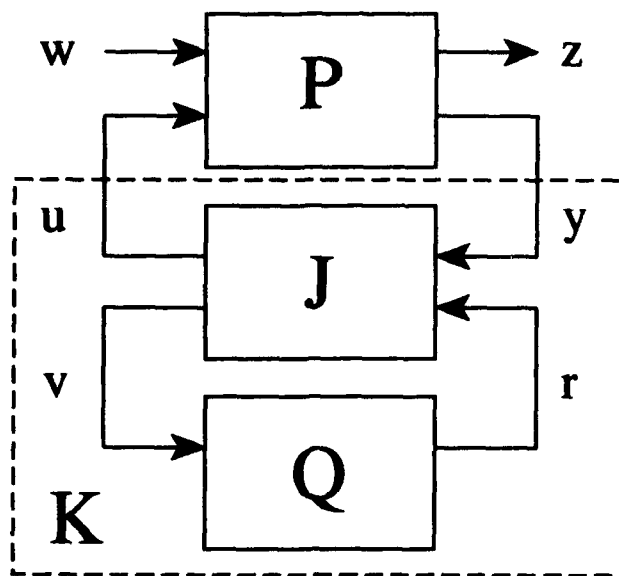


Figure 3.2. H_2 system with parametrized controller

$$K_f = Y_2 C_y^T + B_w D_{yw}^T \quad (3.22)$$

$$K_d = -C_y \quad (3.23)$$

$$K_{f1} = B_u \quad (3.24)$$

and X_2 and Y_2 are the real, unique, symmetric positive semidefinite solutions to the AREs

$$(A - B_u D_{zu}^T C_z)^T X_2 + X_2 (A - B_u D_{zu}^T C_z) - X_2 B_u B_u^T X_2 + \hat{C}_z^T \hat{C}_z = 0 \quad (3.25)$$

where

$$\hat{C}_z = (I - D_{zu} D_{zu}^T) C_z \quad (3.26)$$

and

$$(A - B_w D_{yw}^T C_y) Y_2 + Y_2 (A - B_w D_{yw}^T C_y)^T - Y_2 C_y^T C_y Y_2 + \hat{B}_w \hat{B}_w^T = 0 \quad (3.27)$$

where

$$\hat{B}_w = B_w(I - D_{yw}^T D_{yw}) \quad (3.28)$$

The family of controllers which produce $\|T_{zw}\|_2 \leq \alpha$ can now be parametrized by

$$K(s) = F_t[J(s), Q(s)] \quad (3.29)$$

where Q can be chosen to be any $Q \in H_2$ such that

$$\|Q\|_2^2 \leq \alpha^2 - \underline{\alpha}^2 \quad (3.30)$$

The optimal H_2 controller is attained through the above parametrization when Q is chosen to be identically equal to zero, and the resulting optimal controller is

$$K_{2opt} = \left[\begin{array}{c|c} A_J & K_f \\ \hline -K_c & 0 \end{array} \right] \quad (3.31)$$

3.3 H_∞ Optimization

H_∞ optimization was originated in the seminal paper by Zames [42]. The original problem was posed in an operator-theoretic framework as a model matching problem which can be reduced to a Nehari problem [17]. A state space solution, based on a two ARE approach originally developed by Doyle, *et al* [11], will be presented here.

Figure 3.3 represents the H_∞ feedback system, where d is a bounded energy exogenous input with $\|d\|_\infty \leq 1$, and the controlled output is e . In general, the symbols w and z will be used for H_2 inputs and outputs, and d and e will be used for H_∞ inputs and outputs.

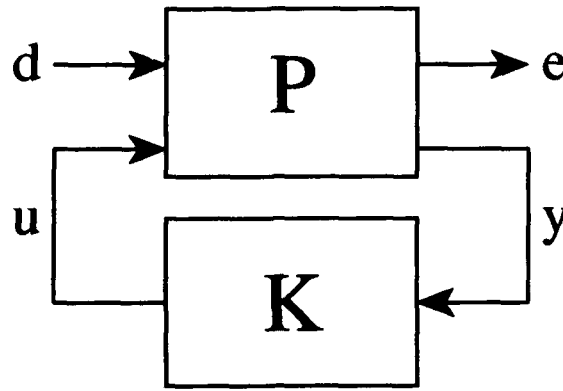


Figure 3.3. H_∞ feedback system

The plant P can be partitioned

$$P = \begin{bmatrix} P_{ed} & P_{eu} \\ P_{yd} & P_{yu} \end{bmatrix} \quad (3.32)$$

such that

$$\begin{aligned} e &= P_{ed}d + P_{eu}u \\ y &= P_{yd}d + P_{yu}u \end{aligned} \quad (3.33)$$

The H_∞ optimization problem is to design a stabilizing controller K which minimizes the maximum energy of the output e , given a bounded energy input, or

$$\inf_{K \text{ stabilizing}} \sup_{\|d\|_2 \leq 1} \|e\|_2 := \inf_{K \text{ stabilizing}} \|T_{ed}\|_\infty \quad (3.34)$$

$$= \inf_{K \text{ stabilizing}} \|P_{ed} + P_{eu}K(I - P_{yu}K)^{-1}P_{yd}\|_\infty \quad (3.35)$$

A state space realization of (3.32) is given by

$$\begin{aligned} \dot{x} &= Ax + B_d d + B_u u \\ e &= C_e x + D_{ed} d + D_{eu} u \\ y &= C_y x + D_{yd} d + D_{yu} u \end{aligned} \quad (3.36)$$

The following assumptions are made:

- i. $D_{ed} = 0$
- ii. $D_{yu} = 0$
- iii. (A, B_u) is stabilizable and (C_y, A) is detectable
- iv. $D_{eu}^T D_{eu} = I$ and $D_{yd} D_{yd}^T = I$
- v. $\begin{bmatrix} A - j\omega I & B_u \\ C_e & D_{eu} \end{bmatrix}$ has full column rank for all ω
- vi. $\begin{bmatrix} A - j\omega I & B_d \\ C_y & D_{yd} \end{bmatrix}$ has full row rank for all ω

Conditions i and ii are not required for a solution to exist, but reduce the complexity of the solution. Condition iii is necessary for the existence of stabilizing controllers. Condition iv is a regularity condition which is equivalent to requiring a direct penalty on all controls and no perfect measurements. The condition can be relaxed to a full rank requirement through scaling [41]. Finally, conditions v and vi in combination with iii guarantee the two Hamiltonian matrices corresponding to the following solution are in $\text{dom}(\text{Ric})$.

The infimum of the norm in (3.34) over the set of stabilizing controllers is denoted $\underline{\gamma}$ and, in general, the controller which achieves the infimum is not unique. Furthermore, $\underline{\gamma}$ is found through an iterative method based on the solution to two AREs and a coupling condition. This method is based on the parametrization of all sub-optimal controllers where

$$\|T_{ed}\|_{\infty} < \gamma \quad (3.37)$$

for some $\gamma > \underline{\gamma}$. This approach excludes the infimum, but allows it to be approached to any desired tolerance. The family of all admissible controllers which satisfy (3.37) is given by the LFT (Figure 3.4)

$$K(s) = F_{\ell}[J(s), Q(s)] \quad (3.38)$$

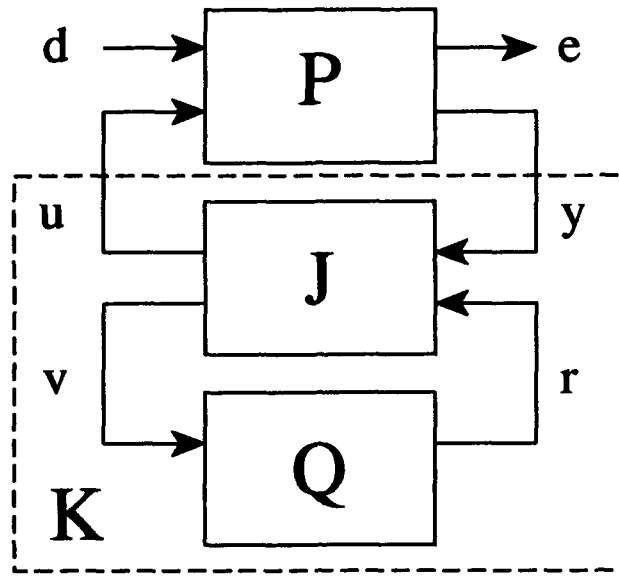


Figure 3.4. H_∞ system with parametrized controller

The parametrization is defined by

$$J(s) = \begin{bmatrix} J_{uy} & J_{ur} \\ J_{vy} & J_{vr} \end{bmatrix} = \left[\begin{array}{c|cc} A_J & K_f & K_{fl} \\ \hline -K_c & 0 & I \\ K_{cl} & I & 0 \end{array} \right] \quad (3.39)$$

where

$$A_J = A - K_f C_y - B_u K_c + \gamma^{-2} Y_\infty C_e^T (C_e - D_{eu} K_c) \quad (3.40)$$

$$K_c = (B_u X_\infty + D_{eu}^T C_e) (I - \gamma^{-2} Y_\infty X_\infty)^{-1} \quad (3.41)$$

$$K_f = Y_\infty C_y^T + B_d D_{yd}^T \quad (3.42)$$

$$K_{cl} = -(\gamma^{-2} D_{yd} B_d^T X_\infty + C_y) (I - \gamma^{-2} Y_\infty X_\infty)^{-1} \quad (3.43)$$

$$K_{fl} = \gamma^{-2} Y_\infty C_e^T D_{eu} + B_u \quad (3.44)$$

The matrices X_∞ and Y_∞ are the solutions of the AREs

$$\begin{aligned} & (A - B_u D_{eu}^T C_e)^T X_\infty + X_\infty (A - B_u D_{eu}^T C_e) \\ & + X_\infty (\gamma^{-2} B_d B_d^T - B_u B_u^T) X_\infty + \hat{C}_e^T \hat{C}_e = 0 \end{aligned} \quad (3.45)$$

where

$$\hat{C}_e = (I - D_{eu} D_{eu}^T) C_e \quad (3.46)$$

and

$$\begin{aligned} & (A - B_d D_{yd}^T C_y) Y_\infty + Y_\infty (A - B_d D_{yd}^T C_y)^T \\ & + Y_\infty (\gamma^{-2} C_e^T C_e - C_y^T C_y) Y_\infty + \hat{B}_d \hat{B}_d^T = 0 \end{aligned} \quad (3.47)$$

where

$$\hat{B}_d = B_d (I - D_{yd}^T D_{yd}) \quad (3.48)$$

Finally, Q can be chosen to be any $Q \in H_\infty$ such that

$$\|Q\|_\infty < \gamma \quad (3.49)$$

The above parametrization of a controller K is valid if and only if the following three conditions hold:

- i. $H_X \in \text{dom}(\text{Ric})$ with $X_\infty = \text{Ric}(H_X) \geq 0$
- ii. $H_Y \in \text{dom}(\text{Ric})$ with $Y_\infty = \text{Ric}(H_Y) \geq 0$
- iii. $\rho(Y_\infty X_\infty) < \gamma^2$

where

$$H_X = \begin{bmatrix} A - B_u D_{eu}^T C_e & \gamma^{-2} B_d B_d^T - B_u B_u^T \\ -\hat{C}_e^T \hat{C}_e & -(A - B_u D_{eu}^T C_e)^T \end{bmatrix} \quad (3.50)$$

$$H_Y = \begin{bmatrix} A - B_d D_{yd}^T C_y & \gamma^{-2} C_e^T C_e - C_y^T C_y \\ -\hat{B}_d \hat{B}_d^T & -(A - B_d D_{yd}^T C_y)^T \end{bmatrix} \quad (3.51)$$

are the Hamiltonians associated with (3.45) and (3.47), respectively.

To find a controller which results in a closed-loop infinity-norm arbitrarily close to $\underline{\gamma}$, select an initial value of γ and check the above three conditions. If any condition fails, increase γ and repeat the process. If all three conditions are met, reduce γ and repeat the process. In this manner, the controller which minimizes the infinity-norm can be found to any desired accuracy (within numerical constraints). A more refined method of determining $\underline{\gamma}$ based on the convexity of the AREs over the set of admissible γ has been developed by Li and the reader is referred to [43] for details.

3.4 The Complex Structured Singular Value

The final topic to be discussed in this chapter is the *structured singular value* μ . This section will introduce μ and how to find an upper bound on μ through H_∞ optimization techniques. Chapter VII will discuss the application of μ -synthesis to optimal control problems to guarantee robust stability and robust performance. For a tutorial on the complex structured singular value, see [2].

3.4.1 Structured Singular Value. The structured singular value is a matrix function based on the underlying structure of a set of block diagonal matrices

$$\Delta := \left\{ \text{diag}[\delta_1 I_{r_1}, \dots, \delta_S I_{r_S}, \Delta_1, \dots, \Delta_F] \mid \delta_i \in \mathcal{C}, \Delta_j \in \mathcal{C}^{m_j \times m_j} \right\} \quad (3.52)$$

where $\delta_i I_{r_i}$ is the i th scalar block of order r_i and Δ_j is the j th full block of order m_j . For simplicity of development, it will be assumed that Δ is square, but the theory

applies as well for non-square perturbations. The dimension n of $\Delta \in \Delta$ is given by

$$n = \sum_{i=1}^S r_i + \sum_{j=1}^F m_j \quad (3.53)$$

The set of all block diagonal matrices which also have an infinity-norm bounded by γ^{-1} is defined by

$$\mathbf{B}\Delta := \left\{ \Delta \in \Delta \mid \bar{\sigma}(\Delta) \leq \gamma^{-1} \right\} \quad (3.54)$$

The structured singular value of a real matrix M defined over the set of perturbations Δ is

$$\mu_{\Delta}(M) := \frac{1}{\min \{ \bar{\sigma}(\Delta) \mid \Delta \in \Delta, \det(I - M\Delta) = 0 \}} \quad (3.55)$$

unless there is no $\Delta \in \Delta$ which makes $I - M\Delta$ singular, in which case $\mu_{\Delta}(M) := 0$.

From the definition of $\mu_{\Delta}(M)$, it can be seen that the maximum singular value of M is always an upper bound; however, this bound can be conservative. One method of reducing the conservativeness of the upper bound is to consider a transformation which does not affect the value of $\mu_{\Delta}(M)$ but does affect the value of $\bar{\sigma}(M)$. First define a set of scaling transfer functions \mathbf{D} which has the same block diagonal structure as the perturbations Δ . These transfer functions are given by

$$\mathbf{D} := \left\{ \left[D_1, \dots, D_S, d_1 I_{m_1}, \dots, d_{F-1} I_{m_{F-1}}, I_{m_F} \right] \mid \right. \\ \left. D_i \in \mathbb{C}^{r_i \times r_i}, D_i = D_i^* > 0, d_j \in \mathbb{R}, d_j > 0 \right\} \quad (3.56)$$

Now, an improved upper bound is given by the following:

Theorem 3.4.1 *Assume $M \in \mathbb{C}^{n \times n}$, Δ is defined by (3.52), and \mathbf{D} is defined by (3.56). Then*

$$\mu_{\Delta}(M) \leq \inf_{D \in \mathbf{D}} \bar{\sigma}(DMD^{-1}) \quad (3.57)$$

Proof: See [44], Theorem 2.3.3. ■

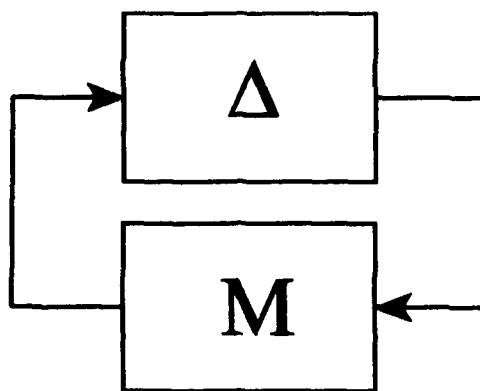


Figure 3.5. M- Δ system

Therefore, we can reduce the calculation of an upper bound on μ to computing the maximum singular value of a matrix.

Consider the system in Figure 3.5 where M and Δ can be partitioned as

$$M = \begin{bmatrix} M_{11} & M_{12} \\ M_{21} & M_{22} \end{bmatrix} \quad (3.58)$$

$$\Delta \in \mathbf{\Delta} = \left\{ \left[\begin{array}{cc} \Delta_1 & 0 \\ 0 & \Delta_2 \end{array} \right] \mid \Delta_1 \in \mathbf{\Delta}_1, \Delta_2 \in \mathbf{\Delta}_2 \right\} \quad (3.59)$$

The main result from μ analysis follows.

Theorem 3.3.2 (Main Loop Theorem) *The following are equivalent:*

- i. $\mu_{\mathbf{\Delta}}(M) < \gamma$
- ii. (a) $\mu_{\mathbf{\Delta}_2}(M_{22}) < \gamma$, and
 (b) $\max_{\Delta_2 \in \mathbf{B}\mathbf{\Delta}_2} \mu_{\mathbf{\Delta}_1}[F_2(M, \Delta_2)] < \gamma$

Proof: See [2], Corollary 4.7. ■

The importance of this theorem is that a single test on the transfer function M allows us to infer information about the response to each perturbation block. Let

$\mu_{\Delta_2}(M_{22}) < \gamma$ be a desired measure of performance and $\mu_{\Delta_1}(M) < \gamma$ be a requirement for stability. Then from the Main Loop Theorem, $\mu_{\Delta}(M) < \gamma$ implies our performance condition is satisfied and the system is robustly stable. Furthermore, by exchanging Δ_1 and Δ_2 in the theorem, $\mu_{\Delta}(M) < \gamma$ implies our system has robust performance for all perturbations. Thus far we have only considered the case where M is a constant matrix. The next section will expand these concepts to include matrices which vary over frequency.

3.4.2 Frequency Domain μ -synthesis. Suppose $G(s)$ is a MIMO transfer function with n_d inputs and n_e outputs. Assume $\Delta \subset \mathcal{C}^{n_d \times n_e}$ has the block structure given in (3.52). Define the set of all dynamic perturbations which have the desired diagonal structure as

$$\mathcal{M}(\Delta) := \{ \Delta(s) \in \mathfrak{RH}_{\infty} \mid \Delta(s_0) \in \Delta \text{ for all } s_0 \in \overline{\mathcal{C}^+} \} \quad (3.60)$$

where $\overline{\mathcal{C}^+}$ is the extended closed right-half complex plane.

Now, the complex structured singular value of a dynamic transfer matrix $G(s)$ over the structured perturbations $\Delta(s) \in \mathcal{M}(\Delta)$ is defined by

$$\|G(s)\|_{\Delta} = \sup_{\omega \in \mathfrak{R}} \mu_{\Delta} [G(j\omega)] \quad (3.61)$$

Notice that we use the norm symbol for the structured singular value of a dynamic matrix, but in fact, it is not a true norm since it does not satisfy the triangle inequality. However, we will use this notation for convenience.

Define the set \mathbf{D} of scaling transfer functions which have the same block diagonal structure as Δ , where each individual block has the property $D_i = D_i^* > 0$. Then, an upper bound on the structured singular value of a transfer matrix is given

by

$$\|G(s)\|_{\Delta} \leq \sup_{\omega \in \mathfrak{R}} \inf_{D \in \mathfrak{D}} \bar{\sigma}(DM D^{-1}) \quad (3.62)$$

$$= \inf_{D \in \mathfrak{D}} \|DM D^{-1}\|_{\infty} \quad (3.63)$$

Thus, for the purpose of control synthesis, (3.63) converts the μ problem into an H_{∞} problem combined with the selection of the scaling matrix D . The closed-loop transfer function M is determined by some open-loop plant P and a feedback controller K . The H_{∞} problem can be solved for any given scaling D by solving a standard H_{∞} optimization problem. Through an iterative process of closing the loop with an H_{∞} optimal controller K and determining an optimal scaling D , the infimum in the above problem can be approached. This method is known as *D-K iteration*. The method is not guaranteed to converge to the optimal scaling D , but in practice provides an acceptable method of approximating the optimal scaling. This limitation is a current subject of research. The D-K iteration method results in a controller order equal to the plant order plus twice the order of the scaling transfer functions. Furthermore, since μ -synthesis is based on designing an H_{∞} controller, it can result in a non-strictly proper controller.

Computation of μ for dynamic systems is currently accomplished by computing the D scaling over a large range of frequencies, then finding a $D(s)$ which matches the resulting point by point scaling. The order of $D(s)$ is chosen to give the best match, but a trade-off must be made since the order of the resulting H_{∞} controller which minimizes the upper bound in (3.63) is equal to the order of the original plant plus twice the order of $D(s)$ (in general, minus one at optimal). Recently, Safonov and Chiang have proposed a new approach to μ -synthesis which avoids the curve fitting problems; see [45] for details.

3.5 Summary

We began this chapter by introducing the Youla parametrization of all stabilizing controllers. This allowed us to parametrize a non-convex set of controllers over a convex set. Next the solution to a regular H_2 problem was developed. The set of controllers which result in a closed-loop transfer function with a two-norm less than some *a priori* value was shown to be an LFT of a particular matrix and a convex set in H_2 . Similarly, the set of controllers which satisfy an H_∞ constraint on the closed-loop transfer function was shown to be an LFT of a fixed matrix and a convex set in H_∞ . The fixed matrix is based on the solution of two AREs which are coupled. Finally, μ -synthesis was introduced for fixed and frequency varying matrices. A method of computing an upper bound based on an H_∞ problem, known as D-K iteration, was introduced. In the next chapter we will begin to explore the optimal H_2/H_∞ problem.

IV. The Optimal H_2/H_∞ Controller

The mixed H_2/H_∞ problem consists of an H_2 objective function with an H_∞ constraint. The H_2 problem is formed by selecting the outputs for which we wish to minimize the energy due to a set of white Gaussian noise inputs. Weighting transfer functions are often augmented at the output to emphasize certain frequency ranges of the response and to deemphasize other frequency ranges. Additionally, weighting transfer functions can be augmented at the input to provide a colored noise. The H_∞ problem is set up by selecting a second set of outputs for which we wish minimize the energy of due to bounded energy inputs. Again, weighting transfer functions can be augmented at the input and output to control the frequency response. Stable weighting transfer functions will be used to avoid the addition of unstable modes to the problem. For further information on methods of applying H_2 and H_∞ optimal control, the reader is referred to [19, 39].

This chapter will pose the general mixed problem in an operator-theoretical framework and characterize the optimal controller using convex analysis. While a complete analytical solution is not presented, the formulation of the problem in this framework provides considerable insight into the nature of the solution and limits of performance. The chapter will first set up the mixed optimal control problem as a convex program using the Youla parametrization. Using this setup, the uniqueness of the optimal solution for the mixed problem with one H_∞ constraint will be shown. Furthermore, a dual approach will be used to characterize the order of the optimal controller for a special case of the H_∞ constraint.

4.1 Parametrization of the H_2/H_∞ Controller

Consider the general control system shown in Figure 4.1, where w is a unit intensity white Gaussian noise input, d is a bounded energy input, and z and e are controlled (possibly fictitious) outputs. It is assumed that there is no *a priori*

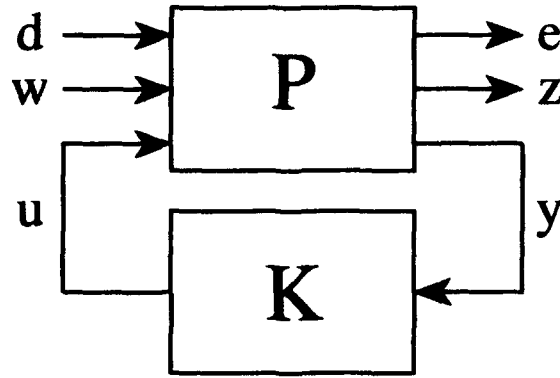


Figure 4.1. General mixed H_2/H_∞ optimization problem

relationship between w and d or z and e . The measured output is y and the control law is $u = K(s)y$.

The mixed H_2/H_∞ problem is to design a controller $K(s)$ such that the transfer function from w to z has minimum energy subject to maintaining the maximum gain of the transfer function from e to d below some predetermined value γ . The former problem is an H_2 optimization problem and the constraint is an H_∞ optimization problem. The full plant $P(s)$ is formed from some underlying plant $G(s)$ augmented with stable weighting transfer functions on the inputs d and w and the outputs e and z . The general form of the system is

$$\begin{bmatrix} e \\ z \\ y \end{bmatrix} = \begin{bmatrix} P_{ed} & P_{ew} & P_{eu} \\ P_{zd} & P_{zw} & P_{zu} \\ P_{yd} & P_{yw} & P_{yu} \end{bmatrix} \begin{bmatrix} d \\ w \\ u \end{bmatrix} \quad (4.1)$$

This system can be reduced to two separate problems: the H_2 problem, which is to find an internally stabilizing controller $K(s)$ that minimizes $\|T_{zw}\|_2$, where

$$T_{zw} = P_{zw} + P_{zu}K(I - P_{yu}K)^{-1}P_{yw} \quad (4.2)$$

and the H_∞ problem, which is to find an internally stabilizing controller $K(s)$ that satisfies $\|T_{ed}\|_\infty \leq \gamma$ for some γ , where

$$T_{ed} = P_{ed} + P_{eu}K(I - P_{yu}K)^{-1}P_{yd} \quad (4.3)$$

To simplify the discussion, the following definitions are made:

$$\underline{\gamma} := \inf_{K \text{ admissible}} \|T_{ed}\|_\infty \quad (4.4)$$

$$\underline{\alpha} := \inf_{K \text{ admissible}} \|T_{zw}\|_2 \quad (4.5)$$

$$K_{2opt} := \text{the unique } K(s) \text{ that makes } \|T_{zw}\|_2 = \underline{\alpha} \quad (4.6)$$

$$\bar{\gamma} := \|T_{ed}\|_\infty \text{ when } K(s) = K_{2opt} \quad (4.7)$$

$$K_{mis} := \text{a solution to the } H_2/H_\infty \text{ problem for some } \gamma > \underline{\gamma} \quad (4.8)$$

$$\gamma^* := \|T_{ed}\|_\infty \text{ when } K(s) = K_{mis} \quad (4.9)$$

$$\alpha^* := \|T_{zw}\|_2 \text{ when } K(s) = K_{mis} \quad (4.10)$$

where the admissible set of controllers is the set of all stabilizing controllers. Furthermore, we will assume the following:

- i. T_{zw} has a finite two-norm which implies P_{zw} is strictly proper
- ii. z cannot be decoupled from w which implies $\underline{\alpha} > 0$
- iii. $P_{zu} \neq 0$ and $P_{yw} \neq 0$
- iv. P_{zu} and P_{yw} have full rank for all $\omega \in \mathfrak{R}$

The assumption i ensures T_{zw} is in H_2 . Assumption ii eliminates the uninteresting case where a controller can completely decouple the output from the input. Assumption iii ensures that the $\|T_{zw}\|_2$ is a function of the controller K . Finally, assumption

iv is a regularity condition on the H_2 problem. It ensures all controls have some direct penalty and there are no perfect measurements.

To characterize the stabilizability of the individual problems, define

$$P_2 := \begin{bmatrix} P_{zw} & P_{zu} \\ P_{yw} & P_{yu} \end{bmatrix} \quad (4.11)$$

$$P_\infty := \begin{bmatrix} P_{ed} & P_{eu} \\ P_{yd} & P_{yu} \end{bmatrix} \quad (4.12)$$

Lemma 4.1.1 *Assume P_{yu} is stabilizable and P_2 , P_∞ , and P are formed by augmenting the plant $G(s)$ with stable weighting transfer functions at the inputs d and w and outputs e and z . Then the following are equivalent:*

- i. K stabilizes P_{yu}
- ii. K stabilizes P_2
- iii. K stabilizes P_∞
- iv. K stabilizes P

Proof: Since no unstable modes are introduced by augmenting stable transfer functions at the input and output, P_{yu} stabilizable implies that P_2 , P_∞ , and P are stabilizable. Thus, from Theorem 2.2.2, i implies ii, iii, and iv. Conversely, ii, iii, and iv each imply i. ■

The mixed H_2/H_∞ problem can be stated as: find a stabilizing controller $K(s)$ which minimizes the two-norm of T_{zw} and satisfies the constraint that the infinity-norm of T_{ed} is less than or equal to some fixed γ . This is a mathematical programming problem with a convex objective function and constraint, but the set of all admissible controllers is not convex. Thus, convex programming cannot be directly applied to solve the problem. However, through the use of the Youla parametrization of all stabilizing controllers, this problem can be transformed into a convex programming

problem. We begin by defining the doubly-coprime factorization of P_{yu} ,

$$P_{yu} = NM^{-1} = \tilde{M}^{-1}\tilde{N} \quad (4.13)$$

and

$$\begin{bmatrix} \tilde{Y} & -\tilde{X} \\ -\tilde{N} & \tilde{M} \end{bmatrix} \begin{bmatrix} M & X \\ N & Y \end{bmatrix} = I \quad (4.14)$$

Thus, the set of all K which stabilize P_{yu} is parametrized over $Q \in H_\infty$ by

$$K = (X + MQ)(Y + NQ)^{-1} \quad (4.15)$$

$$= (\tilde{Y} + Q\tilde{N})^{-1}(\tilde{X} + Q\tilde{M}) \quad (4.16)$$

Letting $K_0 := K(Q = 0) = XY^{-1} = \tilde{Y}^{-1}\tilde{X}$ and defining

$$J = \begin{bmatrix} K_0 & -\tilde{Y}^{-1} \\ Y^{-1} & -Y^{-1}N \end{bmatrix} \quad (4.17)$$

it can be seen that all stabilizing K are formed by a lower fractional transformation of J and Q , $F_\ell(J, Q)$, as shown in Figure 4.2. Notice that the term common to both T_{zw} and T_{ed} is

$$K(I - P_{yu}K)^{-1} = -(X + MQ)\tilde{M} \quad (4.18)$$

Therefore, we can rewrite equation (4.2) as

$$T_{zw} = P_{zw} - P_{zu}X\tilde{M}P_{yw} - P_{zu}MQ\tilde{M}P_{yw} \quad (4.19)$$

$$= T_{1_2} + T_{2_2}QT_{3_2} \quad (4.20)$$

where

$$T_{1_2} = P_{zw} - P_{zu}X\tilde{M}P_{yw} \quad (4.21)$$

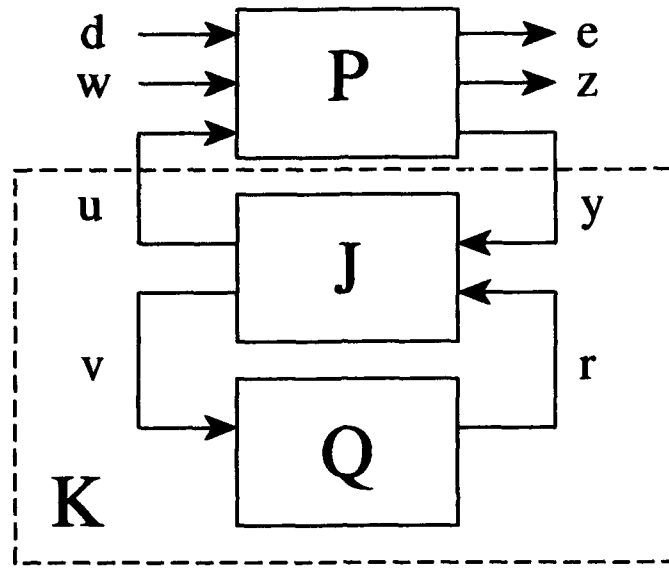


Figure 4.2. Q-parametrization

$$T_{2_2} = -P_{zu}M \quad (4.22)$$

$$T_{3_2} = \tilde{M}P_{yw} \quad (4.23)$$

Similarly, we can rewrite (4.3) as

$$T_{ed} = P_{ed} - P_{eu}X\tilde{M}P_{yd} - P_{zu}MQ\tilde{M}P_{yd} \quad (4.24)$$

$$= T_{1_\infty} + T_{2_\infty}QT_{3_\infty} \quad (4.25)$$

where

$$T_{1_\infty} = P_{ed} - P_{eu}X\tilde{M}P_{yd} \quad (4.26)$$

$$T_{2_\infty} = -P_{eu}M \quad (4.27)$$

$$T_{3_\infty} = \tilde{M}P_{yd} \quad (4.28)$$

It is possible to choose the doubly-coprime factorization such that K_0 is $K_{2_{opt}}$, thus

$$T_{zw}(Q = 0) = T_{1_2} \implies \|T_{1_2}\|_2 = \alpha \quad (4.29)$$

Note that it is not necessary to pick this particular K_0 , it is just convenient for this development. Additionally, for the two-norm of T_{zw} to remain bounded, Q must be restricted to $Q \in H_2$.

Finally, the doubly-coprime factorization of P_{yu} must be found from an n_2 order realization of P_{yu} , where n_2 is the minimal order of P_2 —in particular, from

$$P_2 = \left[\begin{array}{c|cc} A_2 & B_w & B_{u_2} \\ \hline C_z & D_{zw} & D_{zu} \\ \hline C_{y_2} & D_{y_w} & D_{y_{u_2}} \end{array} \right] \quad (4.30)$$

or

$$P_{yu} = C_{y_2}(sI - A_2)^{-1}B_{u_2} + D_{y_{u_2}} \quad (4.31)$$

Now, our problem can be restated as the convex program: Find a $Q \in H_2$ which satisfies

$$\mathcal{P}_{mix} \begin{cases} \alpha = \inf_{Q \in H_2} \|T_{1_2} + T_{2_2}QT_{3_2}\|_2 \\ \text{subject to} \\ \|T_{1_\infty} + T_{2_\infty}QT_{3_\infty}\|_\infty \leq \gamma \end{cases} \quad (4.32)$$

4.2 Uniqueness of the Optimal (Order-Free) H_2/H_∞ Controller

To characterize the optimal controller, we will need the following lemma.

Lemma 4.2.1 *If $T_{zw} \in H_2$, then $\|T_{zw}(Q)\|_2$ is a strictly convex real functional of Q on H_2 .*

Proof: Let $Q_1, Q_2 \in H_2$ and let $\alpha \in (0, 1)$. Then

$$\|T_{1_2} + T_{2_2}[\alpha Q_1 + (1 - \alpha)Q_2]T_{3_2}\|_2$$

$$= \|\alpha T_{1_2} + \alpha T_{2_2} Q_1 T_{3_2} + (1 - \alpha) T_{1_2} + (1 - \alpha) T_{2_2} Q_2 T_{3_2}\|_2 \quad (4.33)$$

$$= \|\alpha [T_{1_2} + T_{2_2} Q_1 T_{3_2}] + (1 - \alpha) [T_{1_2} + T_{2_2} Q_2 T_{3_2}]\|_2 \quad (4.34)$$

$$\leq \alpha \|T_{1_2} + T_{2_2} Q_1 T_{3_2}\|_2 + (1 - \alpha) \|T_{1_2} + T_{2_2} Q_2 T_{3_2}\|_2 \quad (4.35)$$

where equality holds only if the vectors in (4.35) are colinear [46]. However, this implies

$$T_{1_2} + T_{2_2} Q_1 T_{3_2} = \beta (T_{1_2} + T_{2_2} Q_2 T_{3_2}) \quad (4.36)$$

$$\Rightarrow T_{2_2} Q_1 T_{3_2} = (\beta - 1) T_{1_2} + \beta T_{2_2} Q_2 T_{3_2} \quad (4.37)$$

$$\Rightarrow Q_1 = (\beta - 1) T_{2_2}^{-1} T_{1_2} T_{3_2}^{-1} + \beta Q_2 \quad (4.38)$$

but $T_{2_2}^{-1} T_{1_2} T_{3_2}^{-1} \notin H_2$ [39], which implies $Q_1 \notin H_2$ which violates the assumption; thus, a contradiction. Therefore, the two-norm is a strictly convex functional. ■

Armed with the above information we can now show that the optimal mixed controller is unique.

Theorem 4.2.1 *Let $\gamma > \underline{\gamma}$ be given. Then the controller which satisfies the convex program (4.32) is unique. Furthermore, the following hold:*

- i. *if $\gamma \geq \bar{\gamma}$, the resulting controller is the optimal H_2 controller*
- ii. *If $\underline{\gamma} < \gamma \leq \bar{\gamma}$, $\gamma^* = \gamma$ at the optimal (i. e., the solution will satisfy the H_∞ constraint with equality).*

Proof: The problem is a convex program with an active convex constraint. From Lemma 4.2.1, the two-norm is a strictly convex functional over Q , therefore from Theorem 2.6.2, there is a unique $Q \in H_2$ which is the optimal solution to the convex program.

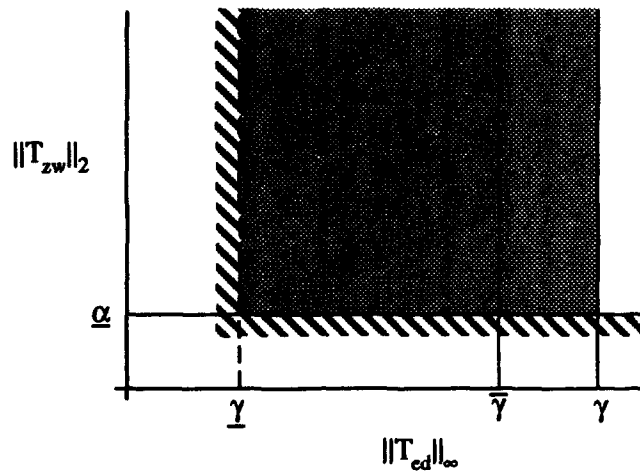


Figure 4.3. Admissible region, $\gamma \geq \bar{\gamma}$

i. Define the Lagrangian

$$\mathcal{L} = \|T_{zw}\|_2 + \lambda(\|T_{ed}\|_\infty - \gamma) \quad (4.39)$$

and assume the solution is not on the constraint boundary, but falls somewhere in admissible region shown as the shaded area in Figure 4.3 (i.e., $\gamma^* < \gamma$). Then, from Theorem 2.6.1, $\lambda = 0$ and (4.39) reduces to

$$\mathcal{L} = \|T_{zw}\|_2 \quad (4.40)$$

The unique controller which satisfies the conditions in Theorem 2.6.1 is $K_{2_{opt}}$ which is in the admissible region; thus, it is the solution.

ii. Let $\underline{\gamma} < \gamma \leq \bar{\gamma}$ and assume $\gamma^* < \gamma$. Again, using Theorem 2.6.1, this implies $\lambda = 0$ and the Lagrangian (4.39) reduces to (4.40). As before, $K_{2_{opt}}$ is the only controller which satisfies the KT conditions. However, as can be seen in Figure 4.4, $K_{2_{opt}}$ is not in the admissible region (shaded area); thus, Theorem 2.6.1 implies $\gamma^* = \gamma$.

■

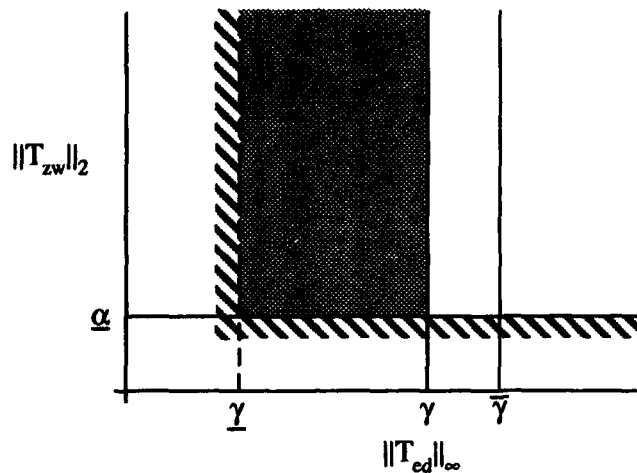


Figure 4.4. Admissible region, $\gamma \leq \bar{\gamma}$

4.3 Dual Approach to H_2/H_∞

The previous section showed the uniqueness of the optimal H_2/H_∞ controller based on a Lagrange multiplier approach. This section will examine the solution to the mixed problem using a minimum norm approach. All of the previous assumptions on the system hold. In addition, for this section only, the system is assumed to be a SISO mixed optimal control problem. This assumption is made to simplify the notation and can be removed. Again, our problem is: Find a controller $K(s)$ which satisfies the following:

- i. $K(s)$ is internally stabilizing
- ii. $\|T_{zw}\|_2$ is minimized
- iii. $\|T_{cd}\|_\infty \leq \gamma$ where $\gamma \in (\underline{\gamma}, \bar{\gamma})$

To investigate the solution to the above problem define a less restrictive problem: Find a controller $K(s)$ which satisfies the following:

- i. $K(s)$ is internally stabilizing
- ii. $\|T_{zw}\|_2$ is minimized
- iii. $\|Q\|_\infty \leq \gamma$ where $\gamma \in (\underline{\gamma}, \bar{\gamma})$

This problem will be solved using minimum norm duality. Furthermore, the problem is related to the mixed norm problem and gives some insight into techniques which might be applied to find a solution to the general problem. To date, however, the full mixed problem has not been solved through this approach.

To begin, the problem is simplified by combining terms in (4.20) to get

$$T_{zw} = T_{1_2} + T_{23_2}Q \quad (4.41)$$

where T_{1_2} and $T_{23_2} = T_{2_2}T_{3_2}$ are determined from the Youla parametrization of the controller. We can now rewrite the problem as: Find $Q \in H_\infty$ such that

$$\alpha = \inf_{\|Q\|_\infty \leq \gamma} \|T_{1_2} + T_{23_2}Q\|_2 \quad (4.42)$$

Using an inner-outer factorization [17] we will transform the problem to a minimum distance from a point (function) in L_2 and convex set in H_2 . Let $T_{23_2} = T_{23_2_i}T_{23_2_o}$, where $T_{23_2_i}$ is a unitary inner function and $T_{23_2_o}$ is a stable and minimum phase outer function. Then,

$$\|T_{1_2} + T_{23_2}Q\|_2 = \|T_{23_2_i}^{-1}T_{1_2} + T_{23_2_o}Q\|_2 \quad (4.43)$$

$$= \|R - X\|_2 \quad (4.44)$$

where $R := T_{23_2_i}^{-1}T_{1_2}$, $S = -T_{23_2_o}$, and $X := SQ$. Furthermore, $\|T_{zw}\|_2$ is finite only if $X \in H_2$ which implies $Q \in H_2$.

Thus, our problem is to find the minimum distance between a point, R , and a convex set in L_2 , where the convex set is defined by the continuous mapping S of an infinity-norm ball in H_2 . Our problem is now to find $Q \in H_2$ which achieves

$$\alpha = \inf_{X \in K} \|R - X\|_2 \quad (4.45)$$

where the set K is defined as

$$K = \{SQ \in H_2 \mid Q \in H_2, \|Q\|_\infty \leq \gamma\} \quad (4.46)$$

From Theorem 2.7.2 we get

$$\alpha = \max_{\|X^*\|_2 \leq 1} [\langle R, X^* \rangle - h(X^*)] \quad (4.47)$$

where $X^* \in L_2^*$, which is the dual of L_2 , $\langle \cdot, \cdot \rangle$ denotes an inner product, and $h(X^*)$ is the support functional for the set K defined by

$$h(X^*) = \sup_{X \in K} \langle X, X^* \rangle \quad (4.48)$$

The first step in solving the minimum distance problem is to determine the support functional $h(X^*)$ of the set K . Since L_2 is a Hilbert space, $L_2 \cong L_2^*$ and functionals can be defined from Theorem 2.7.1 as inner products. With some abuse of notation, the support functional can be written as

$$h(X^*) := \sup_{X \in K} \langle X, X^* \rangle = \sup_{X \in K} \frac{1}{2\pi} \int_{-\infty}^{+\infty} X^*(j\omega) X^*(j\omega) d\omega \quad (4.49)$$

$$\leq \sup_{X \in K} \frac{1}{2\pi} \|Q\|_\infty \int_{-\infty}^{+\infty} |S^*(j\omega) X^*(j\omega)| d\omega \quad (4.50)$$

$$= \frac{\gamma}{2\pi} \int_{-\infty}^{+\infty} |S^*(j\omega) X^*(j\omega)| d\omega. \quad (4.51)$$

Thus, (4.51) is an upper bound on the supremum. To determine if it is actually the desired supremum, we will develop a sequence and see if it approaches the upper bound as its index approaches infinity. Let

$$\{\langle X, X^* \rangle\} = \{\langle X_n, X^* \rangle\} \quad (4.52)$$

where $X_n = SQ_n$ and

$$Q_n = \begin{cases} \gamma \operatorname{sgn}(S^*X^*) & \text{if } \omega \in [-n, n] \\ 0 & \text{otherwise} \end{cases} \quad (4.53)$$

Then

$$\langle X_n, X^* \rangle = \frac{1}{2\pi} \int_{-n}^n Q_n^*(j\omega) S^*(j\omega) X^*(j\omega) d\omega \quad (4.54)$$

$$= \frac{1}{2\pi} \int_{-n}^n \gamma \operatorname{sgn}[S^*(j\omega)X^*(j\omega)] S^*(j\omega) X^*(j\omega) d\omega \quad (4.55)$$

$$= \frac{\gamma}{2\pi} \int_{-n}^n |S^*(j\omega)X^*(j\omega)| d\omega \quad (4.56)$$

which approaches (4.51) as n approaches infinity. Thus, $h(X^*)$ is defined by (4.51).

With this definition the problem becomes

$$\alpha = \max_{\|X^*\|_2 \leq 1} \left[\langle R, X^* \rangle - \frac{\gamma}{2\pi} \int_{-\infty}^{+\infty} |S^*(j\omega)X^*(j\omega)| d\omega \right] \quad (4.57)$$

$$= \max_{\|X^*\|_2 \leq 1} \left[\frac{1}{2\pi} \int_{-\infty}^{+\infty} R^*(j\omega)X^*(j\omega) d\omega - \frac{\gamma}{2\pi} \int_{-\infty}^{+\infty} |S^*(j\omega)X^*(j\omega)| d\omega \right] \quad (4.58)$$

$$\leq \max_{\|X^*\|_2 \leq 1} \left[\frac{1}{2\pi} \int_{-\infty}^{+\infty} (|R(-j\omega)| - \gamma|S(-j\omega)|) |X^*(j\omega)| d\omega \right] \quad (4.59)$$

$$= \max_{\|X^*\|_2 \leq 1} \left[\frac{1}{2\pi} \int_{E_\gamma} (|R(-j\omega)| - \gamma|S(-j\omega)|) |X^*(j\omega)| d\omega \right] \quad (4.60)$$

where E_γ is defined as

$$E_\gamma = \{\omega \in \Re \mid |R(-j\omega)| > \gamma|S(-j\omega)|\} \quad (4.61)$$

Notice, (4.60) will be maximized when X^* is colinear with $(|R(-j\omega)| - \gamma|S(-j\omega)|)$; therefore, X^* has the form

$$X^* = \begin{cases} 0 & \text{if } \omega \in E_\gamma^c \\ c[|R(-j\omega)| - \gamma|S(-j\omega)|] & \text{if } R(-j\omega) > \gamma|S(-j\omega)| \\ -c[|R(-j\omega)| - \gamma|S(-j\omega)|] & \text{if } -R(-j\omega) > \gamma|S(-j\omega)| \end{cases} \quad (4.62)$$

where $c := \frac{1}{\| |R(-j\omega)| - \gamma|S(-j\omega)| \|_2^{-1}}$ to make $\|X^*\|_2 = 1$. Thus, we get

$$\alpha = \frac{1}{2\pi} \int_{E_\gamma} c(|R(-j\omega)| - \gamma|S(-j\omega)|)^2 \quad (4.63)$$

$$= \frac{\int_{E_\gamma} [|R(-j\omega)| - \gamma|S(-j\omega)|]^2}{\left\{ 2\pi \int_{E_\gamma} [(|R(-j\omega)| - \gamma|S(-j\omega)|)^* (|R(-j\omega)| - \gamma|S(-j\omega)|)] \right\}^{\frac{1}{2}}} \quad (4.64)$$

Equation (4.64) gives a method of determining the optimal two-norm of a mixed control problem for a given γ . However, it does not provide a direct method for determining the optimal controller. If the infimum in (4.42) is achieved for some $Q_0 \in H_2$, we can use the alignment condition in Theorem 2.7.2 to determine the unique Q_0 . In this case,

$$\langle (R - X_0), X_0^* \rangle = \|R - X_0\|_2 \|X_0^*\|_2 \quad (4.65)$$

where $X_0 = SQ_0$. However, from the definition of X^* , it can be seen that the alignment condition will force Q_0 to be a piecewise continuous function. This implies that the controller which minimizes the two-norm of T_{zw} and satisfies the H_∞ constraint will be piecewise continuous and not an \mathfrak{RH}_2 function. However, it will be the limit of a sequence of \mathfrak{RH}_2 functions since H_2 is the closure of \mathfrak{RH}_2 .

The above derivation is based on the assumptions $T_{1\infty} = 0$ and $T_{2\infty}T_{3\infty} = I$. Relaxing these conditions, we return to the original SISO mixed H_2/H_∞ problem.

This can be written as: find the $Q \in H_2$ which achieves

$$\alpha = \inf_{\|T_{1\infty} + T_{23\infty}Q\|_{\infty} \leq \gamma} \|T_{12} + T_{23_2}Q\|_2 \quad (4.66)$$

As before, use an inner-outer factorization to get $T_{23_2} = T_{23_2_i}T_{23_2_o}$ and $T_{23\infty} = T_{23\infty_i}T_{23\infty_o}$. Define $R := T_{23_2_i}^{-1}T_{12}$, $S := -T_{23_2_o}$, $U := T_{23\infty_i}^{-1}T_{1\infty}$, and $V := -T_{23\infty_o}$. Then (4.65) becomes

$$\alpha = \inf_{\|U+VQ\|_{\infty} \leq \gamma} \|R - SQ\|_2 \quad (4.67)$$

Once again, this is a minimum distance problem between a function and a convex set in L_2 . An equivalent problem in L_2 is

$$\alpha = \inf_{X \in K} \|R - X\|_2 \quad (4.68)$$

where

$$K := \{SQ \in H_2 \mid Q \in H_2, \|U + VQ\|_{\infty} \leq \gamma\} \quad (4.69)$$

Applying Theorem 2.7.2, the problem is transformed to

$$\alpha = \max_{\|X^*\|_2 \leq 1} [\langle R, X^* \rangle - h(X^*)] \quad (4.70)$$

The problem now is to find the support functional $h(X^*)$. This is still an open problem. It would appear that this would be a simple extension of the previous development since the infinity-norm constraint is an affine function of Q . However, since the constraint is an infinity-norm ball in L_2 , the definition of the support functional results in a complex inner product. Further investigation into the problem is necessary to complete the theoretical approach for designing the optimal controller for a mixed problem.

4.4 Summary

In this chapter the mixed H_2/H_∞ optimal control problem was set up and parametrized over a convex set $Q \in H_2$. Using this parametrization we were able to show that the optimal controller for a given γ is unique. The optimal solution was shown to be $K_{2,op}$ if $\gamma \geq \bar{\gamma}$. Furthermore, the optimal solution must satisfy the H_∞ constraint with equality if $\underline{\gamma} < \gamma \leq \bar{\gamma}$. Finally, for the SISO mixed problem, the special case $T_{1\infty} = 0$ and $T_{2\infty}T_{3\infty} = I$ was investigated using a dual minimum norm approach. It was shown that the optimal controller in this case is piecewise continuous and cannot be represented by a rational function.

One must remember that the optimal controller discussed thus far is based on a free controller order; if the order is fixed to some arbitrary value, the mixed solution may not necessarily be able to achieve the same two-norm as the optimal order controller. However, for applications, a fixed-order controller of low order is desirable. The next chapter will develop the necessary conditions for an *optimal fixed-order* controller for the mixed H_2/H_∞ optimization problem.

V. Fixed-Order H_2/H_∞ Optimal Control

The previous chapter characterized the optimal (order-free) controller for the mixed H_2/H_∞ optimization problem. While the controller order has not been determined analytically, numerical results suggest the optimal order is larger than the order of the full system including all the H_2 and H_∞ weights. Wells and Ridgely [47] have conjectured the optimal controller order is infinite. This conjecture is based partly on the evolution of the loop shape of the closed-loop system as the order is increased. For control applications, infinite order controllers are impractical. In fact, it is desirable for the controller order to be as low as possible. However, a trade-off is usually necessary between the controller order and system performance and robustness. This chapter will develop the necessary conditions for an optimal fixed-order mixed controller.

Ridgely, *et al* [10], developed a fixed-order solution for the general mixed H_2/H_∞ problem with output feedback. However, their development is based on a controller order equal to the order of the underlying system augmented with both the H_2 weightings and the H_∞ weightings. Maintaining the lowest possible controller order is an important consideration in control synthesis. Therefore, the first objective of this development is to allow the controller order to be reduced to as low as that of the system augmented with only the H_2 weights. This objective has the additional advantage of allowing complicated (i.e., increased order) H_∞ weightings to be introduced into the problem without increasing the controller order directly. The increased freedom in selecting H_∞ constraint weightings allows a more desirable final loop shape to be used in the model matching problem. However, there is still a penalty to be paid in computation time for increased order constraints, as will be seen in the next chapter. Furthermore, the H_2 order solution may not be capable of achieving the desired model match, but there is still a trade-off available as the order

is increased from that of the H_2 problem to that of the system augmented with both the H_2 weightings and the H_∞ weightings.

Another assumption in [10] is that the constraint forms a regular H_∞ problem. In the original formulation of the H_∞ problem, Zames [42] desired to minimize the sensitivity of a closed-loop system. However, this results in a singular H_∞ optimization problem (one in which the control usage is not directly penalized and/or perfect measurements are allowed). In general, this problem can be treated sub-optimally by placing limits on the controls and/or by adding disturbances into the measurements. In the recent literature, this problem has received much attention. Copeland and Safonov [48] take a generalized system approach in which this problem is solved by perturbing the singular problem to a neighboring regular H_∞ problem. They showed that the perturbed solution converged to the solution of the singular problem as the perturbation approached zero. Stoorvogel [49] developed conditions which must exist for the singular H_∞ control problem with measurement feedback to be solvable, and his solution is equivalent to the above work. Finally, Juang, *et al* [50], use the structural algorithm [51] to transform the singular H_∞ problem into a regular one. However, all the above techniques result in a controller which is not guaranteed to be proper, and in general, will be improper for the optimal H_∞ controller. Therefore, the second objective of this chapter is to solve the mixed H_2/H_∞ problem as formulated by [10] with the regularity assumption on the H_∞ constraint relaxed. In the mixed H_2/H_∞ problem, the objective function (the H_2 problem) always results in a strictly proper controller. Thus, appending singular H_∞ constraints will not lead to improper controllers. It should be noted that this problem has been addressed in the literature by Juang, *et al* [50], but their solution only provides an overbound to the two-norm.

Finally, to simplify the development, Ridgely, *et al* [10], assumed there was no feedforward term in the H_∞ constraint. However, this assumption restricts the H_∞ constraint weightings to strictly proper transfer functions. To accomplish this, the

weights must be rolled off at high frequency. However, consider a model matching problem for the complementary sensitivity. There is no physical reason to roll off the high frequency weight. In fact, it is desirable to maintain a reasonable weight at high frequency to ensure unmodeled high frequency modes are not ignored. Thus, the feedforward assumption is an unnecessary restriction which limits the options of the designer. Therefore, the final objective of this chapter is to reformulate the mixed problem with the feedforward assumption on the H_∞ problem in [10] relaxed. This will allow proper H_∞ weights.

5.1 State Space Formulation

Consider the system in Figure 5.1, where d and w are exogenous inputs and e and z are the controlled outputs. The measured output is y and u is the control, where the control law is $u = Ky$. It is assumed, in general, that there is no relationship between e and z or d and w . The input w is unit intensity zero mean, white-Gaussian noise and the input d is of bounded energy. The transfer function P is formed by augmenting stable weighting transfer functions from an H_2 problem (w to z) and an H_∞ problem (d to e) around the original system $G(s)$, resulting in the state space form

$$P = \left[\begin{array}{c|ccc} \tilde{A} & \tilde{B}_d & \tilde{B}_w & \tilde{B}_u \\ \hline \tilde{C}_e & \tilde{D}_{ed} & \tilde{D}_{ew} & \tilde{D}_{eu} \\ \tilde{C}_z & \tilde{D}_{zd} & \tilde{D}_{zw} & \tilde{D}_{zu} \\ \tilde{C}_y & \tilde{D}_{yd} & \tilde{D}_{yw} & \tilde{D}_{yu} \end{array} \right] \quad (5.1)$$

where $(\tilde{\cdot})$ are the matrices associated with the system augmented by the H_2 and H_∞ weights. The order of the individual H_2 and H_∞ problems will usually be less than that of P . The state space equations of the individual H_2 and H_∞ problems can be written as

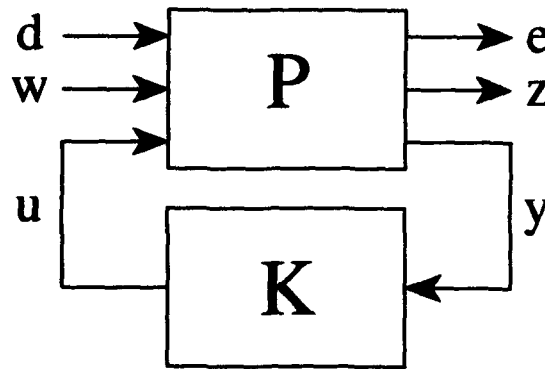


Figure 5.1. General mixed H_2/H_∞ optimization problem

$$\begin{aligned} \dot{x}_2 &= A_2 x_2 + B_w w + B_{u_2} u \\ z &= C_z x_2 + D_{zw} w + D_{zu} u \end{aligned} \quad (5.2)$$

$$\begin{aligned} y &= C_{y_2} x_2 + D_{y_2} w + D_{y_2} u \\ \dot{x}_\infty &= A_\infty x_\infty + B_d d + B_{u_\infty} u \\ e &= C_e x_\infty + D_{ed} d + D_{eu} u \end{aligned} \quad (5.3)$$

$$y = C_{y_\infty} x_\infty + D_{y_d} d + D_{y_u} u$$

where x_2 is the state vector for the underlying H_2 problem and x_∞ is the state vector for the underlying H_∞ problem.

The mixed H_2/H_∞ problem is: Find a controller $K(s)$ which satisfies

$$\inf_{K \text{ stabilizing}} \|T_{zw}\|_2 \text{ subject to } \|T_{ed}\|_\infty \leq \gamma$$

where

$$T_{zw} = C_z (sI - A_2)^{-1} B_w + D_{zw} \quad (5.4)$$

$$T_{ed} = C_e(sI - A_{\infty})^{-1}B_d + D_{ed} \quad (5.5)$$

are the closed-loop transfer functions from w to z and e to d , respectively. The various matrices in (5.4) and (5.5) will be defined shortly.

To solve this problem, the following assumptions are made:

- i. $D_{zw} = 0$
- ii. $D_{yu} = 0$
- iii. (A_2, B_{u_2}) stabilizable, (C_{y_2}, A_2) detectable
- iv. $D_{zu}^T D_{zu}$ full rank, $D_{yw} D_{yw}^T$ full rank
- v. $\begin{bmatrix} A_2 - j\omega I & B_{u_2} \\ C_z & D_{zu} \end{bmatrix}$ has full column rank for all ω
- vi. $\begin{bmatrix} A_2 - j\omega I & B_w \\ C_{y_2} & D_{yw} \end{bmatrix}$ has full row rank for all ω

Assumptions i–vi are made for the reasons given in Section 3.2 for an H_2 problem. Since the H_2 problem is a regular problem, it will guarantee a proper stabilizing controller will result; therefore, the H_{∞} assumptions from Section 3.3 are relaxed. In particular, D_{ed} is *not restricted to zero* and *no assumptions* are made as to the ranks of D_{eu} and D_{yd} . Furthermore, *no restriction* is placed on $j\omega$ -axis zeros of the associated Hamiltonians. Therefore, singular and non-strictly proper H_{∞} constraints are allowed in this development.

The controller in Figure 5.1 is given by

$$\begin{aligned} \dot{x}_c &= A_c x_c + B_c y \\ u &= C_c x_c + D_c y \end{aligned} \quad (5.6)$$

Combining (5.2) with (5.6) produces the closed-loop state space equations for T_{zw} ,

$$\begin{aligned}\dot{x}_2 &= (A + B_{u_2} D_c C_{y_2}) x_2 + B_{u_2} C_c x_c + (B_w + B_{u_2} D_c D_{yw}) w \\ \dot{x}_c &= B_c C_{y_2} x_2 + A_c x_c + B_c D_{yw} w \\ z &= (C_z + D_{zu} D_c C_{y_2}) x_2 + D_{zu} C_c x_c + D_{zu} D_c D_{yw} w\end{aligned}\tag{5.7}$$

Notice that $D_{zu} D_c D_{yw}$ must be identically zero for the two-norm of T_{zw} to be finite; therefore, assumption iv implies $D_c = 0$. Thus, we can assume without loss of generality that the controller K is strictly proper. It should be noted that the set of admissible fixed-order controllers may not achieve the same minimum value of the infinity-norm of T_{ed} as the set of all stabilizing controllers. Therefore, $\underline{\gamma}$ may not be the same as in the optimal order case.

Closing the loop of our system we get

$$\begin{aligned}\dot{x}_2 &= \mathcal{A}_2 x_2 + B_w w \\ z &= C_z x_2 \\ \dot{x}_{\infty} &= \mathcal{A}_{\infty} x_{\infty} + B_d d \\ e &= C_e x_{\infty} + D_{ed} d\end{aligned}\tag{5.8}$$

where

$$x_2 = \begin{bmatrix} x_2 \\ x_c \end{bmatrix}\tag{5.9}$$

$$x_{\infty} = \begin{bmatrix} x_{\infty} \\ x_c \end{bmatrix}\tag{5.10}$$

$$\mathcal{A}_2 = \begin{bmatrix} A_2 & B_{u_2} C_c \\ B_c C_{y_2} & A_c \end{bmatrix}\tag{5.11}$$

$$A_{\infty} = \begin{bmatrix} A_{\infty} & B_{u_{\infty}} C_c \\ B_c C_{y_{\infty}} & A_c \end{bmatrix} \quad (5.12)$$

$$B_w = \begin{bmatrix} B_w \\ B_c D_{yw} \end{bmatrix} \quad (5.13)$$

$$B_d = \begin{bmatrix} B_d \\ B_c D_{yd} \end{bmatrix} \quad (5.14)$$

$$C_z = \begin{bmatrix} C_z & D_{zu} C_c \end{bmatrix} \quad (5.15)$$

$$C_e = \begin{bmatrix} C_e & D_{eu} C_c \end{bmatrix} \quad (5.16)$$

$$D_{ed} = D_{ed} \quad (5.17)$$

5.2 The Lagrangian and Necessary Conditions

The mixed H_2/H_{∞} problem is now to determine a $K(s)$ such that:

- i. A_z and A_{∞} are stable
- ii. $\|T_{ed}\|_{\infty} \leq \gamma$ for some given $\gamma > \underline{\gamma}$
- iii. $\|T_{zw}\|_2$ is minimized.

The following theorem will be necessary for the development of this problem.

Theorem 5.2.1 *Let (A_c, B_c, C_c) be given and assume there exists a $Q_{\infty} = Q_{\infty}^T \geq 0$ satisfying*

$$A_{\infty} Q_{\infty} + Q_{\infty} A_{\infty}^T + (Q_{\infty} C_e^T + B_d D_{ed}^T) R^{-1} (Q_{\infty} C_e^T + B_d D_{ed}^T)^T + B_d B_d^T = 0 \quad (5.18)$$

where $R = (\gamma^2 I - D_{ed} D_{ed}^T) > 0$. Then the following are equivalent:

- i. (A_{∞}, B_d) is stabilizable

ii. \mathcal{A}_∞ is stable

iii. \mathcal{A}_2 is stable.

Moreover, if the above hold then the following are true:

iv. $\|T_{ed}\|_\infty \leq \gamma$

v. the two-norm of the transfer function T_{zw} is given by

$$\|T_{zw}\|_2^2 = \text{tr}[C_z Q_2 C_z^T] = \text{tr}[Q_2 C_z^T C_z]$$

where $Q_2 = Q_2^T \geq 0$ is the solution to the Lyapunov equation

$$\mathcal{A}_2 Q_2 + Q_2 \mathcal{A}_2^T + B_w B_w^T = 0$$

vi. all real symmetric solutions Q_∞ of (5.18) are positive semidefinite

vii. there exists a unique minimal solution Q_∞ to (5.18) in the class of real symmetric solutions

viii. Q_∞ is the minimal solution of (5.18) iff

$$\text{Re}[\lambda_i(\mathcal{A}_\infty + B_d D_{ed}^T R^{-1} C_e + Q_\infty C_e^T R^{-1} C_e)] \leq 0 \text{ for all } i$$

ix. $\|T_{ed}\|_\infty < (\leq) \gamma$ iff $\text{Re}[\lambda_i(\mathcal{A}_\infty + B_d D_{ed}^T R^{-1} C_e + Q_\infty C_e^T R^{-1} C_e)] < (\leq) 0$ where Q_∞ is the minimal solution to (5.18).

Proof: i \Rightarrow ii: From the dual of Theorem 2.5.7, $(\mathcal{A}_\infty, B_d)$ stabilizable implies \mathcal{A}_∞ is stable. ii \Rightarrow i: \mathcal{A}_∞ stable implies $(\mathcal{A}_\infty, B_d)$ stabilizable. ii \Leftrightarrow iii: Implication comes directly from Lemma 4.1.1 and the definition of internally stability. With \mathcal{A} stable, iv comes directly from Theorem 2.5.11. v is directly from the discussion of two-norms in Section 2.3.1. vi is from the dual of Theorem 2.5.6. vii and viii come from the dual of Theorem 2.5.5. Finally, ix follows from the duals of Theorems 2.5.5, 2.5.8, 2.5.9, and 2.5.10. ■

The key result of this theorem is that, given a controller which is closed-loop stable for the H_2 problem, we can determine the minimum level of the H_∞ constraint by determining the minimum value of γ for which a positive semidefinite solution to (5.18) exists.

Using Theorem 5.2.1 the mixed problem can be restated as: Determine the $K(s)$ which minimizes

$$J(A_c, B_c, C_c) = \text{tr}[Q_2 C_z^T C_z] \quad (5.19)$$

where Q_2 is the real, symmetric, positive semidefinite solution to

$$A_2 Q_2 + Q_2 A_2^T + B_w B_w^T = 0 \quad (5.20)$$

and such that

$$A_\infty Q_\infty + Q_\infty A_\infty^T + (Q_\infty C_e^T + B_d D_{ed}^T) R^{-1} (Q_\infty C_e^T + B_d D_{ed}^T)^T + B_d B_d^T = 0 \quad (5.21)$$

has a real, symmetric, positive semidefinite solution. To solve this minimization problem with two equality constraints, a Lagrange multiplier approach is used. The Lagrangian is

$$\begin{aligned} \mathcal{L} = & \text{tr}[Q_2 C_z^T C_z] + \text{tr}\{[A_2 Q_2 + Q_2 A_2^T + B_w B_w^T] \mathcal{X}\} \\ & + \text{tr}\{[A_\infty Q_\infty + Q_\infty A_\infty^T + (Q_\infty C_e^T + B_d D_{ed}^T) R^{-1} (Q_\infty C_e^T + B_d D_{ed}^T)^T \\ & + B_d B_d^T] \mathcal{Y}\} \end{aligned} \quad (5.22)$$

where \mathcal{X} and \mathcal{Y} are symmetric Lagrange multiplier matrices. This approach is similar to the one used by Ridgely, *et al* [10], but it incorporates the feedforward (D_{ed}) term. Furthermore, Theorem 5.2.1 allows the case where the H_∞ constraint is singular.

The first order necessary conditions for the minimum of this Lagrangian are

$$\frac{\partial \mathcal{L}}{\partial A_c} = X_{12}^T Q_{12} + X_2 Q_2 + Y_{12}^T Q_{ab} + Y_2 Q_b = 0 \quad (5.23)$$

$$\begin{aligned} \frac{\partial \mathcal{L}}{\partial B_c} = & X_{12}^T Q_1 C_{v_2}^T + X_2 Q_{12}^T C_{v_2}^T + X_{12}^T V_{12} + X_2 B_c V_2 + Y_{12}^T Q_a C_{v_\infty}^T \\ & + Y_2 Q_{ab}^T C_{v_\infty}^T + Y_{12}^T V_{ab} + Y_2 B_c V_b + (Y_{12}^T Q_a + Y_2 Q_{ab}^T) C_e^T M \\ & + (Y_{12}^T Q_{ab} + Y_2 Q_b) C_c^T D_{eu}^T M = 0 \end{aligned} \quad (5.24)$$

$$\begin{aligned} \frac{\partial \mathcal{L}}{\partial C_c} = & B_{u_2}^T X_1 Q_{12} + B_{u_2}^T X_{12} Q_2 + R_{12}^T Q_{12} + R_2 C_c Q_2 + B_{u_\infty}^T Y_1 Q_{ab} \\ & + B_{u_\infty}^T Y_{12} Q_b + R_{ab}^T Q_a Y_1 Q_{ab} + R_{ab}^T Q_a Y_{12} Q_b + R_{ab}^T Q_{ab} Y_{12}^T Q_{ab} \\ & + R_{ab}^T Q_{ab} Y_2 Q_b + R_b C_c Q_{ab}^T Y_1 Q_{ab} + R_b C_c Q_b Y_{12}^T Q_{ab} \\ & + R_b C_c Q_{ab}^T Y_{12} Q_b + R_b C_c Q_b Y_2 Q_b \\ & + P_1(Y_1 Q_{ab} + Y_{12} Q_b) + P_2(Y_{12}^T Q_{ab} + Y_2 Q_b) = 0 \end{aligned} \quad (5.25)$$

$$\frac{\partial \mathcal{L}}{\partial \mathcal{X}} = A_2 Q_2 + Q_2 A_2^T + B_w B_w^T = 0 \quad (5.26)$$

$$\frac{\partial \mathcal{L}}{\partial Q_2} = A_2^T \mathcal{X} + \mathcal{X} A_2 + C_z^T C_z = 0 \quad (5.27)$$

$$\begin{aligned} \frac{\partial \mathcal{L}}{\partial \mathcal{Y}} = & A_\infty Q_\infty + Q_\infty A_\infty^T + (Q_\infty C_e^T + B_d D_{ed}^T) R^{-1} (Q_\infty C_e^T + B_d D_{ed}^T)^T \\ & + B_d B_d^T = 0 \end{aligned} \quad (5.28)$$

$$\begin{aligned} \frac{\partial \mathcal{L}}{\partial Q_\infty} = & (A_\infty + B_d D_{ed}^T R^{-1} C_e + Q_\infty C_e^T R^{-1} C_e)^T \mathcal{Y} \\ & + \mathcal{Y} (A_\infty + B_d D_{ed}^T R^{-1} C_e + Q_\infty C_e^T R^{-1} C_e) = 0 \end{aligned} \quad (5.29)$$

where

$$M = R^{-1} D_{ed} D_{yd}^T \quad (5.30)$$

$$P_1 = D_{eu}^T R^{-1} D_{ed} B_d^T \quad (5.31)$$

$$P_2 = D_{eu}^T M B_c^T \quad (5.32)$$

$$Q_2 = \begin{bmatrix} Q_1 & Q_{12} \\ Q_{12}^T & Q_2 \end{bmatrix} \quad (5.33)$$

$$\mathcal{X} = \begin{bmatrix} X_1 & X_{12} \\ X_{12}^T & X_2 \end{bmatrix} \quad (5.34)$$

$$Q_\infty = \begin{bmatrix} Q_a & Q_{ab} \\ Q_{ab}^T & Q_b \end{bmatrix} \quad (5.35)$$

$$\mathcal{Y} = \begin{bmatrix} Y_1 & Y_{12} \\ Y_{12}^T & Y_2 \end{bmatrix} \quad (5.36)$$

$$\begin{aligned} B_w B_w^T &= \begin{bmatrix} B_w \\ B_c D_{yw} \end{bmatrix} \begin{bmatrix} B_w^T & D_{yw}^T B_c^T \end{bmatrix} \\ &= \begin{bmatrix} V_1 & V_{12} B_c^T \\ B_c V_{12}^T & B_c V_2 B_c^T \end{bmatrix} \end{aligned} \quad (5.37)$$

$$\begin{aligned} B_d (D_{ed}^T R^{-1} D_{ed} + I) B_d^T &= \begin{bmatrix} B_d \\ B_c D_{yd} \end{bmatrix} (D_{ed}^T R^{-1} D_{ed} + I) \begin{bmatrix} B_d^T & D_{yd}^T B_c^T \end{bmatrix} \\ &= \begin{bmatrix} V_a & V_{ab} B_c^T \\ B_c V_{ab}^T & B_c V_b B_c^T \end{bmatrix} \end{aligned} \quad (5.38)$$

$$\begin{aligned}
C_z^T C_z &= \begin{bmatrix} C_z^T \\ C_c^T D_{zu}^T \end{bmatrix} \begin{bmatrix} C_z & D_{zu} C_c \end{bmatrix} \\
&= \begin{bmatrix} R_1 & R_{12} C_c \\ C_c^T R_{12}^T & C_c^T R_2 C_c \end{bmatrix} \tag{5.39}
\end{aligned}$$

$$\begin{aligned}
C_e^T R^{-1} C_e &= \begin{bmatrix} C_e^T \\ C_c^T D_{eu}^T \end{bmatrix} R^{-1} \begin{bmatrix} C_e & D_{eu} C_c \end{bmatrix} \\
&= \begin{bmatrix} R_a & R_{ab} C_c \\ C_c^T R_{ab}^T & C_c^T R_b C_c \end{bmatrix} \tag{5.40}
\end{aligned}$$

These equations have not been solved analytically but do provide some insight into the nature of the solution. In particular, (5.29) implies that either $\mathcal{Y} = 0$ or $(A_\infty + B_d D_{ed}^T R^{-1} C_e + Q_\infty C_e^T R^{-1} C_e)$ is neutrally stable. The former condition means the solution is off the boundary of the H_∞ constraint (where the boundary is defined by the constraint being satisfied with equality), and the latter condition implies the solution lies on the boundary of the H_∞ constraint and Q_∞ is the neutrally stabilizing solution for the H_∞ Riccati equation (5.21). This relation will be used to develop the solution to the problem.

5.3 H_2 Order or Greater Order Solution

The order of the controller is now fixed to an order greater than or equal to the order of the underlying H_2 problem, n_2 , and the mixed H_2/H_∞ problem is solved. Since the controller order is greater than or equal to n_2 , the unique optimal solution $K_{2,opt}$ is admissible and the H_∞ constraint achieves an infinity-norm of $\bar{\gamma}$ with this controller. Thus, for the mixed H_2/H_∞ problem with $\gamma \geq \bar{\gamma}$ the optimal controller is simply the H_2 optimal controller. Similarly, no controller of any order exists which can reduce γ below the level of the optimal H_∞ controller, $\underline{\gamma}$; therefore, for the mixed H_2/H_∞ problem, no solution exists for $\gamma < \underline{\gamma}$. Finally, the two-norm of the

H_2 problem associated with the optimal H_∞ controller is, in general, infinite. Thus, the only region remaining is $\underline{\gamma} < \gamma < \bar{\gamma}$.

Returning to the last of the first order necessary conditions (5.29), the solution to the problem must either lie on the boundary, $\gamma^* = \gamma$, or it must be off the boundary, $\underline{\gamma} < \gamma^* < \gamma$. The latter condition results in $\mathcal{Y} = 0$ and the Lagrangian (5.22) reduces to

$$\mathcal{L} = tr[Q_2 C_2^T C_2] + tr\{[A_2 Q_2 + Q_2 A_2^T + B_w B_w^T] \mathcal{X}\} \quad (5.41)$$

which is the Lagrangian associated with the H_2 optimization problem. These facts lead to the following theorem.

Theorem 5.3.1 *Assume $n_c \geq n_2$. Then the following hold:*

- i. *If $\gamma < \underline{\gamma}$, no solution to the mixed H_2/H_∞ problem exists*
- ii. *If $\underline{\gamma} < \gamma \leq \bar{\gamma}$, K_{mix} is such that $\gamma^* = \gamma$*
- iii. *If $\gamma \geq \bar{\gamma}$, $K_{2_{opt}}$ is the solution to the mixed H_2/H_∞ problem.*

Proof:

- i. Assume $\gamma < \underline{\gamma}$. Then there is no controller which can satisfy the H_∞ constraint.
- ii. Assume $\underline{\gamma} < \gamma \leq \bar{\gamma}$ and $\gamma^* < \gamma$. This implies $\mathcal{Y} = 0$ and the Lagrangian (5.22) reduces to (5.41). From Lemma 1 in [10], the only controller which satisfies the first order necessary conditions for a minimum of (5.41) is the unique $K_{2_{opt}}$. However, this solution lies outside the admissible region; thus, a contradiction. Therefore, $\gamma^* = \gamma$.
- iii. Assume $\gamma \geq \bar{\gamma}$ and $\gamma^* < \gamma$. Again, this implies $\mathcal{Y} = 0$ and the optimal solution is $K_{2_{opt}}$, which is admissible. If $\gamma = \bar{\gamma}$, the Lagrangian reduces to (5.41) and $K_{2_{opt}}$ is the optimal solution.

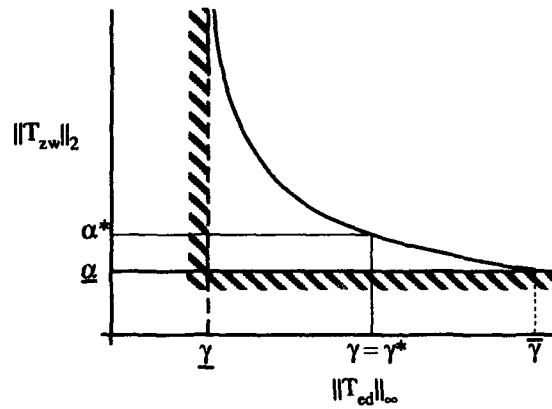


Figure 5.2. Typical mixed H_2/H_∞ α versus γ curve

For a controller with order greater than or equal to the order of the H_2 problem, the solution to the mixed H_2/H_∞ problem with $\underline{\gamma} < \gamma < \bar{\gamma}$ lies on the boundary of the H_∞ constraint, $\gamma^* = \gamma$. Moreover, for $\underline{\gamma} < \gamma \leq \bar{\gamma}$, Theorem 5.3.1 implies there are no extrema except those on the boundary of the H_∞ constraint. Thus in this region, α^* is a monotonically decreasing function of γ as shown in Figure 5.2. Finally, the solution to the Riccati equation (5.21) must be the neutrally stabilizing solution. The following theorem states this connection formally.

Theorem 5.3.2 Assume A is stable and $R = (\gamma^2 I - D_{ed} D_{ed}^T) > 0$. If there exists a $Q_\infty \geq 0$ satisfying

$$\mathcal{A}_\infty Q_\infty + Q_\infty \mathcal{A}_\infty^T + (Q_\infty C_e^T + B_d D_{ed}^T) R^{-1} (Q_\infty C_e^T + B_d D_{ed}^T)^T + B_d B_d^T = 0 \quad (5.42)$$

then the following are equivalent:

- i. $\|T_{ed}\|_\infty = \gamma$
- ii. $(\mathcal{A}_\infty + B_d D_{ed}^T R^{-1} C_e + Q_\infty C_e^T R^{-1} C_e)$ is neutrally stable

Furthermore, in this case Q_∞ is unique.

Proof: This is directly from Theorems 2.5.9, 2.5.10, and 2.5.11 and Theorem 5 in [10]. ■

5.4 Summary

This chapter developed the first order necessary conditions for a fixed-order mixed controller. The assumptions made in previous work were relaxed to allow singular H_∞ constraints and those with a feedforward term. Further, the order of the controller can be reduced to as low as the H_2 order. Finally, the necessary conditions were used to show that the controller must satisfy the H_∞ constraint with equality whenever the constraint is active (and feasible). Currently, there is no way of applying these conditions directly to find analytic solutions to the mixed H_2/H_∞ problem. In the next chapter a numerical approach, based on the results in this chapter, will be developed for the mixed problem.

VI. Numerical Approach

The previous two chapters characterized the optimal (order-free) solution and determined the necessary conditions for a fixed-order solution. However, the development thus far has not provided a technique for synthesizing controllers. This chapter will develop numerical approaches to the mixed problem which will approach an optimal fixed-order solution. The resulting controller is usually *super-optimal*, a controller which does not satisfy the constraint but is as close as numerically possible to the desired solution. *Sub-optimal* solutions, those which satisfy the constraint, but are not optimal, can also be found in many cases.

Ridgely, *et al* [9], developed a numerical method for synthesizing solutions to the general mixed H_2/H_∞ optimization problem. The technique is based on a homotopy method. A connection between the H_∞ central controller (the controller found by the method in Section 3.3 with $Q=0$) and the mixed controller is used to develop a new performance index

$$J_\mu = (1 - \mu) \|T_{zw}\|_2^2 + \mu \operatorname{tr}[Q_\infty C_e^T C_e] \quad (6.1)$$

where $\mu \in (0, 1]$. As μ is varied from one to zero, the resulting controller approaches the desired mixed controller. For $\mu = 1$, the optimal controller is the central H_∞ controller. Using this as an initial condition, μ is decreased and a new controller is found which minimizes J_μ using a Davidon-Fletcher-Powell (DFP) method [37]. This process is continued until the two-norm is converged.

There are several drawbacks to Ridgely's numerical solution to the H_2/H_∞ control problem. First, this method requires a considerable amount of computation time due to a DFP search being accomplished for each increment of the homotopy parameter μ . Furthermore, each run produces only a single controller for a fixed γ on the curve shown in Figure 5.2. The computation time required to find one point

on the curve is on the order of one week. Thus, the first objective of this chapter is to develop a numerical approach which reduces the computation time.

Another limitation of Ridgely's approach is it assumes the controller order is equal to or greater than the plant augmented with the H_2 and H_∞ weights. In addition, the method assumes the H_∞ constraint is strictly proper. As was discussed in the previous chapter, there are several reason why these assumptions need to be relaxed. Therefore, the next two objectives are to reduce the order of the controller to as low as the H_2 problem and to incorporate a feedforward term in the H_∞ constraint.

Finally, the greatest limitation of Ridgely's method is it is based on the central controller. Therefore, it does not allow singular H_∞ constraints, since the central controller may not be strictly proper (or even proper) if the underlying H_∞ constraint is singular, this poses a serious problem if the H_∞ constraint is singular. As we saw in the last chapter, this places a limitation on the designer if only regular H_∞ constraints are allowed. Therefore, the last objective of this chapter will be to develop a method which allows singular H_∞ constraints.

Two numerical methods will be developed in this chapter—one will treat the H_∞ constraint as an equality constraint and the other will treat it as an inequality constraint. Furthermore, methods of computing the gradients for the objectives and constraints will be discussed. Finally, an F-16 longitudinal control design problem will be used to demonstrate the numerical approach.

6.1 Numerical Method

An alternative method for solving this problem was motivated by Figure 5.2. Since the optimal H_2 controller is relatively easy to calculate and it provides a point on the desired curve, it was selected as the initial controller for the new method. The problem now is to start from the optimal H_2 controller and step along the α versus γ curve by progressively reducing γ from $\bar{\gamma}$ to $\underline{\gamma}$ by some increment. This is

a new approach to the mixed problem which has resulted in a significant reduction in computation time. The primary reduction is due to the fact that each iteration of the method results in a new point on the α versus γ curve. The reduction in computation time will be discussed further at the end of this chapter.

6.1.1 Equality Constraint Approach. Applying the results from the previous section, it is seen that the optimal mixed H_2/H_∞ controller for a fixed γ will have the property that $\|T_{ed}\|_\infty = \gamma$. This suggests an equality constraint approach. To enforce the equality constraint, the square of the error between the constraint and its desired value are adjoined to the objective function. While this does not guarantee the constraint is satisfied, it will result in a method which attempts to minimize the objective function while concurrently reducing the error in the H_∞ constraint. This approach results in the following performance index

$$J_\gamma = \|T_{zw}\|_2^2 + \lambda (\|T_{ed}\|_\infty - \gamma)^2 \quad (6.2)$$

where λ is a penalty on the error between the desired γ and the infinity-norm of the transfer function. Define the vector Z as

$$Z = \left[a_{c_1}^T \quad \dots \quad a_{c_{n_c}}^T \quad b_{c_1}^T \quad \dots \quad b_{c_p}^T \quad c_{c_1}^T \quad \dots \quad c_{c_m}^T \right]^T \quad (6.3)$$

where a_{c_j} , b_{c_j} , and c_{c_j} are the columns of A_c , B_c and C_c , respectively. The first order necessary conditions for J_γ to be a minimum are

$$\begin{aligned} \frac{\partial J_\gamma}{\partial z_i} &= \frac{\partial \|T_{zw}\|_2^2}{\partial z_i} + \frac{\partial [\lambda (\|T_{ed}\|_\infty - \gamma)^2]}{\partial z_i} \\ &= \frac{\partial \|T_{zw}\|_2^2}{\partial z_i} + 2\lambda (\|T_{ed}\|_\infty - \gamma) \frac{\partial \|T_{ed}\|_\infty}{\partial z_i} = 0 \end{aligned} \quad (6.4)$$

for $i = 1, \dots, n_z$ and $n_z = n_c \times n_c + n_c \times p + n_c \times m$, where z_i are the elements of Z .

A DFP algorithm [37] is used to minimize the performance index. The one dimensional search in the algorithm uses a parabola fit to reduce the number of function evaluations required to converge to the minimum. The DFP iterations are continued until a predetermined maximum number of iterations (normally, 20) is reached or $|\nabla J_\gamma^T H \nabla J_\gamma|$ is below some preset tolerance, where ∇J_γ is gradient vector and H is the DFP curvature matrix. Further, if no convergence is found by the one dimensional search, the DFP routine is exited, the step in γ is increased, and the search is continued. This allows a relatively large step size for γ to be used. As γ approaches $\underline{\gamma}$, the step size is decreased so as to keep $\gamma > \underline{\gamma}$. The basic algorithm is as follows:

- i. Compute the optimal H_2 controller and set up the initial Z vector
- ii. Compute $\bar{\gamma}$ and set $\gamma = \bar{\gamma}$
- iii. Decrement γ
- iv. Perform DFP search over the Z vector space for minimum J_γ
- v. Store resulting controller and repeat from step iii.

To avoid unstable closed-loop systems, J_γ is set to a value of 10^{20} if the closed-loop A_2 matrix has any unstable eigenvalues. This results in an "artificial wall" which insures the algorithm only searches in the direction of stabilizing controllers.

Initially, the algorithm can be run with loose tolerances on the DFP search to define the desired α versus γ curve, then the convergence tolerances can be tightened and a particular point can be refined to desired accuracy. In addition, this new algorithm can be applied from any initial condition, not just the optimal H_2 controller, by substituting the appropriate initial Z vector and γ .

6.1.2 Inequality Constraint Approach. Unfortunately, there are several numerical drawbacks to equality constraint approaches for numerical optimization. However, these can be overcome using an inequality constraint approach. Consider

the program

$$\mathcal{P} \begin{cases} \min_{K \text{ stabilising}} f(Z) \\ \text{subject to} \\ g(Z) \leq 0 \end{cases} \quad (6.5)$$

where $f(Z) = \|T_{zw}(Z)\|_2^2$ and $g(Z) = \|T_{ed}(Z)\|_\infty - \gamma$. One approach to minimize this performance index is called sequential quadratic programming (SQP) [52]. This technique converts the nonlinear program into a quadratic subproblem with a linear constraint. The objective function is expanded in a Taylor Series around a nominal Z vector. The constant term is dropped and the expansion is truncated at the quadratic term. The constraint is expanded in a Taylor Series and truncated after the linear term. The resulting subproblem is

$$\begin{cases} \min_{d \in \mathbb{R}^{n_z}} \frac{1}{2} d^T H_k d + \nabla f(Z_k)^T d \\ \text{subject to} \\ \nabla g(Z_k)^T d + g(Z_k) \leq 0 \end{cases} \quad (6.6)$$

where Z_k is the value of the Z vector at the k th iteration, H_k is a positive definite approximation of the Hessian matrix and n_z is the length of the Z vector. This subproblem can be solved using available quadratic programming algorithms [37, 52, 53] and results in search direction d_k for the k th iteration. The Z vector is then updated by

$$Z_{k+1} = Z_k + \alpha_k d_k \quad (6.7)$$

where α_k is determined from a one dimensional search. The Hessian matrix can be updated in several ways, but a common method is the Broyden-Fletcher-Goldfarb-Shanno (BFGS) method [37] as follows

$$H_{k+1} = H_k + \frac{q_k q_k^T}{q_k^T s_k} - \frac{H_k^T H_k}{s_k^T H_k s_k} \quad (6.8)$$

where $s_k := Z_{k+1} - Z_k$ and

$$q_k := \nabla f(Z_{k+1}) + \lambda \nabla g(Z_{k+1}) - \nabla f(Z_k) \lambda \nabla g(Z_k) \quad (6.9)$$

where λ is an estimate of the Lagrange multiplier. The same algorithm proposed in the previous section can be used, substituting the SQP minimization for the DFP minimization in step iv.

Another advantage of the SQP approach is it allows infeasible solutions. This allows the optimization routine to approach the solution from both the feasible and infeasible region. This has the advantage of not forcing the routine to bias its search direction to ensure it remains in the feasible region. If the SQP converges with a stability constraint violation, the point will have to be reattempted with a smaller step in γ . In general, this was not found to be a problem. For the problem at hand, this means we can allow controllers which result in unstable closed-loop systems. This is done by adding a second constraint

$$h(Z) = \max_i \{\Re\{\lambda_i(\mathcal{A}_2)\}\} \quad (6.10)$$

This constraint is added into the program (6.5). Since the closed-loop system can be unstable, a stable/antistable projection of the H_2 transfer function must be used to compute the two-norm (see Section 2.3.1). A central difference method can be used to compute the gradient of the Lagrangian corresponding to the stability constraint. Analytical gradients for the stability constraint were not considered, but may be possible.

6.1.3 Computing Gradients of the Two-Norm. The gradient of the square of the two-norm can be computed using the results of the previous chapter. Recall

$$\|T_{sw}\|_2^2 = \text{tr} [Q_2 C_z^T C_z] \quad (6.11)$$

where Q_2 is the real, positive semidefinite solution to the Lyapunov equation

$$A_2 Q_2 + Q_2 A_2^T + B_w B_w^T = 0 \quad (6.12)$$

Forming a Lagrangian,

$$\mathcal{L} = \text{tr} [Q_2 C_z^T C_z] + \text{tr} [(A_2 Q_2 + Q_2 A_2^T + B_w B_w^T) \mathcal{X}] \quad (6.13)$$

the resulting gradients are

$$\frac{\partial \mathcal{L}}{\partial A_c} = X_{12}^T Q_{12} + X_2 Q_2 \quad (6.14)$$

$$\frac{\partial \mathcal{L}}{\partial B_c} = X_{12}^T Q_1 C_{y_2}^T + X_2 Q_{12}^T C_{y_2}^T + X_{12}^T V_{12} \quad (6.15)$$

$$\frac{\partial \mathcal{L}}{\partial C_c} = B_{w_2}^T X_1 Q_{12} + B_{w_2}^T X_{12} Q_2 + R_{12}^T Q_{12} + R_2 C_c Q_2 \quad (6.16)$$

$$\frac{\partial \mathcal{L}}{\partial Q_2} = A_2^T \mathcal{X} + \mathcal{X} A_2 + C_z^T C_z = 0 \quad (6.17)$$

$$\frac{\partial \mathcal{L}}{\partial \mathcal{X}} = A_2 Q_2 + Q_2 A_2 + B_w B_w^T = 0 \quad (6.18)$$

where the various matrices are defined as they were in the previous chapter. The method for actually computing the gradient $\nabla \|T_{zw}\|_2^2$ at some Z_k is as follows:

- i. Solve (6.17) for \mathcal{X} and (6.18) for Q_2
- ii. Compute $\frac{\partial \mathcal{L}}{\partial A_c}$, $\frac{\partial \mathcal{L}}{\partial B_c}$, and $\frac{\partial \mathcal{L}}{\partial C_c}$ from (6.14), (6.15), and (6.16), respectively
- iii. Compute the gradient by

$$\frac{\partial \mathcal{L}}{\partial Z} = \left[\begin{array}{cccc} \left(\frac{\partial \mathcal{L}}{\partial A_c}\right)_1^T & \cdots & \left(\frac{\partial \mathcal{L}}{\partial A_c}\right)_{n_c}^T & \left(\frac{\partial \mathcal{L}}{\partial B_c}\right)_1^T & \cdots \\ & & & \left(\frac{\partial \mathcal{L}}{\partial B_c}\right)_p^T & \left(\frac{\partial \mathcal{L}}{\partial C_c}\right)_1^T & \cdots & \left(\frac{\partial \mathcal{L}}{\partial C_c}\right)_m^T \end{array} \right]^T \quad (6.19)$$

6.1.4 Computing Gradients of the Infinity-Norm. The gradient of the infinity-norm represents complex matrix relations and is not easy to evaluate analytically. There are two different approaches which have been taken in this work. The first method uses a modified central difference method. An improved approach to computing the infinity-norm of a closed-loop system is also developed for use with the central differences. The second uses the sensitivity of the maximum singular value of a matrix developed in [54].

6.1.4.1 Central Differences. The basic central difference formula is

$$\frac{\partial \|T_{ed}(Z)\|_{\infty}}{\partial z_i} = \frac{\|T_{ed}(Z + \delta Z_i)\|_{\infty} - \|T_{ed}(Z - \delta Z_i)\|_{\infty}}{2\delta z_i} \quad (6.20)$$

where

$$\delta Z_i = \begin{bmatrix} 0 \cdots 0 & \delta z_i & 0 \cdots 0 \end{bmatrix} \quad (6.21)$$

If the closed-loop A_{∞} matrix of the perturbed system has any unstable eigenvalues, the infinity-norm is set to a value of 10^{20} . This results in an "artificial wall" which insures the algorithm only searches in the direction of stabilizing controllers. Furthermore, to avoid computing a false partial derivative due to the artificial wall, a one-sided difference is used at those points. If the resulting slope reduces J_{γ} in the direction of the artificial wall, the derivative is set to zero; otherwise, the one-sided difference is used.

As was pointed out by Ridgely [9], the computation of the infinity-norm of a transfer function using the Hamiltonian method is not numerically stable enough for accurate numerical partial derivatives. This is due to the numerical ill conditioning of the Hamiltonian. However, Gahinet [55] suggests using the generalized eigenproblem to improve the numerical robustness of the infinity-norm computation. This can be accomplished by finding an associated matrix pencil which has a similar eigenstructure to the original problem. Since the generalized eigenproblem does not

require an inversion of the Hamiltonian, it is numerically better conditioned. In [55] Gahinet develops such a generalized eigenproblem by defining the generalized Hamiltonian

$$\mathcal{H} = \begin{bmatrix} A & 0 & 0 & B \\ 0 & -A^T & C^T & 0 \\ C & 0 & \gamma I & D \\ 0 & -B^T & D^T & \gamma I \end{bmatrix} \quad (6.22)$$

$$\mathcal{I} = \begin{bmatrix} I_{2n} & 0 \\ 0 & 0_{m+p} \end{bmatrix} \quad (6.23)$$

where $A \in \mathbb{R}^{n \times n}$, $B \in \mathbb{R}^{n \times m}$, and $C \in \mathbb{R}^{p \times n}$. The generalized spectrum of the pencil $\mathcal{H} - \lambda \mathcal{I}$ coincides with the spectrum of the Hamiltonian plus $m + p$ infinite eigenvalues associated with the singular part of \mathcal{I} . The QZ algorithm [56] can be used to find the generalized spectrum. To implement the generalized eigenproblem algorithm, the lower bound on γ is set to zero. An upper bound $\gamma = \gamma_{upper}$ is selected and the QZ algorithm is used to compute the generalized spectrum. If the real part of any eigenvalue is within epsilon of the $j\omega$ -axis, then γ_{upper} is increased and the routine is repeated. Once an upper and lower bound on the infinity-norm are found, a bisection method [57] is used to refine the value. Since the eigenvalues of the generalized eigenproblem are symmetric about the origin, they will always approach the $j\omega$ -axis in pairs and separate along the $j\omega$ -axis in opposite directions as γ is decreased. To improve the accuracy of the bisection method, two tests on γ are used to determine the $j\omega$ -axis intercept: is the real part of the eigenvalue within some epsilon of the $j\omega$ -axis, and is the difference in the imaginary part of the two eigenvalues within epsilon? Figure 6.1 graphically presents the region of the $j\omega$ -axis intercept. Since the eigenvalues of the pencil $\mathcal{H} - \lambda \mathcal{I}$ are symmetric about

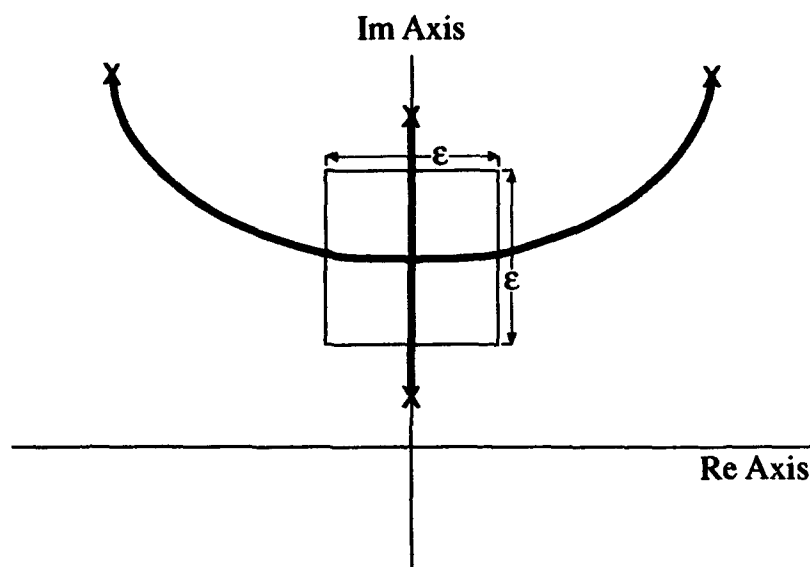


Figure 6.1. $j\omega$ -axis intercept

the real axis, one must account for all the eigenvalues on the imaginary axis. This was incorporated into the algorithm by computing the difference between all pairs of eigenvalues on the imaginary axis and then ensuring the sum of the results is less than some epsilon. This results in a more numerically robust method for determining the axis intercept. By incorporating both the generalized eigenproblem approach and the combined real and imaginary test, the overall robustness of the infinity-norm computation has been improved enough to provide sufficiently accurate numerical derivatives for a DFP algorithm to be used.

6.1.4.2 Singular Value Sensitivity. A second approach for computing the gradient value of the infinity-norm is based on the sensitivity of the singular value of a matrix developed by Giesy and Lim [54]. Assuming the maximum singular value of T_{ed} evaluated at Z has a single peak for $\omega \in \mathfrak{R}^+$, the derivative of the infinity-norm can be written as

$$\frac{\partial \|T_{ed}\|_{\infty}}{\partial z_i} = \Re \left[u_1^H \left(\frac{dT_{ed}(\omega_0)}{dz_i} \right) \Big|_{Z_{nom}} v_1 \right] \quad (6.24)$$

where u_1 and v_1 are the singular vectors associated with the maximum singular value of T_{ed} , ω_0 is the frequency where the the maximum singular value reaches its peak value, and Z_{nom} is the nominal Z vector. The derivative of the transfer function can be determined from

$$\left. \frac{dT_{ed}(\omega_0)}{dz_i} \right|_{Z_{nom}} = \left. \frac{d \left[C_e (j\omega_0 - A_{\infty})^{-1} B_d + D_{ed} \right]}{dz_i} \right|_{Z_{nom}} \quad (6.25)$$

The advantage of this approach is that it eliminates the bisection search required in the central difference approach. This can result in a significant savings in computation time as the size of the Z vector grows for complicated problems. In addition, the accuracy of the gradient is better than that of the central difference approach. This is due to the fact that we are not taking differences of small numbers which often results in bad information due to truncation and roundoff errors. Furthermore, since there is no requirement to search for the γ which causes the real part of the eigenvalues of the Hamiltonian to go to zero, the sensitivity method is better posed numerically. Finally, the gradient of the infinity-norm of the H_{∞} constraint is often a piecewise continuous function of the controller (Z vector). This is due to the norm definition; it is the peak magnitude of the function. As the controller is perturbed, the frequency where the peak magnitude occurs can change and the gradient associated with the peak at the new frequency is usually not the same as the gradient at the previous peak. Thus, a central differences approach can result in an incorrect gradient. The sensitivity method does not have this problem since it only provides information on the unperturbed transfer function.

The sensitivity method does have some disadvantages. The first and most often encountered problem is when the maximum singular value reaches its maximum at multiple frequencies. As discussed above, this results in a point where the gradient is discontinuous. Thus, the infinity-norm is a continuous, but not smooth, function of Z . Another limitation of the sensitivity method is it depends on determining

the peak of the maximum singular value over frequency. This is accomplished by selecting a finite frequency range and computing the maximum singular value. While *a priori* knowledge of the behavior of T_{ed} can be used to determine the proper range of frequencies, there is no guarantee that the range will remain fixed as the optimization routine iterates. Therefore, when using this method, a check must be made to ensure the maximum actually occurs in the selected range. Finally, the peak value of the singular value is determined by searching over a finite set of frequencies. This set must be fine enough to ensure an accurate peak is determined. If the selected grid is too coarse, the computed maximum singular value can be in error. One method to overcome this drawback is to take a two-step approach. First find the maximum singular value with a coarse grid, then refine the grid and find the maximum again. This method was not included in the original code used in this work, but has subsequently been incorporated.

Both of these methods have been implemented for SISO and MIMO problems. To date, the sensitivity method has been found to provide better results than the central difference method, due to the reduced computation time required and the improved numerical accuracy. All the examples in this work used the SQP approach.

6.1.5 Initial Conditions and Controller Realizations. The two algorithms described above use the optimal H_2 controller as an initial condition for starting the routines. This controller was chosen due to its ease of computation; however, the algorithms can be applied from any initial controller, not just the optimal H_2 controller, by substituting the appropriate initial Z vector and γ . In general, both methods can result in either sub-optimal or super-optimal solutions, depending on the particular choice of γ . However, as the minimum infinity-norm is approached, both routines generally result in super-optimal solutions only. This is due to the limitation of the numerical accuracies in the gradients described above. If it is imperative that a sub-optimal solution be found, the value of γ can be reduced below the desired level and the method applied.

Finally, the Z vector was defined with a fully populated state space form; by using canonical forms, the number of variables can be reduced. However, there are drawbacks to using some canonical forms such as the controllability canonical form due to numerical instability which can result. The modal canonical form is more numerically stable [58, 59] and has been used successfully to reduce the parameter space. However, the drawback to this form is it only allows eigenvalues with partial multiplicities of one. This has not been a problem for the controllers used in this work, but should be a consideration for any future implementations, especially for controllers with a large order where repeated eigenvalues are more likely to occur. One approach to handle partial multiplicities greater than one is to put the controller into a modified Jordan Canonical form [60]. While this adds a second super-diagonal of the A_c matrix to the Z vector, and thus increases the size of the parameter space, it does account for all possible controllers. Incorporation of this form should be accomplished in follow-on research.

6.2 Numerical Example: SISO F-16 Longitudinal Controller

An F-16 longitudinal controller design is used to demonstrate the numerical method. The system consists of a short period approximation of a continuous, linear, time-invariant normal acceleration command system. The plant is augmented with a first order pre-filter at the input to model the servo dynamics. The filter is a simplified model of an hydraulic actuator and captures the lag inherent in such a system. Additionally, a first order post-filter is augmented at the output of the plant to model the control delay. This delay accounts for the measurement hold in the accelerometer.

The plant states are the angle of attack (α) and the pitch rate (q). The input is the stabilator deflection (δ_e) and the output is normal acceleration (n_z). The plant is given in Appendix A. The objective is to design a controller which provides good noise rejection, state regulation, and minimizes control usage while concurrently

providing acceptable tracking of a normal acceleration step input as well as achieving acceptable vector gain and phase margins.

This problem is solved using the mixed H_2/H_∞ method. The H_2 portion will minimize the effect of the wind disturbances, measurement noise, and provide state regulation and limit control power. The H_∞ portion will be used to incorporate tracking performance and margins.

6.2.1 H_2 Problem. The H_2 problem is: Find the internally stabilizing controller which minimizes the response of the normal acceleration and weighted control due to the wind disturbance and measurement noise. The weight on the control is added to ensure the control usage is limited to a realistic range. However, since only the energy of the control usage is penalized, unrealistic peak deflection and control rates can result from the H_2 problem. To ensure that the controller as designed will work, a truth model of the system which includes magnitude and rate limiters must be used to analyze the closed-loop system. However, the primary purpose of this example is to demonstrate the mixed H_2/H_∞ control design method, and a complete analysis of the resulting controller will not be performed.

This problem is the standard LQG problem. A block diagram of the H_2 problem is given in Figure 6.2, where the control weight is $\rho = 10.0$ and the state weighting matrix H is identical to the system C matrix (i.e., we are regulating the normal acceleration rather than the states). The wind disturbance is modeled as a white-Gaussian noise (WGN) with a strength of 5.0×10^{-4} rad²-sec which enters the system as a pitch rate perturbation resulting in

$$\Gamma = \begin{bmatrix} 0.996 \\ -0.96 \\ 0 \\ 0 \end{bmatrix} \quad (6.26)$$

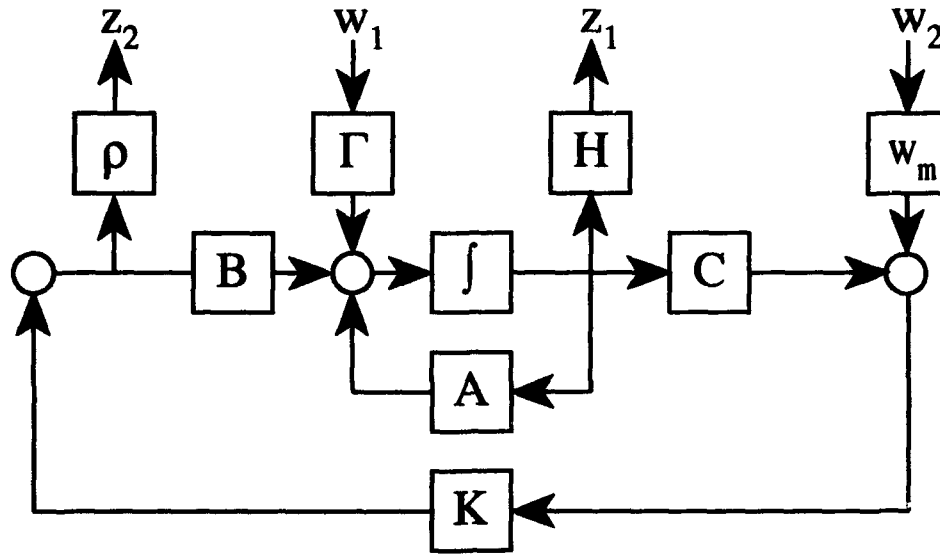


Figure 6.2. F-16 H_2 block diagram

While feeding in the process noise as a pitch rate disturbance is not physically the best approach, it done here simply to provide an example LQG controller with poor tracking and margins. The next example in this chapter will address the more realistic problem with the process noise modeled as an angle of attack perturbation.

The measurement noise is modeled as WGN of strength $1.6 \times 10^{-5} \text{ g}^2\text{-sec}$ and $w_m = 1$. The resulting H_2 matrices are

$$A_2 = \begin{bmatrix} -1.491 & 0.996 & -0.188 & 0 \\ 9.753 & -0.96 & -19.04 & 0 \\ 0 & 0 & -20.0 & 0 \\ 35.264 & -0.334 & -4.366 & -40.0 \end{bmatrix} \quad (6.27)$$

$$B_w = \begin{bmatrix} 0.02271 & 0 \\ -0.021466 & 0 \\ 0 & 0 \\ 0 & 0 \end{bmatrix} \quad B_{w_2} = \begin{bmatrix} 0 \\ 0 \\ 20.0 \\ 0 \end{bmatrix} \quad (6.28)$$

$$C_z = \begin{bmatrix} -35.264 & 0.334 & 4.366 & 80.0 \\ 0 & 0 & 0 & 0 \end{bmatrix} \quad (6.29)$$

$$C_{y2} = \begin{bmatrix} -35.264 & 0.334 & 4.366 & 80.0 \end{bmatrix} \quad (6.30)$$

$$D_{zw} = \begin{bmatrix} 0 & 0 \\ 0 & 0 \end{bmatrix} \quad D_{zu} = \begin{bmatrix} 0 \\ 10.0 \end{bmatrix} \quad D_{yw} = \begin{bmatrix} 0 & 0.004 \end{bmatrix} \quad D_{yu} = \begin{bmatrix} 0 \end{bmatrix} \quad (6.31)$$

The resulting LQG design does a reasonable job of regulating the normal acceleration following an initial 5° angle of attack perturbation as shown in Figure 6.3. Also, response to low and high frequency disturbances is minimal. As previously stated, this LQG problem was deliberately set up with poor step tracking. As a result, the system does not track a normal acceleration unit step command, as shown in Figure 6.4. The control usage for the initial perturbation and the unit step are given in Figures 6.5 and 6.6, respectively. The regulator does not demand too much control for these tasks, but Figure 6.6 shows an increasing ramp-up in control which may lead to unacceptable control demands. Figure 6.7 presents the desired loop shape at low frequency for good tracking and disturbance rejection and at high frequency for sensor noise and unmodeled dynamics rejection. The H_2 open-loop GK avoids the high frequency barrier, but does not clear the low frequency barrier. We will use the mixed approach to modify the controller to clear this barrier.

Finally, the vector margins are examined to determine how robustly stable the system is with the optimal H_2 controller. These margins represent the largest independent variation in either the gain or phase for which the system remains stable. For a SISO system, the gain margin is the union of the complementary sensitivity gain margin and the sensitivity gain margin. However, for MIMO systems, this is not the case; thus, in general, both forms of the gain margins should be presented. For more information on the vector margins, see [61]. For this problem, $[-4.0 \ 6.0]dB$ gain margin and a phase margin of greater than 30° are desired. With the H_2 controller, the complementary sensitivity and sensitivity gain margins are $[-0.473 \ 0.448] dB$

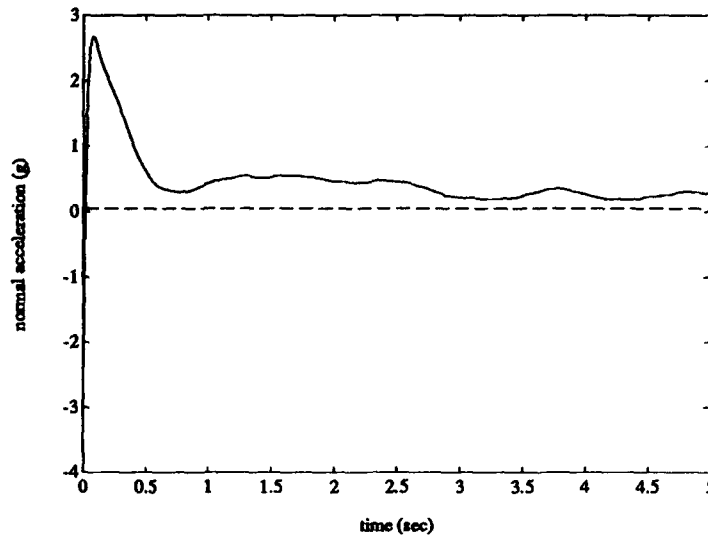


Figure 6.3. F-16, H_2 controller, response to initial 5° angle of attack perturbation and $[-0.473 \ 0.500]$ dB, respectively. The phase margin is 3.21° . These vector margins are unacceptable. The H_∞ portion of the mixed problem will be used to improve these margins.

6.2.2 H_∞ Problem. The H_∞ problem is a closed-loop model matching problem, as given in Figure 6.8. A performance and stability bound on the open-loop transfer function, GK, is defined; then the desired closed-loop sensitivity is derived as

$$S(s) = \frac{1}{1 + G(s)K(s)} \quad (6.32)$$

Figure 6.7 gives the desired bounds and the desired open-loop GK shape. The low frequency bound is chosen to give good noise rejection and step tracking. The high frequency bound is set to attenuate system response to high frequency sensor noise and unmodeled dynamics. For a good discussion on how to pick these bounds, see [19] or [61]. The desired open-loop GK shape has a crossover frequency of 1 rad/sec. This was selected as a first cut to a desired loop-shape; however, the closed-loop bandwidth is affected by the open-loop crossover. The closed-loop bandwidth can be

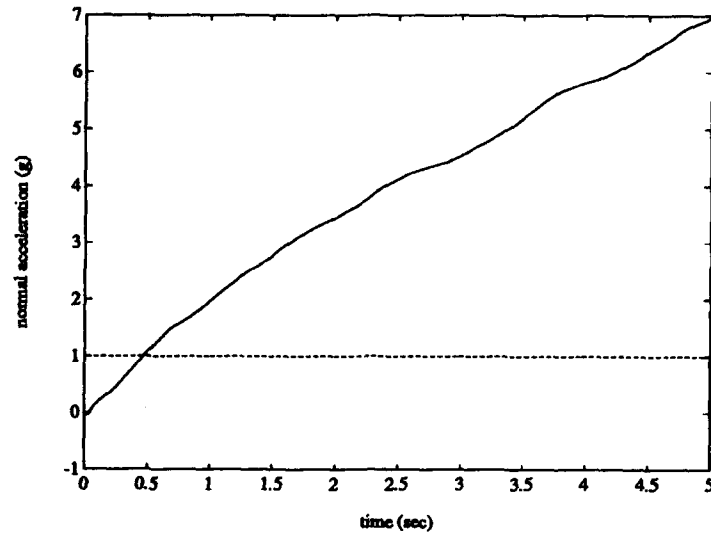


Figure 6.4. F-16, H_2 controller, response to unit normal acceleration step

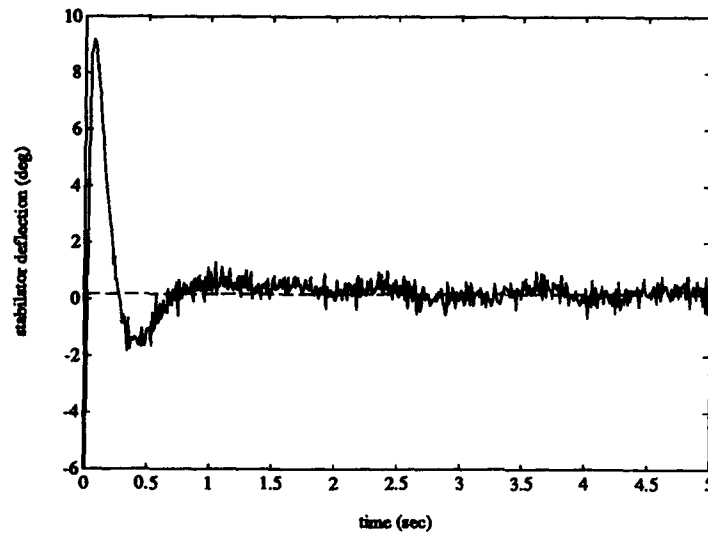


Figure 6.5. F-16, H_2 controller, control usage for initial 5° angle of attack perturbation

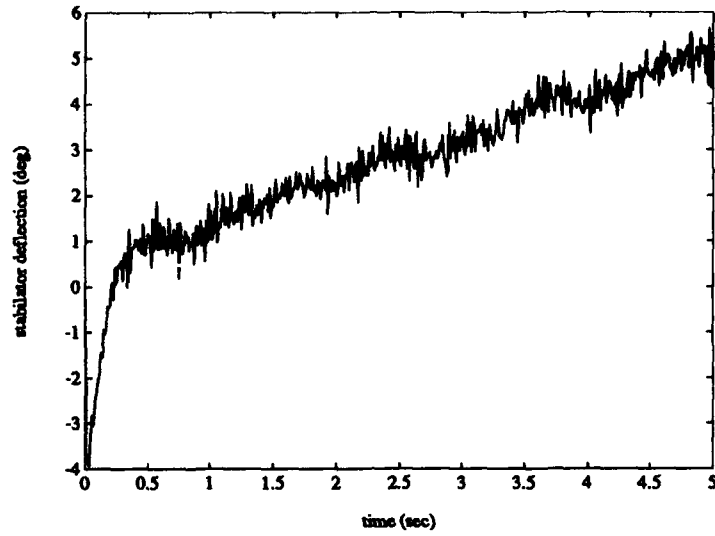


Figure 6.6. F-16, H_2 controller, control usage for unit normal acceleration step

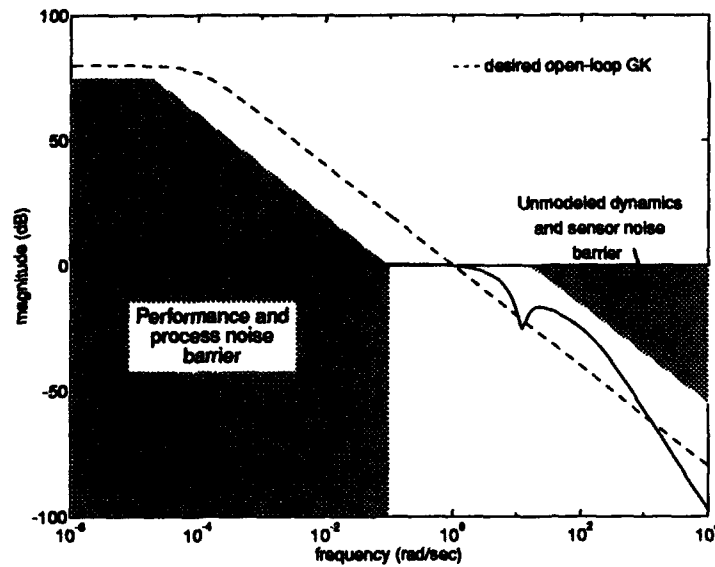


Figure 6.7. F-16, H_2 controller, open-loop GK

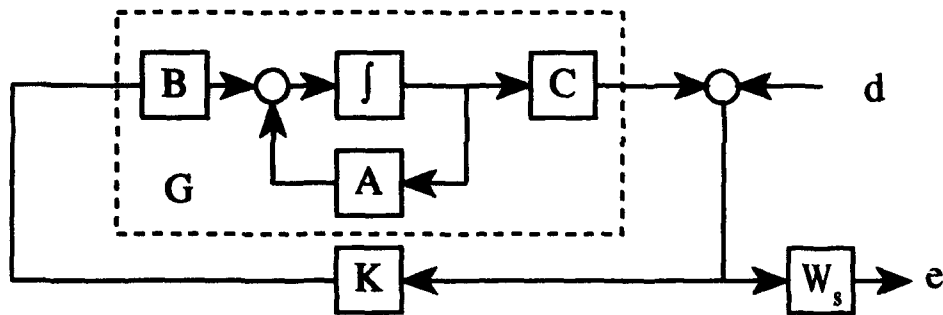


Figure 6.8. F-16 H_∞ block diagram

increased by increasing the desired open-loop crossover. To completely understand the sensitivity of the resulting closed-loop bandwidth to the open-loop crossover, several open-loop shapes should be chosen and the control problem should be repeated for these designs. Since this example is only a demonstration of the mixed H_2/H_∞ method, only one loop shape will be used.

The H_∞ problem is set up to minimize the weighted sensitivity ($W_s S$), where the weight is the inverse of the desired sensitivity, given by

$$W_s = \frac{s + 1.0}{s + 0.0001} \quad (6.33)$$

The resulting H_∞ matrices are

$$A_\infty = \begin{bmatrix} -1.491 & 0.996 & -0.188 & 0 & 0 \\ 9.753 & -0.96 & -19.04 & 0 & 0 \\ 0 & 0 & -20.0 & 0 & 0 \\ 35.264 & -0.334 & -4.366 & -40.0 & 0 \\ -35.264 & 0.334 & 4.366 & 80.0 & -0.0001 \end{bmatrix} \quad (6.34)$$

$$B_d = \begin{bmatrix} 0 \\ 0 \\ 0 \\ 0 \\ 1.0 \end{bmatrix} \quad B_{u\infty} = \begin{bmatrix} 0 \\ 0 \\ 20.0 \\ 0 \\ 0 \end{bmatrix} \quad (6.35)$$

$$C_e = \begin{bmatrix} -35.264 & 0.334 & 4.366 & 80.0 & 1.0 \end{bmatrix} \quad (6.36)$$

$$C_{y\infty} = \begin{bmatrix} -35.264 & 0.334 & 4.366 & 80.0 & 0 \end{bmatrix} \quad (6.37)$$

$$D_{ed} = \begin{bmatrix} 1.0 \end{bmatrix} \quad D_{eu} = \begin{bmatrix} 0 \end{bmatrix} \quad D_{yd} = \begin{bmatrix} 1.0 \end{bmatrix} \quad D_{yu} = \begin{bmatrix} 0 \end{bmatrix} \quad (6.38)$$

It is desirable to determine the minimum γ ($\underline{\gamma}$) for which the H_∞ constraint can be achieved. Since the H_∞ constraint is a singular H_∞ problem ($D_{eu} = 0$; therefore, there is no direct penalty on the control usage), the optimal γ cannot be determined using available methods. To overcome this limitation, an almost singular H_∞ problem was solved by adding a small perturbation to D_{eu} , making the problem a regular one. As the perturbation was reduced, the optimal infinity-norm converged to $\underline{\gamma} = 1.274$. The feedback-loop in the singular problem was closed using the controller resulting from the perturbed problem. However, the resulting closed-loop system was unstable. Thus, the perturbed problem was only able to give us an estimate of $\underline{\gamma}$ for the singular problem. While this does not allow a direct comparison of our results to an H_∞ controller, it does provide a known lower bound for our H_∞ constraint.

6.2.3 Results. The initial controller for the numerical mixed solution is the optimal H_2 controller. A fourth order controller is designed to demonstrate the method for controller order equal to the H_2 order. The SQP method is used to find the mixed H_2/H_∞ solutions as γ is reduced from $\bar{\gamma}$ to $\underline{\gamma}$. The resulting α versus γ curve is given in Figures 6.9 and 6.10. The points marked on the curve

Table 6.1. F-16 H_2/H_∞ Vector Margins

α	γ	Complementary Sensitivity GM(dB)	Sensitivity GM (dB)	PM (°)
4th Order Controllers				
0.3116	178375.7400	[-0.473 0.448]	[-0.473 0.500]	3.21
0.3120	109041.6000	[-0.762 0.701]	[-0.762 0.836]	5.26
0.3139	59340.3730	[-1.352 1.170]	[-1.352 1.602]	9.66
0.3147	200.0969	[-0.756 0.696]	[-0.756 0.828]	5.21
0.3158	100.0144	[-0.756 0.696]	[-0.756 0.828]	5.21
0.3175	50.0256	[-1.160 1.023]	[-1.159 1.338]	8.19
0.3272	10.0176	[-2.488 1.932]	[-2.481 3.486]	19.03
0.3428	5.5869	[-2.277 1.803]	[-2.260 3.063]	17.09
0.3493	3.3604	[-3.514 2.495]	[-3.476 5.884]	28.49
0.3567	2.0091	[-5.129 3.203]	[-3.937 7.399]	33.32
0.3664	1.7627	[-5.376 3.296]	[-3.946 7.434]	33.42
0.4088	1.4900	[-5.900 3.481]	[-4.588 10.340]	40.72
8th Order Controller				
0.4500	1.2808	[-6.270 3.604]	[-5.013 13.186]	45.96

are used to generate the remaining plots in this section. It can be seen that these curves are not monotonically decreasing; this is due to numerical accuracies. If it is desired, the curves can be regenerated with increased tolerances on the convergence, but the additional computation time required will not add to this example and thus was not accomplished. Table 6.1 gives the resulting two-norms and infinity-norms of the controllers. Notice that the infinity-norm can be reduced significantly with little increase in the two-norm. This allows a large increase in both margins and performance with little loss of noise rejection.

Figures 6.11 and 6.12 show the recovery of the desired sensitivity shape and the resulting complementary sensitivity as γ is reduced. Notice that the low frequency sensitivity is reduced as desired for the performance bound while the desired 40 dB roll-off is maintained. This can also be seen in the evolution of the open-loop GK as

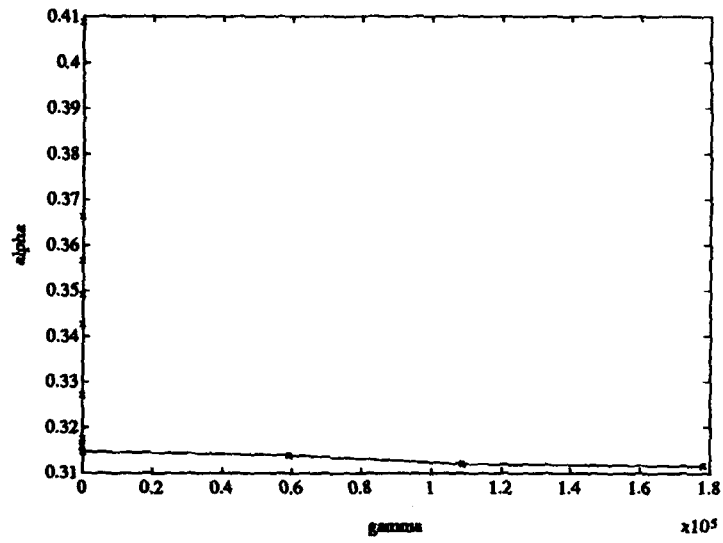


Figure 6.9. F-16, α versus γ

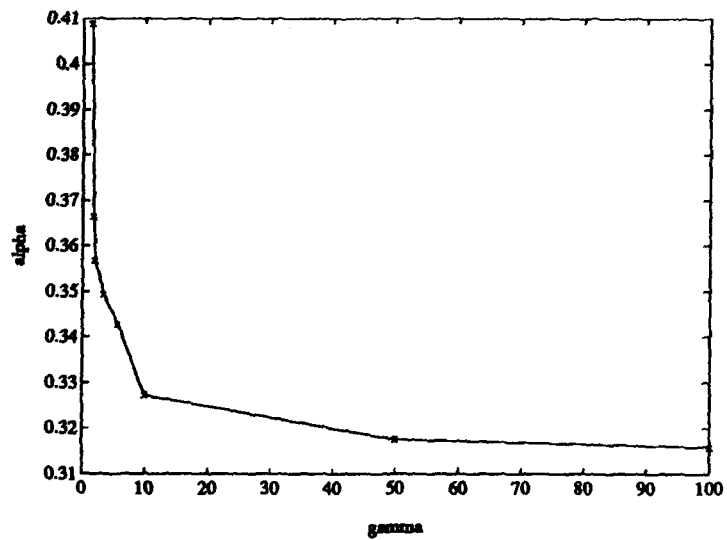


Figure 6.10. F-16, α versus γ , expanded

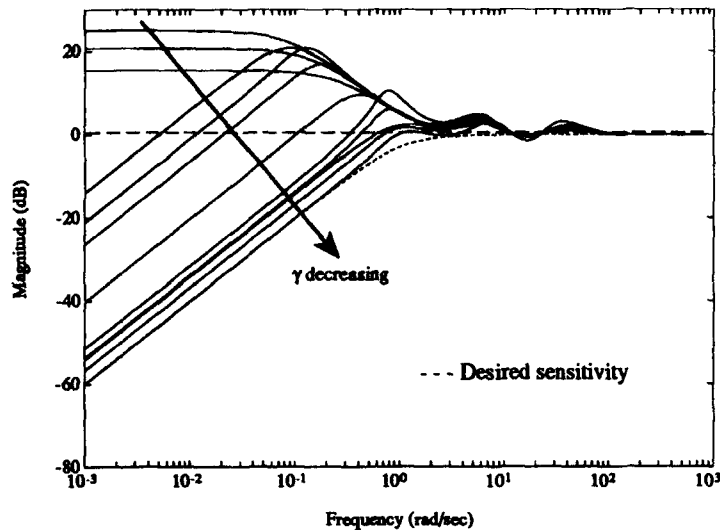


Figure 6.11. F-16, H_2/H_∞ , $n_c = 4$, closed-loop sensitivity

γ is decreased (Figure 6.10). Further, the open-loop shape clears all the barriers at the final value of γ .

The performance of the system is determined by its ability to track a unit step in normal acceleration. The performance improvement with decreasing γ can be seen in Figure 6.14. Moreover, there is little noticeable increase in noise in this plot as γ is decreased. Thus, substantial performance improvement has been made with minimal loss of noise rejection. To compare the control usage of the mixed controller, only the system corresponding to the lowest γ in Table 6.1 is plotted. Figure 6.15 shows the control usage has increased for the mixed controller. Moreover, the initial control response is 2.5 times greater than the H_2 case. This is due to the larger system gain at low frequency for the mixed controller. The increased control is part of the reason the two-norm increases as γ decreases.

The system maintains good regulation with all the mixed controllers as can be seen in Figure 6.16. This is not surprising since all the controllers result in sufficient low frequency gain for regulation performance. Again, Figure 6.17 shows that the

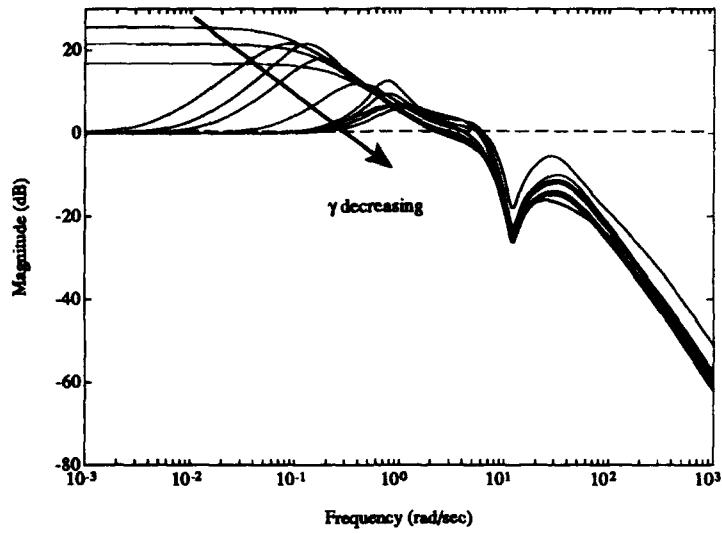


Figure 6.12. F-16, H_2/H_∞ , $n_c = 4$, closed-loop complementary sensitivity

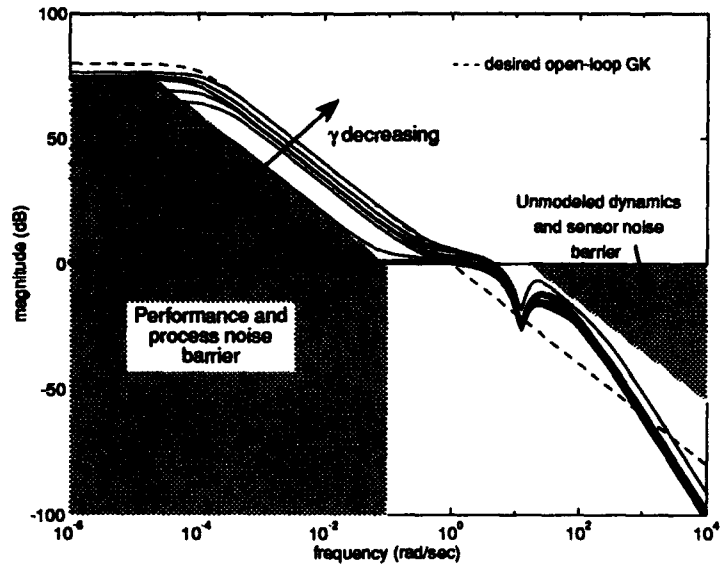


Figure 6.13. F-16, H_2/H_∞ , $n_c = 4$, open-loop GK

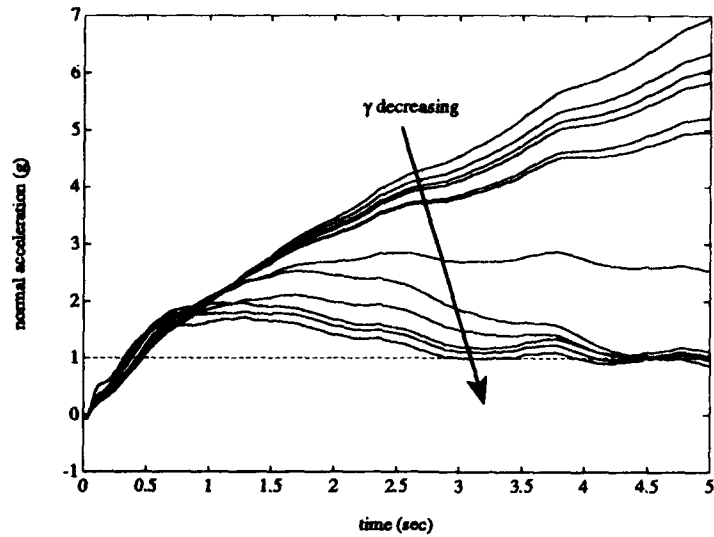


Figure 6.14. F-16, H_2/H_∞ , $n_c = 4$, response to a unit step in normal acceleration

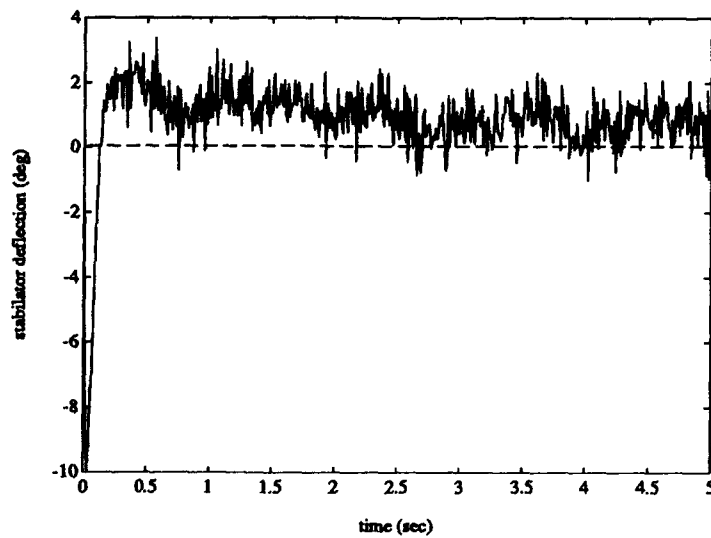


Figure 6.15. F-16, H_2/H_∞ , $n_c = 4$, control usage for a unit step in normal acceleration

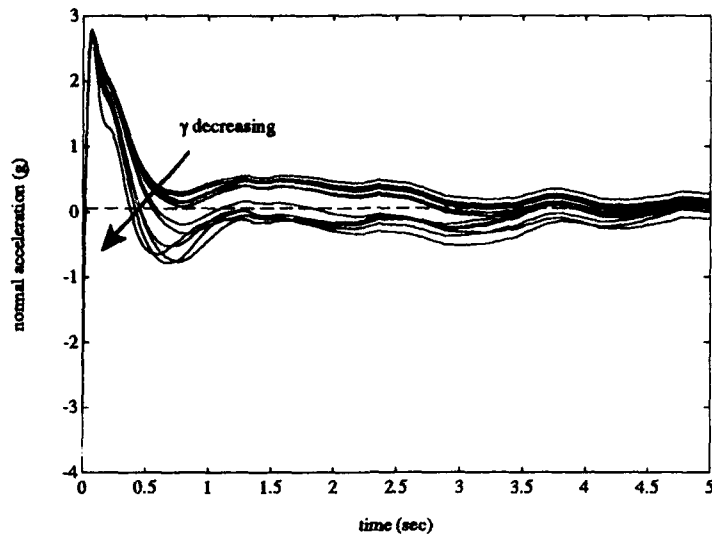


Figure 6.16. F-16, H_2/H_∞ , $n_c = 4$, response to a 5° initial angle of attack perturbation

system with the lowest γ has a large initial control deflection. This is expected since the low frequency gain of the system is large.

Referring back to Table 6.1, improvement in the vector gain margin (GM) and phase margins (PM) as γ is decreased is clear. This is another measure which can be used in a trade-off analysis to determine the best γ for the desired system. As γ approaches $\underline{\gamma}$ (1.274), there is a point where the margins decrease as γ is reduced further. The cause of this fluctuation is clearly seen in the sensitivity and complementary sensitivity plots (Figures 6.11 and 6.12). As γ is decreased from $\bar{\gamma}$, the majority of the recovery is made at low frequency, and the margins and performance reflect the improvement in the loop shape. As γ approaches $\underline{\gamma}$, the margins sometimes decrease as the performance improves. This fluctuation in the margins is due to the process attempting to match the desired sensitivity. As the low frequency portion (performance) of the sensitivity is reduced, it forces the high frequency portion (margins) to increase. The resulting waterbed effect drives the margins up and down as the infinity-norm of the weighted sensitivity is reduced.

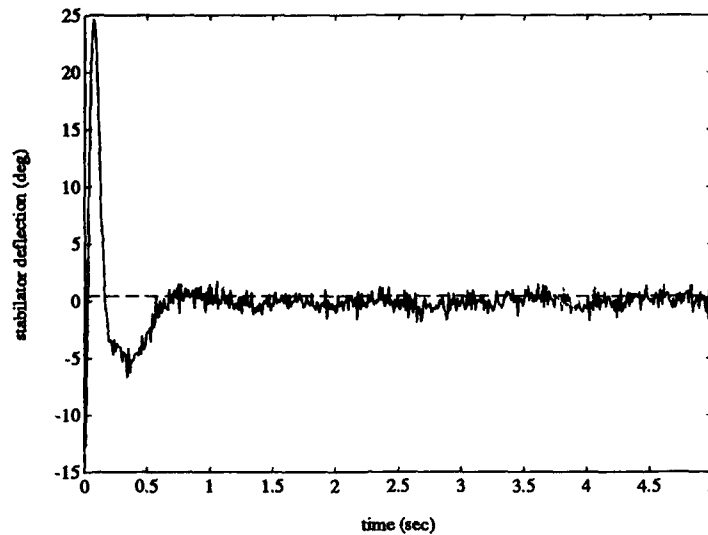


Figure 6.17. F-16, H_2/H_∞ , $n_c = 4$, control usage for a 5° initial angle of attack perturbation

Next, the controller order was doubled to $n_c = 8$ and the SQP algorithm was used to converge to the lowest γ possible. The last row of Table 6.1 presents the margins for this controller. The additional degrees of freedom have allowed the margins to be reduced further than was possible with the fourth order controller (this may also be due to numerical difficulties, as will be discussed later). The performance of the controller is shown in Figure 6.18 and 6.19, where the scale has been chosen to allow a direct comparison to the previous results. Regulation was not significantly changed (not shown). Notice that the overshoot is comparable to the best fourth order controller, but the settling time is decreased. The sensitivity of this system is given in Figure 6.20.

While the eighth order controller does provide better margins and tracking than any of the fourth order controllers, this is at the expense of doubling the controller order. The design engineer must determine which one of these factors will influence his decision the most. However for the purpose of this example, the flexibility of trading off controller order, noise rejection, tracking performance, and vector margins using the mixed H_2/H_∞ approach has been clearly demonstrated.

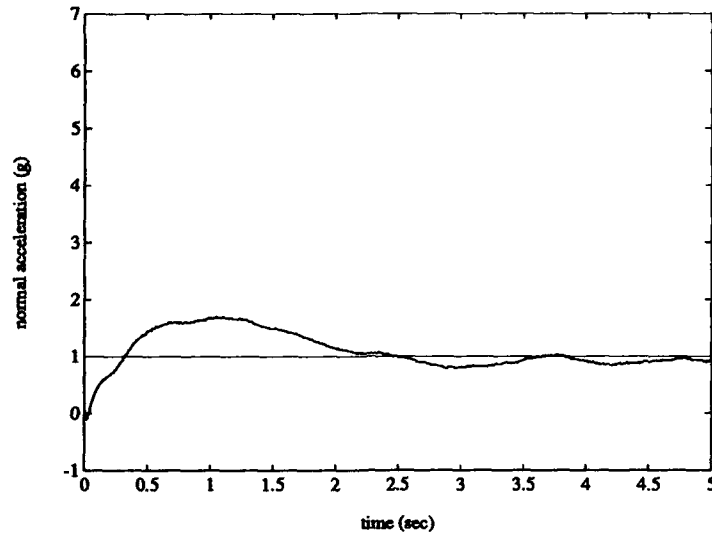


Figure 6.18. F-16, H_2/H_{∞} , $n_c = 8$ and $n_c = 4$, response to a unit step in normal acceleration

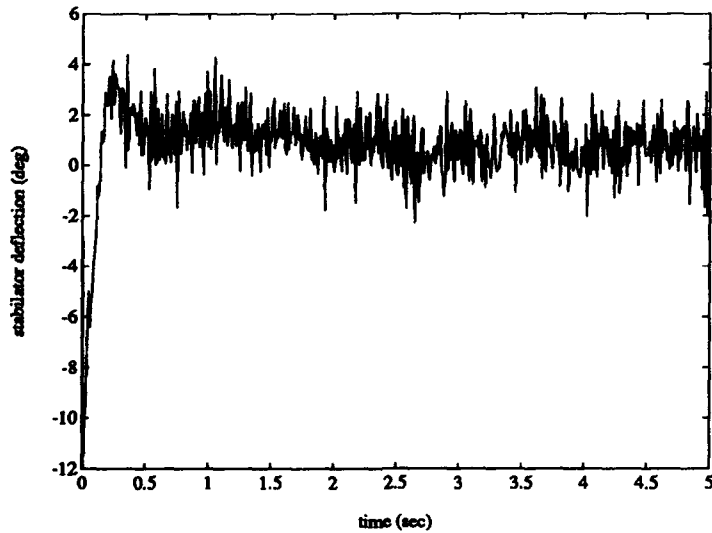


Figure 6.19. F-16, H_2/H_{∞} , $n_c = 8$, control usage for a unit step in normal acceleration

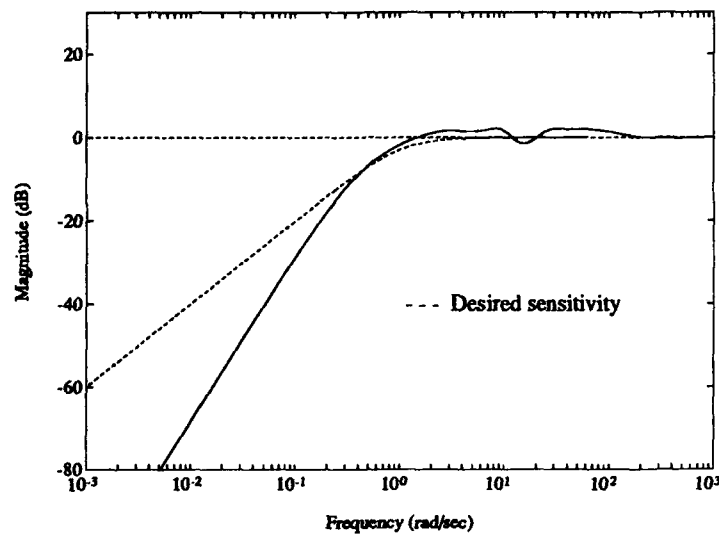


Figure 6.20. F-16, H_2/H_∞ , $n_c = 8$, closed-loop sensitivity

6.2.4 Modified H_2 Problem. As discussed in Section 6.2.1, the wind noise model used in the previous problem was not realistic. An improved model is given here where the wind disturbance enters the plant as an angle of attack perturbation. To accomplish this we must modify Γ by using

$$\Gamma = \begin{bmatrix} -1.491 \\ 9.753 \\ 0 \\ 0 \end{bmatrix} \quad (6.39)$$

This results in B_w becoming

$$B_w = \begin{bmatrix} -0.0333 & 0 \\ 0.2181 & 0 \\ 0 & 0 \\ 0 & 0 \end{bmatrix} \quad (6.40)$$

The remainder of the problem is the same as above.

The problem was solved by determining the optimal H_2 controller and then applying the SQP approach to iteratively decrease γ to as low a value as the numerical approach would achieve. Only the results for the optimal H_2 controller and the mixed controller with the lowest infinity-norm ($\gamma = 1.45$) will be discussed.

For this example, there was significantly more low frequency noise present in the H_2 design; therefore, the resulting open-loop GK transfer function had more low frequency gain as seen in Figure 6.21. This result can also be seen in Figure 6.22 which shows the low frequency sensitivity is below 0 dB. However, Figure 6.23 reveals that there is not enough gain to achieve the desired tracking performance. The $[-9.5 \ 8.9]dB$ vector gain margin and 38.8° vector phase margin which result with the optimal H_2 controller are acceptable. Finally, $\underline{\alpha} = 0.84$ and $\bar{\gamma} = 4981.0$.

After completing the mixed design, the final controller, with $\gamma^* = 1.45$ and $\alpha^* = 0.91$, was selected for comparison to the H_2 controller. As can be seen in Figures 6.21 and 6.22 the mixed controller meets the desired loop-shape and it matches the desired sensitivity much better than the H_2 controller. Furthermore, the tracking performance shown in Figure 6.23 is significantly improved. This improvement in performance has come at the expense of a reduction of the vector gain margin. The mixed controller results in a $[-5.8 \ 10.3]dB$ gain margin and 40.7° phase margin. The reduction in the lower gain margin is acceptable considering the improvement in performance.

Comparing this example to the previous one, it can be seen that the addition of a larger process noise in the H_2 design resulted in better low frequency performance and margins. The previous example showed that these objectives can also be achieved by incorporating a weighted sensitivity H_∞ constraint to the H_2 problem. Therefore, it may be possible to use the H_2 portion of the mixed problem to determine the high frequency properties of the resulting system (something H_∞ optimization has problems with). While the low frequency process noise in the H_2 problem cannot be reduced to zero, it can be artificially lowered below its expected

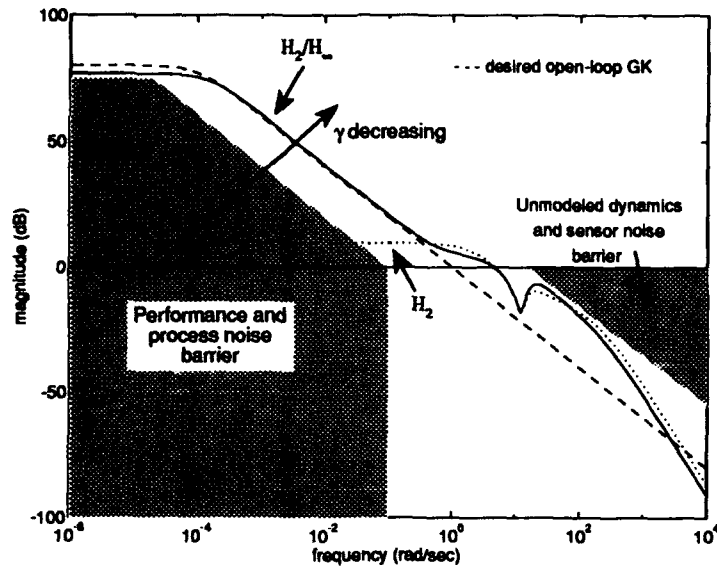


Figure 6.21. F-16, H_2/H_∞ , $n_c = 4$, open-loop GK, improved process noise

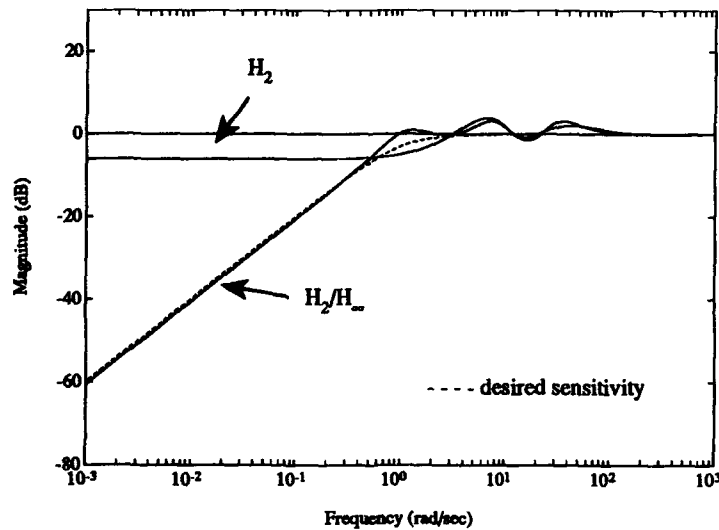


Figure 6.22. F-16, H_2/H_∞ , $n_c = 4$, closed-loop sensitivity, improved process noise

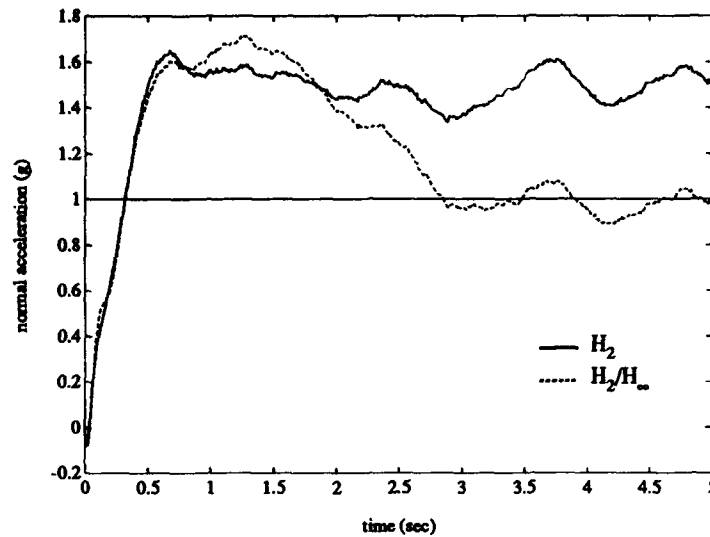


Figure 6.23. F-16, H_2/H_∞ , $n_c = 4$, response to a unit step in normal acceleration, improved process noise

level. In this manner, mixed H_2/H_∞ optimization can be used to design a controller which achieves desired objectives at both low and high frequency.

6.2.5 Convergence. To conclude this example, a discussion of the convergence of the numerical search algorithm is needed. Using Ridgely's method [9] on a Sun System SPARC 2, converging one point on the mixed curve took approximately one week of computation time. The DFP approach developed here can converge a controller in approximately one hour. Finally, the SQP method can converge a controller in a matter of minutes. All of these computation times increase as γ approaches $\underline{\gamma}$, as will be discussed below. While the SQP and DFP methods have a significant computation time advantage over previous methods, they are not yet refined enough for control design applications. The major problem with the methods arise at the "knee" of the curve, the point where there is a significant trade-off in α for γ . This knee has usually been found to occur in the neighborhood of $\underline{\gamma}$, as one should expect. This is due to the two-norm of the system tending to infinity as the optimal H_∞ controller is approached.

At the knee of the curve, problems with multiple peaks in the maximum singular value curve are present. The multiple peaks result in the gradient of the infinity-norm being piecewise continuous over the optimization parameter space. Thus, for any given nominal point, the resulting gradient may only be good for a small neighborhood of the point. This results in numerous small steps being taken in order to converge to a desired γ . In addition, if too large a step is taken, the search may depart the desired region. These issues are still open and will require further refinement to improve the method to the point where it is ready for everyday application by control engineers.

Finally, the SQP method was able to converge to controllers with a lower value of γ than the DFP method. This was partly due to the SQP method admitting unstable closed-loop system during the search. If the artificial wall approach is used, the DFP and SQP methods had about the same performance as far as reducing γ . However, the SQP method converged to a desired γ with a lower two-norm. Moreover, the SQP required fewer iterations and function evaluations to achieve these better results. Therefore, the SQP method was determined to be a better approach for solving the mixed problem numerically.

6.3 Summary

This chapter presented two approaches for computing mixed H_2/H_∞ controllers numerically. The first method converts an equality constraint to a penalty function and uses the Davidon-Fletcher-Powell optimization method. The second approach appends the H_∞ constraint as an inequality constraint and uses sequential quadratic programming to converge to solutions. Both methods have advantages over the existing method. First, they allow singular H_∞ constraints. Next, feed-forward terms in the constraint are allowed. Thirdly, the order of the controller can be reduced to as low as the H_2 order. Finally, both methods have significant computation advantages over the previous method.

The SQP method was found to converge to lower values of the H_∞ constraint due to the fact it admits infeasible solutions. In particular, it allows controllers which result in an unstable closed-loop system. Thus, the SQP method imposes less constraints on the search direction and results in faster convergence to greater tolerances. The numerical method was demonstrated on an F-16 longitudinal control problem. The example demonstrated the trade-off between controller order, noise rejection, performance, and margins available to the designer using the mixed H_2/H_∞ method.

VII. Mixed H_2/μ Optimal Control

The F-16 example in the last chapter demonstrated how mixed H_2/H_∞ optimization can be used to achieve some measure of robust stability. In addition, the closed-loop system had the desired level of nominal performance. Recently, there has been a great deal of interest in formulating controllers which have robust performance in light of expected system uncertainties (see [2] for references). Further, it is desired that a system have minimal response to noise perturbations. The robust performance problem has been successfully addressed in the μ framework [2], while the noise rejection problem can be formulated as an H_2 problem. This chapter considers the joint problem of designing a controller which rejects noise while simultaneously providing robust performance.

One technique for designing controllers with an upper bound on μ is the D-K iteration developed in Section 3.4.2. This approach is an iterative method which determines an optimal scaling matrix D and an associated H_∞ controller K . The method results in a controller order equal to that of the original plant augmented with the scaling matrices. One key attribute of this μ -synthesis method is it uses H_∞ techniques for controller design. The controller order can be reduced using any one of several available order reduction methods, but we desire to reduce the controller order in an "optimal" fashion, where optimal is defined by the mixed H_2/μ problem. Thus, we desire a mixed H_2/H_∞ optimization problem which minimizes the two-norm of an H_2 transfer function and provides an upper bound on μ through an H_∞ transfer function. Furthermore, μ -synthesis can result in a non-strictly proper controller which results in an unbounded two-norm for the H_2 transfer function in the mixed problem. By incorporating the mixed H_2/H_∞ -synthesis method into the "K" portion of the D-K iteration process, the order of the controller and bounds on the two-norm can be addressed.

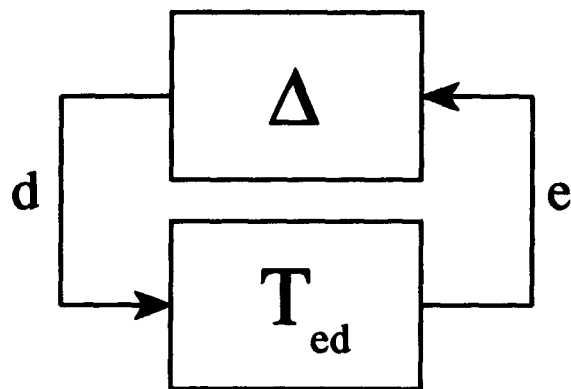


Figure 7.1. Perturbed closed-loop system

This chapter will develop the H_2/μ problem. The method is based on a fixed-order controller, and the order can be reduced to as low as that of the underlying H_2 problem. Next, the robust stability and robust performance problems will be recast into the mixed framework. The numerical approach from Chapter VI will be modified to handle this problem, and demonstrated on a SISO F-16 normal acceleration control design problem and a MIMO HIMAT longitudinal control design problem.

7.1 Mixed H_2/μ

This section incorporates μ -synthesis into the fixed-order mixed H_2/H_∞ framework from Chapter V. Consider the closed-loop system T_{ed} with a block diagonal structured perturbation Δ shown in Figure 7.1. Recall from Chapter III that the set of all dynamic perturbations which have the desired diagonal structure is given by

$$\mathcal{M}(\Delta) := \left\{ \Delta(s) \in \mathfrak{RH}_\infty \mid \Delta(s_0) \in \Delta \text{ for all } s_0 \in \overline{\mathcal{C}}^+ \right\} \quad (7.1)$$

The complex structured singular value of a dynamic transfer matrix $T_{ed}(s)$ over the structured perturbations $\Delta(s) \in \mathcal{M}(\Delta)$ is defined by

$$\|T_{ed}(s)\|_\Delta = \sup_{\omega \in \mathbb{R}} \mu_\Delta [T_{ed}(j\omega)] \quad (7.2)$$

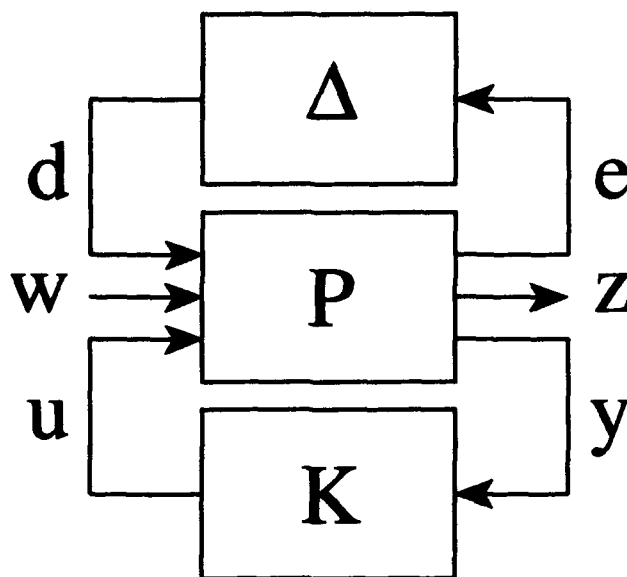


Figure 7.2. Mixed H_2/μ problem

Define the set of scaling transfer functions \mathbf{D} which have the same block diagonal structure as Δ , where each individual block has the property $D_i = D_i^* > 0$. Then, an upper bound on the structured singular value of a transfer matrix is given by

$$\|T_{ed}(s)\|_{\Delta} \leq \sup_{\omega \in \mathbb{R}} \inf_{D \in \mathbf{D}} \bar{\sigma}(DT_{ed}D^{-1}) \quad (7.3)$$

$$= \inf_{D \in \mathbf{D}} \|DT_{ed}D^{-1}\|_{\infty} \quad (7.4)$$

Thus we can convert a μ constraint into an H_{∞} constraint.

Let T_{ed} be the closed-loop transfer function from d to e in Figure 7.2 with the PK loop closed, T_{zw} be the H_2 transfer function of interest and Δ be a bounded energy structured perturbation. Let $D_{opt} \in \mathbf{D}$ represent a scaling transfer function which achieves the infimum in (7.4), and define

$$T_{us} := D_{opt}T_{ed}D_{opt}^{-1} \quad (7.5)$$

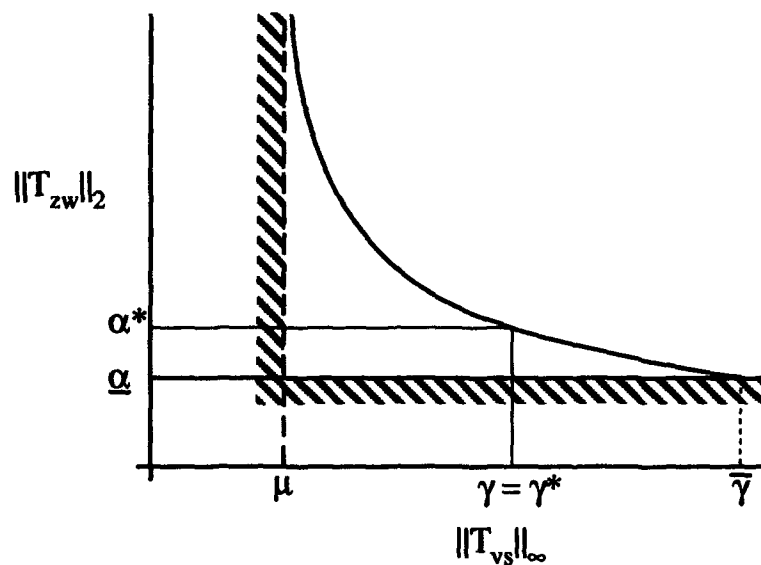


Figure 7.3. Mixed H_2/μ boundary plot

An upper bound on μ can now be determined by finding the infimum of T_{vs} over all K (i. e., the final step in a D-K iteration). Thus $\underline{\gamma}$ is the minimum upper bound on μ ; that is, the minimum achievable value of μ from D-K iteration, assuming the controller order is selected to be large enough. Moreover, T_{zw} achieves a minimum of $\underline{\alpha}$ with the controller $K_{2,opt}$, and there is a corresponding $\bar{\gamma}$ ($\geq \underline{\gamma}$) which is the upper bound on μ corresponding to $K_{2,opt}$. Thus, the problem reduces to a trade-off between H_2 performance and μ performance along the γ versus α curve given in Figure 7.3 for $\underline{\gamma} < \gamma \leq \bar{\gamma}$.

One of the assumptions made in setting up the mixed H_2/μ problem is that the scaling transfer function D_{opt} is known, which is generally not the case. However, this transfer function can be approximated using existing μ -synthesis methods. The proposed algorithm for solving the mixed H_2/μ optimal control problem is as follows:

- i. Compute D_{opt} using μ -synthesis
- ii. Define $T_{vs} := D_{opt}T_{ed}D_{opt}^{-1}$
- iii. Compute $K_{2,opt}$, $\underline{\alpha}$, and $\bar{\gamma}$

- iv. Set γ^* to the desired value
- v. Compute K_{mix} and α^* using H_2/H_∞ -synthesis

7.2 Robust Controllers Using H_2/μ

7.2.1 Robust Stability. Consider the perturbed system given in Figure 7.1, where T_{ed} is the closed-loop system and Δ is a structured uncertainty with $\Delta \in \mathcal{M}(\Delta)$, the set of all stable proper transfer functions which have the desired structure. Then the following theorem provides a less conservative approach to robust stability than H_∞ optimization combined with the Small Gain Theorem (Theorem 1.1.1).

Theorem 7.2.1 *Let $\gamma > 0$. The loop shown in Figure 7.1 is well-posed and internally stable for all $\Delta \in \mathcal{M}(\Delta)$ with $\|\Delta\|_\infty < \frac{1}{\gamma}$ if and only if*

$$\|T_{ed}\|_\Delta = \sup_{\omega \in \mathbb{R}} \mu_\Delta [T_{ed}(j\omega)] \leq \gamma \quad (7.6)$$

Proof: See [44], Theorem 3.6. ■

Thus, using this theorem and the algorithm from above, we can determine an upper bound on the largest perturbation under which the system is guaranteed to be robustly stable. Combining this with the mixed framework, a trade-off can now be made. Either the level of noise rejection can be determined for a given level of perturbation, or the maximum perturbation can be determined for a given level of noise rejection. More likely, the trade-off involves finding some level of noise rejection which is acceptable given the resulting level of robustness.

7.2.2 Robust Performance. Consider the robust performance problem given in Figure 7.4, where $T_{e_2 d_2}$ is the transfer function for the desired performance objective, $\|T_{e_2 d_2}\|_\infty \leq \gamma$ (for example, output sensitivity), with n_{d_2} inputs and n_{e_2} outputs. T_{ed} is the closed-loop system and Δ is a structured uncertainty where

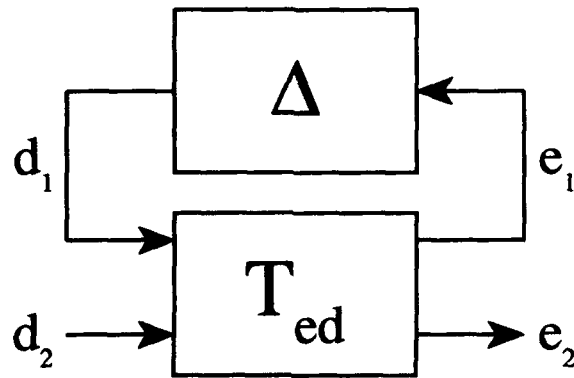


Figure 7.4. Robust performance closed-loop system

$\Delta \in \mathcal{M}(\Delta)$, the set of all stable proper transfer functions which have the desired structure. The transfer function $T_{e_2 d_2}$ can be written as an upper fractional transformation of T_{ed} and Δ , denoted $T_{e_2 d_2} = F_u(T_{ed}, \Delta)$. Our performance objective can be combined into the perturbation by defining an augmented perturbation

$$\Delta_p := \left\{ \left[\begin{array}{cc} \Delta & 0 \\ 0 & \Delta_F \end{array} \right] \mid \Delta \in \Delta, \Delta_F \in C^{n_{d_2} \times n_{e_2}} \right\} \quad (7.7)$$

where Δ_F is a fictitious perturbation. Robust performance can now be determined using the following theorem.

Theorem 7.2.2 *Let $\gamma > 0$. For all $\Delta \in \Delta$ with $\|\Delta\|_\infty < \frac{1}{\gamma}$, the loop in Figure 7.4 is well posed, internally stable, and $\|T_{e_2 d_2}\|_\infty \leq \gamma$ iff*

$$\|T_{ed}\|_{\Delta_p} := \sup_{\omega \in \mathfrak{R}} \mu_{\Delta_p} [T_{ed}(j\omega)] \quad (7.8)$$

$$\leq \sup_{\omega \in \mathfrak{R}} \inf_{D \in \mathbf{D}} \bar{\sigma}(DT_{ed}D^{-1}) \leq \gamma \quad (7.9)$$

Proof: See [44], Theorem 3.7. ■

Thus, if our desired level of performance is represented by $\|T_{e_2 d_2}\|_\infty \leq \gamma$, we can guarantee this performance in light of all structured perturbations where $\|\Delta_p\|_\infty < 1/\gamma$ if

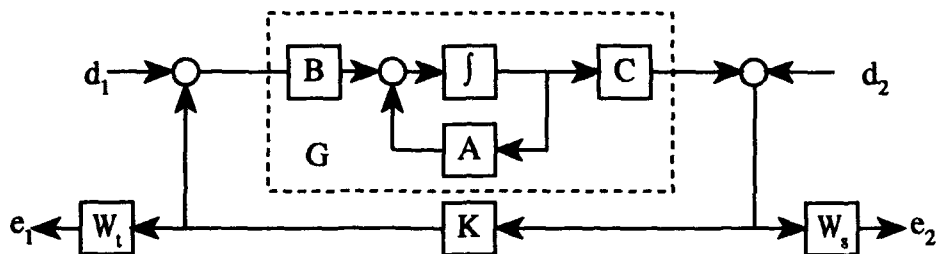


Figure 7.5. μ block diagram

and only if $\|T_{ed}\|_{\Delta_P} \leq \gamma$. Another interpretation of this theorem is: if $\|T_{ed}\|_{\Delta_P} = \gamma$, then robust performance is guaranteed to a level of $\|T_{e_2 d_2}\|_{\infty} \leq \gamma$ for all perturbations such that $\|\Delta_P\|_{\infty} < 1/\gamma$. Now, the mixed structure developed in the previous section can be used by defining $T_{us} := D_{opt} T_{ed} D_{opt}^{-1}$ and applying the algorithm. Again, a trade-off can now be made between the achievable level of robust performance and H_2 performance.

7.3 Examples

7.3.1 SISO F-16 Design. The SISO F-16 longitudinal controller design problem from the previous chapter is used to demonstrate the above method. The system consists of a short period approximation of a continuous, linear, time-invariant normal acceleration command system augmented with a pre-filter for the servo dynamics and a post-filter to model the control delay. The plant is given in Appendix A.

7.3.1.1 Problem Setup. This problem is solved using the mixed H_2/μ method, where the H_2 portion minimizes the effect of the wind disturbance and measurement noise, provides state regulation, and minimizes control power. The μ portion incorporates performance robustness.

The H_2 portion of this problem is identical to that in Section 6.2.4. The μ problem is shown in Figure 7.5. The performance objective is to minimize the weighted output sensitivity in light of an input multiplicative perturbation. The

sensitivity weight is a low-pass filter selected to improve tracking of a step input based on the desired open-loop GK from Section 6.2.2. The weight is given by

$$W_s = \frac{s + 1.0}{s + 0.0001} \quad (7.10)$$

The input perturbation represents uncertainty in the nominal model including uncertainties in the control actuators, aerodynamics, flight conditions, aircraft geometry, structural bending, and other unmodeled high frequency dynamics. The weighting associated with this perturbation is a high-pass filter given by

$$W_t = \frac{50(s + 100)}{s + 10000} \quad (7.11)$$

This weight emphasizes the high frequency content of the perturbation set we are trying to model. For a good discussion on the choice of both sensitivity and complementary sensitivity weights, the reader is referred to [19].

The closed-loop system T_{ed} is now formed as

$$T_{ed} = \begin{bmatrix} W_t K G (I - K G)^{-1} & W_t K (I - K G)^{-1} \\ W_s G (I - G K)^{-1} & W_s (I - G K)^{-1} \end{bmatrix} \quad (7.12)$$

The scaling D_{opt} is determined using the *hinfsyn*, *mu*, and *musynfit* routines from MATLABTM μ -Toolbox [44]. These routines are combined to perform D-K iterations. First *hinfsyn* is used to determine a nominal closed-loop system. Then, *mu* is used to determine the value of μ and the optimal scaling for this controller. Finally, *musynfit* is used by the operator to interactively select the order of the scaling D which best approximates the optimal scaling. The process is repeated until μ is converged to some desired level. The H_∞ transfer function is then formed as $T_{vs} = D_{opt} T_{ed} D_{opt}^{-1}$, where D_{opt} is the last D from the above process. The H_∞ matrices are

$$A_{\infty} = \begin{bmatrix} -3849.04 & 5737.46 & 17039.10 & -161.38 & -2110.08 \\ -5737.46 & -18685.07 & 11506.45 & -108.98 & -1424.93 \\ 0 & 0 & -1.49 & 1.00 & -0.19 \\ 0 & 0 & 9.75 & -0.96 & -19.04 \\ 0 & 0 & 0 & 0 & -20.00 \\ 0 & 0 & 35.26 & -0.334 & -4.37 \\ 0 & 0 & -35.26 & 0.334 & 4.37 \\ 0 & 0 & 0 & 0 & 0 \\ 0 & 0 & 0 & 0 & 0 \\ 0 & 0 & 0 & 0 & 0 \end{bmatrix}$$

$$\begin{bmatrix} -38654.94 & -483.14 & 0 & -4247.39 & 2868.25 \\ -26103.56 & -326.26 & 0 & -2868.25 & 1936.92 \\ 0 & 0 & 0 & 0 & 0 \\ 0 & 0 & 0 & 0 & 0 \\ 0 & 0 & 0 & 0 & 0 \\ -40.00 & 0 & 0 & 0 & 0 \\ 80.00 & -0.0001 & 0 & 8.79 & -5.94 \\ 0 & 0 & -10000.00 & 0 & 0 \\ 0 & 0 & 0 & 398.35 & 2869.22 \\ 0 & 0 & 0 & -2869.22 & -20621.99 \end{bmatrix}$$

(7.13)

$$B_s = \begin{bmatrix} -8.79 & 0 \\ -5.94 & 0 \\ 0 & 0 \\ 0 & 0 \\ 0 & 20.00 \\ 0 & 0 \\ 0.02 & 0 \\ 0 & 0 \\ 8.79 & 0 \\ 5.94 & 0 \end{bmatrix} \quad B_{u_\infty} = \begin{bmatrix} 0 \\ 0 \\ 0 \\ 0 \\ 20.0 \\ 0 \\ 0 \\ 50.0 \\ 0 \\ 0 \end{bmatrix} \quad (7.14)$$

$$C_v = \begin{bmatrix} 483.19 & -326.29 & -1938.38 & 18.36 & 240.04 \\ 0 & 0 & 0 & 0 & 0 \\ 4397.42 & 54.96 & 0 & 483.19 & -326.29 \\ 0 & 0 & -9900.00 & 0 & 0 \end{bmatrix} \quad (7.15)$$

$$C_{y_\infty} = \begin{bmatrix} 0 & 0 & -35.26 & 0.334 & 4.37 & 80.00 & 0 & 0 & 8.79 & -5.94 \end{bmatrix} \quad (7.16)$$

$$D_{vs} = \begin{bmatrix} 1.00 & 0 \\ 0 & 0 \end{bmatrix} \quad D_{vu} = \begin{bmatrix} 0 \\ 50.0 \end{bmatrix} \quad D_{ys} = \begin{bmatrix} 0.02 & 0 \end{bmatrix} \quad D_{yu} = [0] \quad (7.17)$$

7.3.1.2 Results. The process is initiated by computing the tenth order μ -synthesis controller given in the last row and column of Table 7.1. A Schur model reduction is used to compute reduced order controllers. This method models the plant as a reduced order plant with an additive perturbation. It attempts to reduce the infinity-norm of the perturbation and therefore, the modeling error. A

Table 7.1. F-16 H_2/μ Optimization Results

Controller order	H_2/μ		μ -synthesis (model reduction)	
	α	μ	α	μ
4	0.895	2.34	<i>unstable</i>	
6	0.935	1.98	6.36	1.81
8	0.940	1.77	6.36	1.597
10	0.953	1.71	4.41	1.591

Schur decomposition is used where needed and the resulting method is more numerically robust than the often used balanced order reduction. The reader is referred to [62] for more information on Schur decomposition, Schur model order reduction, and balanced order reduction. The tenth order controller is reduced to the eighth and sixth order μ -synthesis controllers given in Table 7.1. A stabilizing fourth order controller could not be found using the available model reduction methods in MATLABTM [44]. The tenth, eighth, and sixth order μ -synthesis results were used as initial controllers for the numerical H_2/μ optimization, and mixed controllers were designed. The resulting mixed controllers which gave the best trade-off between H_2 and μ performance are given in Table 7.1. The optimal H_2 controller is used as the initial controller for the fourth order mixed controller and the resulting best mixed controller is also given in Table 7.1.

The tenth order μ controller has the best level of robust performance, but it also has a high level of high frequency noise response, as shown in Figure 7.6. By comparison, the tenth order H_2/μ controller has robust performance for slightly smaller perturbations since the upper bound on μ is 8% higher; therefore, the nominal performance is also decreased as is seen in Figure 7.7. However, the mixed controller has better high frequency noise response, as is expected, since the two-norm is about one fourth the size of the two-norm with the μ controller. Moreover, Figures 7.8 and 7.9 show that the control usage is considerably reduced with the mixed controller. Again, this result is expected since the H_2 portion of the mixed controller includes a

penalty on control usage, while μ -synthesis does not take this into account. Similar results can be seen for the eighth and sixth order results shown in Figures 7.10–7.17.

One advantage of the mixed approach in this example is the consistent ability to find a stabilizing controller at orders as low as the H_2 order; in this case fourth order. Model reduction techniques resulted in non-stabilizing fourth order controllers for the μ -synthesis approach, but the mixed approach is able to compute a stabilizing fourth order controller. As can be seen in Table 7.1, the upper bound on μ for the fourth order controller is 47% greater than the μ -synthesis tenth order controller; thus, the perturbation size for robust performance is reduced. Nominal performance is also decreased with the peak overshoot increased from about 0.5 g to 0.7 g, and the settling time is about the same for both. The high frequency noise rejection is improved fourfold with the mixed fourth order controller as compared to the tenth order μ -synthesis controller. These results can be seen in Figures 7.18 and 7.19.

The vector margins for the resulting controllers are given in Table 7.2. As can be seen, the tenth order μ -synthesis controller resulted in the best margins. Although the tenth and eighth order H_2/μ controllers resulted in decreased margin, it is an acceptable trade-off for the increased noise rejection. Notice that the sixth order H_2/μ controller has better upper gain margin and phase margin than the tenth and eighth order H_2/μ controllers. This is due to the trade-off between performance and margins which occurs at the knee of the α versus γ curve; as γ is approached, there is an underlying trade-off which is made to minimize γ . The fourth order H_2/μ controller resulted in significantly reduced margins. Therefore, a design decision must be made between the order and the desired margins.

Finally, the response of the system to an initial 5° angle of attack perturbation is given in Figure 7.20. Notice that there is no significant difference in regulation between the controllers. This indicates that the increased two-norm is due almost entirely to the increase in response to high frequency noise and increased control usage, as is seen in the time responses.

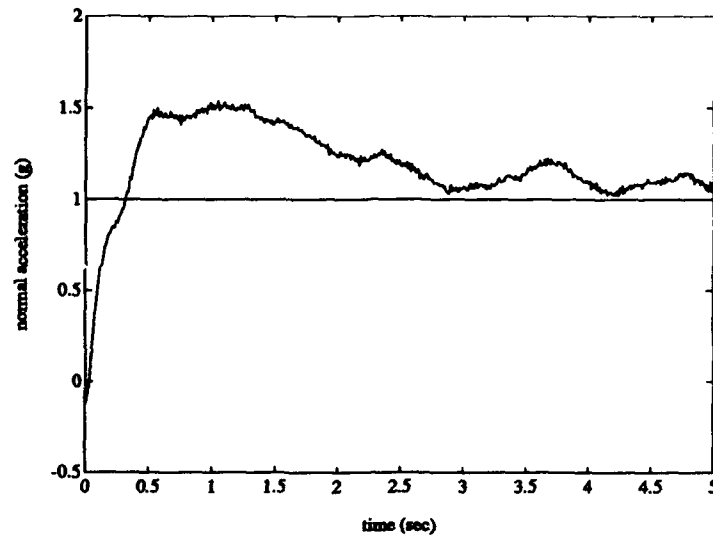


Figure 7.6. F-16, step response, 10th order μ controller

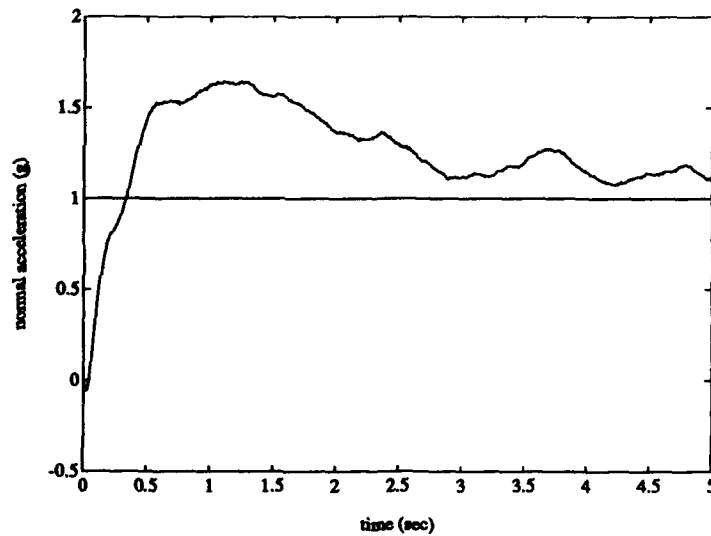


Figure 7.7. F-16, step response, 10th order H_2/μ controller

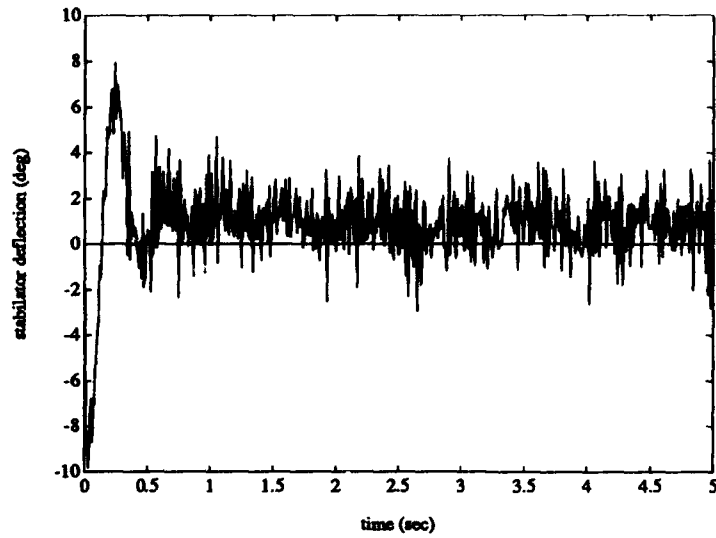


Figure 7.8. F-16, control usage for step response, 10th order μ controller

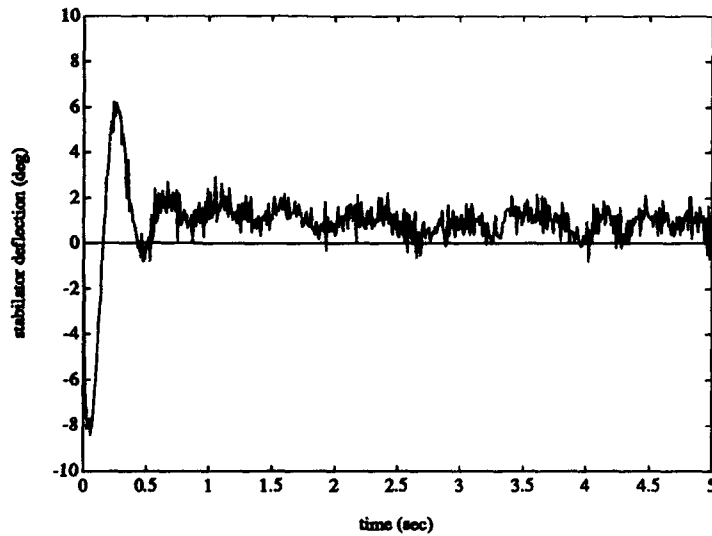


Figure 7.9. F-16, control usage for step response, 10th order H_2/μ controller

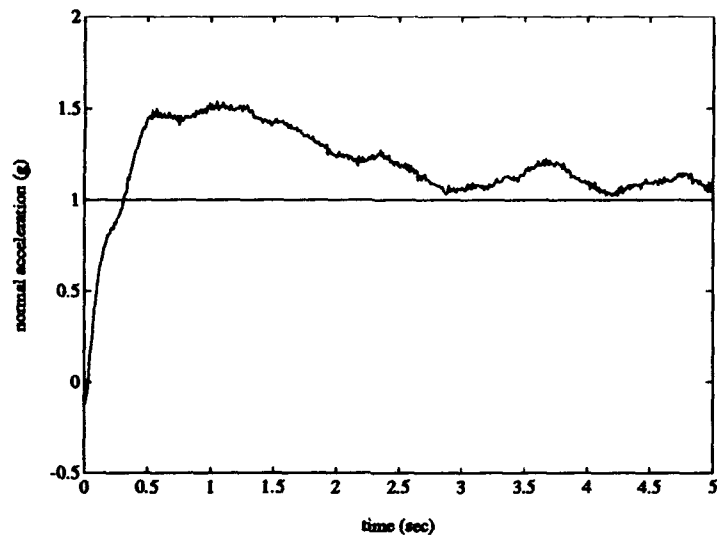


Figure 7.10. F-16, step response, 8th order μ controller

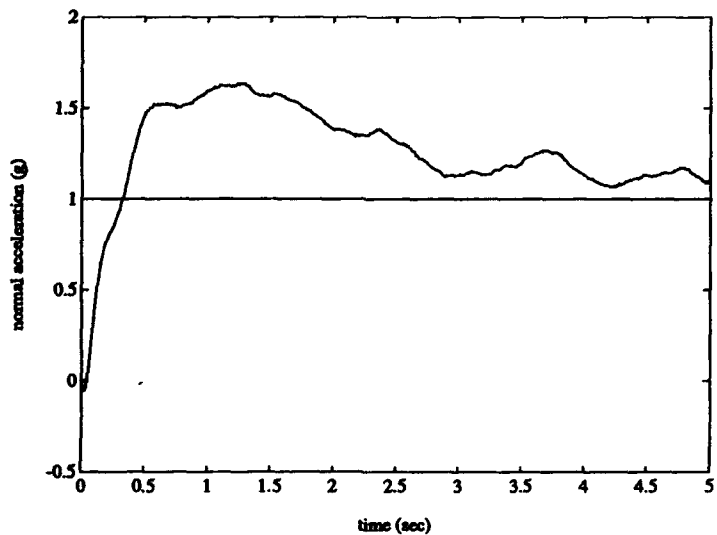


Figure 7.11. F-16, step response, 8th order H_2/μ controller

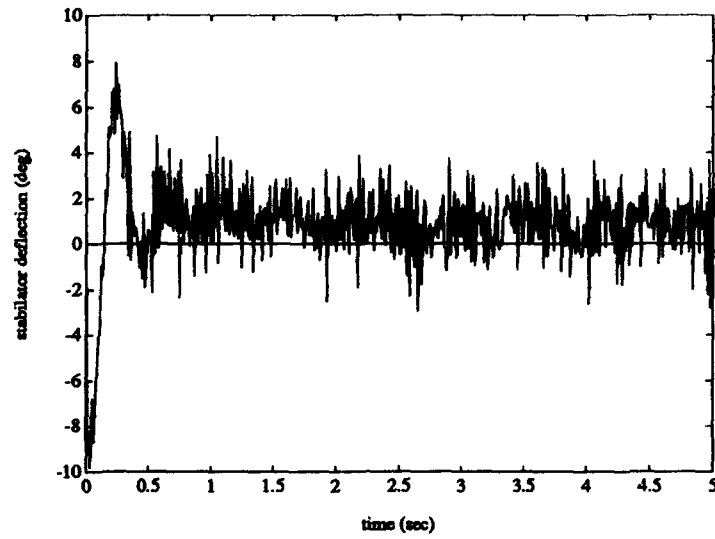


Figure 7.12. F-16, control usage for step response, 8th order μ controller

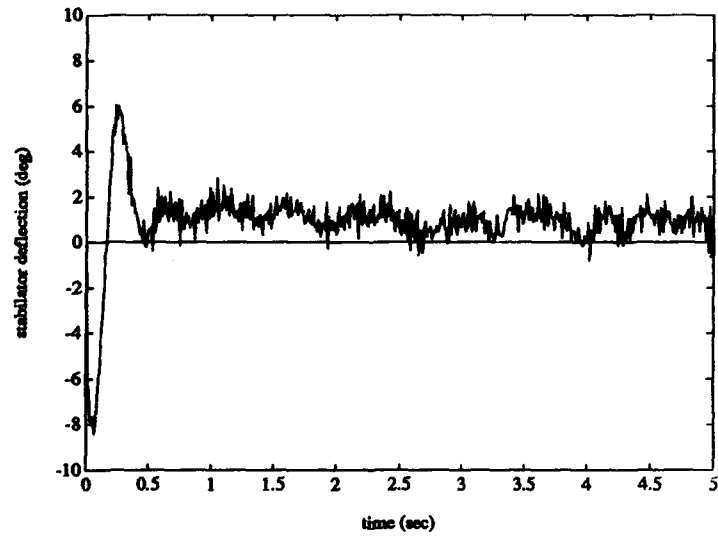


Figure 7.13. F-16, control usage for step response, 8th order H_2/μ controller

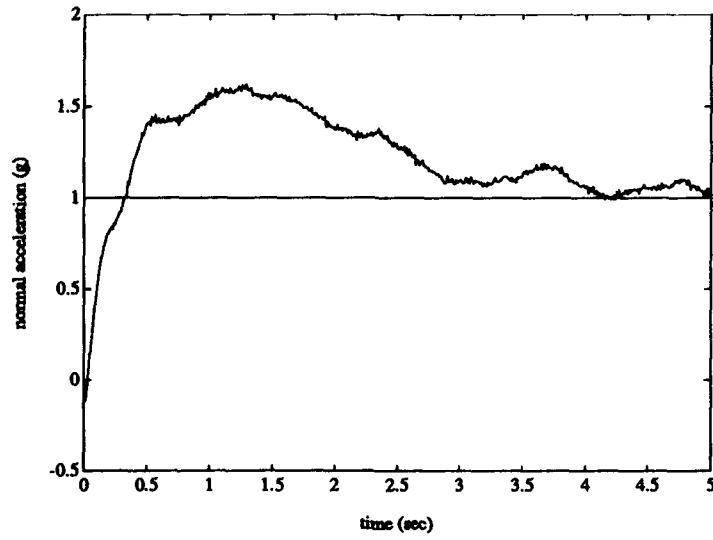


Figure 7.14. F-16, step response, 6th order μ controller

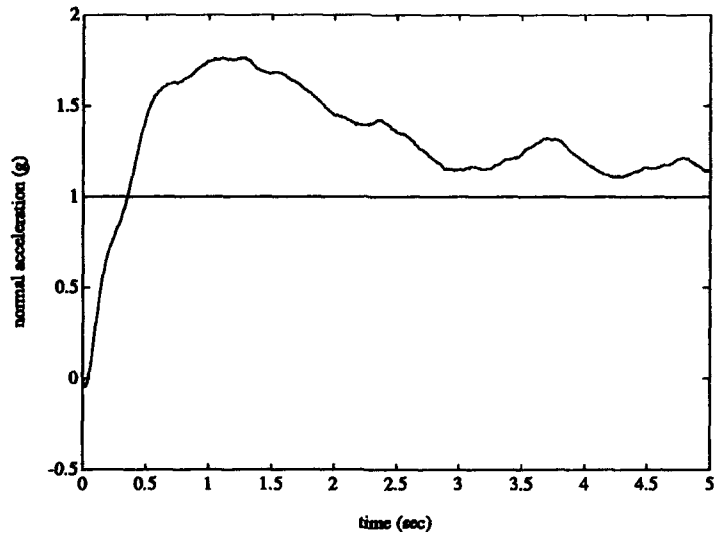


Figure 7.15. F-16, step response, 6th order H_2/μ controller

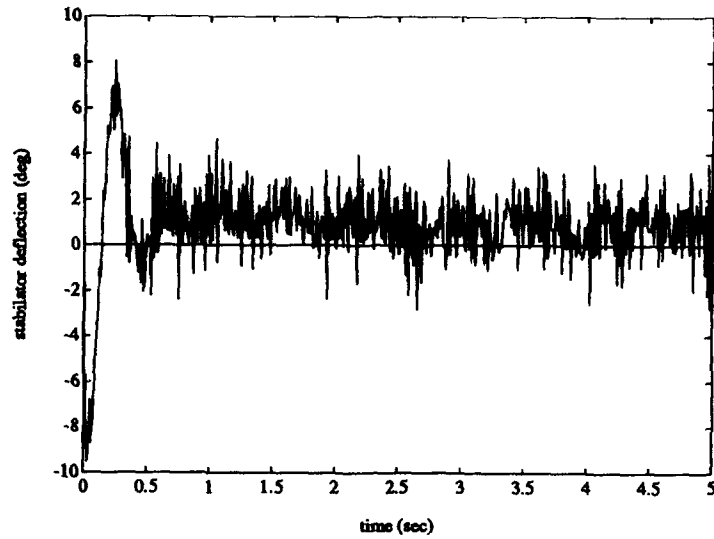


Figure 7.16. F-16, control usage for step response, 6th order μ controller

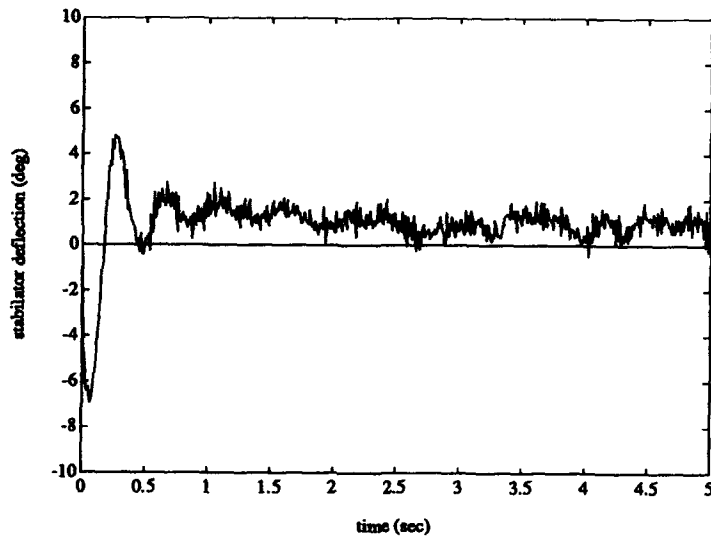


Figure 7.17. F-16, control usage for step response, 6th order H_2/μ controller

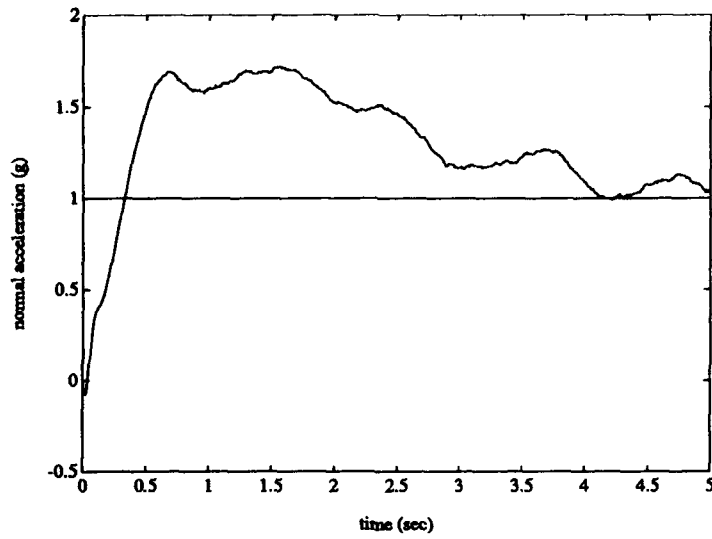


Figure 7.18. F-16, step response, 4th order H_2/μ controller

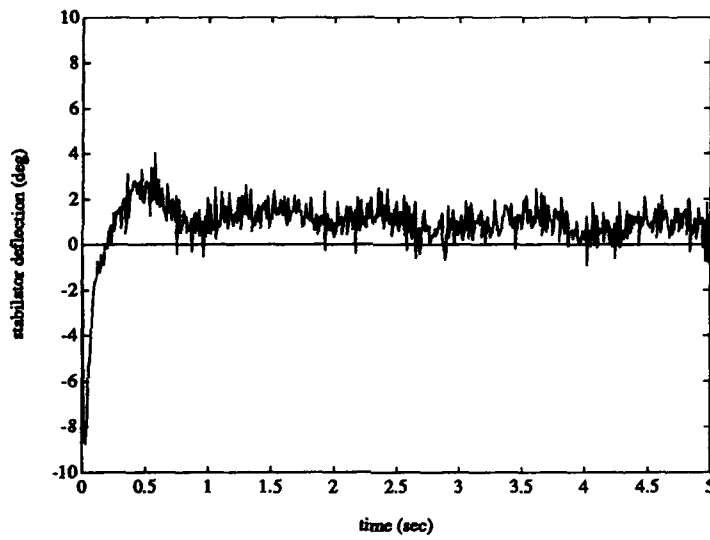


Figure 7.19. F-16, control usage for step response, 4th order H_2/μ controller

Table 7.2. F-16 H_2/μ Vector Margins

Controller order	H_2/μ		μ -synthesis (model reduction)	
	Complementary Sensitivity GM (dB)	Sensitivity GM (dB)	Complementary Sensitivity GM (dB)	Sensitivity GM (dB)
4	[-5.89 3.48]	[-3.92 7.33]	33.11	<i>unstable</i>
6	[-6.77 3.76]	[-4.83 11.84]	43.68	[-4.88 12.21]
8	[-7.50 3.96]	[-4.63 10.60]	41.27	[-4.93 12.56]
10	[-7.57 3.98]	[-4.68 10.84]	41.77	[-4.93 12.56]
				PM (°)
				44.34
				44.94
				44.95

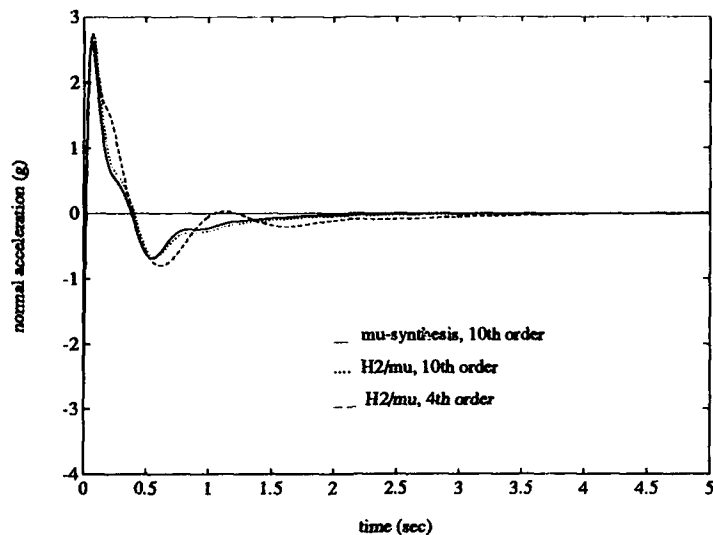


Figure 7.20. F-16, initial 5° angle of attack perturbation response

Based on these results, the designer must make a choice of controller order. Since performance is not considerably different for all the mixed controllers, the primary factor in the decision is the trade-off between order and robustness. If the expected perturbations are known to have an infinity-norm less than $1/2.34$, then the fourth order controller is the best choice. However, if larger perturbations are expected, the controller order will have to be increased to remain robust.

7.3.2 MIMO HIMAT Design. A longitudinal controller design problem for the HIMAT, a highly maneuverable, remotely piloted, technology demonstration vehicle, is used to demonstrate the mixed approach for MIMO problems and to demonstrate further application of mixed H_2/μ . The model is taken from data for the HIMAT vehicle [44]. The model is a four-state, continuous, linear, time-invariant, description of the short period and phugoid modes. The control inputs are elevon (δ_e) and canard (δ_c) deflections and the measured outputs are angle of attack (α) and aircraft attitude (θ). A block diagram of the system is given in Figure 7.21. The plant and simulation truth model are given in Appendix B.

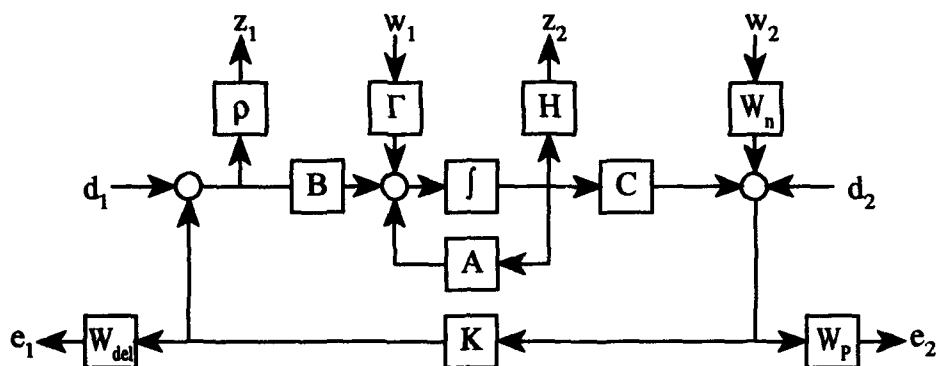


Figure 7.21. HIMAT system block diagram

7.3.2.1 H_2 Regulator. The H_2 portion of the control design is based on a standard Linear Quadratic Gaussian (LQG) problem. A wind disturbance is modeled as an angle of attack perturbation by a zero-mean white Gaussian noise of intensity 5.0×10^{-4} rad²-sec and

$$\Gamma = \begin{bmatrix} -36.6 \\ -1.90 \\ -11.7 \\ 0 \end{bmatrix} \quad (7.18)$$

The measurements are corrupted by zero-mean, white Gaussian noises of strength 1.6×10^{-5} deg²-sec ($W_n = I$). The controlled outputs for the LQG design are control usage and state perturbations with unit weightings ($\rho = 10$ and $H = I$).

Thus, the H_2 problem is set up to design a minimum control/state regulator operating in the face of process and measurement noises. No attempt is made to force the system to track a step or guarantee vector margins for the closed-loop system. Robust performance will be achieved through the use of μ constraints. The resulting controller is fourth order, and the minimum two-norm of the closed-loop system with $K_{2,opt}$ is $\underline{\alpha} = 0.20$.

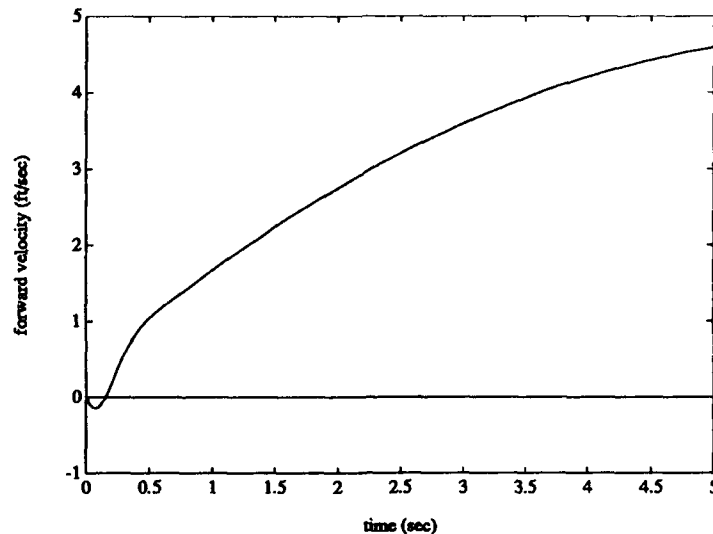


Figure 7.22. HIMAT, H_2 controller-velocity response to initial 5° angle of attack perturbation

The H_2 regulation is shown in Figures 7.22-7.25 for a initial 5° angle of attack perturbation. The H_2 controller provides good regulation with minimal noise response. The control usage in Figure 7.26 shows there is little response to high frequency noises.

The response of the system to unit step in angle of attack and pitch angle are given in Figures 7.27—7.32. Notice that the H_2 solution is not an acceptable tracker, but does have acceptable noise rejection, particularly at high frequency. Furthermore, the control usage is minimal, but not unexpected since there is no apparent tracking.

7.3.2.2 Robust Performance. The mixed controller objective is to design a controller such that the closed-loop system has robust performance measured at the output with an input disturbance perturbation. This problem is solved by appending the performance objective as a fictitious perturbation and combining it with the disturbance into a structured perturbation. The controller is then designed using the mixed framework.

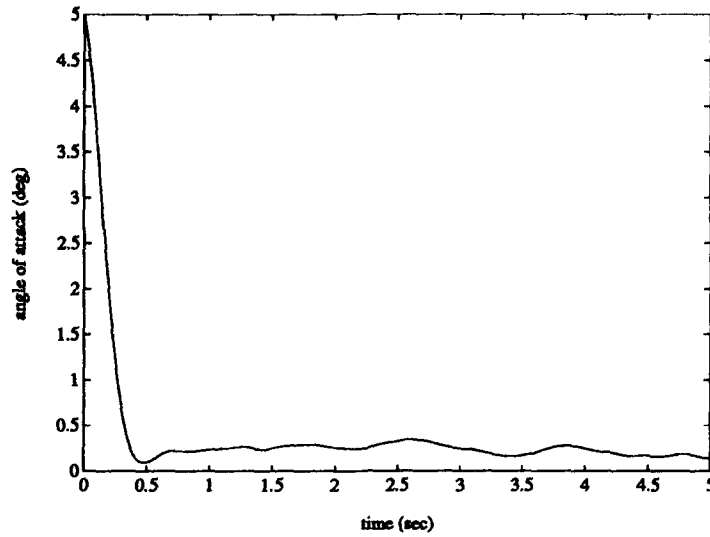


Figure 7.23. HIMAT, H_2 controller-angle of attack response to initial 5° angle of attack perturbation

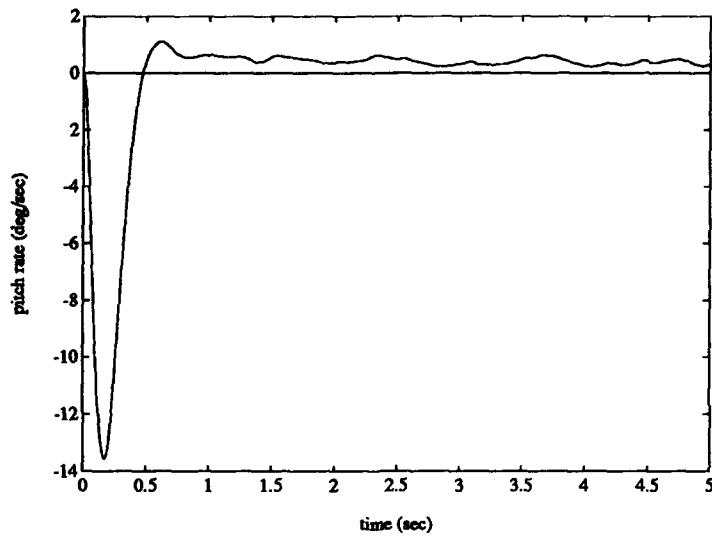


Figure 7.24. HIMAT, H_2 controller-pitch rate response to initial 5° angle of attack perturbation

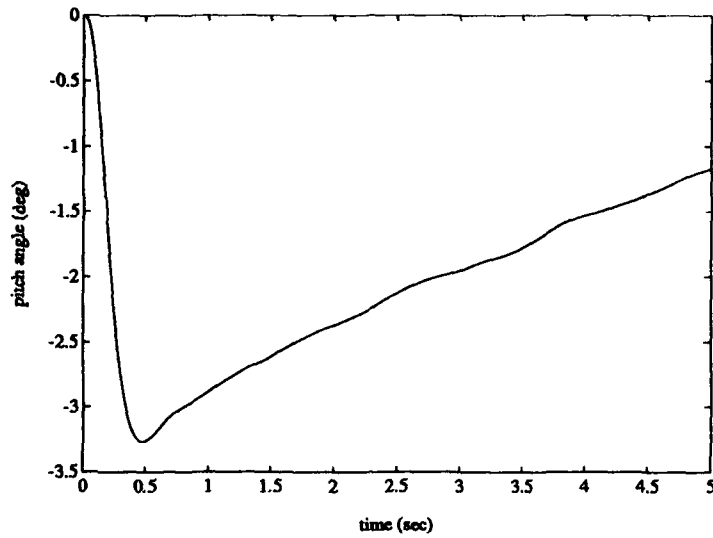


Figure 7.25. HIMAT, H_2 controller-pitch angle response to initial 5° angle of attack perturbation

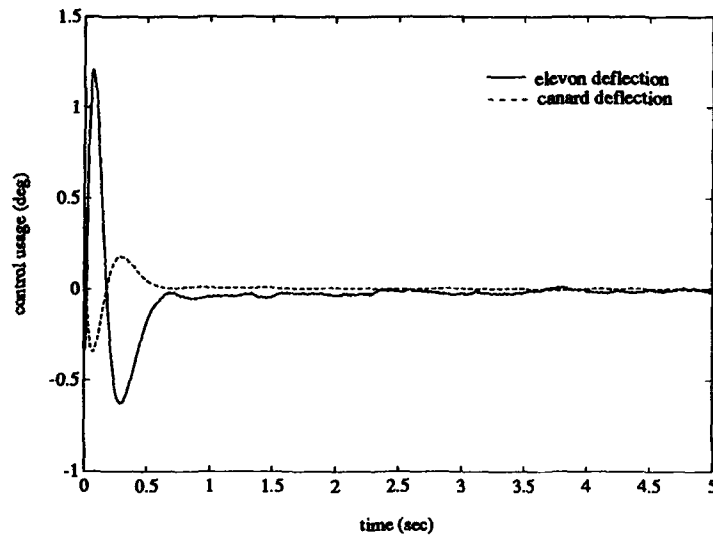


Figure 7.26. HIMAT, H_2 controller-control usage for an initial 5° angle of attack perturbation

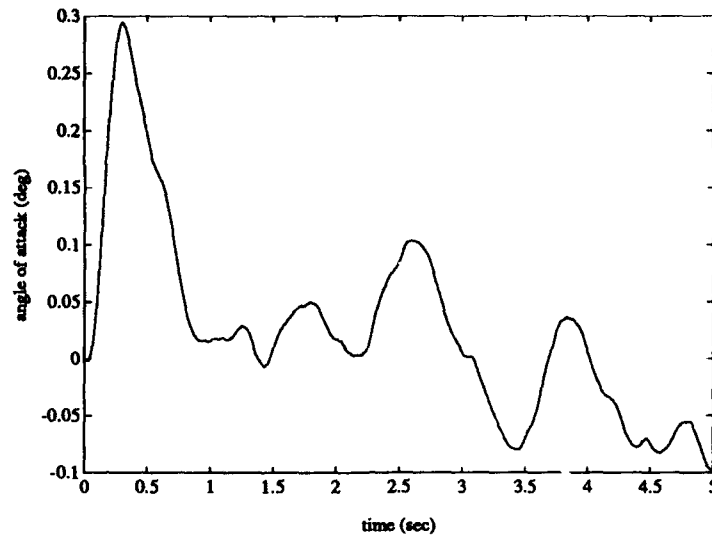


Figure 7.27. HIMAT, H_2 controller-angle of attack response to angle of attack unit step input

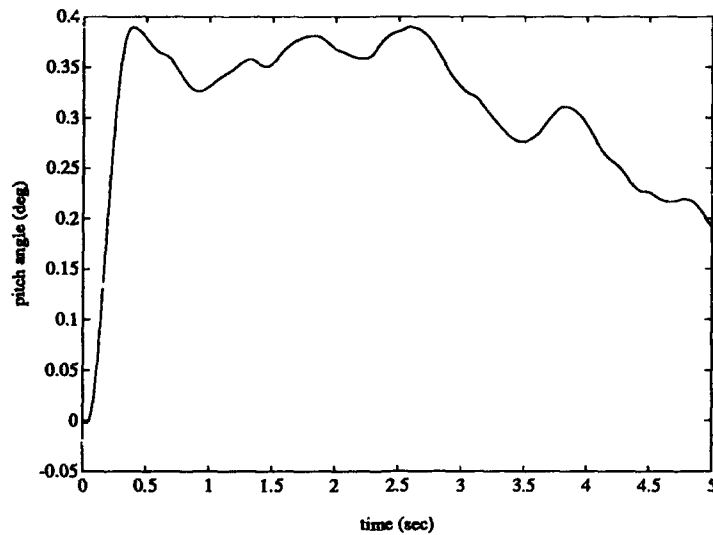


Figure 7.28. HIMAT, H_2 controller-pitch angle response to angle of attack unit step input

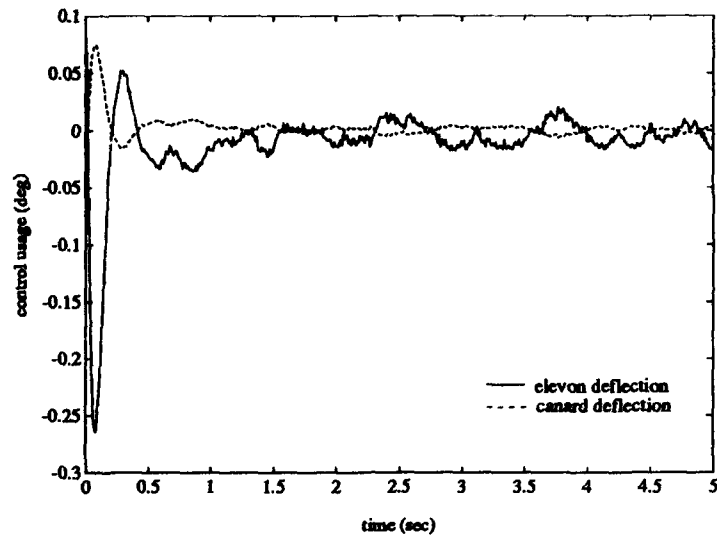


Figure 7.29. HIMAT, H_2 controller-control usage for angle of attack unit step input

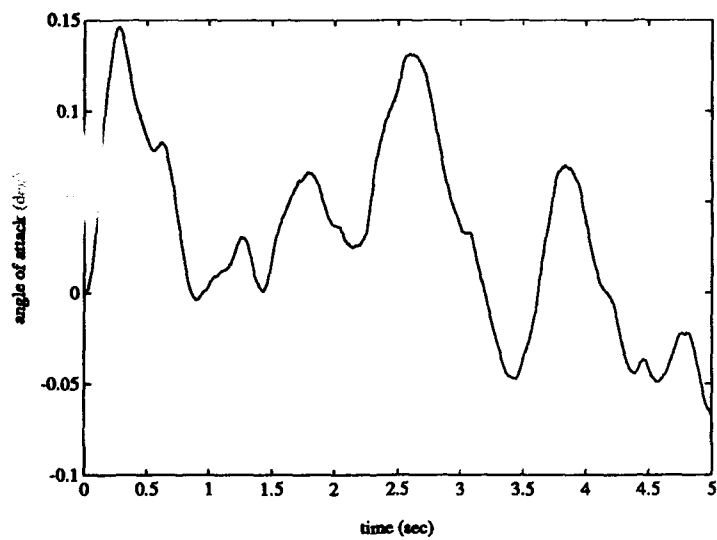


Figure 7.30. HIMAT, H_2 controller-angle of attack response to pitch angle unit step input

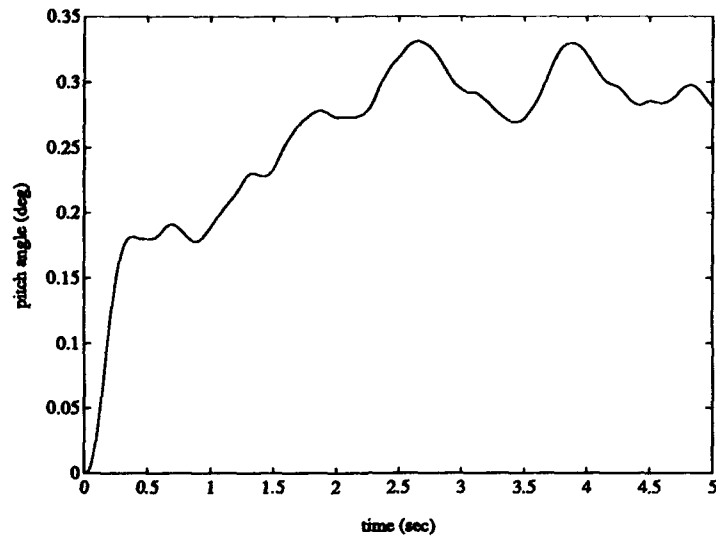


Figure 7.31. HIMAT, H_2 controller-pitch angle response to pitch angle unit step input

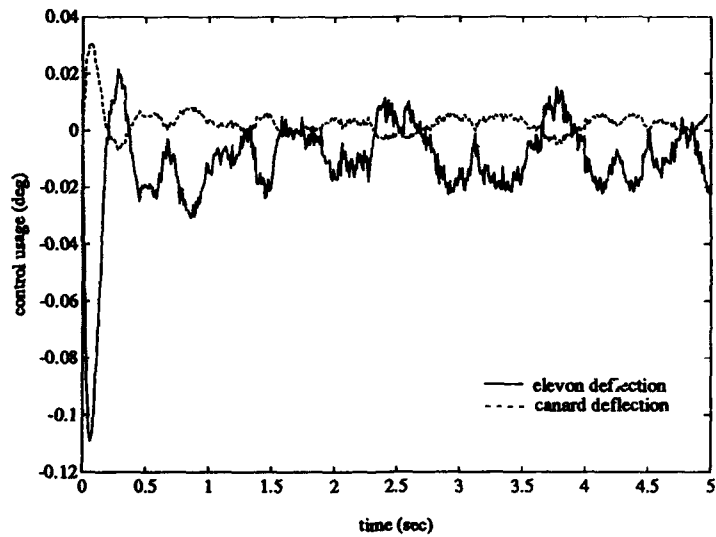


Figure 7.32. HIMAT, H_2 controller-control usage for pitch angle unit step input

The disturbance enters the system at the input to the plant and is modeled as a high frequency perturbation by appending a high-pass filter at the output e_1 . The perturbation filter transfer function is

$$W_{del}(s) = \frac{50(s + 100)}{s + 10000} I_2 \quad (7.19)$$

The performance objective is to track a step at the output. The fictitious "performance perturbation" is modeled by a low-pass filter appended at the output e_2 . The performance filter transfer function is

$$W_P(s) = \frac{0.5(s + 3)}{s + 0.03} I_2 \quad (7.20)$$

The system is considered to have robust performance to structured perturbations $\Delta \in \mathcal{M}(\Delta)$ where $\|\Delta\|_\infty < \gamma$ if

$$\|T_{ed}\|_\Delta < \frac{1}{\gamma} \quad (7.21)$$

where T_{ed} is the closed-loop system

$$T_{ed} = \begin{bmatrix} W_{del}KG(I - KG)^{-1} & W_{del}K(I - KG)^{-1} \\ W_PG(I - GK)^{-1} & W_P(I - GK)^{-1} \end{bmatrix} \quad (7.22)$$

In this particular case, it is desired to have $\gamma \leq 1$.

The first step in the process is to compute the best μ controller. A 20th order controller is found using the MATLABTM *musynfit* function [44] which achieves the desired level of robust performance. A third order fit is used which results in a sixth order D transfer function. The resulting controller order is the sum of the four model states, the two performance weighting states, the two perturbation, and two times the six states of the scaling matrix D , or 20th order. The response of the system to unit steps in angle of attack and pitch angle are given in Figures 7.33–7.38. This

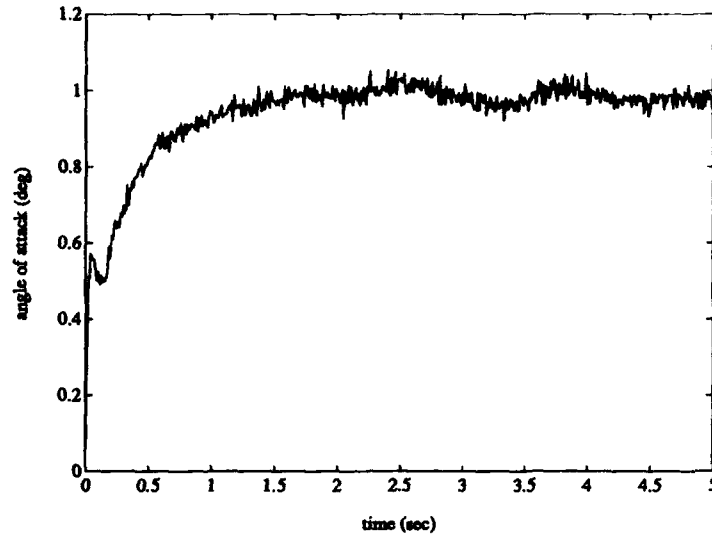


Figure 7.33. HIMAT, μ controller—angle of attack response to angle of attack unit step input

controller possesses good tracking of both angle of attack and pitch angle inputs. Further, the control usage is not excessive after an initial large transient. Notice that the response to high frequency noise is increased over that of the H_2 system.

The objective now is to attempt to reduce the order of the controller and improve the high frequency response using the mixed approach. It should be mentioned that model reduction of the μ controller can be used. In this case, a Schur model reduction method was attempted for 16th, 12th, 8th, and 4th order controllers, but all the resulting controllers suffered from large increases in μ and thus did not provide an acceptable level of performance robustness.

7.3.2.3 H_2/μ . The mixed optimization problem is set up by defining

$$T_{us} = D_{opt} T_{ed} D_{opt}^{-1} \quad (7.23)$$

where D_{opt} is determined from the previous μ -synthesis. The mixed problem is then solved using the inequality constraint approach with an SQP algorithm. It is desired

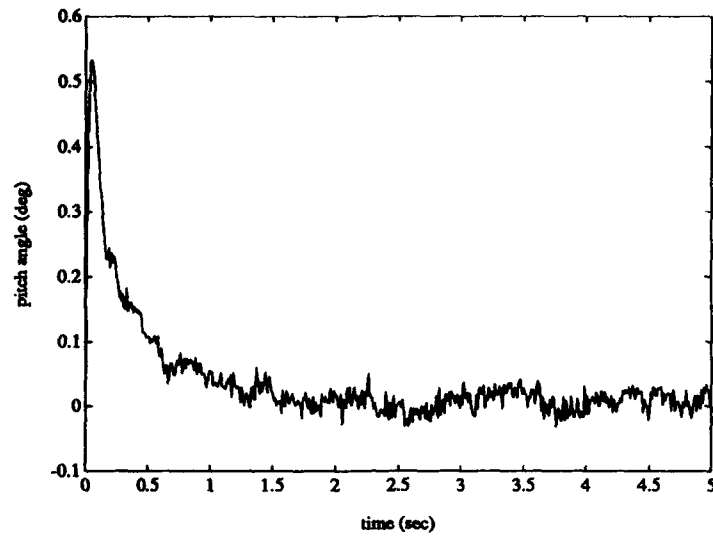


Figure 7.34. HIMAT, μ controller-pitch angle response to angle of attack unit step input

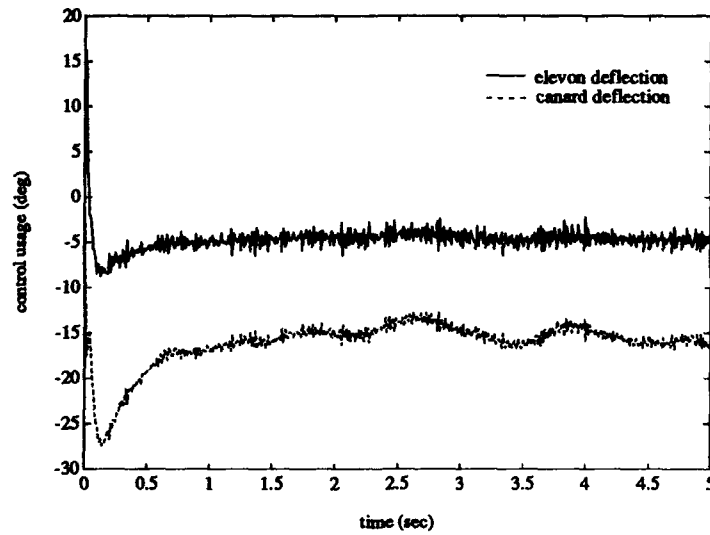


Figure 7.35. HIMAT, μ controller-control usage for angle of attack unit step input

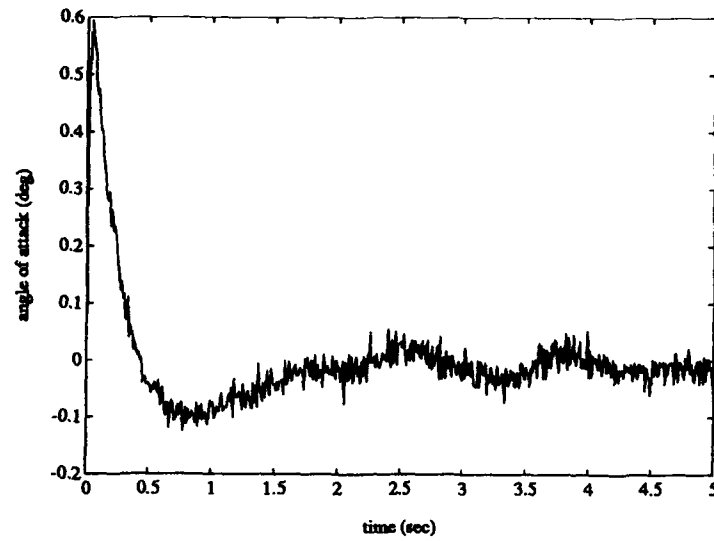


Figure 7.36. HIMAT, μ controller-angle of attack response to pitch angle unit step input

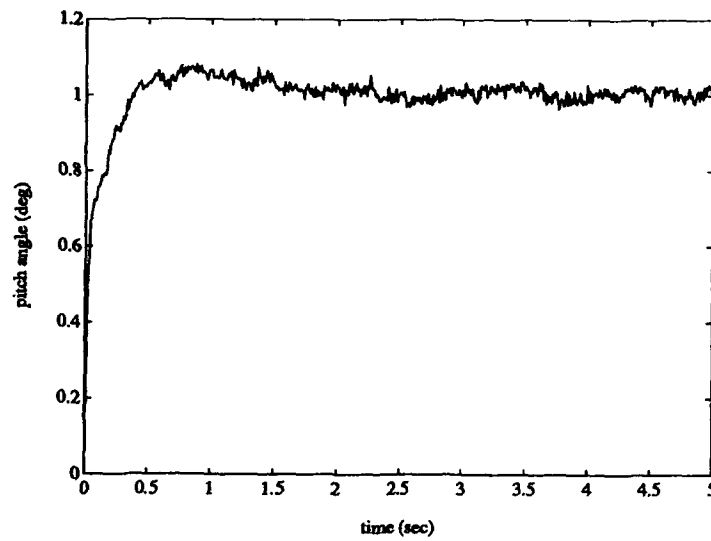


Figure 7.37. HIMAT, μ controller-pitch angle response to pitch angle unit step input

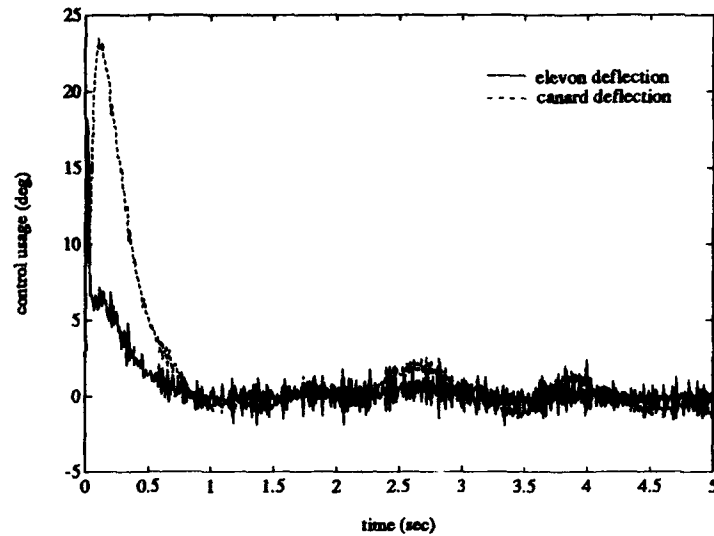


Figure 7.38. HIMAT, μ controller—control usage for pitch angle unit step input

Table 7.3. HIMAT H_2/μ Optimization Results

	Controller		
	order	α	μ
H_2	4	0.20	6808.1
μ	20	44.2	0.987
H_2/μ	4	7.0	1.20
H_2/μ	8	6.9	1.11

to find a low order controller; in this case, the order of the H_2 problem or $n_c = 4$. This does not imply that lower order controllers don't exist; in fact, this approach can be applied to design controllers with order less than the H_2 order, but there is no guarantee that $\gamma^* = \gamma$ for the optimum or even that a stabilizing controller exists.

Table 7.3 presents a comparison of the H_2 , μ , and mixed H_2/μ results. Notice that the fourth order mixed controller provides robust performance to perturbations that have a norm bound which is 83% of desired. Furthermore, this controller has a two-norm which is almost an order of magnitude less than the two-norm of the μ controller, but nearly two orders of magnitude greater than the H_2 controller.

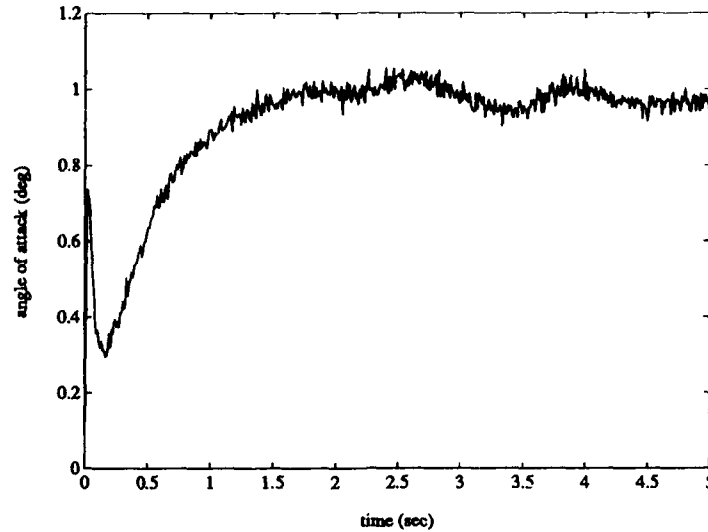


Figure 7.39. HIMAT, H_2/μ , $n_c = 4$, angle of attack response to angle of attack unit step input

Figures 7.39–7.44 show the impact of these results. Comparing the step responses to those of the 20th order μ controller, it is seen that the fourth order mixed controller has a slower initial response to a step, but reaches steady state at approximately the same time as the μ controller. Moreover, the high frequency noise rejection is seen to be about the same—in fact, the mixed controller results in slightly better noise rejection, but it is not significantly better than the noise rejection when the μ controller is used. Notice that the initial control usage is higher for the mixed controllers but then it drops off faster as steady state is approached. Finally, the μ controller and the fourth order mixed controller regulate the states equally well to an initial angle of attack perturbation (not shown).

The last controller computed for this problem is an eighth order mixed controller. As can be seen from Table 7.3, the eighth order mixed controller has a greater level of robustness than the fourth order, but still does not meet the desired level of 1.0. The time responses for this controller are comparable to that of the fourth order and are not shown. This process could be continued with high order controllers until the desired level of robustness is met. Since robust performance is obtained by

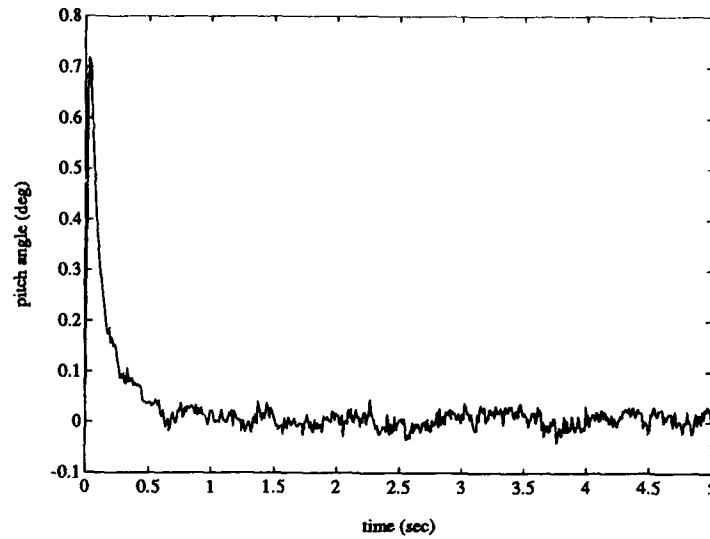


Figure 7.40. HIMAT, H_2/μ , $n_c = 4$, pitch angle response to angle of attack unit step input

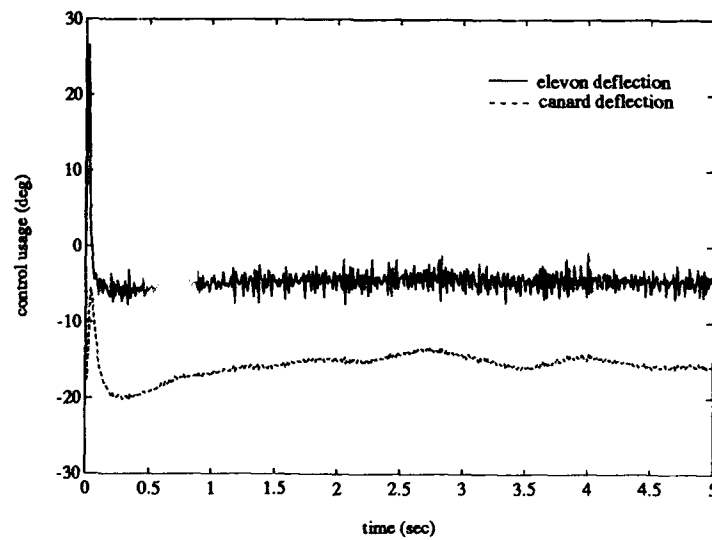


Figure 7.41. HIMAT, H_2/μ , $n_c = 4$, control usage for angle of attack unit step input

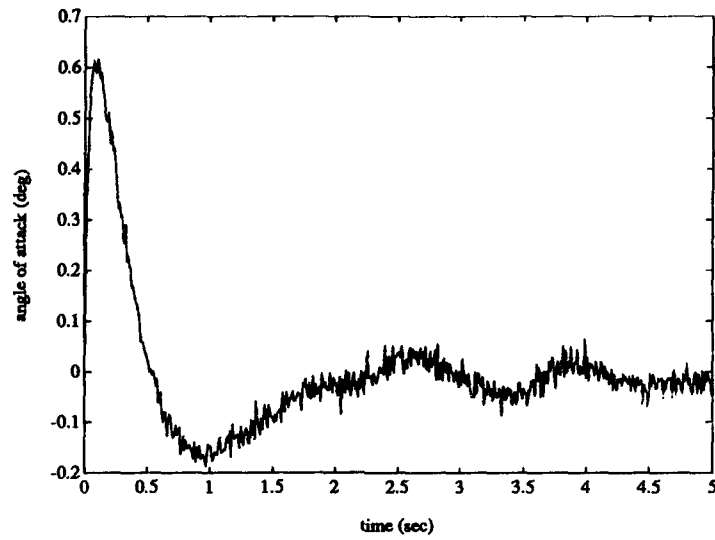


Figure 7.42. HIMAT, H_2/μ , $n_c = 4$, angle of attack response to pitch angle unit step input

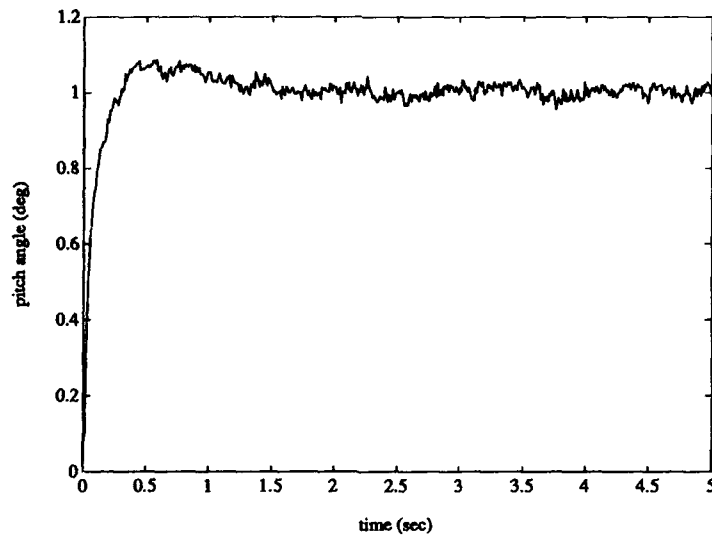


Figure 7.43. HIMAT, H_2/μ , $n_c = 4$, pitch angle response to pitch angle unit step input

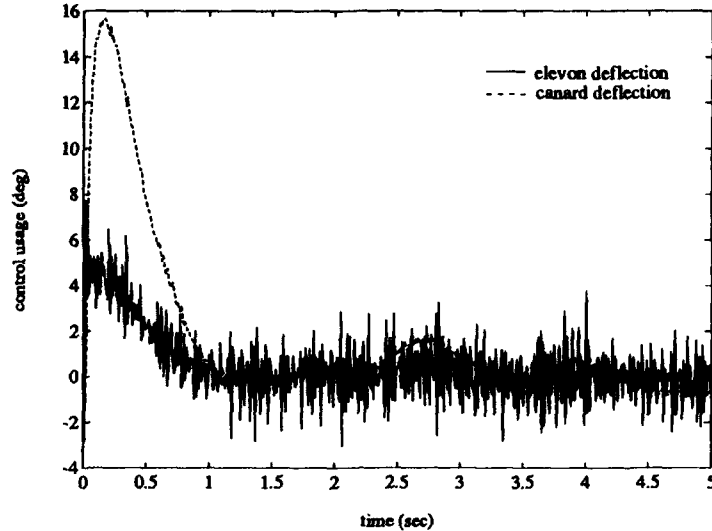


Figure 7.44. HIMAT, H_2/μ , $n_c = 4$, control usage for pitch angle unit step input the 20th order μ controller, a mixed controller which guarantees robust performance with order less than or equal to 20 exists. This example has demonstrated the capability of the mixed H_2/μ method to reduce the controller order. Furthermore, the reduced order controller retained desirable robustness qualities.

7.4 Summary

μ -analysis and synthesis were seen to provide the design engineer with an improved measure of robust stability. Moreover, μ is currently the best way for designing systems with robust performance. However, μ controllers cannot handle white noise inputs, and generally result in high order controllers. By incorporating μ into the mixed H_2/H_∞ approach, both of these limitations were addressed. The H_∞ constraint was formed by scaling the transfer function with the D transfer function from the last D-K iteration step of a μ design. Then the mixed method from the previous chapter was applied. An F-16 and HIMAT longitudinal control design examples demonstrated the H_2/μ optimization. Significant reduction in both controller order and high frequency noise response were obtained using the mixed

approach rather than just the μ controller. This improvement was at the expense of some reduction in the robust performance of the system.

VIII. Multiple H_∞ Constraints

Multiple H_∞ constraints arise in many control problems. Consider the multiple input/multiple output system in Figure 8.1, where G represents the plant to be controlled, K is the controller to be designed, $W_1\Delta_1$ represents an input perturbation to the system, and $W_2\Delta_2$ represents a fictitious "performance perturbation". The problem is to design a controller which is robustly stable to perturbations at the input and has nominal performance at the output. One approach to this problem is to combine the perturbations into a single Δ , bringing the weights W_1 and W_2 into the system as shown in Figure 8.2.

The resulting H_∞ problem is to find a controller which reduces the infinity-norm of the closed-loop transfer function M to a value less than or equal to the inverse of the infinity-norm of the perturbation Δ , or

$$\|M\|_\infty \leq \frac{1}{\|\Delta\|_\infty} \quad (8.1)$$

where

$$\Delta = \begin{bmatrix} \Delta_1 & 0 \\ 0 & \Delta_2 \end{bmatrix} \quad (8.2)$$

A common choice of M [39] is

$$M = \begin{bmatrix} W_1T & \star \\ \star & W_2S \end{bmatrix} \quad (8.3)$$

where T and S are the input complementary sensitivity and the output sensitivity, respectively, and \star are picked to make the problem a regular H_∞ problem. This approach guarantees the stability and performance requirements are met when the inequality (8.1) is satisfied. Generally, the resulting controller is very conservative with regard to the actual perturbations Δ_1 and Δ_2 .

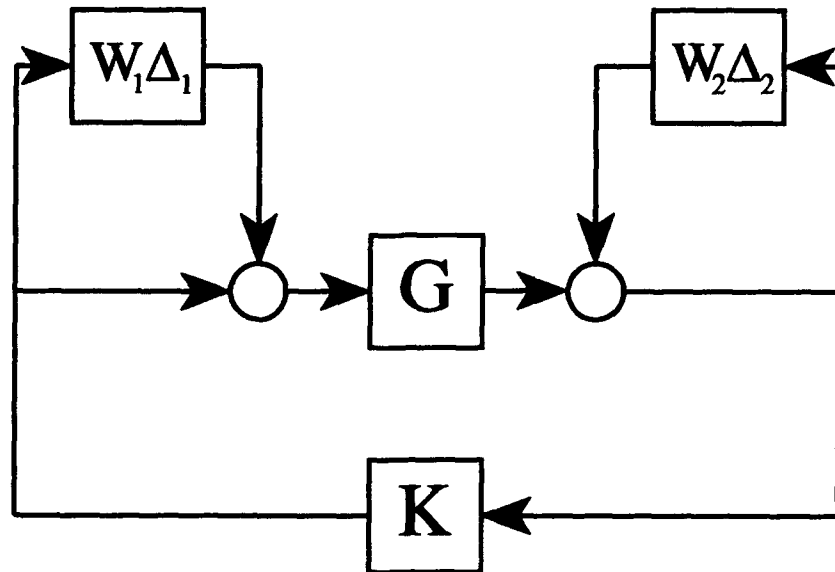


Figure 8.1. System with uncertainties

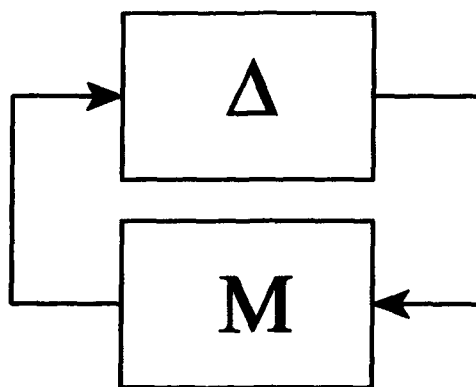


Figure 8.2. System with uncertainties "pulled out"

A less conservative choice for M is

$$M = \begin{bmatrix} W_1 T \\ W_2 S \end{bmatrix} \quad (8.4)$$

While this is less conservative, the problem cannot usually be solved by available state-space techniques since it results in a singular H_∞ problem.

An even less conservative approach is to separate the perturbations into two H_∞ problems

$$\|W_1 T\|_\infty \leq \frac{1}{\|\Delta_1\|_\infty} \quad (8.5)$$

$$\|W_2 S\|_\infty \leq \frac{1}{\|\Delta_2\|_\infty} \quad (8.6)$$

There is no convenient way of solving this problem under the current H_∞ optimal control theory. However, a controller which meets the desired H_∞ constraints can be found using mixed H_2/H_∞ optimal control. This method has the added advantage of minimizing the effect of white noise on selected controlled outputs from the system.

Another approach to solving this problem is to use μ -synthesis through D-K iterations. This method has the advantage of not only finding a controller which provides robust stability and nominal performance, but also provides a measure of robust performance. The ability of μ -synthesis to provide robust performance is due to its exploitation of frequency information as well as the block-diagonal structure of the perturbation. The mixed H_2/H_∞ optimal control method exploits the block-diagonal structure of the perturbation, but only contains peak gain information provided by the infinity-norm and does not have the same frequency information as μ -synthesis. Furthermore, the cross-terms in 8.3 are not considered by the multiple H_∞ constraint approach as they are in μ -synthesis. Therefore, the resulting controller will not guarantee robust performance. The mixed approach does, however, guarantee

a controller which provides robust stability and nominal performance at controller orders as low as the H_2 order.

The above example is the simplest case of a multiple constraint problem. However, the design engineer is often interested in performance and margins at more than just one point in the system. Using the multiple H_∞ constraint framework, robustness to multiplicative perturbations at the input and the output as well as additive perturbations (and the inverses of all of the above) can be accounted for simultaneously. Further, any other desired constraint such as control power limits can be augmented to the problem in this framework. Thus, the mixed H_2/H_∞ optimal control problem with multiple H_∞ constraints is a powerful tool which provides substantial flexibility in control design and trade-off analysis. The application of multiple constraint mixed optimization problems which include μ will be examined further in the next chapter.

The objective of the first section of this chapter is to characterize the optimal (order-free) solution to the mixed H_2/H_∞ optimization problem with multiple constraints. The conditions for fixed-order controllers will then be presented. Finally, the numerical methods developed in Chapter VI will be extended to include multiple constraints and the F-16 longitudinal control problem will be used to demonstrate the methods.

8.1 Uniqueness of the Optimal Controller

This section will extend the results of Chapter IV to the H_2/H_∞ optimal control problem with multiple H_∞ constraints. Consider the system in Figure 8.3, where $d_i, i = 1, \dots, n_\infty$, are of bounded energy and w is zero-mean, white Gaussian noise.

The transfer function P is the underlying plant G with all weights associated with the problem absorbed. It is assumed, in general, that there is no relationship between $e_i, i = 1, \dots, n_\infty$, and z or $d_i, i = 1, \dots, n_\infty$, and w . As before, the aug-

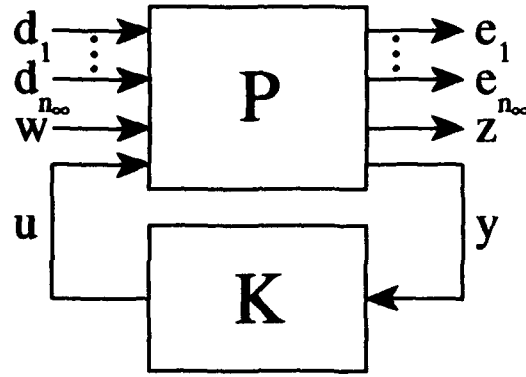


Figure 8.3. General mixed H_2/H_∞ optimization problem

mented plant P is formed by wrapping the weights from an H_2 problem from w to z and the weights of the H_∞ problems from d_i to e_i around the basic system. To simplify the discussion, the following additional definitions are made:

$$\gamma_i := \inf_{K \text{ admissible}} \|T_{ed_i}\|_\infty \quad (8.7)$$

$$\bar{\gamma}_i := \|T_{ed_i}\|_\infty \text{ when } K(s) = K_{2opt} \quad (8.8)$$

$$K_{mis} := \text{a solution to the } H_2/H_\infty \text{ problem for some set } \{\gamma_1, \dots, \gamma_{n_\infty}\} \quad (8.9)$$

$$\gamma_i^* := \|T_{ed_i}\|_\infty \text{ when } K(s) = K_{mis} \quad (8.10)$$

As in the Chapter IV, this problem can be formulated as a convex program through a Youla parametrization as shown in Figure 8.4. The convex program is: find a $Q \in H_2$ which satisfies

$$\mathcal{P} = \begin{cases} \alpha = \inf_{Q \in H_2} \|T_{zw}\|_2 \\ \text{subject to} \\ \|T_{ed_i}\|_\infty \leq \gamma_i \text{ for } i = 1, \dots, n_\infty \end{cases} \quad (8.11)$$

This problem is more complicated than the single constraint problem due to the nature of the regions where solutions can exist. In the single constraint problem

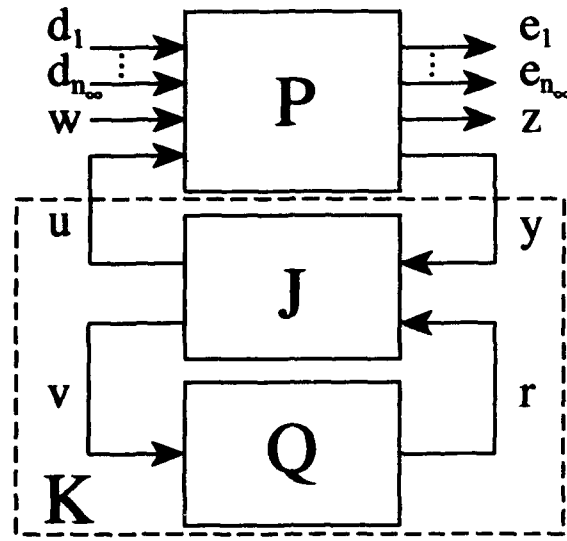


Figure 8.4. J-Q parametrization of the mixed H_2/H_∞ problem

shown in Figures 4.3 and 4.4, there are only two possibilities; either the controller is the optimal H_2 controller, or it is a controller which satisfies the H_∞ constraint with equality. However, for the multiple H_∞ constraint problem, there are more regions to consider in order to determine the nature of the mixed controller.

Consider the mixed problem with two H_∞ constraints, where γ_1 and γ_2 are specified. Figure 8.5 presents the four possible regions in the H_∞ constraint plane where the values of γ_1 and γ_2 can be chosen. Note that the point (γ_1, γ_2) in this plane indicates the point at which both inequality constraints are satisfied with equality. We will denote the actual mixed solution by (γ_1^*, γ_2^*) . Region IV is defined as the region where $\gamma_1 \geq \bar{\gamma}_1$ and $\gamma_2 \geq \bar{\gamma}_2$. Region II is defined by $\gamma_1 < \bar{\gamma}_1$ and γ_2 greater than or equal to the value of $\|T_{ed_2}\|_\infty$ when a K_{mix} from the $H_2/\|T_{ed_1}\|_\infty$ curve (that is, the single constraint mixed controller) is used to form T_{ed_2} at a given value of γ_1 . This value of γ_2 will be denoted $\tilde{\gamma}_2$. Similarly, Region III is defined like Region II but with γ_1, γ_2 and T_{ed_1}, T_{ed_2} changing roles, and $\tilde{\gamma}_1$ is the value of γ_1 on the optimal mixed $H_2/\|T_{ed_2}\|_\infty$ curve. Finally, Region I is defined by the values of γ_1 and γ_2 less than those given by the optimal mixed single constraint curves, but greater than

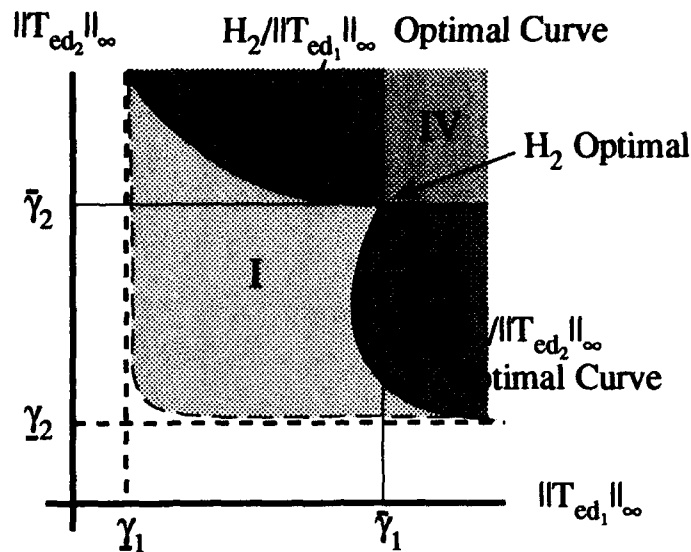


Figure 8.5. Admissible solution regions

the minimal values achievable for a two-constraint problem. The lower left corner of Region I does not necessarily reach the intersection of the lines $\gamma_1 = \underline{\gamma}_1$ and $\gamma_2 = \underline{\gamma}_2$; this is due to existence questions in this region which will be discussed later. In particular, the point $(\underline{\gamma}_1, \underline{\gamma}_2)$ is most likely not achievable.

Figure 8.6 shows a three-dimensional plot of the surface formed by plotting corresponding values of α^* , γ_1^* , and γ_2^* . This is the mixed $\|T_{zw}\|_2 / \|T_{ed_1}\|_{\infty} / \|T_{ed_2}\|_{\infty}$ surface. With this surface in mind, we will use some geometric insight to determine the nature of the solution for each region. Starting with Region IV, one can see from Figure 8.7 that the optimal H_2 controller is in the admissible region—since this is the global optimal, it is the solution to the mixed problem in this region. Thus, for (γ_1, γ_2) in Region IV, the optimal mixed solution is $(\gamma_1^*, \gamma_2^*) = (\bar{\gamma}_1, \bar{\gamma}_2)$.

In Region II, the admissible region can be seen in Figure 8.8. The minimum value of α will be achieved on the optimal $H_2 / \|T_{ed_1}\|_{\infty}$ curve. Thus, $(\gamma_1^*, \gamma_2^*) = (\gamma_1, \bar{\gamma}_2)$ in Region II. Similar results will occur for Region III, so $(\gamma_1^*, \gamma_2^*) = (\bar{\gamma}_1, \gamma_2)$ in Region III.

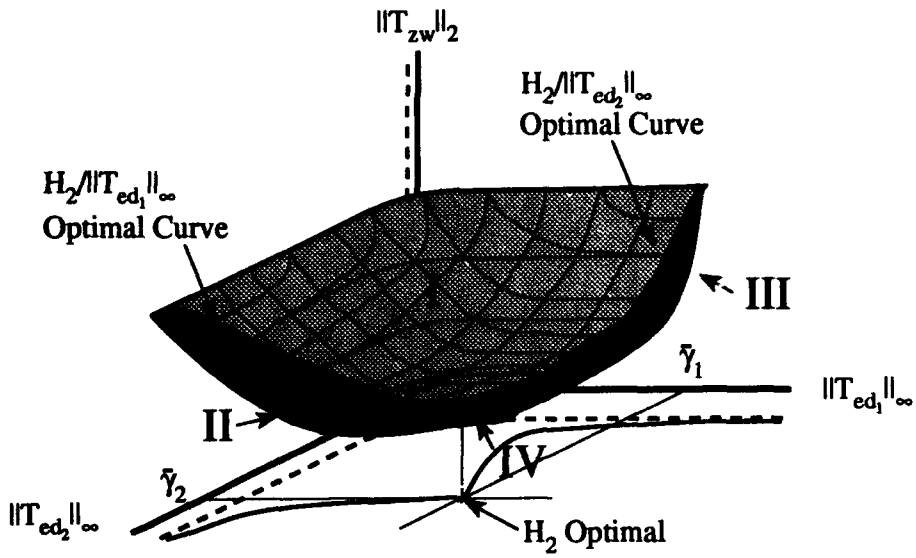


Figure 8.6. $\|T_{zw}\|_2/\|T_{ed_1}\|_\infty/\|T_{ed_2}\|_\infty$ surface

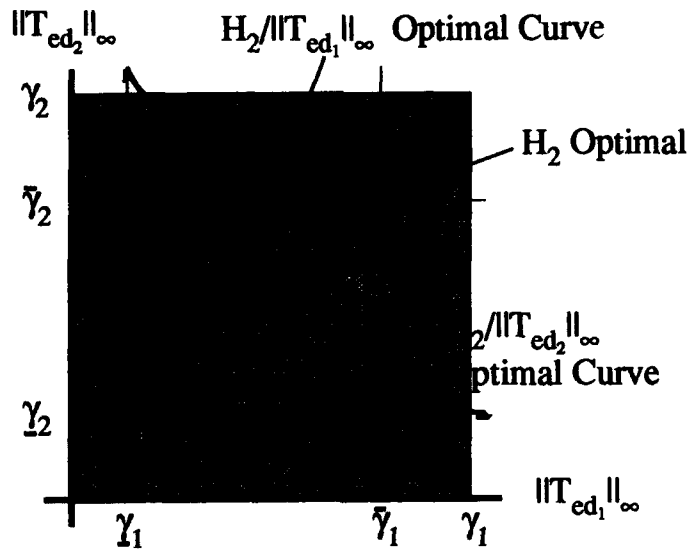


Figure 8.7. Admissible solutions—Region IV

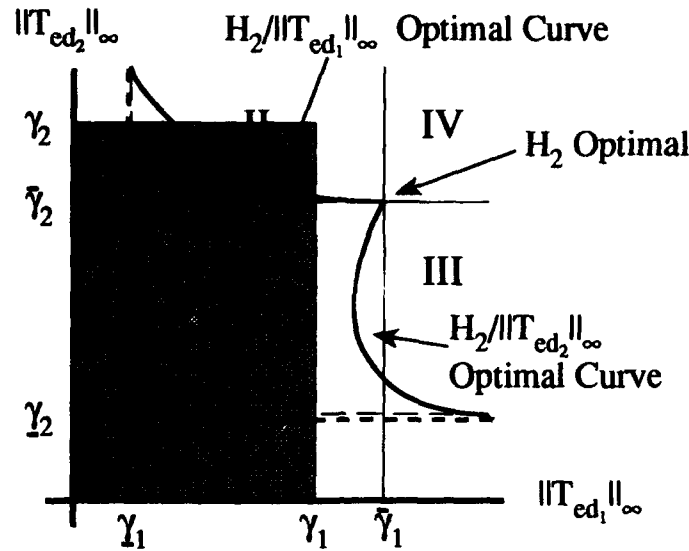


Figure 8.8. Admissible solutions-Region II

For Region I, the admissible region is shown in Figure 8.9. The geometric insight from Figure 8.6 is that the solution will fall at the intersection of the constraint boundaries; i. e., $(\gamma_1^*, \gamma_2^*) = (\gamma_1, \gamma_2)$

The following theorem will confirm this insight. First, define $K_{mix_1}(\gamma_1)$ as the unique optimal controller for the mixed $H_2/\|T_{ed_1}\|_\infty$ problem at a fixed γ_1 . $K_{mix_2}(\gamma_2)$ is defined in a similar fashion.

Theorem 8.1.1 Assume $n_\infty = 2$ (i. e., there are 2 d_i 's and 2 e_i 's) and let γ_1 and γ_2 be given. If a controller K which solves the convex program (8.11) exists, then it is unique and K is given by:

- i. If $\gamma_1 \leq \bar{\gamma}_1$ and $\gamma_2 \leq \bar{\gamma}_2$ (Region I) then the optimal controller K must satisfy both H_∞ constraints with equality.
- ii. If $\gamma_2 \geq \bar{\gamma}_2$ and $\gamma_1 \leq \bar{\gamma}_1$ (Region II) then $K = K_{mix_1}(\gamma_1)$
- iii. If $\gamma_1 \geq \bar{\gamma}_1$ and $\gamma_2 \leq \bar{\gamma}_2$ (Region III) then $K = K_{mix_2}(\gamma_2)$
- iv. If $\gamma_1 \geq \bar{\gamma}_1$ and $\gamma_2 \geq \bar{\gamma}_2$ (Region IV) then $K = K_{2_{opt}}$.

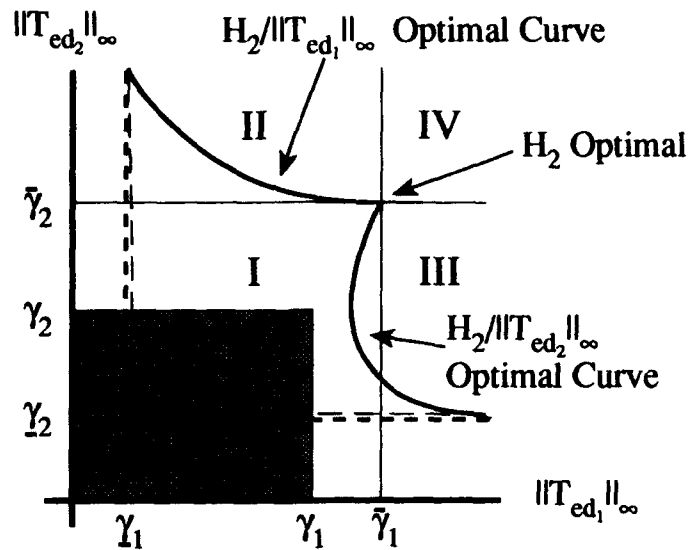


Figure 8.9. Admissible solutions—Region I

Proof: From Lemma 4.1.1, the two-norm is a strictly convex functional; therefore, from the corollary to Theorem 9.4.1 [35], any solution to the convex program (8.11) is unique.

i. Define the Lagrangian

$$\mathcal{L} = \|T_{zw}\|_2 + \lambda_1 (\|T_{ed_1}\|_{\infty} - \gamma_1) + \lambda_2 (\|T_{ed_2}\|_{\infty} - \gamma_2) \quad (8.12)$$

If neither constraint is satisfied with equality, then the Kuhn-Tucker conditions imply $\lambda_1 = \lambda_2 = 0$. The problem reduces to the optimal H_2 control problem which has the unique solution $K_{2,opt}$. However, referring to Figure 8.9, it can be seen that this solution is not admissible. Therefore, at least one constraint must be satisfied with equality. Now, assume $\gamma_1^* = \gamma_1$ and $\gamma_2^* \neq \gamma_2$, which implies $\lambda_2 = 0$. The Lagrangian reduces to

$$\mathcal{L} = \|T_{zw}\|_2 + \lambda_1 (\|T_{ed_1}\|_{\infty} - \gamma_1) \quad (8.13)$$

which is the Lagrangian associated with the mixed $H_2/\|T_{ed_1}\|_\infty$ optimal control problem, which was shown in Theorem 4.2.1 to have a unique solution. Again referring to Figure 8.9, it can be seen that this solution is not in the admissible region; thus, $\gamma_2^* = \gamma_2$. A similar argument can be made for $\gamma_2^* = \gamma_2$ and $\gamma_1^* \neq \gamma_1$. Thus, the only remaining possibility is $(\gamma_1^*, \gamma_2^*) = (\gamma_1, \gamma_2)$.

- ii. Assume neither constraint is satisfied with equality. Again, the only controller which satisfies the Kuhn-Tucker conditions is $K_{2_{opt}}$, which is not in the admissible region as shown in Figure 8.8. Thus, at least one constraint must be satisfied with equality. Assume now that $\gamma_1^* = \gamma_1$ and $\gamma_2^* \neq \gamma_2$ which implies $\lambda_2 = 0$. The Lagrangian then reduces to (8.13) for which the Kuhn-Tucker conditions are satisfied by the unique $K_{mix_1}(\gamma_1)$, which is in the admissible region. Since the optimal solution is unique, $K_{mix_1}(\gamma_1)$ is the optimal controller for Region II.
- iii. The proof is analogous to that of ii.
- iv. Assume neither constraint is satisfied by equality. Then (8.12) reduces to the H_2 problem and $K_{2_{opt}}$ is admissible; therefore, it is the optimal solution.

■

The question of existence of a solution still needs to be addressed. In the single constraint problem, controllers existed for all $\gamma > \underline{\gamma}$. For the two-constraint problem where the constraint intersection falls in Regions II, III, and IV, the existence of a solution is guaranteed by the definition of the boundaries. However, in Region I, there is a question of existence of solutions in the neighborhood of the intersection of $\underline{\gamma}_1$ and $\underline{\gamma}_2$, as depicted by the dashed curve in Figure 8.5. There is no guarantee that a solution to the mixed problem will exist which satisfies $\gamma_1 = \underline{\gamma}_1$ and $\gamma_2 = \underline{\gamma}_2$, concurrently. In fact, numerical results have suggested that there is some limit of performance in this region. Since no analytical approach has been devised thus

far to determine the existence or non-existence of controllers, numerical studies are required to determine where controllers can be found.

8.2 Fixed-order Solutions

8.2.1 State Space Formulation. Thus far, the order of the controller has been free, but for practical design problems it is necessary to fix the controller order. This section will develop the fixed-order problem and determine characteristics of the solutions. Unfortunately, with a fixed-order controller, it is no longer possible to use the Youla parametrization to parametrize the problem over a convex set. However, conditions can be derived which must be satisfied for an extremal using the first order necessary conditions of a particular Lagrangian.

Returning to the system in Figure 8.3, the state space of P is formed by wrapping the stable weights from the H_2 problem from w to z and the stable weights of the H_∞ problems from d_i to u_i around the system G resulting in the augmented plant

$$P = \begin{bmatrix} \bar{A} & \bar{B}_{d_1} & \cdots & \bar{B}_{d_{n_\infty}} & \bar{B}_w & \bar{B}_u \\ \hline \bar{C}_{e_1} & \bar{D}_{e_1 d_1} & \cdots & \bar{D}_{e_1 d_{n_\infty}} & \bar{D}_{e_1 w} & \bar{D}_{e_1 u} \\ \vdots & \vdots & \vdots & \vdots & \vdots & \vdots \\ \bar{C}_{e_{n_\infty}} & \bar{D}_{e_{n_\infty} d_1} & \cdots & \bar{D}_{e_{n_\infty} d_{n_\infty}} & \bar{D}_{e_{n_\infty} w} & \bar{D}_{e_{n_\infty} u} \\ \bar{C}_z & \bar{D}_{z d_1} & \cdots & \bar{D}_{z d_{n_\infty}} & \bar{D}_{z w} & \bar{D}_{z u} \\ \bar{C}_y & \bar{D}_{y d_1} & \cdots & \bar{D}_{y d_{n_\infty}} & \bar{D}_{y w} & \bar{D}_{y u} \end{bmatrix} \quad (8.14)$$

where $[\bar{\cdot}]$ are the matrices associated with the system augmented by the H_2 and H_∞ weights. The order of the individual H_2 and H_∞ problems will generally be less than that of P, since P incorporates all the H_2 and H_∞ weighting states. The state space equations of the H_2 and H_∞ problems can be written as

$$\dot{x}_2 = A_2 x_2 + B_w w + B_{u_2} u \quad (8.15)$$

$$z = C_z x_2 + D_{zw} w + D_{zu} u \quad (8.16)$$

$$y = C_{y_2} x_2 + D_{yw} w + D_{yu} u \quad (8.17)$$

$$\dot{x}_{\infty i} = A_{\infty i} x_{\infty i} + B_{d_i} d_i + B_{u_{\infty i}} u \quad (8.18)$$

$$e_i = C_{e_i} x_{\infty i} + D_{ed_i} d_i + D_{eu_i} u \quad (8.19)$$

$$y = C_{y_{\infty i}} x_{\infty i} + D_{yd_i} d_i + D_{yu} u \quad (8.20)$$

where x_2 is the state vector for the underlying H_2 problem and $x_{\infty i}$ are the state vectors for the underlying H_{∞} problems.

The mixed H_2/H_{∞} problem is: Find a controller $K(s)$ which satisfies

$$\inf_{K \text{ stabilizing}} \|T_{zw}\|_2 \text{ subject to } \|T_{ed_i}\|_{\infty} \leq \gamma_i, \quad i = 1, 2, \dots, n_{\infty}$$

where

$$T_{zw} = C_z (sI - A_2)^{-1} B_w + D_{zw} \quad (8.21)$$

$$T_{ed_i} = C_{e_i} (sI - A_{\infty i})^{-1} B_{d_i} + D_{ed_i} \quad (8.22)$$

are the closed-loop transfer functions from w to z and d_i to e_i , respectively. The various matrices in (8.21) and (8.22) will be defined shortly.

To solve this problem the following assumptions are made:

- i. $D_{zw} = 0$
- ii. $D_{yu} = 0$

iii. (A_2, B_{u2}) stabilizable, (C_{y2}, A_2) detectable

iv. $D_{zu}^T D_{zu}$ full rank, $D_{yw} D_{yw}^T$ full rank

v. $\begin{bmatrix} A_2 - j\omega I & B_{u2} \\ C_z & D_{zu} \end{bmatrix}$ has full column rank for all ω

vi. $\begin{bmatrix} A_2 - j\omega I & B_w \\ C_{y2} & D_{yw} \end{bmatrix}$ has full row rank for all ω

The rationale for these assumptions is the same as given in Section 5.1.

As in the single constraint problem, $D_{zu} D_c D_{yw}$ must be identically zero for a finite two-norm of T_{zw} to exist; condition iv then implies $D_c = 0$. Thus, consider the controller $K(s)$ in state space form

$$\dot{x}_c = A_c x_c + B_c y \quad (8.23)$$

$$u = C_c x_c \quad (8.24)$$

Closing the loop of our system we get

$$\begin{aligned} \dot{x}_2 &= A_2 x_2 + B_w w \\ z &= C_z x_2 \\ \dot{x}_{ooi} &= A_{ooi} x_{ooi} + B_{di} d_i \\ e_i &= C_{ei} x_{ooi} + D_{edi} d_i \end{aligned} \quad (8.25)$$

where

$$x_2 = \begin{bmatrix} x_2 \\ x_c \end{bmatrix} \quad (8.26)$$

$$x_{ooi} = \begin{bmatrix} x_{ooi} \\ x_c \end{bmatrix} \quad (8.27)$$

$$A_2 = \begin{bmatrix} A_2 & B_{u_2} C_c \\ B_c C_{y_2} & A_c \end{bmatrix} \quad (8.28)$$

$$A_{\infty i} = \begin{bmatrix} A_{\infty i} & B_{u_{\infty i}} C_c \\ B_c C_{y_{\infty i}} & A_c \end{bmatrix} \quad (8.29)$$

$$B_w = \begin{bmatrix} B_w \\ B_c D_{yw} \end{bmatrix} \quad (8.30)$$

$$B_{d_i} = \begin{bmatrix} B_{d_i} \\ B_c D_{y d_i} \end{bmatrix} \quad (8.31)$$

$$C_z = \begin{bmatrix} C_z & D_{zu} C_c \end{bmatrix} \quad (8.32)$$

$$C_{e_i} = \begin{bmatrix} C_{e_i} & D_{eu_i} C_c \end{bmatrix} \quad (8.33)$$

$$D_{ed_i} = D_{ed_i} \quad (8.34)$$

8.2.2 The Lagrangian and Necessary Conditions. The mixed H_2/H_∞ problem is now to determine a $K(s)$ such that:

- i. A_2 and $A_{\infty i}$ are stable for all i
- ii. $\|T_{ed_i}\|_\infty \leq \gamma_i$ for some given set of $\gamma_i > \underline{\gamma}_i$
- iii. $\|T_{zw}\|_2$ is minimized.

Extending Theorem 5.2.1 to the multiple H_∞ constraint case, one obtains the following.

Theorem 8.2.1 *Let (A_c, B_c, C_c) be given and assume there exist a set of solutions $Q_{\infty i} = Q_{\infty i}^T \geq 0$ satisfying*

$$A_{\infty i} Q_{\infty i} + Q_{\infty i} A_{\infty i}^T + (Q_{\infty i} C_{e_i}^T + B_{d_i} D_{ed_i}^T) R_i^{-1} (Q_{\infty i} C_{e_i}^T + B_{d_i} D_{ed_i}^T)^T + B_{d_i} B_{d_i}^T = 0 \quad (8.35)$$

for all i , where $R_i = (\gamma_i^2 I - D_{ed_i} D_{ed_i}^T) > 0$. Then, for each i , the following are equivalent:

- i. (A_{∞_i}, B_{d_i}) is stabilizable
- ii. A_{∞_i} is stable
- iii. A_2 is stable.

Moreover, if i, ii, and iii hold, then the following are true:

- iv. $\|T_{ed_i}\|_{\infty} \leq \gamma_i$ for all i
- v. the two-norm of the transfer function T_{zw} is given by

$$\|T_{zw}\|_2^2 = \text{tr}[C_z Q_2 C_z^T] = \text{tr}[Q_2 C_z^T C_z]$$

where $Q_2 = Q_2^T \geq 0$ is the solution to the Lyapunov equation

$$A_2 Q_2 + Q_2 A_2^T + B_w B_w^T = 0$$

- vi. all real symmetric solutions Q_{∞_i} of (8.95) are positive semidefinite for all i
- vii. there exists a unique minimal solution Q_{∞_i} to (8.95) in the class of real symmetric solutions for each i
- viii. Q_{∞_i} are the minimal solutions of (8.95) iff $\text{Re}[\lambda_j(A_{\infty_i} + B_{d_i} D_{ed_i}^T R_i^{-1} C_{e_i} + Q_{\infty_i} C_{e_i}^T R_i^{-1} C_{e_i})] \leq 0$ for all j
- ix. $\|T_{ed_i}\|_{\infty} < (\leq) \gamma_i$ iff $\text{Re}[\lambda_j(A_{\infty_i} + B_{d_i} D_{ed_i}^T R_i^{-1} C_{e_i} + Q_{\infty_i} C_{e_i}^T R_i^{-1} C_{e_i})] < (\leq) 0$ for all j , where Q_{∞_i} are the minimal solutions to (8.95) for each i .

Proof: This is an extension of Theorem 5.2.1 for multiple H_{∞} constraints. ■

Using Theorem 8.2.1, the problem can be restated as: Determine the $K(s)$ which minimizes

$$J(A_c, B_c, C_c) = \text{tr}[Q_2 C_z^T C_z] \quad (8.36)$$

where Q_2 is the real, symmetric, positive semidefinite solution to

$$A_2 Q_2 + Q_2 A_2^T + B_w B_w^T = 0 \quad (8.37)$$

and such that

$$A_{\infty i} Q_{\infty i} + Q_{\infty i} A_{\infty i}^T + (Q_{\infty i} C_{e_i}^T + B_{d_i} D_{e d_i}^T) R_i^{-1} (Q_{\infty i} C_{e_i}^T + B_{d_i} D_{e d_i}^T)^T + B_{d_i} B_{d_i}^T = 0 \quad (8.38)$$

has a real, symmetric, positive semidefinite solution $Q_{\infty i}$ for each i . To solve this minimization problem with equality constraints, a Lagrange multiplier approach is used. The Lagrangian is

$$\begin{aligned} \mathcal{L} = & \operatorname{tr}[Q_2 C_x^T C_x] + \operatorname{tr}\{[A_2 Q_2 + Q_2 A_2^T + B_w B_w^T] \mathcal{X}\} \\ & + \sum_{i=1}^{n_{\infty}} \operatorname{tr}\{[A_{\infty i} Q_{\infty i} + Q_{\infty i} A_{\infty i}^T + (Q_{\infty i} C_{e_i}^T + B_{d_i} D_{e d_i}^T) R_i^{-1} (Q_{\infty i} C_{e_i}^T + B_{d_i} D_{e d_i}^T)^T \\ & + B_{d_i} B_{d_i}^T] \mathcal{Y}_i\} \end{aligned} \quad (8.39)$$

where \mathcal{X} and \mathcal{Y}_i are symmetric Lagrange multiplier matrices. The resulting first order necessary conditions are

$$\frac{\partial \mathcal{L}}{\partial A_c} = X_{12}^T Q_{12} + X_2 Q_2 + Y_{12_i}^T Q_{ab_i} + Y_2 Q_{b_i} = 0 \quad (8.40)$$

$$\begin{aligned} \frac{\partial \mathcal{L}}{\partial B_c} = & X_{12}^T Q_1 C_{y_2}^T + X_2 Q_{12}^T C_{y_2}^T + X_{12}^T V_{12} + X_2 B_c V_2 + Y_{12_i}^T Q_{a_i} C_{y_{\infty}}^T \\ & + Y_2 Q_{ab_i}^T C_{y_{\infty}}^T + Y_{12_i}^T V_{ab_i} + Y_2 B_c V_{b_i} + (Y_{12_i}^T Q_{a_i} + Y_2 Q_{ab_i}^T) C_{e_i}^T M_i \\ & + (Y_{12_i}^T Q_{ab_i} + Y_2 Q_{b_i}) C_c^T D_{c u_i}^T M_i = 0 \end{aligned} \quad (8.41)$$

$$\begin{aligned} \frac{\partial \mathcal{L}}{\partial C_c} = & B_{u_2}^T X_1 Q_{12} + B_{u_2}^T X_{12} Q_2 + R_{12}^T Q_{12} + R_2 C_c Q_2 + B_{u_{\infty}}^T Y_{1_i} Q_{ab_i} \\ & + B_{u_{\infty}}^T Y_{12_i} Q_{b_i} + R_{ab_i}^T Q_{a_i} Y_{1_i} Q_{ab_i} + R_{ab_i}^T Q_{a_i} Y_{12_i} Q_{b_i} + R_{ab_i}^T Q_{ab_i} Y_{12_i}^T Q_{ab_i} \end{aligned}$$

$$\begin{aligned}
& + R_{ab_i}^T Q_{ab_i} Y_2 Q_{b_i} + R_{b_i} C_c Q_{ab_i}^T Y_{12_i} Q_{b_i} + R_{b_i} C_c Q_{b_i} Y_2 Q_{b_i} \\
& + R_{b_i} C_c Q_{ab_i}^T Y_1 Q_{ab_i} + R_{b_i} C_c Q_{b_i} Y_{12_i}^T Q_{ab_i} \\
& + P_{1_i} (Y_1 Q_{ab_i} + Y_{12_i} Q_{b_i}) + P_{2_i} (Y_{12_i}^T Q_{ab_i} + Y_2 Q_{b_i}) = 0
\end{aligned} \tag{8.42}$$

$$\frac{\partial \mathcal{L}}{\partial \chi} = \mathcal{A}_2 Q_2 + Q_2 \mathcal{A}_2^T + \mathcal{B}_w \mathcal{B}_w^T = 0 \tag{8.43}$$

$$\frac{\partial \mathcal{L}}{\partial Q_2} = \mathcal{A}_2^T \chi + \chi \mathcal{A}_2 + \mathcal{C}_z^T \mathcal{C}_z = 0 \tag{8.44}$$

$$\begin{aligned}
\frac{\partial \mathcal{L}}{\partial \mathcal{Y}_i} & = \mathcal{A}_{\infty_i} Q_{\infty_i} + Q_{\infty_i} \mathcal{A}_{\infty_i}^T + (Q_{\infty_i} \mathcal{C}_{e_i}^T + \mathcal{B}_{d_i} \mathcal{D}_{ed_i}^T) R_i^{-1} (Q_{\infty_i} \mathcal{C}_{e_i}^T + \mathcal{B}_{d_i} \mathcal{D}_{ed_i}^T)^T \\
& + \mathcal{B}_{d_i} \mathcal{B}_{d_i}^T = 0
\end{aligned} \tag{8.45}$$

$$\begin{aligned}
\frac{\partial \mathcal{L}}{\partial Q_{\infty_i}} & = (\mathcal{A}_{\infty_i} + \mathcal{B}_{d_i} \mathcal{D}_{ed_i}^T R_i^{-1} \mathcal{C}_{e_i} + Q_{\infty_i} \mathcal{C}_{e_i}^T R_i^{-1} \mathcal{C}_{e_i})^T \mathcal{Y}_i \\
& + \mathcal{Y}_i (\mathcal{A}_{\infty_i} + \mathcal{B}_{d_i} \mathcal{D}_{ed_i}^T R_i^{-1} \mathcal{C}_{e_i} + Q_{\infty_i} \mathcal{C}_{e_i}^T R_i^{-1} \mathcal{C}_{e_i}) = 0
\end{aligned} \tag{8.46}$$

where

$$M_i = R_i^{-1} D_{ed_i} D_{yd_i}^T \tag{8.47}$$

$$P_{1_i} = D_{eu_i}^T R_i^{-1} D_{ed_i} \mathcal{B}_{d_i}^T \tag{8.48}$$

$$P_{2_i} = D_{eu_i}^T M_i \mathcal{B}_c^T \tag{8.49}$$

$$Q_2 = \begin{bmatrix} Q_1 & Q_{12} \\ Q_{12}^T & Q_2 \end{bmatrix} \tag{8.50}$$

$$\chi = \begin{bmatrix} X_1 & X_{12} \\ X_{12}^T & X_2 \end{bmatrix} \tag{8.51}$$

$$Q_{\infty_i} = \begin{bmatrix} Q_{a_i} & Q_{ab_i} \\ Q_{ab_i}^T & Q_{b_i} \end{bmatrix} \tag{8.52}$$

$$\mathcal{Y}_i = \begin{bmatrix} Y_{1i} & Y_{12i} \\ Y_{12i}^T & Y_{2i} \end{bmatrix} \quad (8.53)$$

$$\begin{aligned} B_w B_w^T &= \begin{bmatrix} B_w \\ B_c D_{yw} \end{bmatrix} \begin{bmatrix} B_w^T & D_{yw}^T B_c^T \end{bmatrix} \\ &= \begin{bmatrix} V_1 & V_{12} B_c^T \\ B_c V_{12}^T & B_c V_2 B_c^T \end{bmatrix} \end{aligned} \quad (8.54)$$

$$\begin{aligned} B_{d_i} (D_{ed_i}^T R_i^{-1} D_{ed_i} + I) B_{d_i}^T &= \begin{bmatrix} B_{d_i} \\ B_c D_{yd_i} \end{bmatrix} (D_{ed_i}^T R_i^{-1} D_{ed_i} + I) \begin{bmatrix} B_{d_i}^T & D_{yd_i}^T B_c^T \end{bmatrix} \\ &= \begin{bmatrix} V_{a_i} & V_{ab_i} B_c^T \\ B_c V_{ab_i}^T & B_c V_{b_i} B_c^T \end{bmatrix} \end{aligned} \quad (8.55)$$

$$\begin{aligned} C_z^T C_z &= \begin{bmatrix} C_z^T \\ C_c^T D_{zu}^T \end{bmatrix} \begin{bmatrix} C_z & D_{zu} C_c \end{bmatrix} \\ &= \begin{bmatrix} R_1 & R_{12} C_c \\ C_c^T R_{12}^T & C_c^T R_2 C_c \end{bmatrix} \end{aligned} \quad (8.56)$$

$$\begin{aligned} C_{e_i}^T R_i^{-1} C_{e_i} &= \begin{bmatrix} C_{e_i}^T \\ C_c^T D_{eu_i}^T \end{bmatrix} R_i^{-1} \begin{bmatrix} C_{e_i} & D_{eu_i} C_c \end{bmatrix} \\ &= \begin{bmatrix} R_{a_i} & R_{ab_i} C_c \\ C_c^T R_{ab_i}^T & C_c^T R_{b_i} C_c \end{bmatrix} \end{aligned} \quad (8.57)$$

As in the single constraint case, these necessary conditions have not been solved analytically but do provide some insight into the nature of the solution. In particular, (8.46) implies that either $\mathcal{Y}_i = 0$ or $(A_{\infty i} + B_{d_i} D_{ed_i}^T R_i^{-1} C_{e_i} + Q_{\infty i} C_{e_i}^T R_i^{-1} C_{e_i})$ is neutrally stable for all i . The former condition means the solution is off the boundary of the corresponding H_∞ constraint, and the latter condition implies the solution lies on the

boundary of the corresponding H_∞ constraint, and Q_∞ is the neutrally stabilizing solution for that H_∞ Riccati equation. This relation will be used to develop the solution to the problem.

8.2.3 H_2 Order or Greater Solution. The order of the controller, n_c , is assumed to be fixed at an order greater than or equal to that of the underlying H_2 problem, n_2 , and the mixed H_2/H_∞ problem is solved. Since $n_c \geq n_2$, the unique optimal controller $K_{2,opt}$ is admissible and the associated H_∞ problems achieve infinity-norms of $\bar{\gamma}_i$ with this controller. Thus, for the fixed-order mixed H_2/H_∞ problem with $\gamma_i \geq \bar{\gamma}_i$ for all i , the optimal mixed controller is simply the H_2 optimal controller. Similarly, no controller of any order exists which can reduce γ_i below the level of an optimal H_∞ controller, $\underline{\gamma}_i$; therefore, for the mixed H_2/H_∞ problem, no solution exists if any $\gamma_i < \underline{\gamma}_i$. As was discussed at the end of Section 8.1, a region where solutions do not exist can exist inside Region I. Currently, this area can only be determined numerically.

To simplify the discussion, for the remainder of this section it will be assumed that there are only two active H_∞ constraints. From the first order necessary conditions, the following theorem can be developed.

Theorem 8.2.2 *Assume n_c is fixed to a value greater than or equal to n_2 and $n_\infty = 2$. Then the following hold:*

- i. *if $\gamma_1 \geq \bar{\gamma}_1$ and $\gamma_2 \geq \bar{\gamma}_2$, the solution to the mixed H_2/H_∞ problem exists and is $K_{2,opt}$.*
- ii. *if $\gamma_1 \leq \bar{\gamma}_1$ or $\gamma_2 \leq \bar{\gamma}_2$, and a solution to the mixed H_2/H_∞ problem exists, it will satisfy at least one of the H_∞ constraints with equality.*

Proof:

- i. Since the global optimal $K_{2,opt}$ is admissible, it is the solution.

- ii. Assume the solution is off both boundaries (i. e., neither constraint is satisfied with equality). This implies $\mathcal{Y}_1 = \mathcal{Y}_2 = 0$ and the Lagrangian (8.39) reduces to

$$\mathcal{L} = \text{tr}[Q_2 C_x^T C_x] + \text{tr}\{[A_2 Q_2 + Q_2 A_2^T + B_w B_w^T] \mathcal{X}\} \quad (8.58)$$

From Lemma 1 in [10], the only controller which satisfies the first order necessary conditions for a minimum of (8.58) is the unique $K_{2_{opt}}$. However, this solution lies outside the admissible region; thus, a contradiction. Therefore the optimal solution satisfies at least one of the H_∞ constraints with equality. ■

Notice, inside Region I, we cannot claim that both constraints will be satisfied with equality as was true in the single constraint problem. While Theorem 8.2.2 does not fully characterize the solution to the fixed-order mixed problem with multiple constraints, it does provide insight into methods of solving the problem. For a strictly sub-optimal solution, the problem can be split into two problems, one with an equality constraint on the first constraint and an inequality constraint on the second, and vice versa. The solution will then be the controller which minimizes the two-norm of H_2 problem, while satisfying both constraints.

However, if super-optimal solutions are acceptable (i. e., solutions which do not necessarily satisfy one or both of the constraints, but are within some tolerance of satisfying them), both constraints can be appended to the H_2 problem as minimum distance constraints such as the square of the error from equality. The solution to this problem will be a fixed-order controller which is minimum distance in a two-norm sense from the optimal. Since $K_{2_{opt}}$ is always in some neighborhood of the global optimal (unconstrained order), a solution to the fixed-order problem, with order greater than or equal to n_2 , is guaranteed to exist. The uniqueness of the solution, however, is not guaranteed. The super-optimal approach has been

successfully applied to the multiple constraint mixed problem, as reported by Ullauri, *et al* [63].

Finally, the constraints can both be appended to the objective as inequality constraints. While this is easier to implement than a one equality/one inequality constraint method, it can lead to numerical difficulties if the region of convergence is highly non-convex. In practice, this has not been found to be a problem.

8.3 Numerical Solution

Two approaches have been developed to compute controllers which solve the mixed H_2/H_∞ problem for multiple constraints. The first method, called the *Grid Method*, computes the set of controllers which satisfy the H_∞ constraints in the region of interest. This is accomplished by holding all but one constraint constant and varying the remaining constraint. The second method, or *Direct Method*, attempts to simultaneously reduce all the H_∞ constraints. For the remainder of the discussion it will be assumed that there are only two H_∞ constraints. The results can be extended as necessary to handle larger constraint sets. Both methods are based on the inequality constraint program

$$\left\{ \begin{array}{l} \min_{K \text{ stabilizing}} \|T_{zw}\|_2 \\ \text{subject to} \\ \|T_{ed_1}\|_\infty - \gamma_1 \leq 0 \\ \|T_{ed_2}\|_\infty - \gamma_2 \leq 0 \end{array} \right. \quad (8.59)$$

However, both methods could be modified for equality constraints if desired.

8.3.1 Grid Method. The grid method consists of solving a series of mixed problems by holding one H_∞ constraint constant and reducing the second. Once the optimal curve has been determined, the first constraint is decremented and the process is repeated. The initial controllers for the method are determined by solving

the two single constraint mixed H_2/H_∞ problems to define the region of interest. The process results in a surface defined by α versus γ_1 versus γ_2 . An example of a surface generated using the grid method is given in Figure 8.10. The values of γ_1 and γ_2 corresponding to the optimal H_2 solution is denoted in the figure, and the boundaries extending from the optimal H_2 point are the results from the mixed $H_2/\|T_{ed_1}\|_\infty$ and the $H_2/\|T_{ed_2}\|_\infty$ optimal control problems.

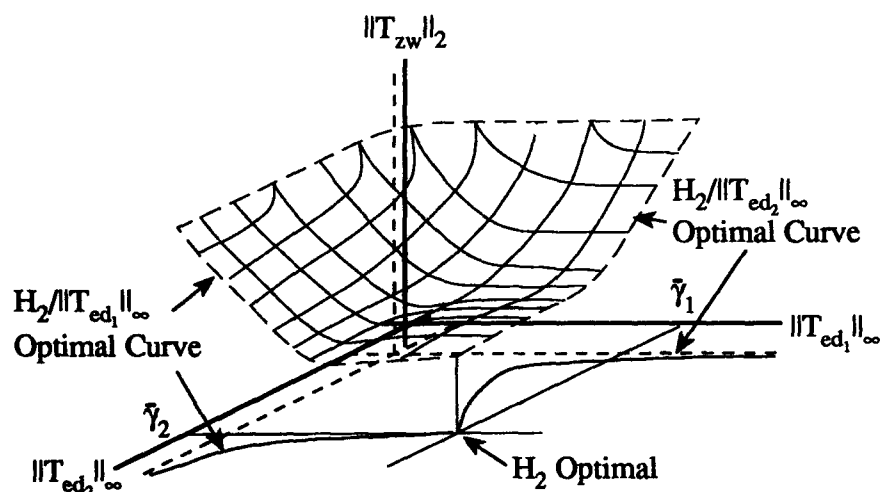


Figure 8.10. Typical surface generated by the grid method

8.3.2 Direct Method. As was discussed in the introduction to this chapter, design objectives are often stated as H_∞ constraints. Since the design objectives are often limited to one region of the constraint hyperplane, one approach to synthesizing a controller would be drive all H_∞ constraints concurrently to the desired region without computing the entire grid described in the previous approach. The direct method is an iterative approach where all the constraints are decremented from some initial point and a solution is found. The process continues until all the constraints are in the desired region.

For the two-constraint problem, the process used in this approach is to begin at the optimal H_2 controller and simultaneously reduce γ_1 and γ_2 until a controller is

found which meets both objectives. This results in a controller of fixed-order which meets both the H_∞ constraints and has the smallest two-norm for the H_2 transfer function. An advantage of the direct method is that the initial controller can be chosen as any stabilizing controller with order greater than or equal to n_2 . Numerically, the direct method has been found to work better in the neighborhood of $\underline{\gamma}_i$ than the grid method. One reason for this is the direct method approaches the minimum point from a better conditioned portion of the curve. The grid method attempts to track the solution along a minimum γ curve and is generally less numerically well conditioned. Once a controller is found via the direct method which satisfies the design objectives, a reduced size grid approach can be used to determine design trade-offs in the admissible region.

8.4 SISO F-16 Example

The SISO F-16 longitudinal controller design from Chapter V is used to demonstrate the multiple H_∞ constraint method. This example demonstrates the application of the grid and direct methods for finding solutions to multiple-constraint mixed problems. However, it is not intended as an in-depth analysis of a controller design with all trade-offs explored. A source for such an exploration is [63].

Recall that the problem is to design a normal acceleration tracker which also has good noise rejection properties and margins. In the previous example, the H_2 portion of the mixed control design was used to minimize response to noise, regulate the states, and limit control usage. The H_∞ constraint was a sensitivity model matching problem designed to achieve the performance objective and provide acceptable vector margins. As was seen in the example, there was a trade-off between the margins and the performance as the solution approached an acceptable tracker. To exploit this trade-off, a second H_∞ constraint is appended to improve margins. Thus, the problem will be an LQG design with a weighted input complementary constraint to recover margins and weighted output sensitivity constraint to improve

performance. Since this is a SISO plant, the margins and performance at the input and output of the plant are the same; however, the methodology which is presented here can be applied to a MIMO plant to recover acceptable margins and performance at both ends of the plant. See [63] for a MIMO example of the multiple-constraint mixed optimization.

8.4.1 Problem Setup. The H_2 problem is the same one defined in the F-16 example in Section 6.2.4. The H_∞ constraints consist of the same transfer functions used in the H_2/μ example in Section 7.3.1.1, except the constraints will be treated individually. Thus, T_{ed_1} will be the model matching input complementary sensitivity which is used to provide a measure of robust stability. The second constraint (T_{ed_2}) is an output sensitivity model matching problem which provides a measure of nominal performance.

The objective is to concurrently:

- i. reduce the value of $\|T_{ed_1}\|_\infty$ below 1 to guarantee robust stability to expected perturbations
- ii. reduce the value of $\|T_{ed_2}\|_\infty$ to as low a value as possible for nominal performance
- iii. minimize $\|T_{zw}\|_2$ to provide noise rejection, output regulation, and limit control usage.

The H_2 and the T_{ed_2} matrices are the same as the H_2 and H_∞ matrices in the example in the Sections 6.2.4 and 6.2.2, respectively. The weighting on the complementary sensitivity is selected as a high-pass filter and is given by

$$W_t = \frac{50(s + 100)}{s + 10000} \quad (8.60)$$

The matrices associated with the complementary sensitivity constraint T_{ed_1} are

$$A_{\infty_1} = \begin{bmatrix} -1.491 & 0.996 & -0.188 & 0 & 0 \\ 9.753 & -0.960 & -19.04 & 0 & 0 \\ 0 & 0 & -20.0 & 0 & 0 \\ 35.264 & -0.334 & -4.367 & -40.0 & 0 \\ -35.264 & 0.334 & 4.367 & 80.0 & -10000.0 \end{bmatrix} \quad (8.61)$$

$$B_{d_1} = \begin{bmatrix} 0 \\ 0 \\ 0 \\ 0 \\ 0 \end{bmatrix} \quad B_{u_{\infty_1}} = \begin{bmatrix} 0 \\ 0 \\ 20.0 \\ 0 \\ 0 \end{bmatrix} \quad (8.62)$$

$$C_{e_1} = \begin{bmatrix} -1763.2 & 16.7 & 218.35 & 4000.0 & -495000.0 \end{bmatrix} \quad (8.63)$$

$$C_{y_{\infty_1}} = \begin{bmatrix} -35.264 & 0.334 & 4.367 & 80.0 & 0 \end{bmatrix} \quad (8.64)$$

$$D_{ed_1} = [0] \quad D_{eu_1} = [0] \quad D_{yd_1} = [1.0] \quad D_{yu} = [0] \quad (8.65)$$

8.4.2 Results. A controller order of four was selected so the results could be directly compared to those of the example in Section 6.2. The problem was approached by first solving the single constraint problems $H_2/\|T_{ed_1}\|_{\infty}$ and $H_2/\|T_{ed_2}\|_{\infty}$. The results of these two problems defined the optimal single constraint curves in Figures 8.11–8.13. Additionally, the problems defined the constraint plane region in Figure 8.14, where a trade-off could be made between robust stability and nominal performance. Of particular interest in Figure 8.14 is that there is no real trade-off until γ_2 is reduced below 60000. However, for our particular problem, we are interested in the region close to $\underline{\gamma}_1$ and $\underline{\gamma}_2$. Thus, a direct approach was used to minimize both constraints concurrently. The result of this search was a controller that yields

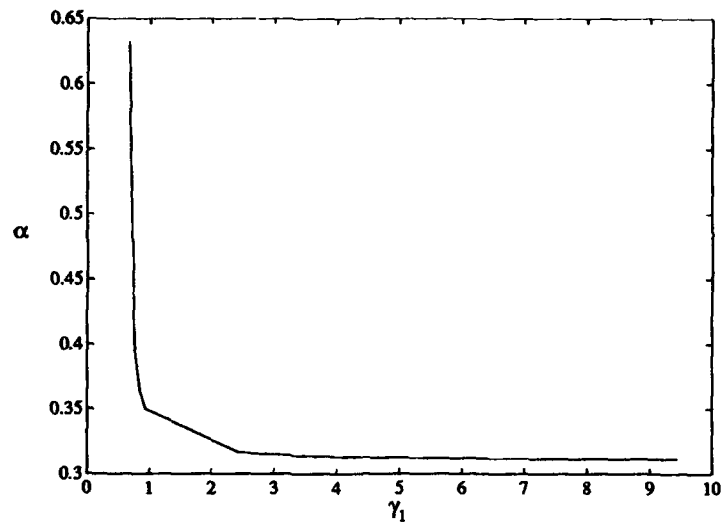


Figure 8.11. F-16, $H_2/\|T_{ed_1}\|_\infty$ α versus γ_1 curve

$\gamma_1 = 0.861$, $\gamma_2 = 1.78$, and $\alpha = 0.411$. This controller produced the lowest values of γ_1 possible using the available numerical methods.

Now that the minimum point has been determined, it is desired to find the trade-off of γ_1 , γ_2 , and α that can be made in the neighborhood of the minimum point. Thus, a grid method was used. The initial controller was the optimal $H_2/\|T_{ed_2}\|_\infty$ controller corresponding to $\gamma_2 = 200$. This resulted in $\tilde{\gamma}_2 = 9.37$. The grid was generated by first fixing the value of γ_2 and reducing the value of γ_1 . The value of γ_2 was then decremented and the process was repeated. The values of γ_1 used were 200, 100, 50, 20, 10, 5, 2, and 1. To complete the grid, the roles of γ_1 and γ_2 were reversed, and another grid was generated using γ_2 values of 8, 6, 4, 2, 1, and 0.5. The surface which resulted is given in Figure 8.15. The shape of the surface is as expected, with an obvious trade-off between H_2 performance and the constraints. Since our first objective is to obtain robust stability, we can accept any solution which results in $\gamma_1 < 1$. Figure 8.16 is the projection of the mixed surface in the constraint plane. Any solution in the acceptable region will guarantee robust stability. Therefore, the

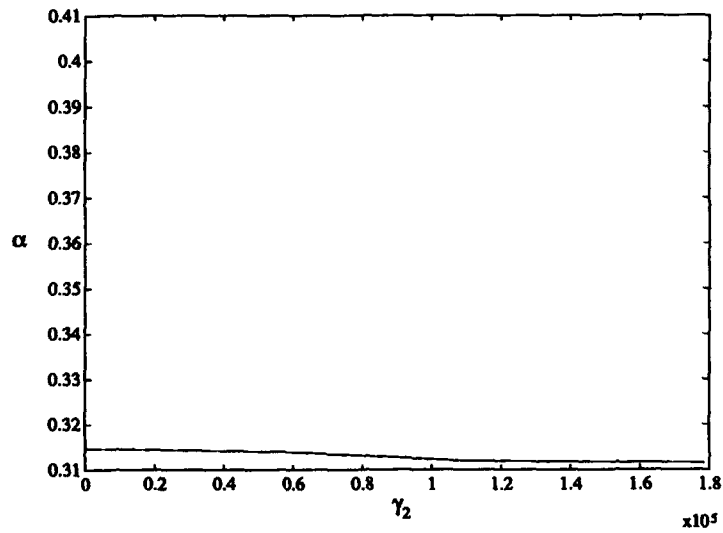


Figure 8.12. F-16, $H_2/\|T_{ed_2}\|_\infty \alpha$ versus γ_2 curve

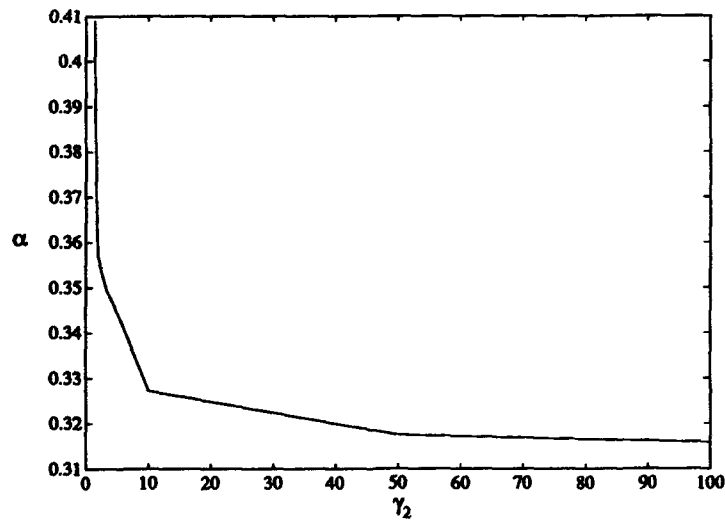


Figure 8.13. F-16, $H_2/\|T_{ed_2}\|_\infty \alpha$ versus γ_2 curve, expanded

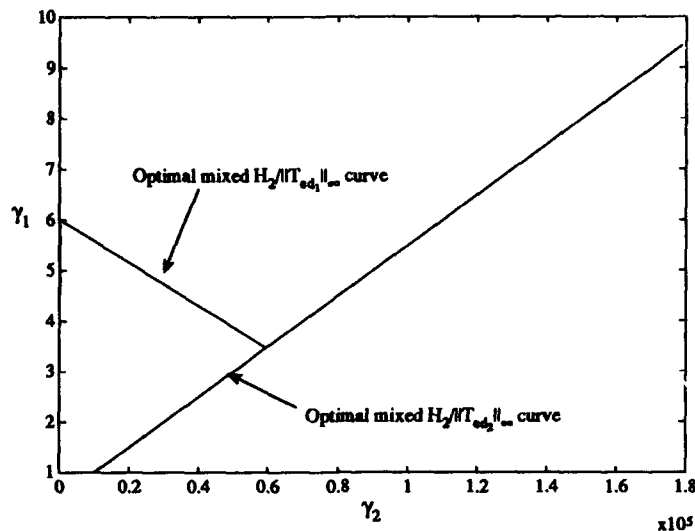


Figure 8.14. F-16, constraint plane solution regions

problem reduces to a trade-off analysis between γ_2 and α . If it is desired, the grid can be further refined in the acceptable region to determine the best solution.

One interesting result of this particular problem is that the controller with the best robust stability ($\alpha = 0.411, \gamma_1 = 0.86, \gamma_2 = 1.78$) yields a different controller from the best one found in the single constraint problem given in Section 6.2 ($\alpha = 0.409, \gamma_1 = 1.02, \gamma_2 = 1.49$). The time responses for both controllers are given in Figure 8.17. Notice that we give up some nominal performance in order to increase stability robustness. If we desire, the γ_1 (robust stability) constraint could be relaxed to $\gamma_1 \leq 1.0$ and the minimum γ_2 can be determined. In fact, $\gamma_1 = 1.02$ for the single constraint controller nearly meets our robust stability bound. Thus, for practical purposes, the $\gamma_2 = 1.49$ controller achieves our desired robustness bounds. Finally, the vector margins for the multiple constraint controller are $[-7.55 \ 7.31]dB$ gain margin and 33.8° phase margin. These are lower than the margins resulting from the single constraint controller which are $[-5.9 \ 10.3]dB$ gain margin and 40.7° phase margin. Thus, while the multiple constraint controller has the best robustness to the modeled perturbations, it has less robustness to independent gain and phase varia-

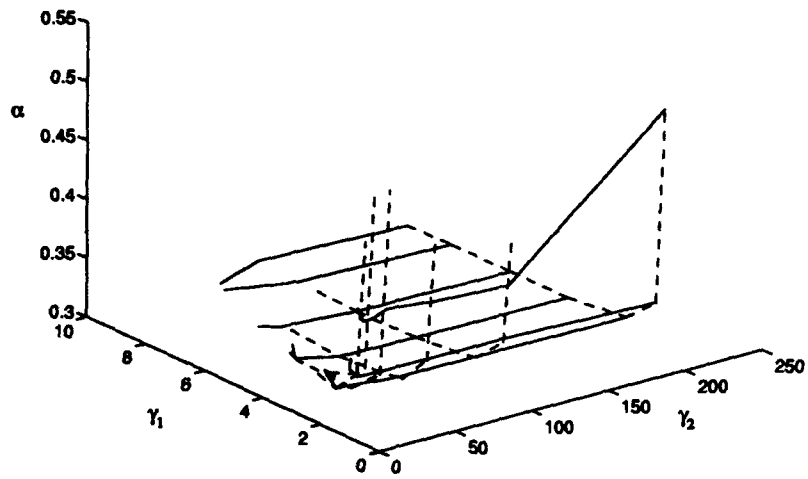


Figure 8.15. F-16, $H_2/\|T_{ed_1}\|_\infty/\|T_{ed_2}\|_\infty$ surface

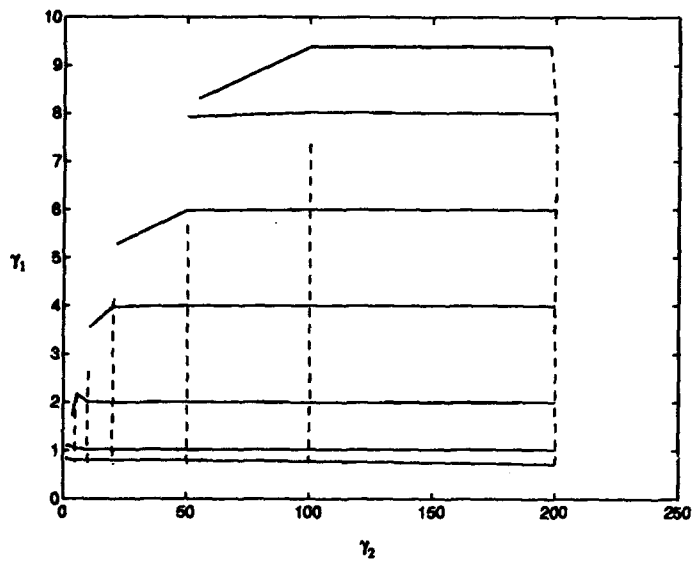


Figure 8.16. F-16, projection of the $H_2/\|T_{ed_1}\|_\infty/\|T_{ed_2}\|_\infty$ surface in the constraint plane

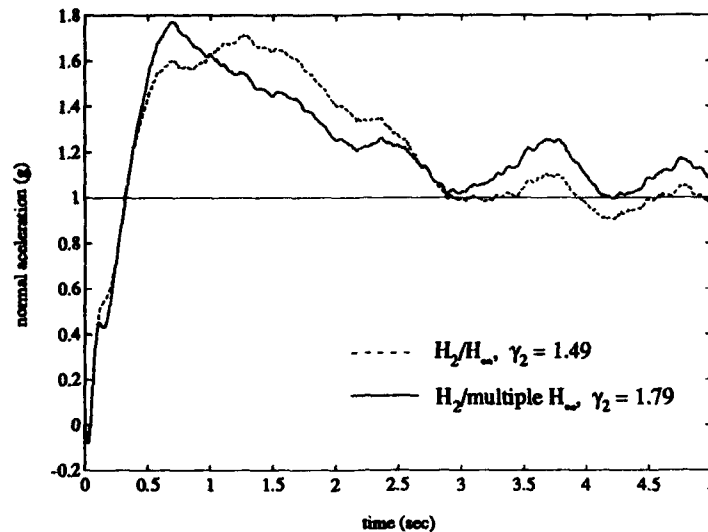


Figure 8.17. F-16, H_2/H_∞ and $H_2/\text{multiple } H_\infty$ controllers, response to unit normal acceleration step

tions. Since the single constraint controller achieves our robustness bound, and also provides better performance and margins, it is a better choice for implementation.

The trade-off in performance to achieve our robust stability bound is not significant for this problem. This is not a surprising result due to the relationship between the input complementary sensitivity and the output sensitivity for a SISO system. However, this will not be true for all problems. In particular, a MIMO system can result in constraints on the input sensitivity and complementary sensitivity as well as the output sensitivity and complementary sensitivity. In addition, there may be constraints on additive perturbations and control usage. Thus, a more significant trade-off is expected, in general, between the different objectives.

8.5 Summary

This chapter extended the H_2/H_∞ control problem to include multiple H_∞ constraints. The optimal solution for this problem was shown to be unique. Further, a set of relationships were developed between the level of the constraints and which

constraints must be satisfied with equality for an optimal solution. Fixed-order controllers were addressed next, and it was shown that the solution is either $K_{2,opt}$ or it must satisfy at least one constraint with equality. Based on this result, two numerical approaches were developed. A grid method can be used to determine the trade-off available between the constraints. A direct approach can be used if a particular level of the constraints is desired. Finally, an F-16 longitudinal control design example was used to demonstrate both numerical methods. It clearly showed the various trade-offs available to the designer between robust stability, nominal performance, and margins.

IX. Mixed H_2/L_1 and $H_2/H_\infty/\mu/L_1$ Optimal Control

Thus far, the problem we have examined is a convex program consisting of an H_2 objective function with a finite set of H_∞ constraints. This problem can be extended to include any finite set of convex constraints. In particular, this chapter will develop a methodology to include an L_1 constraint. Once again, the uniqueness of the optimal (order-free) controller will be shown. Further, a numerical approach based on an equivalent discrete-time system will be suggested. To conclude this discussion, all the constraints discussed in this dissertation will be combined into a multiple-constraint mixed problem.

9.1 Mixed H_2/L_1 Optimization

Often the control engineer is faced with requirements which can include limits on control surface deflections, maximum positive and negative accelerations, limits on angles of rotation, and so forth. In the mixed H_2/H_∞ problem, these limitations have been included as bounded energy limitations. While this often works adequately, it does not ensure that the magnitude limit will be met. A better way of incorporating these requirements is to treat them directly as bounded magnitude limitations. Thus, if we consider a system with a bounded magnitude input r and desire to place a limit on the worst case magnitude of the output m , we can define an induced operator norm on the system as $\|T_{mr}\|$; which, for continuous systems, is just the L_1 -norm of the impulse response of the transfer function from r to m . For discrete systems it is the ℓ_1 -norm of the pulse response of the transfer function.

There is currently a great deal of interest in developing control synthesis methods based on the ℓ_1 -norm (for an in-depth examination of the subject, see [20]). In this work, we are not interested in trying to solve an ℓ_1 control problem; rather, we are just interested in adding an L_1 or ℓ_1 constraint into the framework. This is not as straightforward as the H_∞ constraint since there is no convenient method of com-

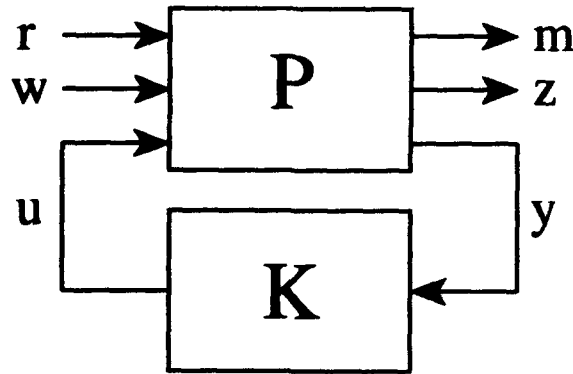


Figure 9.1. General mixed H_2/L_1 optimization problem

puting the L_1 -norm of a frequency domain transfer function. However, we are still dealing with a normed constraint; therefore, the problem remains convex and the previous work will hold. The fixed-order approach will be modified to compute the ℓ_1 -norm of an equivalent discrete transfer function. In general, the problem should be posed in the discrete domain and both the H_2 and ℓ_1 problems solved there. One reason for this approach is that the final implementation will usually be performed in the discrete domain. Therefore, a controller designed in the continuous domain will have to be discretized, which will result in a sub-optimal controller. However, the discrete problem is beyond the scope of this work; this section will only characterize the optimal (order-free) solution for the H_2/L_1 problem and develop a hybrid algorithm for including an ℓ_1 -norm overbound on the L_1 constraint in a frequency domain H_2/L_1 problem.

9.1.1 Uniqueness of the Optimal H_2/L_1 Controller. Consider the general control system shown in Figure 9.1, where w is a unit intensity white Gaussian noise input, r is a bounded magnitude input, and z and m are controlled (possibly fictitious) outputs where it is desired to minimize the energy of z and the magnitude of m . It is assumed that there is no *a priori* relationship between w and r or z and m . The measured output is y and the control law is $u = K(s)y$.

The mixed H_2/L_1 problem is to design a controller $K(s)$ such that the transfer function from w to z has minimum energy subject to maintaining the magnitude gain of the transfer function from r to m below some predetermined value ν . The former problem is an H_2 problem and the constraint is an L_1 problem. As in the H_2/H_∞ problem, the full plant $P(s)$ is formed from some underlying plant $G(s)$ augmented with stable weighting transfer functions on the inputs r and w and the outputs m and z . Partitioning P in a similar fashion to the previous work, this system can be reduced to two separate problems: the H_2 problem, which is to find an internally stabilizing controller $K(s)$ which minimizes $\|T_{zw}\|_2$ where

$$T_{zw} = P_{zw} + P_{zu}K(I - P_{yu}K)^{-1}P_{yw} \quad (9.1)$$

and the L_1 problem, which is to find an internally stabilizing controller $K(s)$ which satisfies $\|T_{mr}\|_1 \leq \nu$ for some ν where

$$T_{mr} = P_{mr} + P_{mu}K(I - P_{yu}K)^{-1}P_{yr} \quad (9.2)$$

As before, it is assumed that T_{zw} is strictly proper and thus has a finite two-norm. The mixed H_2/L_1 problem can be stated as: find a stabilizing controller $K(s)$ which minimizes the two-norm of T_{zw} and satisfies the constraint that the one-norm of T_{mr} is less than or equal to some fixed ν . This mathematical programming problem can be transformed into a convex programming problem through the use of the Youla parametrization. The convex program is

$$\mathcal{P} \begin{cases} \inf_{Q \in \mathcal{H}_2} \|T_{12} + T_{22}QT_{32}\|_2 \\ \text{subject to} \\ \|T_{11} + T_{21}QT_{31}\|_1 \leq \nu \end{cases} \quad (9.3)$$

where T_{i1} are defined in a similar method as $T_{i\infty}$ in Section 4.2. Define $\underline{\nu}$ as the minimum ν for which a controller exists and ν^* as the value of ν when the loop is

closed with the optimal (order-free) mixed controller. Also, define $\bar{\nu}$ as the value of ν when the loop is closed with $K_{2_{opt}}$.

Theorem 9.1.1 *Let $\nu > \underline{\nu}$ be given. The controller which satisfies the convex program (9.3) is unique. Furthermore, the following hold:*

- i. *if $\nu \geq \bar{\nu}$, the controller is the optimal H_2 controller*
- ii. *If $\nu \leq \bar{\nu}$, $\nu^* = \nu$ at the optimal (i. e., the solution will satisfy the L_1 constraint with equality).*

Proof: The proof follows directly from the proof of Theorem 4.2.1. ■

In general, the optimal (order-free) controller will be unique for any convex constraint. In fact, this result is easily extended to include any finite set of convex constraints.

9.1.2 Fixed-Order Controllers—Numerical Approach. Assume the controller order is fixed at a value greater than or equal to the order of the H_2 order. The mixed H_2/L_1 problem can be solved numerically using an approach similar to that used in the mixed H_2/H_∞ problem. There will be no attempt to characterize the nature of the fixed-order controller; rather, an algorithm will be developed which attempts to find a fixed-order controller in a neighborhood of the optimal (order-free) controller. As before, the region of interest for this problem is $\underline{\nu} < \nu < \bar{\nu}$ since, if $\nu \geq \bar{\nu}$ the optimal controller is $K_{2_{opt}}$, and if $\nu < \underline{\nu}$, no solution exists.

Define the program

$$\left\{ \begin{array}{l} \min_{K \text{ stabilizing}} \|T_{zw}\|_2 \\ \text{subject to} \\ \|T_{mv}\|_1 - \nu \leq 0 \end{array} \right. \quad (9.4)$$

Program (9.4) can be minimized using the SQP routine described in Chapter VI. The algorithm will be identical to the previous results with the exception of

the calculation of the constraint and its gradient. As was discussed in Section 2.3.3, there is no convenient way of computing the L_1 -norm. However, the ℓ_1 -norm of an equivalent discrete system can be computed to any desired accuracy. Further, from Theorem 2.3.1, by using an Euler approximation system of the continuous system, we can always insure that the discrete ℓ_1 -norm will be an upper bound to the continuous L_1 -norm.

To compute the ℓ_1 -norm, first put the system into an EAS discrete form using the method described in Section 2.3.3.3. For synthesis, the time step τ in the discretization is fixed based on the bandwidth of the system. Once the equivalent discrete transfer function is determined, the ℓ_1 -norm is determined using the method given in Section 2.3.3.2. The acceptable level of error in the norm is also used to determine N , the point where the infinite sum is truncated.

Finally, the gradient of the constraint is determined analytically. The gradient is

$$\frac{\partial \|T_{mr}^{EAS}\|_1}{\partial x_i} = \frac{\partial \left[\sum_{k=0}^N |C_E A_E^k B_E| + |D_E| \right]}{\partial x_i} \quad (9.5)$$

$$= \frac{\partial \left[\sum_{k=0}^N |C (I - \tau A)^k \tau B| + |D| \right]}{\partial x_i} \quad (9.6)$$

where (A_E, B_E, C_E, D_E) is the EAS equivalent of realization (A, B, C, D) of T_{mr} .

This proposed method has not been implemented to date. However, it would appear to provide a straightforward approach to handling L_1 constraints. Further development along these lines of research are being pursued.

9.2 H_2 Optimization with H_∞ , μ , and L_1 Constraints

To complete this dissertation, we will look at how we can put this all together to solve an aircraft control problem. The various exogenous inputs to the system include

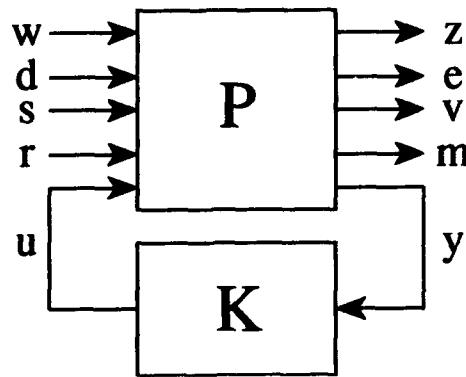


Figure 9.2. General mixed $H_2/H_\infty/\mu/L_1$ optimization problem

white noises from wind disturbances and measurement noises. In addition, there are plant perturbations due to unmodeled dynamics and aerodynamic variations. The primary design objective is to ensure the system remains stable in light of the noises and plant perturbations. Furthermore, the performance objectives include attenuating response to noise and perturbations and providing desired response to commanded inputs. Moreover, it is desired that this performance remain at an acceptable level in light of the perturbations described above. Finally, there may be some catastrophic perturbations, such as the loss of a control surface, which are not desirable to include in the above objectives. However, some limited subset of the stability and performance objectives must be met in light of these catastrophic perturbations.

The above objectives can be recognized as the robust stability and robust performance problems defined in the introduction to this dissertation. Moreover, we have now developed the necessary tools to handle a set of these objectives in an optimal fashion. Consider the block diagram given in Figure 9.2. Following the standard notation from the previous chapters, w represents the white noise inputs, d and s are the bounded energy inputs and r represents the bounded magnitude inputs. The controlled outputs z , e , and v are bounded energy and m is bounded magnitude. As before, no *a priori* relationship between w , d , s , or r and z , e , v , or m is assumed. The problem can now be stated as: Find the controller K which solves

the program

$$\mathcal{P} \begin{cases} \alpha = \inf_{K \text{ stabilizing}} \|T_{zw}\|_2 \\ \text{subject to} \\ \|T_{ed}\|_\infty \leq \gamma \\ \|T_{vs}\|_\infty \leq \beta \\ \|T_{mr}\|_1 \leq \nu \end{cases} \quad (9.7)$$

Through the use of the Youla parametrization from Section 3.1, the problem can be transformed to the convex program

$$\mathcal{P} \begin{cases} \alpha = \inf_{Q \in H_2} \|T_{1_2} + T_{2_2}QT_{3_2}\|_2 \\ \text{subject to} \\ \|T_{1_\infty} + T_{2_\infty}QT_{3_\infty}\|_\infty \leq \gamma \\ \|T_{1_\mu} + T_{2_\mu}QT_{3_\mu}\|_\infty \leq \beta \\ \|T_{1_1} + T_{2_1}QT_{3_1}\|_1 \leq \nu \end{cases} \quad (9.8)$$

where T_{i_2} are associated with T_{zw} , T_{i_∞} are associated with T_{ed} , T_{i_μ} are associated with T_{vs} , and T_{i_1} are associated with T_{mr} .

Theorem 9.2.1 *Assume the convex program*

$$\mathcal{P} \begin{cases} \alpha = \inf_{Q \in H_2} \|T_{1_2} + T_{2_2}QT_{3_2}\|_2 \\ \text{subject to} \\ \|T_{1_i} + T_{2_i}QT_{3_i}\|_{\beta_i} \leq \gamma_i \end{cases} \quad (9.9)$$

where $\beta_i \in \{\infty, 1\}$ and $i = 1, \dots, N$, is consistent. Then the $Q \in H_2$ which achieves the infimum is unique.

Proof: From Lemma 4.1.1, the two-norm is a strictly convex functional, therefore, from the corollary to Theorem 9.4.1 [35], any solution to the convex program (9.9) is unique. ■

The characterization of where the optimal (order-free) solution will fall relative to the constraints is complicated for this problem due to the increased number of constraints. However, the optimal solution must still satisfy the Kuhn-Tucker conditions.

For fixed-order solutions, both the direct and grid methods from Chapter VIII can be extended to include the larger set of constraints. As the number of constraints increases, greater insight into the desired objective bounds will be needed to limit the region of interest. In addition, the increased number of constraints provide the designer with more trade-offs. Thus, by incorporating H_∞ , μ , and ℓ_1 constraints into the H_2 optimization problem, the designer can now account for a larger set of stability and performance objectives in an optimal fashion.

9.3 Application of Mixed Optimization

While this section cannot provide a complete method for solving all control design problems using mixed optimization, some thoughts on applications are appropriate. To begin, it is necessary to determine exactly which portion of the mixed method will be used to handle each design problem faced. It may turn out that a combined approach can be taken where one problem is addressed by a combination of the objective and constraints. Since the H_2 problem is the objective function it is the logical starting point for this discussion.

Traditionally, the H_2 problem is set up to minimize the influence of both low and high frequency noise. Additionally, it has been found that tracking can often be obtained by adding a low frequency noise at the output and minimizing the energy of the output. While this has some merits, the tracking problem can be directly approached by using an H_∞ constraint or an L_1 constraint. Furthermore, we saw in the F-16 problem that a good output tracker also had good low frequency noise rejection. Thus, it may be possible to use the H_2 portion of the mixed problem primarily to limit the response of the system to high frequency noise. Of course,

we assumed that the H_2 problem is regular, so some low frequency noise will be necessary.

The next problem to attack is how to achieve robust stability and performance. As we saw, μ -synthesis provides a method for achieving the desired robustness. Therefore, the expected perturbations and performances requirements should be incorporated into a μ constraint. However, as has been mentioned earlier, there may be some perturbations which have a low probability of occurrence, but for which we desire some minimal level of robustness to. These catastrophic perturbations can be incorporated into the problem as an H_∞ constraint. Therefore, a trade-off can be made between our "normal" capability and the ability to handle catastrophic events. It should be mentioned that the desire is not necessarily to design a controller which provides for every situation, but rather one which provides some level of stability and performance while the catastrophic event is identified and the control laws reconfigured.

Finally a discussion of the level of nominal performance achieved throughout this work is needed. Using H_∞ techniques we have been able to find controllers which track better and have better margins than the LQG regulator we began with. However, we have not achieved the level of tracking performance desired in most applications. In particular, we are often given specifications on the rise time, overshoot, and settling time resulting from tracking a unit step input to the system. All of these are inherently bounded magnitude constraints. Thus, the obvious approach to incorporating these constraints is to define them as L_1 transfer functions and adjoin them to our optimization problem. Therefore, we are able to address a number of concerns of the designer and, through the mixed $H_2/H_\infty/\mu/L_1$ approach, provide a method of designing controllers by trading off the various objectives.

X. Conclusions and Recommendations

10.1 Summary

This dissertation has characterized the mixed norm optimization problem for both order-free and fixed-order controllers. The first problem considered was the general mixed H_2/H_∞ optimization problem for output feedback. It was shown that the problem can be restated as a convex program through application of the Youla parametrization of all stabilizing controllers. This form was then used to prove that the optimal order-free solution is unique. Furthermore, through a duality approach, the controller for a special case of the H_2/H_∞ problem was shown to be non-rational or infinite order.

Due to the real world requirement that controller order be reduced to an implementable level, a fixed-order solution was sought. For the mixed H_2/H_∞ problem, it was shown that optimal fixed-order solutions exist for orders as low as the H_2 problem. Further, the necessary conditions for an optimal fixed-order controller were developed for the mixed problem with both a singular and proper (but not necessarily strictly proper) H_∞ constraint. In addition, the nature of the optimal fixed-order controller was characterized based on the level of the desired H_∞ constraint.

A numerical synthesis method was developed based on the results of the fixed-order solutions. This method is based on the relationship of the optimal two-norm versus infinity-norm curve. It has the advantage of only requiring a regular H_2 problem, and thus can handle singular H_∞ constraints, including those that have associated Hamiltonians with $j\omega$ -axis zeros. The numerical search was based on either a Davidon-Fletcher-Powell or a Sequential Quadratic Programming algorithm. Since the optimal H_2 solution is easily computed, it was selected as a convenient initial controller. Both sub- and super-optimal solutions can be found using the method.

The gradient of the two-norm objective function was derived from Lagrangian

$$\mathcal{L} = \text{tr} [Q_2 C_2^T C_2] + \text{tr} [(A Q_2 + Q_2 A^T + B_w B_w^T) \mathcal{X}] \quad (10.1)$$

The gradient of the H_∞ constraint was based either on a central difference or on an analytical gradient of the associated maximum singular value. The sensitivity method resulted in more accurate gradients and therefore converged to solutions faster and more accurately. However, it is limited due to the piecewise continuous nature of the H_∞ gradient. Both the DFP and SQP methods took significantly less computation time than existing methods. Finally, the SQP method was able to converge to controllers with lower values of γ and required fewer iterations than the DFP method.

The new numerical method was used to demonstrate the application of the mixed problem to a SISO F-16 normal acceleration control design problem. It was found that a significant reduction in the infinity-norm constraint could be made with little increase in the two-norm. This trade-off allowed the mixed controller to improve both stability robustness and tracking performance without suffering loss of noise rejection or excessive control usage.

The mixed problem was also extended to include robust performance through the addition of a μ constraint. This was accomplished by substituting the mixed approach for the last controller design in a D-K iteration. Using mixed H_2/μ optimization, both the robust stability and robust performance problems were developed. The SISO F-16 normal acceleration control problem and a MIMO HIMAT longitudinal control problem were used to demonstrate the usefulness of the mixed H_2/μ problem. In both examples, the order of the controller was reduced significantly below the order resulting from a μ -synthesis design. Furthermore, the F-16 design demonstrated a significant reduction in high frequency noise response and control usage when compared to the μ controller.

To extend the class of problems to which mixed optimization can be applied, multiple H_∞ constraints were incorporated into the H_2/H_∞ problem. It was shown through convex analysis that the optimal (order-free) controller is unique. Further, the necessary conditions for an optimal fixed-order control controller were developed. In particular, it was shown that the optimal fixed-order controller must satisfy certain conditions based on where the intersection of the H_∞ constraints fall in the constraint plane. Two numerical approaches, the grid and direct methods, were developed to find solutions which satisfied design objectives. Again, the SISO F-16 normal acceleration problem was used to demonstrate the methods. The various regions in the constraint plane were found and the direct method was used to find a solution which satisfied the design objectives. Moreover, a grid was produced in the neighborhood of this solution to demonstrate the available trade-offs which could be made between the two-norm and the constraints.

Next, the mixed problem was extended to include L_1 constraints. Again, the uniqueness of the optimal (order-free) solution was shown. In fact, this result can be extended to any set of convex constraints appended to the H_2 problem. A numerical approach to the H_2/L_1 problem was proposed. It is based on computing the ℓ_1 -norm of an equivalent discrete-time system.

Finally, all of the above results have been combined to form an H_2 optimization problem with any finite set of H_∞ , μ , and L_1 constraints. Such problems arise often in aerospace applications. One particular example is a robust performance problem which also has a robust stability objective due to another potential catastrophic perturbation. If the catastrophic perturbation is included in the structured perturbation, it can limit the performance available under "normal" perturbations. Therefore, it is not desirable to include the catastrophic perturbation into the structured perturbation for the μ robust performance constraint. However, with the mixed approach, the catastrophic robust stability objective can be appended to the

problem as an additional H_∞ constraint. Now a trade-off can be made between robust performance and "catastrophic" robust stability.

10.2 Recommendations for Future Research

While this dissertation has contributed to the understanding of mixed norm optimization problems, there still remains a number of questions to be answered. The first of these is what the optimal order of a mixed controller is, and what the optimal mixed curve looks like. While the optimal order appears to be infinite, this has not yet been proven analytically. This problem may possibly be solved through the operator-theoretic approach developed in this work.

Another question which has not been answered is the uniqueness of the optimal fixed-order controller. Numerical results to date tend to indicate the controller is unique. However, due to the lack of convexity of the underlying set, it has not been shown whether or not the optimal fixed-order solution is unique. Perhaps the application of nonconvex analysis to this problem will be able to answer the question.

Thirdly, the synthesis method proposed in this work has not been refined to the point where it is ready for everyday application. In particular, the numerical solution has problems around the knee of the α versus γ curve. The largest contributor to this problem is the nature of the H_∞ constraint. For problems of interest, the gradient of the H_∞ constraint is only piecewise continuous; this leads to the gradient being valid in only a small neighborhood of the nominal solution. Thus, the step size of the one dimensional search must be reduced, resulting in an increased number of iterations to converge to a solution. Another problem is the non-uniqueness of a particular state space realization of the controller transfer function. This has been partially overcome through the use of the modal canonical form, but this does not allow all possible controller transfer functions (i. e., it only allows controllers with first order Jordan blocks). Incorporation of a modified Jordan form [60] should overcome this

limitation. Refinement of the numerical method is an open problem which should yield a significant advance in optimal control synthesis.

The fourth open area is the H_2/L_1 optimization problem. While a continuous approach to this problem has been proposed, the appropriate approach is in the discrete domain. In fact, the entire mixed framework should be rederived in the discrete domain. This has the advantage of producing a controller which can be directly implemented by a digital computer without adding the complicated and sub-optimal step of discretizing a continuous controller. This work is currently underway.

Finally, mixed H_2 optimization with H_∞ , μ , and L_1 constraints needs to be demonstrated on a realistic control design problem. As was suggested, a robust performance problem combined with a catastrophic robust stability objective would be ideal for this. Further, the ever-present noise rejection and state regulation problem can be incorporated into the H_2 problem. Finally, the L_1 constraints can be used to enforce time domain constraints, such as control deflection and normal acceleration limits. Through such control design examples, the flexibility and power of the mixed optimization approach can be further explored and refined.

Appendix A. SISO F-16 Short Period Model

The F-16 normal acceleration command control system is modeled by a continuous, time-invariant linear system shown in Figure A.1. The system consists of a two-state short period approximation of the normal acceleration command system augmented with a pre-filter for the servo dynamics and a post-filter to model the control delay. The plant states are the angle of attack (α) and the pitch rate (q). The input is the stabilator deflection (δ_e) and the output is normal acceleration (n_z). The plant (W_p) is given by

$$\begin{aligned} \begin{bmatrix} \dot{\alpha} \\ \dot{q} \end{bmatrix} &= \begin{bmatrix} -1.491 & 0.996 \\ 9.753 & -0.96 \end{bmatrix} \begin{bmatrix} \alpha \\ q \end{bmatrix} + \begin{bmatrix} -0.188 \\ -19.04 \end{bmatrix} \delta_e \\ \begin{bmatrix} n_z \end{bmatrix} &= \begin{bmatrix} 35.264 & -0.334 \end{bmatrix} \begin{bmatrix} \alpha \\ q \end{bmatrix} + \begin{bmatrix} -4.367 \end{bmatrix} \delta_e \end{aligned} \quad (\text{A.1})$$

The actuator dynamics (W_a) are modeled as a first order relation between the commanded stabilator deflection ($\delta_{e_{com}}$) and the actual deflection given by

$$\dot{\delta}_e = -20.0\delta_e + 20.0\delta_{e_{com}} \quad (\text{A.2})$$

A first order Padé approximation is used for the time delay (W_d) and is given by

$$\begin{aligned} \dot{d} &= -40.0d + n_z \\ n_{z_{delay}} &= 80.0d - n_z \end{aligned} \quad (\text{A.3})$$

where ($n_{z_{delay}}$) is the output of the system.

A wind disturbance is modeled as an angle of attack perturbation by a zero-mean white Gaussian noise with a strength of 5.0×10^{-4} rad²-sec. The measurement is corrupted by zero-mean, white Gaussian noise of strength 1.6×10^{-5} g²-sec. The

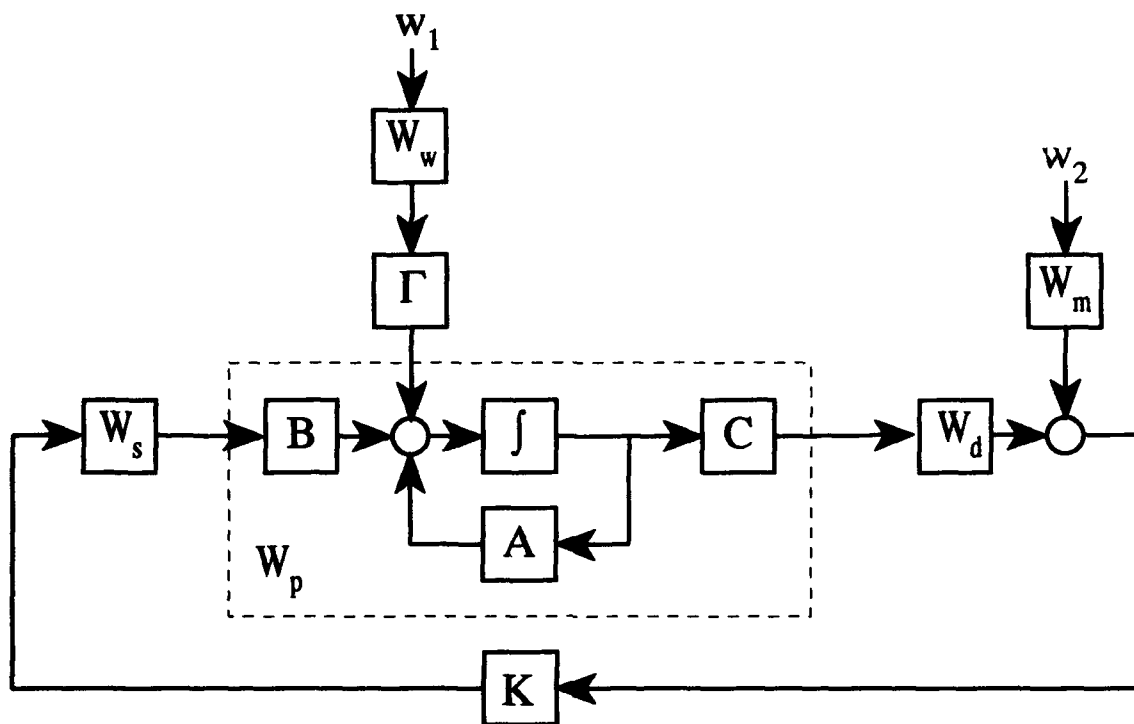


Figure A.1. F-16 model block diagram

strength of the noises were determined by tuning a linear quadratic estimator. The truth model for the tuning and analysis includes a first order Von Karman wind model for the low frequency process noise (W_w), which entered the plant as an alpha perturbation (Γ), and a high-pass filter to model the measurement noise (W_m). These models are given, respectively, as

$$\dot{x}_w = -6.7x_w + 0.0187w_1 \quad (\text{A.4})$$

$$\xi = x_w \quad (\text{A.5})$$

$$\dot{x}_m = -10x_m + 0.004w_2 \quad (\text{A.6})$$

$$\eta = 1.0x_m + 0.004w_2 \quad (\text{A.7})$$

where w_1 and w_2 are unit strength white-Gaussian noises, x_d is the wind state, x_m is the measurement noise state, ξ is the process noise, and η is the measurement noise. Γ is the first column of the plant A matrix given in (A.1).

Appendix B. MIMO HIMAT Model

The model is taken from data for the HIMAT vehicle [44]. The model is a continuous, time-invariant linear system, consisting of the four-state longitudinal dynamics. The states are forward velocity perturbation (δ_v), angle of attack (α_r), pitch rate (q), and aircraft attitude (θ_r). The control inputs are elevon (δ_e) and canard (δ_c) and the measured outputs are angle of attack (α) and aircraft attitude (θ). The plant is given by

$$\begin{aligned}
 \begin{bmatrix} \dot{\delta}_v \\ \dot{\alpha}_r \\ \dot{q} \\ \dot{\theta}_r \end{bmatrix} &= \begin{bmatrix} -0.0226 & -36.6 & -18.90 & -32.1 \\ 0 & -1.90 & 0.983 & 0 \\ 0.0123 & -11.7 & -2.63 & 0 \\ 0 & 0 & 1.0 & 0 \end{bmatrix} \begin{bmatrix} \delta_v \\ \alpha_r \\ q \\ \theta_r \end{bmatrix} \\
 &+ \begin{bmatrix} 0 & 0 \\ -0.414 & 0 \\ -77.80 & 22.40 \\ 0 & 0 \end{bmatrix} \begin{bmatrix} \delta_e \\ \delta_c \end{bmatrix} \tag{B.1} \\
 \begin{bmatrix} \alpha \\ \theta \end{bmatrix} &= \begin{bmatrix} 0 & 57.3 & 0 & 0 \\ 0 & 0 & 0 & 57.3 \end{bmatrix} \begin{bmatrix} \delta_v \\ \alpha_r \\ q \\ \theta_r \end{bmatrix}
 \end{aligned}$$

The design and truth model noise inputs are the same as those given in Appendix A only with the units on the sensor noise changed to deg²-sec. The truth model is shown in Figure B.1, where A, B, and C are defined in the normal way and Γ is the second column of A.

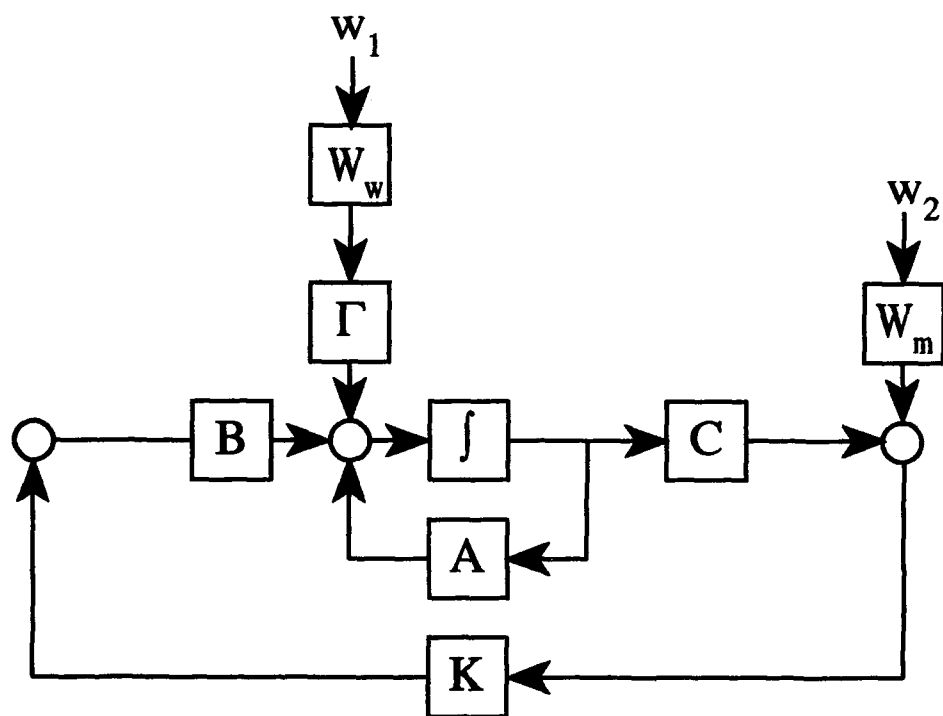


Figure B.1. HIMAT model block diagram

Bibliography

1. J. C. Doyle. Analysis of feedback systems with structured uncertainty. In *IEE Proceedings*, volume 129, Part D, no. 6, pages 242–250, 1982.
2. A. Packard and J. Doyle. The complex structured singular value. *Automatica*, 29(1):71–109, 1993.
3. G. Zames. On the input–output stability of time–varying nonlinear feedback systems, Part I: Conditions derived using concepts of loop gain, conicity, and positivity. *IEEE Trans. Auto. Control*, AC-11:228–238, April 1966.
4. D. S. Bernstein and W. H. Haddad. LQG control with an H_∞ performance bound: A Riccati equation approach. *IEEE Trans. Auto. Control*, AC-34(3):293–305, March 1989.
5. J. Doyle, K. Zhou, and B. Bodenheimer. Optimal control with mixed H_2 and H_∞ performance objectives. In *Proceedings of American Control Conference*, pages 2065–2070, Pittsburgh PA, June 1989.
6. K. Zhou, J. Doyle, K. Glover, and B. Bodenheimer. Mixed H_2 and H_∞ control. In *Proceedings of the American Control Conference*, pages 2502–2507, San Diego CA, May 1990.
7. H. H. Yeh, S. S. Banda, and B-C. Chang. Necessary and sufficient conditions for mixed H_2 and H_∞ optimal control. In *Proceedings of the 29th Conference on Decision and Control*, pages 1013–1017, Honolulu HI, December 1990.
8. M. A. Rotea and P. P. Khargonekar. H_2 -optimal control with an H_∞ -constraint: The state feedback case. *Automatica*, 27(2):307–316, March 1991.
9. D. B. Ridgely, C. P. Mracek, and L. Valavani. Numerical solution of the general mixed H_2/H_∞ optimization problem. In *Proceedings of the American Control Conference*, pages 1353–1357, Chicago IL, June 1992.
10. D. B. Ridgely, L. Valavani, M. Dahleh, and G. Stein. Solution to the general mixed H_2/H_∞ control problem-necessary conditions for optimality. In *Proceedings of the American Control Conference*, pages 1348–1352, Chicago IL, June 1992.
11. J. C. Doyle, K. Glover, P. P. Khargonekar, and B. A. Francis. State-space solutions to standard H_2 and H_∞ control problems. *IEEE Trans. on Auto. Control*, AC-34(8):831–847, August 1989.
12. E. Schomig, M. Sznaier, and U. Ly. A time–domain penalty function approach to mixed H_2/H_∞ -control using parameter optimization methods. In *Proceedings of the 2nd IEEE Conference on Control Applications*, pages 973–976, Vancouver BC, September 1993.

13. A. N. Madiwale. Reduction of conservatism in mixed H_2/H_∞ design. In *Proceedings of the 28th Conference on Decision and Control*, pages 923–925, Tampa FL, December 1989.
14. R. Bambang, E. Shimemura, and K. Uchida. Mixed H_2/H_∞ control of uncertain systems. In *Proceedings of the American Control Conference*, pages 245–247, San Francisco CA, June 1993.
15. P. P. Khargonekar and M. A. Rotea. Mixed H_2/H_∞ control: A convex optimization approach. *IEEE Trans. Auto. Control*, AC-36(7):824–837, July 1991.
16. S. R. Hall and J. P. How. Mixed H_2/μ performance bounds using dissipative theory. In *Proceedings of the 32nd Conference on Decision and Control*, pages 1536–1540, San Antonio TX, December 1993.
17. B. A. Francis. *A Course in H_∞ Control Theory*. Lecture Notes in Control and Information Sciences. Springer-Verlag, 1987.
18. A. W. Naylor and G. W. Sell. *Linear Operator Operator Theory in Engineering and Science*. Applied Mathematical Sciences. Springer-Verlag, 1982.
19. J. C. Doyle, B. A. Francis, and A. R. Tannenbaum. *Feedback Control Theory*. Macmillan, 1992.
20. M. A. Dahleh and I. J. Dias-Bobillo. *Control of Uncertain Systems: A Linear Programming Approach*. Preprint.
21. J. B. Pearson. Introduction to robust ℓ_1 -optimal control. Lecture notes from the ℓ_1 Robust Control Workshop, *American Control Conference*, 1992.
22. F. Blanchini and M. Sznaier. Rational \mathcal{L}^1 suboptimal compensators for continuous-time systems. In *Proceedings of American Control Conference*, pages 635–639, San Francisco CA, June 1993.
23. W. M. Wonham. *Linear Multivariable Control: A Geometric Approach*. Springer-Verlag, 1985.
24. J. Snyders and M. Zakai. On nonnegative solutions of the equation $AD + DA^T = -C^*$. *SIAM Journal of Applied Mathematics*, 18(3):704–714, May 1970.
25. J. C. Willems. Least squares stationary optimal control and the algebraic Riccati equation. *IEEE Trans. Auto. Control*, AC-16(6):621–634, Dec 1971.
26. I. Gohberg, P. Lancaster, and L. Rodman. On Hermitian solutions of the symmetric algebraic Riccati equation. *SIAM Journal of Control and Optimization*, 24(6):1323–1334, Nov 1986.
27. P. Lancaster and L. Rodman. Existence and uniqueness theorems for the algebraic Riccati equation. *International Journal of Control*, 32(2):285–309, 1980.
28. A. Packard and J. Doyle. Lecture notes from μ -synthesis short course. NASA-Langley, VA, 1990.

29. B. P. Molinari. The stabilizing solution of the algebraic Riccati equation. *SIAM Journal of Control*, 11(2):262-271, May 1973.
30. H. K. Wimmer. Monotonicity of maximal solutions of algebraic Riccati equations. *System & Control Letters*, 5:317-319, 1985.
31. K. Glover and J. Doyle. A state-space approach to H_∞ optimal control. In H. Nijmeijer and J. M. Schumacher, editors, *Three Decades of Mathematical Systems Theory*, pages 179-218. Springer-Verlag, 1989. Lecture Notes in Control and Information Sciences, Vol 135.
32. A. V. Balakrishnan. *Applied Functional Analysis*. Applications of Mathematics. Springer-Verlag, 1981.
33. S. P. Boyd and C. H. Barratt. *Linear Controller Design: Limits of Performance*. Prentice-Hall, Inc, 1991.
34. Ivar Ekeland. *Convex Analysis and Variational Problems*. North-Holland, 1976.
35. R. Fletcher. *Practical Methods of Optimization, Volume 2: Constrained Optimization*. John Wiley & Sons. Ltd., 1981.
36. D. G. Luenberger. *Optimization by Vector Space Methods*. John Wiley & Sons, Inc, 1969.
37. A. L. Peressini, F. E. Sullivan, and Jr. J. J. Uhl. *The Mathematics of Nonlinear Programming*. Undergraduate Texts in Mathematics. Springer-Verlag, 1988.
38. D. C. Youla, H. A. Jabr, and J. J. Bongiorno. Modern Wiener-Hopf design of optimal controllers, Part II: The multivariable case. *IEEE Trans. Auto. Control*, AC-21:319-338, 1976.
39. J. M. Maciejowski. *Multivariable Feedback Design*. Addison-Wesley Publishing Company. Inc., 1989.
40. M. G. Safonov, D. J. N. Limebeer, and R. Y. Chiang. Simplifying the H_∞ theory via loop-shifting, matrix-pencils and descriptor concepts. *International Journal of Control*, 50(6):2467-2488, 1989.
41. R. L. Dailey. Lecture notes for the workshop on H_∞ and μ methods of robust control, 1990. In conjunction with the *American Control Conference*, San Diego, CA.
42. G. Zames. Feedback and optimal sensitivity: Model reference transformations, multiplicative seminorms, and approximate inverses. *IEEE Trans. Auto. Control*, AC-23(2):301-320, April 1981.
43. X. Li. *Robust Controller Design by H_∞ Optimization and Structured Singular Value Techniques*. PhD thesis, Drexel University, August 1992.
44. G. J. Balas, J. C. Doyle, K. Glover, A. Packard, and R. Smith. *μ -Analysis and Synthesis Toolbox*. The Mathworks. Inc., 1991.

45. M. G. Safonov and R. Y. Chiang. Real/complex K_m -synthesis without curve fitting. In Leondes, editor, *Control and Dynamic Systems*, pages 1-71. Academic Press, 1993.
46. C. N. Dorny. *A Vector Space Approach to Models and Optimization*. John Wiley & Sons, Inc, 1975.
47. S. R. Wells and D. B. Ridgely. Using increased order controllers in mixed H_2/H_∞ optimization. In *Proceedings of American Control Conference*, pages 1358-1362, Chicago IL, June 1992.
48. B. R. Copeland and M. G. Safonov. A generalized eigenproblem approach to singular control problems-Part II: H_∞ problems. In *Proceedings of the 31st IEEE Conference on Decision and Control*, pages 1453-1458, Tucson AZ, December 1992.
49. A. Stoorvogel. *The H_∞ Control Problem*. Prentice Hall, 1992.
50. J. C. Juang, C. F. Lin, J. R. Cloutier, and J. H. Evers. Generalized singular robust control design. In *Proceedings of the 30th Conference on Decision and Control*, pages 2995-3001, Brighton England, December 1991.
51. L. M. Silverman. Inversion of multivariable linear systems. *IEEE Trans. Auto. Control*, AC-14(3):270-276, June 1969.
52. K. Schittkowski. NLPQP: A fortran subroutine solving constrained nonlinear programming problems. In *Annals of Operation Research*, pages 485-500. J. C. Baltzer A. G., Scientific Publishing Company, 1985/6.
53. A. Grace. *Optimization Toolbox*. The Mathworks. Inc., 1992.
54. D. P. Giesy and K. B. Lim. H_∞ norm sensitivity formula with control system design applications. *Journal of Guidance, Control, and Dynamics*, 16(6):1138-1145, November-December 1993.
55. P. Gahinet and P. Apkarian. Numerical computation of the L_∞ norm revisited. In *Proceedings of the 31st Conference on Decision and Control*, pages 2257-2258, Tucson AZ, December 1992.
56. G. H. Golub and C. F. Van Loan. *Matrix Computations*. Baltimore: The Johns Hopkins University Press, 1983.
57. D. M. Young and R. T. Gregory. *A Survey of Numerical Mathematics*, volume II. Dover, 1973.
58. A. Grace, A.J. Laub, J. N. Little, and C. M. Thompson. *Control System Toolbox*. The Mathworks. Inc., 1992.
59. D. G. Schultz and J. L. Melsa. *State Functions and Linear Control Systems*. McGraw-Hill Book Company, 1967.
60. P. S. Maybeck. *Stochastic Models, Estimation, and Control, Volume 1*. Mathematics in Science and Engineering, Vol 141-1. Academic Press, 1979.

61. D. B. Ridgely and S. S. Banda. *Introduction to Robust Multivariable Control*. AFWAL-TR-85-3102. USAF, 1986.
62. R. Y. Chiang and M. G. Safonov. *Robust Control Toolbox*. The Mathworks. Inc., 1992.
63. J. Ullauri, D. E. Walker, and D. B. Ridgely. Reduced order mixed H_2/H_∞ optimization with multiple H_∞ constraints. To appear in the Proceedings of the *AIAA Guidance, Navigation, and Control Conference*, Scottsdale, AZ, 1994.

Vita

Lieutenant Colonel David E. Walker was born on 12 June 1958, in Denton, Texas. He graduated from SHAPE American High School, Casteau, Belgium, in 1975, and attended the University of Texas at Austin. He completed a Bachelor of Science in Aerospace Engineering in 1979 and a Master of Science in 1980 with specialization in Control and Optimization Theory. In May 1979, he received a commission in the USAF. Lt Col Walker began active duty in the USAF in February 1980 attending Undergraduate Navigator Training at Mather AFB, California. Upon graduation, he completed RF-4C Weapons System Officer training and served tours at Zweibruecken AB, Germany and Shaw AFB, South Carolina as an Instructor Weapons System Officer in the RF-4C. In 1985, Lt Col Walker attended the USAF Test Pilot School, Edwards AFB, CA, and received the R. L. Jones award as the top engineering graduate in June 1986. He remained at Edwards AFB, where he served as the Chief, Avionics Branch, F-15 Combined Test Force for the F-15E developmental test and evaluation. In addition, Lt Col Walker performed flight tests in the F-15, F-4, F-16 and T-38. In 1988, he was selected to serve as the Executive Officer to the Commander, Air Force Flight Test Center until 1990 when he attended the Air Command and Staff College at Maxwell AFB, Alabama. Upon graduation in May 1991, he entered the Graduate School of Engineering, Air Force Institute of Technology.

Permanent address: 7319 Scenic Oaks Circle
Austin, Texas 78745